

A Thesis Submitted for the Degree of PhD at the University of Warwick

Permanent WRAP URL:

<http://wrap.warwick.ac.uk/130613>

Copyright and reuse:

This thesis is made available online and is protected by original copyright.

Please scroll down to view the document itself.

Please refer to the repository record for this item for information to help you to cite it.

Our policy information is available from the repository home page.

For more information, please contact the WRAP Team at: wrap@warwick.ac.uk

3700

**MECHANISMS OF SAND FLOW
AND COMPACTION IN CORE-BLOWING**

by

FARHAD HEYDARI

A thesis submitted for the degree of Doctor of
Philosophy in Engineering.

University of Warwick
Department of Engineering

1990

Dedicated to my Mother Fatemeh

CONTENTS

ACKNOWLEDGEMENTS

LIST OF FIGURES

SYNOPSIS

		Page No.
1.	INTRODUCTION	1
2.	OBJECTIVES	3
3.	LITERATURE SURVEY	4
3.1.	Core-making terminology	4
3.2.	Core sands	6
3.2.1.	Core sand types	6
3.2.1.1.	Silica	6
3.2.1.2.	Zircon	7
3.2.2.	Properties of core sands	8
3.2.3.	Core sand binders	8
3.2.3.1.	Introduction	8
3.2.3.2.	Requirements	8
3.2.3.3.	Binder groups	9
3.2.3.3.1.	Organic binders	9
3.2.3.3.1.1.	Oil based binders	10
3.2.3.3.1.2.	Cereals	10
3.2.3.3.1.3.	Resin binders	11
3.2.3.3.1.4.	Cold setting resins	11
3.2.3.3.1.5.	Thermo setting resins (the shell process)	13
3.2.3.3.2.	Inorganic binders	14
3.2.3.3.2.1.	Sodium silicates	14
3.3.	Mixing	16
3.4.	Core-making	18
3.4.1.	Properties required for core-making	18
3.4.2.	Core-making processes	19
3.4.2.1.	The shell process	19
3.4.2.2.	The hot box process	20
3.4.2.3.	Cold setting core-making processes	20
3.4.2.3.1.	Sodium silicate processes	22
3.4.2.3.1.1.	Silicate CO ₂ process	22
3.4.2.3.1.2.	Powder hardened silicate processes	23
3.4.2.3.1.3.	Ester-silicate process	24
3.4.2.3.2.	Cold setting phenolic furane process	25
3.4.2.3.3.	The SO ₂ process	26
3.4.2.3.3.1.	Furan-SO ₂ process	27
3.4.2.3.3.2.	The epoxy-SO ₂ process	28
3.4.2.3.3.3.	The FRC process	29
3.4.2.3.4.	The cold-box process (Isocure)	30
3.4.2.3.5.	The fascal system	32
3.4.2.3.6.	The betaset process	33
3.5.	Core coating	35

3.6.	Core-boxes	37
3.6.1.	Introduction	37
3.6.2.	Core-box design	37
3.6.3.	Core-box materials	38
3.6.4.	Core-box rigging for production	39
3.6.5.	Cleaning core-boxes	40
3.6.6.	The core-box repairs	41
3.7.	Core-making techniques	42
3.7.1.	Core blowing/shooting	42
3.7.1.1.	Introduction	42
3.7.1.2.	Core-shooting	42
3.7.1.3.	Core-blowing	43
3.7.1.4.	Comparison between core-blowing and core-shooting	43
3.7.1.5.	Blow-plates and blow holes	45
3.7.1.6.	Core-box venting	47
3.7.1.7.	Previous research in core-blowing and core-shooting	48
3.8.	Flow of sand mixture in core-blowing and core-shooting	64
4.	EXPERIMENTAL PROCEDURE	67
4.1.	Introduction	67
4.2.	Experimental equipment	67
4.3.	Experimental groups	70
4.3.1.	Group 1	70
4.3.2.	Group 2	71
4.3.3.	Group 3	72
4.3.4.	Group 4	73
4.3.5.	Group 5	73
4.3.6.	Group 6	74
5.	RESULTS	76
5.1.	Group 1	76
5.1.1.	Group a	76
5.1.2.	Group b	85
5.2.	Group 2	87
5.3.	Group 3	89
5.3.1.	Group a	89
5.3.2.	Group b	91
5.4.	Group 4	92
5.4.1.	Group a	93
5.4.2.	Group b	94
5.5.	Group 5	96
5.6.	Group 6	99
5.6.1.	Group a	99
5.6.2.	Group b	101
5.7.	Summary of results	104

6.	DISCUSSION	106
6.1.	Introduction	106
6.2.	Sand magazine	108
6.3.	Sand/air jets	112
6.4.	Core-box venting	117
6.5.	Compaction	120
6.6.	Discussion of results	126
6.6.1.	Group 1	126
6.6.1.1.	Group a	126
6.6.1.2.	Group b	129
6.6.2.	Group 2	133
6.6.3.	Group 3	134
6.6.4.	Group 4	135
6.6.5.	Group 5	138
6.6.6.	Group 6	140
7.	CONCLUSIONS	142
	REFERENCES	144
	APPENDIX	

ACKNOWLEDGEMENTS

The author wishes to sincerely thank Dr. J. Wallbank for his supervision, financial support, patience and numerous inspirational and stimulating discussions during the course of this work.

Thanks are also due to Dr. V. Kondic from whom helpful discussions were obtained.

The author also wishes to thank the technical staff of the University of Warwick for their help with the experimental work.

Thanks are also due to Mrs. Hazel Taylor for typing this project.

Finally, the author wishes to sincerely thank his forever loved parents for their love, encouragement and support.

LIST OF FIGURES

- Fig. 1. Section through core blower and core box
- Fig. 2. Core reinforcement, EITB Publications(2)
- Fig. 3. Core venting tools, EITB Publications(2)
- Fig. 4. Core chills, EITB Publications(2)
- Fig. 5. Sedimentation processes, Webster(5)
- Fig. 6. U.K. silica sand deposits, Webster(5)
- Fig. 7. Thermal expansion curve for mineral sands, Garnar(4)
- Fig. 8. Basic shapes of sand grains, Webster(5)
- Fig. 9. Basic production sequence in shell moulding, Beeley(7)
- Fig. 10. Examples of systems for carbon dioxide hardening of cores and mould parts, Beeley(7)
- Fig. 11. DMEA recycling plant, Kunsch(48)
- Fig. 12. Schematic representation of the reaction mechanisms of the betaset process, Shephard(51)
- Fig. 13. Alloys successfully cast with the betaset process, Shephard(51)
- Fig. 14. Core-box design, Beeley(7)
- Fig. 15. Section through core-shooter, Gardner(71)
- Fig. 16. Section through core-blower, Gardner(71)
- Fig. 17. Universal, single and double blow plates, Clark(64)
- Fig. 18. Various blow tubes, Clark(64)
- Fig. 19. Various core-box vents, Clark(64)
- Fig. 20. Variation of core weight according to different blow holes and air pressure, Gade(75)
- Fig. 21. Satisfactory air pressure drop shown in diagram of core-blower, Clark(64)
- Fig. 22. Formation of channels in sand magazine, Clark(64)

- Fig. 23. Techniques used to prevent channelling, Clark(64)
- Fig. 24(a). Pressure vs time in core-blower reservoir, Lesnichenko(68)
- Fig. 24(b). Pressure vs time in core-shooter reservoir, Lesnichenko(68)
- Fig. 25. Movement of layered sand in sand sleeve, Geller(80)
- Fig. 26. Movement of layered sand in sand sleeve, Geller(80)
- Fig. 27. Movement of layered sand in sand sleeve, Geller(80)
- Fig. 28. Air pressure variation in sand sleeve, Khurtov(70)
- Fig. 29. Movement of the contrasting substance in the sand stream, Pelczarski(81)
- Fig. 30. Speed of sand stream in core-box vs time, Pelczarski(81)
- Fig. 31. Determination of the horizontal component of the speed of the sand flow, Pelczarski(81)
- Fig. 32. Variation of core density across and along the core-box, Pelczarski(81)
- Fig. 33. The shape of the free surface when filling the core-box with sand, Pelczarski(81)
- Fig. 34. Movement of layered sand in sand magazine, Danko(83)
- Fig. 35. Core box filling by two different sands, Danko(83)
- Fig. 36. Core blower
- Fig. 37. Core box number 1
- Fig. 38. Main body of core box number 1
- Fig. 39. Perspex front of core box number 1
- Fig. 40. Back of core box number 1
- Fig. 41. Front view of core box number 1
- Fig. 42. Cross sections of different channels of core box number 1
- Fig. 43. Core box number 2

- Fig. 44. Core box number 2
- Fig. 45. Core box number 2
- Fig. 46. Core box number 3
- Fig. 47a. Front view of core box number 3
- Fig. 47b. Side view of core box number 3
- Fig. 47c. Plan view of core box number 3
- Fig. 48. Schematic diagram of core box number 2 showing filling time measurement technique
- Fig. 49. Blow holes used in the experiments
- Fig. 50. Order of experiments carried out on core box 2 in group 4. All vents open (a total of 30)
- Fig. 51. Order of experiments carried out on box 2 in group 6. All vents open (a total of 30)
- Fig. 52. Order of experiments carried out on box 1 in group 6. All vents open
- Fig. 53. Schematic diagram of core-box number 1 showing the number of different channels and levels 1' to 3'
- Fig. 54. Preliminary experiments carried out in sub group a of group 1 on box 1
- Fig. 55. Core-box 1, core-weight vs blow hole area
- Fig. 56. Experiments carried out in sub-group a of group 1 on box 1
- Fig. 57. $\phi 5\text{mm}$ blow hole, all vents open
- Fig. 58. $\phi 5\text{mm}$ blow hole, all vents open
- Fig. 59. $\phi 5\text{mm}$ blow hole, all vents open
- Fig. 60. $\phi 5\text{mm}$ blow hole, all vents open
- Fig. 61. $\phi 5\text{mm}$ blow hole, all vents open
- Fig. 62. $\phi 5\text{mm}$ blow hole, all vents open
- Fig. 63. $\phi 5\text{mm}$ blow hole, all vents open
- Fig. 64. $\phi 10\text{mm}$ blow hole, all vents open
- Fig. 65. $\phi 10\text{mm}$ blow hole, all vents open
- Fig. 66. $\phi 10\text{mm}$ blow hole, all vents open
- Fig. 67. $\phi 10\text{mm}$ blow hole, all vents open

- Fig. 68. ϕ 10mm blow hole, all vents open
- Fig. 69. ϕ 10mm blow hole, all vents open
- Fig. 70. ϕ 10mm blow hole, all vents open
- Fig. 71. ϕ 10mm blow hole, all vents open
- Fig. 72. ϕ 10mm blow hole, all vents open
- Fig. 73. ϕ 10mm blow hole, all vents open
- Fig. 74. ϕ 10mm blow hole, all vents open
- Fig. 75. ϕ 15mm blow hole, all vents open
- Fig. 76. ϕ 15mm blow hole, all vents open
- Fig. 77. ϕ 15mm blow hole, all vents open
- Fig. 78. ϕ 15mm blow hole, all vents open
- Fig. 79. ϕ 15mm blow hole, all vents open
- Fig. 80. ϕ 15mm blow hole, all vents open
- Fig. 81. ϕ 15mm blow hole, all vents open
- Fig. 82. ϕ 20mm blow hole, all vents open
- Fig. 83. ϕ 20mm blow hole, all vents open
- Fig. 84. ϕ 20mm blow hole, all vents open
- Fig. 85. ϕ 20mm blow hole, all vents open
- Fig. 86. ϕ 20mm blow hole, all vents open
- Fig. 87. ϕ 15mm blow hole, one vent at the end of each channel open
- Fig. 88. ϕ 15mm blow hole, one vent at the end of each channel open
- Fig. 89. ϕ 15mm blow hole, one vent at the end of each channel open
- Fig. 90. ϕ 15mm blow hole, one vent at the end of each channel open
- Fig. 91. ϕ 15mm blow hole, one vent at the end of each channel open
- Fig. 92. ϕ 15mm blow hole, one vent at the end of each channel open
- Fig. 93. Triangular blow hole = ϕ 15mm, one vent at the end of each channel open

- Fig. 94. Triangular blow hole = $\phi 15\text{mm}$, one vent at the end of each channel open
- Fig. 95. Triangular blow hole = $\phi 15\text{mm}$, one vent at the end of each channel open
- Fig. 96. Triangular blow hole = $\phi 20\text{mm}$, one vent at the end of each channel open
- Fig. 97. Rectangular blow hole = $\phi 20\text{mm}$, one vent at the end of each channel open
- Fig. 98. Rectangular blow hole = $\phi 20\text{mm}$, one vent at the end of each channel open
- Fig. 99. $\phi 5\text{mm}$ blow hole, vents up to 2' and in channel 4 closed
- Fig. 100. $\phi 5\text{mm}$ blow hole, vents up to 2' and in channel 4 closed
- Fig. 101. $\phi 5\text{mm}$ blow hole, vents up to 2' and in channel 4 closed
- Fig. 102. $\phi 5\text{mm}$ blow hole, vents up to 2' and in channel 4 closed
- Fig. 103. $\phi 5\text{mm}$ blow hole, vents up to 2' and in channel 4 closed
- Fig. 104. $\phi 15\text{mm}$ blow hole, vents up to 2' and in channel 4 closed
- Fig. 105. $\phi 15\text{mm}$ blow hole, vents up to 2' and in channel 4 closed
- Fig. 106. $\phi 15\text{mm}$ blow hole, vents up to 2' and in channel 4 closed
- Fig. 107. $\phi 15\text{mm}$ blow hole, vents up to 2' and in channel 4 closed
- Fig. 108. $\phi 15\text{mm}$ blow hole, vents up to 2' and in channel 4 closed
- Fig. 109. $\phi 5\text{mm}$ blow hole, vents up to 1' closed
- Fig. 110. $\phi 5\text{mm}$ blow hole, vents up to 1' closed
- Fig. 111. $\phi 5\text{mm}$ blow hole, vents up to 1' closed
- Fig. 112. $\phi 5\text{mm}$ blow hole, vents up to 1' closed
- Fig. 113. $\phi 5\text{mm}$ blow hole, vents up to 1' closed
- Fig. 114. $\phi 15\text{mm}$ blow hole, vents up to 1' closed
- Fig. 115. $\phi 15\text{mm}$ blow hole, vents up to 1' closed

- Fig. 116. ϕ 15mm blow hole, vents up to 1' closed
- Fig. 117. ϕ 15mm blow hole, vents in channels 2, 4 and 6 open
- Fig. 118. ϕ 15mm blow hole, vents in channels 2, 4 and 6 open
- Fig. 119. ϕ 15mm blow hole, vents in channels 2, 4 and 6 open
- Fig. 120. ϕ 15mm blow hole, vents in channels 2, 4 and 6 open
- Fig. 121. ϕ 15mm blow hole, vents in channels 2, 4 and 6 open
- Fig. 122. ϕ 15mm blow hole, vents in channels 2, 4 and 6 open
- Fig. 123. ϕ 15mm blow hole, vents in channels 2, 4 and 6 open
- Fig. 124. ϕ 15mm blow hole, vents in channels 3, 5 and 7 open
- Fig. 125. ϕ 15mm blow hole, vents in channels 3, 5 and 7 open
- Fig. 126. ϕ 15mm blow hole, vents in channels 3, 5 and 7 open
- Fig. 127. ϕ 15mm blow hole, vents in channels 3, 5 and 7 open
- Fig. 128. ϕ 15mm blow hole, vents in channels 3, 5 and 7 open
- Fig. 129. Sound core
- Fig. 130. Sound core
- Fig. 131. Core containing spongy areas
- Fig. 132. Core containing spongy areas
- Fig. 133. Core containing spongy areas
- Fig. 134. Core containing voids
- Fig. 135. Core containing voids
- Fig. 136. Core-box 1, filling time vs blow hole area
- Fig. 137. Schematic diagram of core-box number 2 showing the position of the vents and the number of different sections
- Fig. 138. Experiments carried out in sub-group b of group 1 on box 2

- Fig. 139. ϕ 10mm blow hole, all vents open
- Fig. 140. ϕ 10mm blow hole, all vents open
- Fig. 141. ϕ 15mm blow hole, all vents open
- Fig. 142. ϕ 15mm blow hole, all vents open
- Fig. 143. ϕ 15mm blow hole, all vents open
- Fig. 144. ϕ 30mm blow hole, all vents open
- Fig. 145. ϕ 30mm blow hole, all vents open
- Fig. 146. ϕ 30mm blow hole, all vents open
- Fig. 147. ϕ 5mm blow hole, all vents open
- Fig. 148. ϕ 5mm blow hole, all vents open
- Fig. 149. ϕ 5mm blow hole, all vents open
- Fig. 150. ϕ 5mm blow hole, all vents open
- Fig. 151. ϕ 5mm blow hole, all vents open
- Fig. 152. Experiments carried out in sub-group b of group 1 on box 2
- Fig. 153. ϕ 15mm blow hole, vents on section 1 open only
- Fig. 154. ϕ 15mm blow hole vents on section 1 open only
- Fig. 155. ϕ 15mm blow hole, vents on section 1 open only
- Fig. 156. ϕ 15mm blow hole, vents on section 1 open only
- Fig. 157. ϕ 15mm blow hole, vents on section 1 open only
- Fig. 158. ϕ 15mm blow hole, vents on left hand side of the core box open only
- Fig. 159. ϕ 15mm blow hole, Top 3 vents on right hand side and Bottom vents of left hand side on section 2 of the core-box open only
- Fig. 160. ϕ 15mm blow hole, Bottom 3 vents on section 2 and vents on section 1 of the core-box open only
- Fig. 161. ϕ 15mm blow hole, Middle 3 vents on section 2 of the core-box open only

- Fig. 162. ϕ 15mm blow hole, Middle 3 vents on section 2 and vents on section 1 of the core-box open only
- Fig. 163. ϕ 15mm blow hole, Top 3 vents of section 2 and vents on section 1 of the core-box open only
- Fig. 164. Experiments carried out in group 2 on box. All vents open (a total of 20)
- Fig. 165. Core box 2, core-weight vs blow hole area
- Fig. 166. Core box 2, core-weight vs air pressure
- Fig. 167. Experiments carried out in sub-group a of group 3 on box 1 (All vents open)
- Fig. 168. Core-box 1, filling time vs air pressure
- Fig. 169. Core-box 1, core-weight vs blow hole area
- Fig. 170. Core-box 1, core-weight vs air pressure
- Fig. 171. Experiments carried out in sub-group b in group 3 on box 2, all vents open (a total of 30)
- Fig. 172. Core-box 2, core-weight vs blow hole area
- Fig. 173. Core-box 2, core-weight vs air pressure
- Fig. 174. Experiments carried out in sub group a of group 4 on box 1. Resin content = 1.05% (All vents open)
- Fig. 175. Experiments carried out in sub-group a of group 4 on box 1. Resin content= 0.35% (All vents open)
- Fig. 176. Core-box 1, core-weight vs blow hole area
- Fig. 177. Core-box 1, core-weight vs air pressure
- Fig. 178. Core-box 1, core-weight vs blow hole area
- Fig. 179. Core-box 1, core-weight vs air pressure
- Fig. 180. Experiments carried out in sub-group b of group 4 on box 2. All vents open (a total of 30)
- Fig. 181. Core-box 2, core-weight vs air pressure
- Fig. 182. Core-box 2, core-weight vs air pressure
- Fig. 183. Core-box 2, core-weight vs air pressure
- Fig. 184. Core-box 2, core-weight vs blow hole area

- Fig. 185. Core-box 2, core-weight vs blow hole area
- Fig. 186. Core-box 2, core-weight vs blow hole area
- Fig. 187. Experiments carried out in group 5 on box 2. All vents open (a total of 30)
- Fig. 188. Core-box 2, core-weight vs air pressure
- Fig. 189. Core-box 2, core-weight vs air pressure
- Fig. 190. Core-box 2, core-weight vs air pressure
- Fig. 191. Core-box 2, core-weight vs blow hole area
- Fig. 192. Core-box 2, core-weight vs blow hole area
- Fig. 193. Core-box 2, core-weight vs blow hole area
- Fig. 194. Experiments carried out in sub-group a of group 6 on box 1. (All vents open)
- Fig. 195a. Core-box 1, core-weight vs blow hole area
- Fig. 195b. Core-box 1, core-weight vs blow hole area
- Fig. 195c. Core-box 1, core-weight vs blow hole area
- Fig. 196a. Core-box 1, core-weight vs air pressure
- Fig. 196b. Core-box 1, core-weight vs air pressure
- Fig. 196c. Core-box 1, Core-weight vs air pressure
- Fig. 197. Experiments carried out in sub-group b of group 6 on box 2.
- Fig. 198a. Core-box 2, core-weight vs blow hole area
- Fig. 198b. Core-box 2, core-weight vs blow hole area
- Fig. 198c. Core-box 2, core-weight vs blow hole area
- Fig. 199a. Core-box 2, core-weight vs air pressure
- Fig. 199b. Core-box 2, core-weight vs air pressure
- Fig. 199c. Core-box 2, core-weight vs air pressure
- Fig. 200. Pressure vs Time, Geller(69)
- Fig. 201. Pressure vs Time, Lesnichenko(86)
- Fig. 202. Film removal of film build-up by sand/air jet opposite blow hole
- Fig. 203. Sand sticking opposite blow hole
- Fig. 204. Core-box 3, ϕ 10mm blow hole, all vents open

- Fig. 205. Core-box 3, ϕ 10mm blow hole, all vents open
- Fig. 206. Core-box 3, ϕ 10mm blow hole, all vents open
- Fig. 207. Core-box 3, ϕ 10mm blow hole, all vents open
- Fig. 208. Core-box 3, ϕ 10mm blow hole, all vents open
- Fig. 209. Distribution of forces during collision of the sand particles, after Danko⁽⁸¹⁾
- Fig. 210. Movement of sand particles on surface of sand layer in core-box
- Fig. 211. Partially and fully resin coated sand particles
- Fig. 212a. Core-box 1, core-weight vs resin content
- Fig. 212b. Core-box 1, core-weight vs resin content
- Fig. 212c. Core-box 1, core-weight vs resin content
- Fig. 212d. Core-box 2, core-weight vs resin content
- Fig. 212e. Core-box 2, core-weight vs resin content
- Fig. 212f. Core-box 2, core-weight vs resin content

SYNOPSIS

The effect of different control variables of the core-blowing process on the mechanism of sand flow inside core-boxes has been studied. These variables included the core-box geometry, the blowing air pressure, the sand/binder mixture, the area and arrangement of the core-box vents, and the area and shape of the blow hole.

A high speed cine-camera (64 frames/sec) was used to record the filling of the three core-boxes used. The blown cores were weighed in the boxes on scales accurate to 0.1 of a gram. They were then cured using sulphur dioxide (SO₂) and checked for soundness.

The results showed that:

- i) The filling pattern within a core-box can be controlled by the blowing conditions. Different patterns of filling can be achieved according to different; blow hole sizes and shapes, blowing air pressure settings and core-box venting arrangements, resulting in different degrees of sand compaction in the core-box.
- ii) For a given blowing condition increasing the blowing air pressure and/or increasing the blow hole area to optimum values, gives rise to increasing the overall compaction of the core and its weight. The rate of change in the core-weight decreases as the optimum values of blowing air pressure and/or blow hole area are approached.
- iii) The filling time of a core-box with sufficient venting is related to the area of the blow hole and the blowing air pressure. Insufficient venting of a core-box can give rise to prolonged filling times.
- iv) Insufficient venting or over venting of a core-box leads to decreasing the core compaction and weight. One sided venting in the core-boxes used, resulted in faster filling and better sand compaction in those sides.
- v) Compaction of the sand in the core-box is achieved under the influence of; the kinetic energy of the sand/air jet entering the core-box (Primary compaction), and the air flowing through the mass of sand in the core-box (Secondary compaction).
- vi) Increasing the binder level in the mix led to the production of stronger cores. However it also led to core defects in the form of voids in areas where compaction is largely achieved as a result of the secondary compaction.

1. INTRODUCTION

1. INTRODUCTION

The art of casting metal has its origins in ancient civilisation. After initial mastery of the art, it became apparent to founders that to produce anything other than the simplest of solid castings, a system would have to be devised to enable internal cavities to be formed within the casting. It was found that this could only be done with cores. The early cores were formed in baked clay which developed into forming cores of sand, mixed with available binding materials. These cores were used in the production of such castings as ancient statues and iron stoves. The casting of bells exerted an influence on core making.

The 19th Century brought about new developments of core making, and equipment was made available for mass production. The cores, usually hand rammed from a sand/organic binder mix, were heated in ovens to harden.

Core-blowing machines were introduced into core making shops around 1910. Early progress of the core-blowing process was slow. However, the importance of the core-blowing machine as a modern means for rapid production of uniform and high quality cores was recognised. Core-blowing has thus become a specialised branch of the foundry trade, and the factors controlling the success of any particular job are many and varied.

In blowing a core, the core-box cavity is filled by introducing sand, suspended in a stream of compressed air which enters the cavity, at high speed through the blowing holes. The core is rammed by abruptly arresting the travel of the sand grains themselves while the air is

allowed to continue on to the atmosphere, exhausted via vents in the core-box, Fig 1.

When confronted with a core which is to be produced on a core-blower, a machine of the proper design and the requirements of the finished cores are known, as far as sand/binder mix, strength, permeability and other core physical characteristics are concerned. However, the questions; how shall the core be placed in the core-box, and where the blow holes and the vents should be arranged, as well as the size and shape of these, to give satisfactory results with a minimum of experimental effort have to be resolved. In view of the variety of sizes, shapes and contours of cores required, difficulties are often encountered in deciding just what are the best blowing conditions. A working knowledge of the essential factors of the core-blowing process is therefore of great interest to pattern-makers and foundry engineers.

Unfortunately, practical knowledge pertaining to blowing cores has been confined largely to those who directly work with core-blowing machine design and are engaged in the manufacture of the equipment.

In order to reduce core-blowing to engineering knowledge, it is necessary to systematically study the process and determine its underlying characteristics. This requires the investigation of the mechanism of sand/air flow (ie; sand/air flow stream flowing from the blowing holes into the core-box cavity), and the motion of sand particles during the filling of the cavity in the core-box and the mechanism of core compaction.

2. OBJECTIVE

2. OBJECTIVE

To investigate the mechanism of sand/air flow (i.e. sand/air stream flowing through the blowing holes into the core-box cavity), motion of sand particles during the filling of the cavity in the core-box and core compaction.

3. LITERATURE SURVEY

3. LITERATURE SURVEY

3.1. Core-making Terminology

A core is an aggregate of partially inert materials, possessing a degree of porosity, and a controlled mechanical strength to allow the aggregate to be assembled without breakage, for the purpose of making internal or external portions of a mould⁽¹⁾. The major function of the core is to form internal cavities surrounded by metal.

Sand cores are made with the aid of core-boxes which can be repeatedly used to produce a particular core. The boxes are usually constructed in two or more parts with pins and guides so that the finished core can be removed. The cavity in the core-box represents the form or pattern which is to be reproduced in the finished core.

The core sand grains used in core-making are bound together with core-binders. With the aid of the binders sand mixtures are set into cores. The mixtures may have to be heated to gain the required strength, using core-drying and core-baking ovens. With some binders gasses are passed through cores, this is known as core hardening by gassing.

Cores can be assembled to build a whole mould (i.e. external and internal parts). This necessitates handling and accurate positioning of the cores which is usually helped by the use of core-prints which are location features on other parts of the core or mould half.

Some cores may need extra reinforcement, Fig 2. The use of sprigs, nails, wire, rod, rod rig construction, and perforated tube, are common in cores of thin cross

sections, i.e. below 12mm and more than 50mm long⁽²⁾. The type of reinforcement is determined by the size and complexity of the core.

Prior to casting, cores may have to be coated using materials known as core-washes or core-coatings in order to promote a smooth casting surface.

During the casting operation gasses are normally evolved from the core binders. These gasses escape through core-vents and through the natural permeability of the core mixture. The venting method chosen is governed by the size and shape of the core, and the core-sand used, Fig 3.

Shrinkage holes can form in cored sections of a casting when a thick section is isolated from the feeder. Core-chills can counteract the formation of such shrinkage holes⁽²⁾. Core-chills are pieces of metal varying in size and shape, which are placed on the faces of bosses, pads, ribs, or in the corners of a core-box. Fig 4 illustrates some different types of core-chills.

3.2. Core Sands

Sand consists of grains of mineral matter ranging from approximately 0.05 to 2mm dia. Common foundry sand is composed of silicon dioxide, SiO_2 . Silica grains are often associated with small amounts of feldspar, mica and other minerals. High grade special sands are sometimes used for cores and moulds where special characteristics, such as increased thermal conductivity are required. Such sands include zircon (Zr SiO_4), chromite ($\text{Fe Cr}_2\text{O}_4$), olivine [$(\text{Mg, Fe})_2 \text{SiO}_4$], staurolite ($\text{Fe Al}_5 \text{Si}_2 \text{O}_{12} \cdot \text{OH}$) and aluminium silicates(3).

Fore modern core practice the basic requirements of core sands are (4);

- dimensional and thermal stability at elevated temperatures
- suitable particle size and shape
- chemical inertness with molten metals
- not readily wettable by molten metals
- low content of volatile elements
- availability in large quantities at reasonable cost
- consistent cleanliness and pH values
- compatible with the binders used.

3.2.1. Core sand types

3.2.1.1. Silica

Silicon combines with oxygen to form an oxide, SiO_2 , which occurs in a variety of forms(1). Most silica sand deposits have formed by weathering, i.e. the geological sedimentary processes and transportation by wind and water, Fig 5. The composition of the deposits depends on the nature of the materials that were eroded

and in the manner in which they were deposited⁽¹⁾. During the depositional processes, classification (i.e. separation) by size, shape, composition and specific gravity can take place.

Commercial silica foundry sands are found widely distributed over the United Kingdom being worked at many localities. Fig 6 illustrate a selection of foundry sands, location, characteristics, and properties.

Silica sands are not thermally stable. They expand by appreciable amount on heating and shrink on cooling. Their binder requirements, pH, acid values, vary from deposit to deposit. They are also of comparatively low density and low thermal conductivity⁽⁴⁾.

3.2.1.2. Zircon

The element zirconium combines with sodium, calcium, manganese, iron, titanium, thorium and oxygen to form eleven different Zr-bearing minerals⁽⁴⁾. Of these, only baddeleyite (ZrO_2) and zircon silicate ($ZrSiO_4$) are mined on a commercial scale. Zircon is widely produced from beach sand deposits. These range in age from very young, as found along the eastern coast of Australia, to very ancient fossil shoreline deposits being mined in Florida and Georgia. Malaysia, India, Sri-Lanka and South Africa are other producers of zircon sands.

Zircon sand has several desirable properties as a foundry sand⁽⁵⁻⁸⁾;

- lowest thermal expansion of any foundry sand, Fig 7
- high thermal conductivity and bulk density giving about four times the cooling rate of silica
- unwetted by most molten metals

- chemical unreactivity
- clean rounded grains which readily accept any type of binder
- superior dimensional and thermal stability at elevated temperatures
- pH is neutral or slightly acid.

3.2.2. Properties of core sands

Based on the origin, the sands vary in grain shape (Fig 8), grain composition, surface characteristics, grain size and distribution. These properties in addition to chemical analysis, sintering point, and expansion, vitally affect the usefulness and ultimate properties of the core.

3.2.3. Core sand binders

3.2.3.1. Introduction

Dry cores are composed of a mixture of sand and some binding material, which causes adhesion between the sand grains, and which have to be hardened after some further treatment. Binders can be classified depending on their; chemical nature, physical form, or hardening process. A simple division is by chemical nature, i.e. organic, and inorganic.

3.2.3.2. Requirements

Whether organic or inorganic, the binder should possess the following requirements;

- high dry strength and sufficient resistance to temperature so as not to collapse before the casting has solidified to retain its shape⁽⁵⁾

- high collapsibility after casting cools to room temperature to allow the sand to be easily removed(1)
- minimum evolution of gas to prevent gaseous effects in castings
- minimum absorption of moisture if cores are to be stored giving a good "shelf life"
- good dispersing properties in mixing(9)
- minimum stickiness not to create additional labour in cleaning core-boxes but allow the sand to "flow" into the box geometry
- reasonable bench life in the unmoulded condition
- no safety or environmental problems
- good economy.

3.2.3.3. Binder groups

3.2.3.3.1. Organic binders

Resin binders are synthetic materials which can be classified together with cold curing oils as organic binders(10). These binders are more expensive than inorganic binders but this is partly offset by the lower percentage addition (less than 2% compared to the more than 3% additions for the inorganic binders(5)). All the organic binders have excellent breakdown properties which makes them ideal for the cores of a casting where accessibility for fettling is difficult, and the resultant reduced fettling costs make these binders economical. In general, it may be said that unlike inorganic binders which are thermally stable and exhibit little degradation of bonding on heating, organic binders burn out upon casting, producing gas and producing a

carbonaceous film on the sand grains⁽¹⁰⁾. These properties are in fact responsible for the good casting surface finish with these materials, plus ease of casting knockout and the reclamation of such sands for further use. A disadvantage is that the generation of gases during casting can, under certain circumstances result in casting defects.

There are three major types of organic binders; oil based, cereals and resins.

3.2.3.3.1.1. Oil based binders

These binders as used in the foundry industry are of two types; natural and processed oils⁽⁵⁾.

Natural oils are vegetable and marine oils; linseed, tung and dehydrated castor oils. These oils dry and harden on standing. The drying power of an oil depends on the degree of unsaturation which is represented by the number of double bonds in the chain ($-C=C-$)⁽⁵⁾. The greater the number of double bonds, the greater the unsaturation and the greater the drying power⁽¹¹⁾.

Processed oils may contain unsaturated mineral oils, synthetic oils and alkyd resins. These oils are relatively cheap and can be produced from a blend of oleic and linoleic acids, with glycerol⁽⁵⁾.

3.2.3.3.1.2. Cereals

Cereal binders are of two types, pregelatinised starch and dextrine⁽⁷⁾. These develop a gelatinous bond with water⁽¹²⁻¹³⁾. Cereals improve initial compacted strength and contribute to collapsibility and ease of knockout, by decomposing at the casting temperatures. They do, however, increase gas evolution and diminish the

resistance of dried cores to the absorption of moisture(7).

3.2.3.3.1.3. Resin binders

In the last 40 years there has been a tendency to replace oils, and inorganic binders such as silicates, with resins for foundry core binders. This is because of many advantages that resin binders offer(5). The main advantages are:

- faster curing and higher production rates
- in-box curing
- increased flowability
- easier core break-down and shake-out
- improved casting quality
- reduced skill requirements in production of cores and moulds
- good economy.

There are many types of resins used, from simple urea and phenol formaldehyde resins to complex furan polyal resins(7).

3.2.3.3.1.4. Cold-setting resins

The use of cold-setting resins in foundries began in the early sixties and coincides with the introduction of furfuryl alcohol. Cold-setting resins are commonly based on resin containing furfuryl alcohol, in which polymerisation reaction results by the addition of a strong univeral acid, forming a green coloured condensation product(10). The reaction is exothermic, which helps to obtain a consistent-through cure. The reaction rate is sensitive to temperature and the nature of the base sand(14).

Urea formaldehyde/furfuryl alcohol resins were later developed which exhibit a stronger bond than that produced with furfuryl alcohol resins, and are more stable to the effect of heat than urea formaldehyde resin alone(10).

Today cold-set resins are represented by a range of materials exhibiting differing physical properties. This range may be sub-divided as follows;

- Urea formaldehyde and furfuryl alcohol modified urea formaldehyde resins known as furanes, (UF/FA resins)
- Phenol formaldehyde (PF resins) and furfuryl alcohol modified phenol formaldehyde resins, (PF/FA resins). Both PF and PF/FA resins are characterised by zero nitrogen contents which eliminate problems due to pinholing in some alloys(10)
- the furfuryl alcohol modified copolymer resins containing both urea and urea formaldehyde components called copolymers (PF/UF resins)
- Polyurethanes (PU), where a phenol formaldehyde resin together with a tertiary amine accelerator is hardened by a dimisoyanate MDI(15) (Methylene-disphenyl-isocyanate)

The PF and PU resins do not contain furfuryl alcohol(10).

The catalysts generally used are either phosphoric acid for furanes(16) (UF/FA) and para toluene sulphonic acid (PTSA)(17) for the phenolic and phenolic furanes. A general guide for copolymer resins is that PTSA is used to catalyse resins with nitrogen contents below 5%, whilst above this level phosphoric acid is employed.

The range of cold curing resins available to foundrymen represents a very efficient type of cold setting process. The main advantages associated with the use of these binders are, the good flowability of the mixed sand, low gas evolution on casting, high hot strengths, excellent breakdown and high tensile strength which enable cores to withstand handling(10)(18).

Against these advantages there are limitations imposed by the physical properties of resins. For instance, the problem of nitrogen pinhole defects exists with certain UF containing resins. Fining flaw problems, can be encountered with PF and PF/FA resins. Owing to the formaldehyde content, unpleasant odours are produced during mixing, leading to unpleasant working conditions if provisions for adequate ventilation is not provided.

3.2.3.3.1.5. Thermo setting resins (the shell process)

The shell process, or the Croning process, consists of mixing sand with powdered phenol formaldehyde (PF) resin of the type known as a novalac(19). A mixture of the PF resin and sand, when blown into a heated core-box, cures by heat to give a rigid shape. However, problems were encountered due to segregation of the resin in the sand mix which gave rise to coating defects(10).

Curing of Novalac resins takes place when reacted with hexamethylene tetramine or hexamine $(\text{CH}_2)_6 \text{N}_4$. The curing takes place at a temperature of 200-230°C. The presence of nitrogen in hexamine could lead to nitrogen/hydrogen pinhole defects in the castings. To eliminate this defect a modified novalac has been produced(5). The process is further improved by using

pre-coated sand containing 2.5% to 4% PF resin. The pre-coating of the sand grains by the resin is carried out by one of two methods; the Warm and the Hot process.

In the Warm process, hexamine is incorporated at the start of the process, together with a wax which acts as a release agent and improves the flowability of the sand(10).

In the Hot process, the mixture is heated to 130°C and then cooled to below the melting point of the resin and the catalyst is introduced in the form of a solution of hexamine in water(10).

In the hot-box process either urea formaldehyde furfuryl alcohol (UF/FA), phenol formaldehyde (PF) or (PF/UF) are used(17). These resins are mixed with solutions of salts usually ammonium chloride, which are stable at ambient temperature, but on heating release acid which reduces the pH of the resin causing a rapid cross linking and thus setting.

The UF resins although cheap and excellent for hot-box production also give rapid breakdown on casting but have a high nitrogen content which limits their unblended use. The furane resins give much faster setting times and higher strengths and low gas evolution(5).

3.2.3.3.2. Inorganic binders

Cement, clays and sodium silicates are classified as inorganic binders. These are the lowest costly binders and some have been used since founding began(20-23).

3.2.3.3.2.1. Sodium silicates

Aqueous sodium silicates have been used as foundry binders for many years in the CO₂ process(19), but more

recently in the cement silicate, fluid sand and ester-silicate processes. The term sodium silicate refers to a three ingredient system; silica, sodium oxide and water giving the $\text{SiO}_2\text{-Na}_2\text{O-H}_2\text{O}$ ternary system(5).

Since the adoption of the carbon dioxide sodium silicate process in the early 1950's the usage of this technique has grown continually with silicate bonded sands being used for both mould and core-making processes(19). On the passage of CO_2 gas through the sand, hardening takes place via two mechanisms; the formation of the silica hydrogen bond and the physical dehydration of the aqueous silicate(10). A characteristic of the hardening process is that in most cases the initial as gassed strength is low requiring care in handling of cores. On storage, the strength levels generally continue to rise owing to further dehydration of any unreacted sodium silicates.

3.3. Mixing

The purpose of mixing is to secure distribution of core mixture constituents to a smooth, lump free consistency. The binder should be finally distributed as a thin film round each sand grain(7).

The mixer units range from batch types such as wheel design mullers, blade mixers and even cement mixers to the continuous mixer units.

Condition of the sand is highly important, free from fine impurities, such as clays, moisture and oily materials(24). Antisegregation devices in storage bins and hoppers are applied to maintain a constant surface area to be coated. These devices prevent fines from reaching the mixers at irregular rates which could have a significant and unexpected effects on the sand mixture properties.

The configuration of the sand grains has also an effect. Angular or irregular shaped grains, require more binder than rounded sand grains. Where sand reclamation is used, angular grains tend to become rounded after several coatings, if the original binder remains on the grain in the form of a fused-on deposit(24).

Mechanical parts of the equipment should be designed so as to prevent excessive scrubbing motion of the sand against itself which could result in removal of any coating. Attrition of the sand mixture is undesirable since it hinders formation of binder on sand grains as well as causing overheating which tends to decrease bench life of the mixed core sand(17).

Mixers are designed to maintain good mechanical performance. Overloading the mixer can cause granular damage or undesired heating which could give rise to evaporation of solvents and consequently, reducing the bench life and tensile strength characteristic of the sand-mix as well as increasing the binder requirements(24).

Mixers of all types should be enclosed to prevent solvent vapour loss as well as objectionable odours.

Sand should be fed into the mixing chamber at a constant rate and temperature(25).

Pumps, when used should be of the variable type with facilities for easy adjustment and recording of volume within fine tolerances(17).

Pumps, valves and plumbing must be compatible with the chemicals they come in contact with. Acid catalysts used with furane and phenolic hot box processes, for example, can be extremely damaging to pumps and valves. The same is true for the peroxides used in epoxy, furane and acrylic/SO₂ processes(25).

3.4. Core-making

In the manufacture of castings often a mould is used to define the outer shape of the castings, whilst the internal configuration is formed by means of a core. Cores are most commonly used as inserts in moulds to form design features which would be difficult or impossible to produce by direct moulding.

3.4.1. Properties required for core-making

It is a prime requirement that both moulds and cores be sufficiently refractory in nature to prevent penetration and erosion by the molten metal⁽¹⁰⁾.

Cores are often almost totally enclosed by molten metal with the core print providing the only means of venting. It follows that the volume, rate of evolution, and chemical nature of any gases generated from the binder are of major consideration if defective castings due to blow holes and pin hole porosity are to be avoided⁽¹⁰⁾. A further requirement is that the binder must degrade at the casting temperature in order to prevent hot tearing and to facilitate removal from the casting at knock-out⁽¹⁾.

The requirement of the sand-binder mix to be rammed or blown into the core-box to produce cores with uniform density implies that the sand mix should be non-sticky and free flowing. Furthermore, in order to ensure that dimensionally accurate castings are produced, the ideal binder system would be such that the curing reaction would be completed prior to stripping from the core-box⁽¹⁰⁾.

The choice of a core-making process involves a consideration of the requirements mentioned, together with the ability to produce dimensionally accurate cores at the optimum rate for the foundry at minimum cost.

3.4.2. Core-making processes

3.4.2.1. The shell process

In its infancy, the shell process was limited to shell mould production. The mixture made was a simple mechanical mixture of sand and powdered resin suitable for dump box operations, Fig 9, but unsuitable for blowing purposes due to the resin segregation that took place in a core blower⁽¹⁹⁾. However, the process presented tremendous possibilities towards complete automation of foundry operations.

In the shell process, sand precoated with a thermo-setting resin, is either blown into an electrically or gas heated core-box usually maintained at 250°C-300°C, or dumped under the influence of gravity onto the pattern plate⁽¹⁰⁾. The former produces a shell of controlled thickness, whereas, in the latter case, the shell thickness is dependent on the pattern temperature and the sand holding time on the pattern.

Since the sand mix is dry it is easily blown into the core-box at relatively low pressure. Cores can be made hollow, thus facilitating the removal of gases generated by core during casting.

Dimensional accuracy of cores is high and excellent breakdown is obtained with all but the low melting point light alloys⁽¹⁰⁾.

Disadvantages of the shell process are; the requirement to heat the core-box to high temperatures, the high cost of metal core-boxes and the high cost of precoated sand(17). Core fumes and operator fatigue due to high temperatures are also inherent disadvantages.

3.4.2.2. The hot-box process

This process, a follow on from the shell process, was possible by the development of sand mixtures based on liquid resin binders, in which curing is accomplished by heating in the presence of a catalyst(5). The fact that hot-box mixtures are wet allows the use of conventional rather than special blowers designed for blowing dry mixtures. As a result of the thermo-setting properties of the resin employed, a hardened cured skin is produced which enables stripping to be carried out in a very short time. Hardening is further continued after stripping hot core to give a uniform curing(10).

The main application of the hot-box process lies in long production runs of similar core designs thus lowering the cost of heating metal core-box. Changing the boxes in production may involve several hours to heat the box to the working temperature. Cores have excellent breakdown properties but also unpleasant fumes associated with the curing process.

2.4.2.3. Cold setting core-making processes

In cold setting processes the sand binder mixture is hardened to a point where the core can be stripped from the box, coated if necessary, and used without the need to heat to the core.

Cold setting processes have revolutionised both mould and core-making processes. They have reduced and in some cases eliminated the need for skilled moulders and core makers(24). The absence of heating permits relatively inexpensive core-boxes and heat related problems such as; expansion, contraction and warpage of boxes are not apparent(17).

Increasing applications of cold setting processes has been at the expense of oil sand binders for the volume production work of small to medium sized cores, and in place of the loam and dry sand cores for larger work(15).

The cold setting processes offer improved dimensional accuracy of castings through consistent accurate core production direct from the core-box. Cores that previously were made in two halves to produce flat surfaces for core drying can be made as one, thus reducing the number of cores required(26).

Improved casting soundness is achieved through higher core rigidity and reduced gas evolution.

Reductions in the core production costs are achieved in terms of labour and production equipment. Cost of manufacture, maintenance and operating of core driers and core sizing machines are eliminated. Floor previously occupied for these operations are thus recovered. Skilled labour can usually be replaced with semi-skilled or unskilled labour.

Main advantages of the cold setting processes lie in the form of energy conservation and other ancillary benefits(24).

3.4.2.3.1. Sodium silicate processes

Experiments with sodium silicate as a binder for sand were carried out in 1898⁽²⁷⁾ in England.

Sodium silicate processes are widely used in many types of foundries, to produce castings from a few grammes in weight to many tonnes, across the whole range of metal alloy compositions⁽¹⁵⁾. Three main types of sodium silicate processes differ mainly in the method by which the sand-binder mix is blended⁽¹⁷⁾;

- Silicate CO₂
- Powder hardened silicate
- Ester-silicate

3.4.2.3.1.1. Silicate CO₂ process

The silicate CO₂ process began to be adopted on a commercial scale in the 1950s, and today the process has achieved widespread use⁽¹⁹⁾.

One of the problems of the CO₂ process that quickly became apparent in the early days, and is still a problem today, is that of poor core breakdown at the shake-out.

The development of the CO₂ process in the 1970s, made a huge impact on the foundry industry⁽²⁶⁾. It consisted of preparing a slightly damp mixture of sodium silicate and sand, which was hand rammed into wooden core-boxes and hardened by the injection of CO₂ gas. The gas, from bottles is injected into the core-box by means of tubes or masking plates. Fig 10 illustrates examples of systems used. The core is hardened in seconds and this makes the process commercially competitive apart from the limitation of poor breakdown⁽²⁶⁾. The attraction offered

in the environmental problems are unmatched by any organic process(28).

The process uses many commercial sands. The main sand requirement is that it should have a low clay content which reduces the ultimate core strength(27).

The sand which contains 3%-6% sodium silicate can be mixed in most types of mixers(10). Mixed sand can be either rammed or blown into the core-boxes. The hardening reactions of carbon dioxide with water present in the sodium silicate solution, produces sodium carbonate and silica gel. The amount of CO₂ gas required to cure a core is affected by the positions and number of vents in the core-box, sand and CO₂ temperatures, gas pressure and volume, and the method used to introduce the gas into the core. The influence of the main process variables have been examined by Atterton(29), Haley(30), Thompson(31), Taylor(32) and Lange(33).

The advantages of the process are(28);

- high dimensional accuracy of the hardened cores
- adaption of the process to suit small quantity production methods, and high volume techniques
- relatively low cost
- freedom from unpleasant fumes either in mixing or casting.

The disadvantages are the comparatively low tensile strengths of the as-gassed cores and the poor breakdown(7).

3.4.2.3.1.2. Powder hardened silicate processes

These processes involve the addition of powder hardeners which, when added to the sand mix, react with

the sodium silicate binder to form a rigid bond. Compared to gaseous and liquid hardeners the powders, finely ground to below 200 BSS mesh, are difficult to mix, and setting is generally slower(17).

The powders used include ferro-silicon, dicalcium silicate and various types of cement.

The ferro-silicon is used in the Nishiyama process(34). This hardening reaction produces hydrogen gas which may give rise to explosion hazards(35).

Dicalcium silicate, as used in the fluid sand process, is a major constituent of a number of metallurgical slags as well as certain types of portland cement. It reacts with sodium silicate by removal of water to produce the silicate glass. The initial reaction rate is slow(15).

All of these latter processes have found limited applications and some have been superseded by the ester-silicate system.

3.4.2.3.1.3. Ester-silicate process

The hardeners used in this process are organic liquids, esters, (an ester is the generic name for the product of a reaction between an organic acid and a polyhydric alcohol(36)). The hardening is achieved by a two part chemical reaction between sodium silicate and organic esters, the most significant reaction being a decomposition of the esters by the alkali to form alcohol and an acid which produces gelling of the sodium silicate. Consistent through hardening is achieved by avoiding over or under gassing of the sand(5).

This process is used for the manufacture of small and heavy castings over a wide range of alloy compositions. The process is also used for moulding as a facing material subsequently to be backed by green sand.

Olivine, chromite or zircon sands are widely used with this process in the steel industry. In some cases it has been found possible to replace these sands with silica sands, since it is possible to obtain glass hard and smooth surfaces on the cores and moulds(15).

Many organic esters such as, monocetin, diacetin, triactin and diethylene glycol diacetate can be used to gel sodium silicate. The various blends produce a range of setting times(17).

The cores produced using this process are free from finning defects sometimes encountered with resins and there are no unpleasant fumes associated with the process. Problems due to nitrogen pinholing are also avoided(37).

3.4.2.3.2. Cold setting phenolic furane process

The many organic synthetic resins, such as, UF/FA, PF/FA, FA/F, and PF are hardened through polymerisation at room temperature under the influence of acid catalysts, such as, para-toluene sulphonic (PTSA), phosphoric and sulphuric acids. By suitable choice of resin and catalyst stripping times from three minutes to three hours can be achieved(15).

Sands of low acid demand are used, the grain size and shape largely determining the binder level for required strengths. Chromite and zircon facing sands are used in some steel applications(17).

This process can be used to manufacture moulds and cores for a wide variety of jobbing castings from less than half a kilo-gram to 50 tonne in most grades of ferrous and non-ferrous alloys(15). The process is sometimes used for boxless moulds in competition with green sand where it is often competitive when capital cost is taken into account.

The most common method for production using this process is the pattern flow system, in which the core-boxes are brought to a continuous mixer by roller track and the mixed sand is discharged into the box. Since the sand is quite flowable either vibration or hand-ramming is sufficient to compact the sand(10).

An alternative system used, to the pattern flow method, is the multi-stage carousel type machine.

If coatings are required, water based types are to be preferred. Spirit based coating can be used provided great care is taken to ensure that excess solvent is not allowed to cause softening of the resin bond resulting in metal penetration and burn on(10).

3.4.2.3.3. The-SO₂ process

The different types of SO₂ process involve the mixing of the sand with organic resins such as phenolic-furane and an oxidising agent such as methyl ethyl ketone peroxide (MEKP). The sand either rammed or blown into core-boxes sets very rapidly as SO₂ gas is passed through it. The SO₂ reacts with the peroxide to form SO₃, which dissolves in the water present in the binder to form sulphuric acid (H₂ SO₄) inducing rapid exothermic polymerisation of the resin.

The system although still used in the U.S.(38) and some parts of Europe(39), has not been extensively used in the industry, primarily because of two problems, firstly environmental problems of SO₂ gas and secondly resin build-up film on the core-boxes which influences dimensional accuracy and stripping of the cores. The removal of this film has also been difficult and costly.

Recent research resulted in the development of new techniques that considerably decreased the film build up, and also enabled the cleaning of the film to be carried out extremely rapidly and cheaply(40).

3.4.2.3.3.1. Furan-SO₂ process

This was the original SO₂ cold-box process(38), in which a chemically bonded system uses resins employed in the self setting phenol-furan processes(17). Resin addition depends upon the sand surface and grain distribution. As little resin as 0.7% of the weight of the sand can be used for the production of high quality cores.

Core blowers/shooters can be used to blow or shoot the sand-binder mixture into the core-boxes. The boxes can be made in a wide variety of materials such as, epoxy resin, aluminium and cast iron.

Gassing is carried out by liquid SO₂ carried by pressurised nitrogen via a vaporiser. All pipes including solenoid valves conveying SO₂ are in stainless steel. Gassing times can be as little as 0.5 sec to as much as 5 sec, depending on the size of the cores. Purging with compressed air is carried out after gassing to remove the residual SO₂ gas. All the fumes are conveyed to a

scrubbing tower containing a 10% solution of caustic soda in water.

Several advantages are offered by the process(38,39,41). The core strength immediately after gassing and the hot strength, are high. This enables the casting of water jackets in engine block heads, or other intricate cored work, with good dimensional accuracy(42). The excellent surface finish allows castings. Superior breakdown of the cores at the shake-out is another advantage. The bench life of the furan-SO₂ sand-binder mix and of cores is also good. Mixed sands can be kept in the machine hoppers up to three or four hours, and still keep a constant core making cycle time(39). The colour changes of the cores could be used as a process control.

3.4.2.3.3.2. The epoxy-SO₂ process

The epoxy-SO₂ process was developed in order to bring about improvements over the already existing furan-SO₂ process(38).

The process consists of a two part binder system. The first part is a combination of epoxy resin and oxidiser. The second part is epoxy resin with synthetic modifiers such as acrylic. Total binder level is based on the weight of the sand and is generally in the range of 0.6%-1.4% depending on the type of sand and physical strengths required of the core(38).

The gassing operation is the same as that employed in furan-SO₂ process with the advantage of roughly halving the gassing and purging cycle times.

The following advantages have been reported(38,39,42); elimination of sand setting in

hoppers and less wasted sand between core-box change have increased up-time and productivity, a major reduction in maintenance time spent to clean sand mixers, hoppers, sand magazines and exhaust valve screens, and delivery belt, consistent flowability and blowability throughout the shift, significant reductions in core scrap at the machine, normally caused by sand in which the binder has degraded with time, absence of nitrogen, water, formaldehyde or phenol in epoxy results in fewer blow defects, higher core strength and hardness are developed at resin levels lower than that of furan-SO₂, thermo-plasticity properties lead to the reduction of veining and hot tearing of castings combined with excellent shake-out.

3.4.2.3.3.3. The FRC process

This process uses an organic binder composed of vinyl unsaturated urethane oligomers which contain reactive carbon-carbon double bonds, an organic hydroperoxide that initiates the free radical polymerisation, silane adhesion promoters which provide cores with excellent shelf life, and a diluted activator gas to induce curing(43).

The curing is induced through the application of nitrogen diluted sulphur dioxide gas with a typical concentration of 1%-10% sulphur dioxide followed by a purge of nitrogen or dry air to flush excess activator gas from the cores(44).

The process has been successfully applied to a wide variety of sands demonstrating wide versatility.

During the casting process, an outstanding feature of the FRC binders is the reduction or the elimination of veins in ferrous castings, while excellent dimensional accuracy during the casting process is maintained(44). The improved dimensional accuracy associated with the FRC binders were apparent early in the development for non-ferrous applications. The original binders were designed to maintain dimensional accuracy in permanent mould applications at 316°C (600°F). The reduction in deformation at this temperature has also been beneficial when cores for ferrous castings are dried after application of core coatings(41).

3.4.2.3.4. The cold-box process (Isocure)

This process is also known as the amine-cured phenolic-isocyanate system(45).

It is a rapid curing cold resin system, which is particularly suitable for high volume production techniques, but can also be adapted for small volume work(46). As the binder is activated by a toxic amine vapour, it is environmentally desirable to produce cores in well ventilated areas of machines with extraction.

The binder system in this process is comprised of two parts. Part one is a phenolic formaldehyde polymer resin blended with suitable solvents, and part two is an isocyanate(47). The two constituent parts are mixed together usually in a continuous mixer and dispensed directly into core blowing/shooting machines. The bench life of the mixture is normally 3-4 hours. The hardening process is carried out in the core-box by the passage of a catalyst gas usually either triethylamine (T.E.A.) or

dimethylethylamine (D.M.E.A.) with an inert carrier gas such as carbon dioxide⁽¹⁷⁾. These catalysts produce an unpleasant smell and can attack the mucous membranes⁽¹⁰⁾, consequently adequate ventilation has to be provided. Purging of the core while still in the box is the normal procedure, it serves to force the amine through the core and drive off any excess unused amine from the core before removal from the core-box. Vapour entry points and core-box vent positions are all important for quick and efficient curing⁽⁴⁵⁾. The success of the curing also depends on the sand-binder mix being free of moisture. Contamination of the mixed sand by moisture must be avoided. The methylene diphenyl isocyanate (M.D.I.) present in the two part resin system has an affinity for moisture. It has been reported that one part moisture in the sand can result in the destruction of twelve parts of M.D.I, thus causing a considerable reduction in the tensile strength of the cores produced⁽¹⁵⁾. Moisture pick up from the atmosphere can also result in some deterioration of the cores.

Metal core-boxes, in particular cast iron are used. Amine vapour does not disperse through cores as easily as CO₂ will disperse through a silicate bonded core⁽¹⁵⁾, which makes positioning of the core-box vents critical. Closely fitted core-box joint faces are also important, since amine vapour escapes through poorly fitting box face joints resulting in excessive amine consumption or partially cured cores.

High degrees of casting accuracy and definition can be obtained with this process. Casting finish is good and

in many cases coatings are not required(47). However, if coatings are required, they can be satisfactorily chosen from newly developed range of cold-box coatings which do not weaken the resin bond(10).

The rate of gas evolution during casting is low and as a result internal venting can be dispensed with(47).

In general breakdown is good, although with light alloys cast at lower temperatures breakdown is inferior to cores produced by such processes as SO₂ or hot-box.

Amine fumes extracted from the core making areas must be cleaned before being released into the atmosphere. There are a few systems available for this purpose such as; impingement scrubbers, acid scrubbers, phosphoric acid bubbler and ion exchange. Another, most recent, process involves the use of a chemical scrubber to recycle amines for the cold-box process(48), Fig 11.

3.4.2.3.5. The fascold system

This process, a development of the cold setting resin processes, is an acid hardened furane system of ultra high speed formulation(26). The process makes use of an organic acid for phenol furane resin and stronger inorganic acids for ureafurane resins(15). The resin and catalyst are separately pre-mixed with sand, and then blended in a final mixer for discharge into the core-boxes. Cores may be stripped in 30 to 40 seconds and may be used after 30 to 120 minutes depending on size(26).

The fascold process offers the following advantages(17); no heat or gassing is required for curing, the bonded sand has very good breakdown and is reclaimable. The process equipment is easily controlled,

giving good quality cores. A relatively low degree of skill and training is required for operators. Furane resin binders are used and the resulting castings have a good dimensional accuracy and finish.

These advantages are offset by discarded excess of sand-mix because of its short bench life. The process can only be used in conjunction with special high speed mixing equipment and/or combined mixing/blowing machines. The temperature of the sand must be kept between 20°-25°C for maximum throughput and strength with minimum binder requirements. Colder sands require considerably more resin and catalyst(15).

3.4.2.3.6. The Betaset process

This process employs as its curing agent the vapour of a volatile ester to cure a specially formulated phenolic resin. The chemistry of the binder is based on an alkali-catalysed phenolic resole. The binder being essentially free from sulphur and nitrogen and low in carbon, can be mixed with a wide variety of sands using a wide variety of sand mixing equipment. The mixed sand has a bench life of up to four hours, and can be blown, shot or manually filled into the core-boxes by conventional means(49).

The mixture of sand and binder is rapidly cured by passage of the vapour of the volatile ester methyl formate. The reaction, described in detail by Lemon(50), consists of the vapour-phase methyl formate ester reacting with the phenolic resin to produce an unstable intermediate complex which readily decomposes to form a polymerised resin, an alkali metal salt and a small

quantity of alcohol (Fig 12). The vapour consumption levels, expected with the correct vent configurations and core-box sealing practices, are normally of the order of 30% by weight of hardener on resin⁽⁴⁹⁾. The properties of Beta-set resin and hardener are illustrated in Fig 13.

The gassing portion of the core-making cycle is normally longer than that of other processes such as amine or SO₂, however, the total gassing interval including purge air is normally similar or shorter. This is due to the elimination of the traditional air purge, which is replaced by a short interval of flushing air to ensure that all generated vapour enters the core-box and does not condense in the vapour delivery lines to the gassing head. Shorter gassing cycles can be achieved especially with heavy cores⁽⁵¹⁾.

The system offers excellent surface castings. The high temperature characteristics of the binder give rise to a significant reduction or elimination of finning or veining defects⁽⁵²⁾.

The environmental advantages are; the resin has little odour and does not exhibit any unpleasant characteristics during sand mixing. The vapour hardener also emits an odour which is neither strong nor cloying and, therefore, all gassing equipment is extracted to the atmosphere⁽⁵³⁾.

3.5. Core coating

Core coatings or dressings are sometimes applied to surfaces of cores to improve the surface finish of castings through reduction of metal penetration resulting in the prevention of the occurrence of such defects as "burn on"(2), and in reduction of cleaning costs.

Sand cores consist of porous masses into which the liquid alloy can penetrate during pouring and solidification. If this penetration is superficial, the surface produced will be uneven and rough, but if it is severe, a metal-sand crust adheres firmly to the surface, and this is known as metal penetration. This can be prevented by application of a coating which seals the pores on the cores(55).

Also the sand may adhere to the surface of castings due to melting or sintering. In this case a refractory coating may prevent the defect(56).

A core surface which is susceptible to erosion can be protected with a coating which is more erosion-resistant than the surface of the core.

Coatings can also be used to reduce or increase gas formation during casting in order to create negative or positive mould gas pressures respectively(54).

All coatings have four basic constituents, a solid filler material, a bonding agent; a suspension agent, and a liquid carrier.

Solid fillers are refractory materials which protect the surface of a core. Examples of filler include; carbon based blacking, graphite, silica, zircon, mica, talc, calcined magnesite, aluminium silicates and chamotte(56).

The coating bonding agent bonds the fine particles of solid filler together on drying out, and helps the coating to stick to the core surface. Dextrins, sulphite lyes, linseed oil, alcohol soluble synthetic resins, bentonites, clays, phosphates and sodium silicates are used(54).

The suspension agent prevents, the solid filler material from setting out, and severe penetration of the carrier liquids into the core material(3). Bentonites, clays, celluloses and alginates are some of the suspension agents used.

The carrier enables the coating to be applied across the core surface. Carriers can be either water, or spirit, the choice of which, depends upon the core-making material binder systems. Water, isopropanol and trichloroethane are some of the mostly used carriers(57).

The common application processes are brushing, dipping, swabbing and spraying. These methods differ greatly from one another in the techniques required. The behaviour of the coating during processing must thus be suited to the application method and the special properties of the process must be taken into account(54).

3.6. Core-boxes

3.6.1. Introduction

The most common method of forming cores is to use a core-box, which contains a cavity in the shape of the desired core. These boxes can be simple wooden structures or precision metal assemblies, depending upon the core-making processes employed(7).

The problem of design and constructing core-boxes is as old as the foundry industry itself. This area of the pattern-maker's skill often needs an extension of knowledge beyond the average needs of pattern equipment design. Understanding laws of hydraulics, thermal response of materials, the behaviour of gaseous fluids when flowing under pressure and many other fundamental phenomenon are required to generate a scientific understanding of the whole aspect of designing core-box equipment, and dynamics of the core-box filling with core sand mixture for high speed, high quality core production(58).

3.6.2. Core-box design

The simplest core-box design is the open sided type producing flat walled cores or half cores which can be turned out directly on to a flat plate. These are especially useful for low strength cores. Other developments in design include; ring or frame type, two piece horizontally parted, vertically split blind bottom, vertically parted pin core-boxes and multiple piece boxes, Fig 14. Where small cores are required in large quantities, multi core cavity core-boxes can be used

enabling a number of cores to be rammed or blown simultaneously reducing production times(7).

Core-box design plays an important part in the production of suitable cores and life expectancy of the tooling involved. The following factors have to be considered when designing a core-box(59-60):-

Dimension of core

Number of cores to be produced

Type of materials being used (sand, binders, etc)

Complexity of shape, undercuts requiring loose sections of core-box

Core-box material (wood, resin, metal, etc.)

The core-making process. If the core process requires a toxic gassing operation extraction provisions are necessary

Type of core-blowing/shooting machine being used

Whether the blowing/shooting technique is horizontal or vertical

Ancillary equipment such as blow plates, gassing and ejector plate systems may be required

Air or hydraulic cylinders to actuate the loose pieces of the box when on high production

Venting system of the core-box

Overall production costs.

3.6.3. Core-box materials

Many materials are suitable for the production of core-boxes; wood, resin, aluminium alloys, cast iron and steel. These materials may be used both individually or in combination to produce core-boxes. The choice of the material depends mainly upon the core-making process,

volumes and technique, for which the box is to be used(61). As an example, all conventional materials can be used in the manufacture of core-boxes employed in the CO₂-silicate process. The choice of core-box material here is only dependent on the core-making method, since the core-making materials used do not react with the core-box materials. For hand rammed low volume cores painted wooden core-boxes could be sufficient, however, if the cores are to be blown/shot, for high production, then a more wear resistant material such as cast iron is used(62). In some processes, such as the hot-box process, because of the high temperatures present for the reaction of the resin coated sand, cast iron or steel are required. In other processes, such as the cold-box processes, epoxies, aluminium and even epoxy lined metal core-boxes can be used(60). Where dimensional accuracy and durability is important, cast iron or steel is selected.

3.6.4. Core- box rigging for production

The objective of core-box rigging is to design production core-boxes to obtain dense cores at a minimum material cost and maximum production rate. Box rigging designs lay the ground-work for high quality and low cost castings. For the pattern shop, it can be the starting point for higher quality cores and higher productivity and quality of castings. Core-box rigging is especially important where solid cores are to be produced by blowing/shooting sand into core-boxes(59).

Many of the sand input and venting principles laboriously learned over the years in the hot-box and

shell processes do not apply to the cold-box. In general, the hot-box technique of shooting sand into the box with small tubes and high blow pressures is not successful in cold-box. In blowing highly fluid cold-box sand the resin is stripped off sand grains onto the core-box surface as it bounces around creating resin 'wipe-off' which necessitates down-time to clean tooling. Also the minimum venting which works for shell and hot-box processes may not be enough to permit either high compaction or fast curing in cold-box(59).

Understanding the basic parameters of core-box rigging ie., sand entry, air entry, air exhaust and input and exhaust piping, together with guide-lines developed during many years of foundry experience and observations will greatly simplify the creation of good tooling(63).

3.6.5. Cleaning core-boxes

The core-box cleaning is a necessary task of the pattern shop to ensure smooth production of quality cores. The cleaning process can be harmful to the tooling if it is not carried out correctly. "Hand cleaning" of the core-boxes is probably the safest means of cleaning especially if it is done by experienced people. Hand tools used in cleaning the boxes include steel wool (wire wool), scrapers, vent knives, wire brushes, fine emery paper and liquid cleaners(61).

Blasting of the boxes with abrasive materials, ranging from crushed nuts to sands, is used in practice. Sandblasting the boxes should be avoided wherever possible, since this can result in the box surface wear.

Other cleaning processes involve the immersion of core-boxes in baths filled with cleaning chemicals.

3.6.6. The core-box repairs

Repair and change is an ongoing requirement of the pattern shop. Repair work to wooden core-boxes can be accomplished with a wide variety of plastic products available today. The usual practice, however, is to use new wood inserts that are adhered to a clean surface on the existing equipment(61).

A popular way to change and repair plastic patterns is to make a plastic duplication of the affected area and work the change or repair in reverse on the duplication. The area on the lay-up is then completely removed. The duplication is semi-permanently attached to the area and a new surface coat and glass cloth lay-up is applied from the reverse side of the existing lay-up. When the patch has hardened and cooled, the duplication is removed and the surface of the existing lay-up and repair is lightly sanded.

One way to avoid repairs in tooling is to use urethane inserts for high use and to avoid abuse. A master mould for the expendable insert is maintained to cast new inserts when required. In this way an ongoing repair and replacement feature is, therefore, figured into the original building of the tooling(61).

3.7. Core-making techniques

3.7.1. Core blowing/shooting

3.7.1.1. Introduction

In 1903 Hewlett⁽¹⁾, and in 1910 Murphy⁽⁶⁴⁾ pioneered the core blowing method of core making. Since then various types of core blowers and shooters have been developed. A coreblower/shooter, when reduced to its most basic form, is a machine which simultaneously fills a core-box with sand and compacts it, using compressed air as a transfer and compaction medium. The rest of the functions of a core blower/shooter are for mechanical handling of core-boxes and cores, sand delivery and metering, process timing, and subsequent control. Some machines act as gassing stations.

3.7.1.2. Core shooting

The sand is contained within a perforated or slotted cylinder which at the top is sealed from the atmosphere and the sand hopper by a slide gate or similar means. The bottom leads to the core-box via shooting holes in the shooting head. An airtight chamber, connected to an air reservoir by the shoot valve, surrounds the perforated or slotted cylinder, Fig 15.

Opening the shoot valve results in an increase in air pressure in the chamber surrounding the sand cylinder. This in turn extrudes the sand from the sand cylinder with little air entrainment. The air reservoir volume is fixed so the shooting action takes place under a reducing air pressure.

Sand is replenished by opening the slide gate to allow sand to fall into the sand cylinder⁽⁶⁰⁾.

3.7.1.3. Core blowing

The sand is contained in a sand chamber normally called the blowing head or sand magazine. The base of this magazine is formed by the blow plate which has holes to allow the passage of sand to the core-box. At the top of the blowing head is the blow valve which is connected to the air main, generally via an air receiver situated close to the blow valve, Fig 16.

On opening the blow valve an increase in pressure throughout the sand magazine occurs which forces the sand through the blow-holes into the core-box. The air in the sand carries the sand until it reaches the core-box or the sand already in the core-box when the sand stops expending its kinetic energy in compacting the sand below. The air is permitted to pass on out of the core-box through vents in the box⁽⁶⁰⁾.

Sand is replenished into the blow head by moving the blow head to a secondary filling position.

3.7.1.4. Comparison between core-blowing and core-shooting

Several authors⁽⁶⁰⁾⁽⁶⁴⁻⁷¹⁾ on core blowing/shooting and a working knowledge of blowing and shooting as well as experience of users and producers have led to the following observations.

1. Maintenance and attention are needed more with core shooters in the area of the sand cylinder than with core blowers. Variations in the size of the slots or perforations can have a significant effect on the ability of the core shooter to make consistent cores. If the bottom half of the sand cylinder is

effectively blanked off, the air will enter the sand through the upper half and the sand flows in a funnel shape, leaving a shell of sand around the lower walls of the sand cylinder. If the top half of the sand cylinder is effectively blocked the air will enter through the lower half of the sand cylinder which will give air entrainment and poor sand movement. To maintain consistent core quality the slots or perforations in the sand cylinder must be kept cleaned at all times. A core blower does not use a sand cylinder and, consequently, requires less attention and maintenance to the blowing head or sand magazine.

2. An outer sleeve of a heavy duty cloth is recommended to be used around the sand cylinder, if a fine sand is to be shot. This is to prevent the carry-back of fine sand through the slots or perforations to the exhaust which can damage the exhaust valve. Core blowers do not suffer from this problem because the air exhaust takes place over a larger area of sand giving lower sand velocity, and the exhaust valve is generally above the sand surface in the blow head.
3. A core blower is said to be able to blow a core up to 75% of the volume of the sand contained in the blowing head and at constant air pressure. A core shooter generally has a shooting head below the sand cylinder in order to span the shooting centres of the core-box. However, the size of core which can be shot is related to the size of the sand cylinder. The minimum weight of core which can be produced is

about 10% of the sand cylinder volume. If a small percentage of sand is used each time the sand in the cylinder can impact, and if a "wet mix" is used, the binder can tend to smear and the sand can form a dense mass which will not flow.

4. The use of a fixed volume of air in a core shooter can mean a lower air consumption than a core blower.
5. Sand abrasion occurs in core blowers and core shooters alike, resulting in core-box wear. This is said to be lower when using a core shooter, thus enabling the possible use of suitably strong wooden core-boxes on a core shooter. The correct design of core-boxes and the blowing/shooting holes plus venting efficiency play a very important part in reducing box wear.

3.7.1.5. Blow-plates and blow holes

A blow-plate is a plate usually of cast iron and about 25mm thick, shaped to follow the outside contour of the sand reservoir⁽⁶⁴⁾. The purpose of the single blow-plate is to seal the bottom of the sand magazine and to direct the sand into the core-box through the blow holes in the plate. The double blow-plate, in Fig 17, serves the same purpose as the single blow-plate and provides additional venting, thereby reducing the number of core-box vents to a minimum⁽⁶⁴⁾. The universal blowing plate is widely used in small and jobbing foundries, where it can replace a large number of regular blow-plates. The blow tubes and vents are interchangeable. Thus by merely moving the blow tubes to the positions needed, the universal plate can be used with many different core-

boxes. The holes in the plate, which do not require blow tubes, are filled with vents.

An important feature in the construction of core blowing equipment is the size and placing of the blow holes. These are the holes drilled through the blow-plate to provide passage for sand from the reservoir to the core-box cavity. There are several schools of thought on deciding the size, number, and positioning of the blow holes. Some authors⁽⁶⁶⁾ claim that many small holes produce better results than a few large ones. Others claim that the holes should be as large as possible without dumping the sand. Those favouring the small holes⁽⁶⁶⁾ believe the sand is sprayed at a greater velocity, getting into difficult corners and packing cores much better.

It is not necessary to use round blow holes⁽⁶⁴⁾. Slotted holes have been used with success in many applications. Fig 18 illustrates the cross-sections of various blow tubes. The use of tubes is important because they can be replaced when worn out. Without tubes, the hole in the blow-plate would be worn by sand blasting of each blow and the plate would have to be replaced.

Some bushings are lined with rubber or plastic or equipped with an adaptable sleeve. Others use a simple short piece of steel or brass tubing. When properly installed they also serve the purpose of providing an air tight connection between the blow plate and the core-box. The bushing should break the sand cleanly and evenly at the core line to save extra cleaning labour. This is done by having the bottom of the blow tube tapered off to the

core line by means of a rubber or steel insert, Fig 18. Another method is the use of a straight tube with the bottom section tapered. The threads then help to break the sand cleanly⁽⁶⁴⁾.

3.7.1.6. Core-box venting

One of the major factors in the core-blowing process is the determination of the size, the number and the positioning of core-box vents. The purpose of the core-box vents is to trap the sand grains in the core-box cavity and at the same time permit the air to flow out of the box. The venting of the box is accomplished in various ways, from the natural leakage at the parting line(s) to ingenious and specially manufactured devices for exhausting the air from the box.

In the past years, designers of core-blowing machines have recommended many different ratios of vent area to blow hole area varying from 1:1 to 6:1. At the present time manufacturers of different core-making equipment offer their own rules and guide-lines mostly appropriate to their own particular equipments.

The type of core-box vents available vary from slotted vents to very fine mesh screen vents, Figure 19. These all have advantages and disadvantages and are suited to different applications. For example, a disadvantage in the use of screen vents is the tendency of the screen to blow down and leave a slight lump on the core. The slotted vents, however, hold their shape better and last longer but are more difficult to keep clean⁽⁶⁴⁾.

3.7.1.7. Previous research on the flow mechanism in core-blowing/shooting

Attempts to blow sand into core-boxes were initiated in 1911. In 1930 several companies involved in the manufacturing of core-blowers began experimental work. A wide diversity of opinion prevailed on the subject, but all agreed that high air pressure of around 8 bars was necessary. The blow holes used were small and the venting problem was scarcely considered(72).

The first experiment was on blowing pin cores, open at both ends in which the air could escape readily. Later, other small cores included, L, T and other shapes which were blown satisfactorily. Subsequently, an old metal core-box was used and the cores proved satisfactory. As the edges of the box used were worn, the joints were loose and the air could escape easily. This suggested the idea to cut slots or file vents, in the sides of the boxes(72).

Since these early developments much has been published on the core-blowing/shooting processes, most of which consists of recommendations and suggestions on different factors involved, observed by foundrymen on their working experiences.

Some of the early research on the subject was carried out by Lincoln and Swink(65,66)(73), Pridmore(72), Degley(67) and Dwyer(74). The following points were made by these authors:-

1. The core must be arranged so that the parting surface will permit the core to be removed from the box after it is blown.

2. It is always desirable to direct the blown stream downward toward the larger sand sections, rather than depend upon the venting arrangement to pull the sand up into pockets.
3. Wherever possible, the blow stream should be introduced through the print sections of the core.
4. It is desirable to utilise to the greatest possible extent the natural venting possibilities of the box at the parting surface or on open print surfaces, thus keeping the necessity for additional venting to a minimum.
5. Where two or more cores are placed in one gang box they should be arranged so that each individual core has its own free venting system to atmosphere thus discouraging any tendency for the blow stream to travel from one core-box cavity to another.
6. In order to maintain a sufficient velocity of the blow stream, blow holes should not be too large and the average sizes used were usually from 5 to 20mm in diameter.

In 1950, Grade⁽⁷⁵⁾ carried out experiments on the influence of blow hole diameter, vent area and air pressure in core-blowing. The cores produced in the investigations reported were bars 25 x 25 x 20mm. They were blown in the horizontal position on a cartridge type core-blower. The sand was admitted through a single orifice located over the centre of the core-boxes.

Two core-boxes were used. The first, was a conventional metal core-box vented by commercial screen vents located in the two 25 x 25mm slides at the ends of

the box. The total vent area was approximately 155mm². The second, was almost entirely of wire screen. It consisted of an internal box made of 200-mesh wire cloth supported by an external box of 24-mesh nickel screen.

It can be seen, from the results presented in Fig 20, that a blow hole diameter of around 19mm (3/4 Inch) yielded the heaviest cores with both venting arrangements. For blowhole diameters smaller than the above, the normally vented core-box yielded heavier cores than the box with the maximum amount of venting.

Within the range of air pressures used, increasing the pressure increased the core weight but the advantage obtained with successive increases in pressure became progressively less.

The data reported neither confirm nor contradict Lincoln's⁽⁶⁶⁾ contention that a small blow hole will increase the "throwing power" of the sand. The data, however, suggest an alternative method for accomplishing the desired result, namely, employing the optimum blow hole size and using vents to direct the sand to the more inaccessible parts of the core.

The basic principle of core-blowing is to floatate sand into the core-box by using the medium of compressed air. It was recommended by Clark⁽⁶⁴⁾ in 1956, that the velocity of the air must be kept high to obtain the desired velocity of the sand particles, thus insuring their deposit in the remote corners of the core-box. It follows, therefore, that the air pressure within the box must be relieved by adequate venting. The example

illustrated in Fig 21, was claimed to show the air pressure in a well vented core-box.

Clarke⁽⁶⁴⁾ further suggested that the air must be introduced as quickly as possible and through a sufficiently large air inlet (60-100mm) to minimise the effects of channelling in the sand magazine. Fig 22 illustrates the channelling effect. This could be prevented by agitation within the sand magazine as illustrated in Fig 23.

In the early 1960s, Lesnichenko⁽⁶⁸⁾ also described the channelling effect with core-blowers, in which the air entered from the top of the sand magazine. These channels were eliminated when experimenting with core-blowers, in which the air was supplied to the lower part of the reservoir through a gauze covered shell, and as the sand was blown out it was loosened by a rotating rake.

Lesnichenko⁽⁶⁸⁾, postulated that the performance of a core blower or shooter was largely determined by the performance of the reservoir. Hence he investigated the pressure changes in the reservoirs of both core-blowers and shooters. Measurements of pressure and time were taken using an oscilloscope and appropriate graphs produced, Fig 24.

The graph of pressure changes in a core-blower reservoir, Fig 24a, drawn from an experimental oscillograph, can be divided into four characteristic sections⁽⁶⁸⁾.

The curvature of the first section 0-I depends on the initial air pressure in the receiver and its volume,

the cross-sectional area of the air line from the receiver to the valve, the valve working cross-section, the volume of the air-blower reservoir and the total cross-sectional area of the inlet orifices.

The length of the curve in section I-II depends mainly on the same factors as the length of the first section, plus the volume and ventilation of the core-box. The start of the third section is defined by the point of maximum pressure. In this section the pressure is steady and the curve is almost parallel to the horizontal axis. The fourth section shows the rate of pressure drop in the reservoir after the inlet valve has been closed.

It was observed that the start of the flow of the sand into the box coincided almost exactly with the start of pressure rise in the reservoir, the delay did not exceed 0.04 secs.

Since at this instance, the pressure inside the reservoir does not exceed 2.5 bars, the flow rate of the sand-air stream is small. On practical grounds the sections O-I should be kept to a minimum. This can be achieved by reducing the dynamic resistance in the path from receiver to reservoir by fitting quick-action valves and selecting optimum reservoir dimensions. From the duration of section I-II, it is possible to estimate the kinetics of the core-box filling process, but it is not always possible to determine accurately the instance at which the core-box is filled⁽⁶⁸⁾. It cannot be maintained that the end of filling is invariably defined by point II on the curve. In order to find what this moment is, it is necessary to supplement recordings of reservoir pressure

by recording the pressure in the top of the box, where maximum ventilation is provided⁽⁶⁸⁾. The pressure curve in the core-box will indicate the end of a filling process. At the instance the core-box becomes full and the vents in the plate are blocked with sand, the air pressure at the top of the box increases, and as the oscillograph indicates the pressure drop suddenly becomes smaller. The time required to fill the box depends on the rate of pressure increase in it, and this is determined by the number and position of the vents⁽⁶⁸⁾.

The reservoir pressure graph for core shooters, Fig 24b, can be divided into three characteristic sections. The first section is a steep, almost vertical, pressure rise, the second a steady pressure section and the third a rapid pressure drop. In contrast to the reservoir pressure graph for core-blowers, there is no slow pressure rise section and the duration of section O-I does not exceed 0.04 secs. It can be assumed that sand starts to flow when the air pressure in the reservoir is at a maximum⁽⁶⁸⁾. The instantaneous pressure rise in the receiver amounts to a minor explosion. The effect is intensified by the fact that the conical reservoir floor, blocked with sand, constitutes a considerable dynamic resistance, particularly in the first 0.04-0.08 secs. This is confirmed by the fact that sand starts to flow 0.04-0.08 secs after the injection valve is opened. The start of the steady section indicates the duration of propagation of the minor explosion wave. It can be supposed that at the start of section I-II the air fulfils the same functions as the compressed gases from

the cartridge in a rifle barrel. From the pressure curves for the air in the receiver, that at top of the reservoir, and that in the blow hole, it can be seen that the pressure in the blow hole does not increase until sand is flowing out through it. The duration at this stage is indicated by the steady section on the curve and it does not exceed 0.12-0.16 secs⁽⁶⁸⁾.

Section II-III Fig 24b, covers the period of air pressure drop in the reservoir after the injection valve has been closed and the exhaust valve opened. These two valves operate simultaneously, the pressure drop period lasts 0.2-0.24 secs, and the entire cycle is no longer than 0.6 secs, as a result of fitting the rapid-action combined valve.

The method of venting, depends on the design and depth of the core-box. In the shallow and closed core-boxes the vents are provided in the bottom of the box. Up to 25 per cent of the vents should be placed in the cavities and recesses. The total number of vents is determined by the ratio of their squares and those of the injection orifices, which should be 0.5-1.0 for core-blowers and 0.3-0.5 for core-shooters⁽⁶⁸⁾.

For open core-boxes deeper than 70mm, it is best to use top venting, equipping the core-blower with universal blowing-plates. When blowing open core-boxes on machines equipped with a venting plate, vents should be provided over the entire surface of the plate between the injection bushes. When making moulds, particularly if large blow holes are used, the ratio indicated above should be reduced to 0.1-0.5⁽⁶⁸⁾.

On the mechanism of sand compaction in the core-boxes, Lesnichenko⁽⁶⁸⁾ confirms, previous authors⁽⁷⁶⁻⁷⁹⁾, that compaction is due to combined influence of kinetic energy of the sand injected into the box, and the pressure drop in the core-box due to the passage of air through the sand layer.

In 1965, Geller and Poplavskii⁽⁶⁹⁾⁽⁸⁰⁾ carried out core-shooting experiments using a core-shooter with a transparent reservoir and a transparent core-box. High speed cine photographs were taken of the sand flow from the reservoir and in the core-box, with simultaneous oscillographic records of the air pressures in the reservoir and the core-box. The sleeve of the sand magazine was filled with dark core sand-binder mix separated by layers of light coloured dry quartz sand. This technique helped the observations of the movements of the sand during the shooting process.

The results revealed that three basic modes of sand flow are possible inside the sleeve⁽⁸⁰⁾.

In the first case the core is shot with all slots in the sleeve open. The sand layers in the sleeve moves bodily without curling or changing in thickness. In other words, the sand is not compacted while moving within the sleeve. In the blow-hole, with its tapering walls, the layers of sand are distorted; near the walls they are compressed, while in the centre over the exit orifice they are expanded, thus assuming a certain funnel shape, Fig 25.

When the slots in the bottom of the sleeve are substantially reduced in section or closed altogether,

the operation conditions in the reservoir undergo a fundamental change. The sand column is compacted within the reservoir, forming a depression on the free surface, and when it starts to move, it undergoes longitudinal compression and compaction. The sand around the side walls does not join in the downward movement, a crater forms in the column and sand flow ceases, Fig 26.

When the slots in the top of the sleeve are reduced in cross-section or closed, sand flow from the reservoir is accompanied by a general structural loosening of the column. The horizontal layers appear thicker, indicating that the compressed air enters and opens up the column, while at the same time a gap appears between the sand and the sleeve walls. At first the sand moves as if its packing density is unaffected, but as it becomes more inflated with air the flow pattern becomes increasingly randomised and eventually the sleeve contains a structureless fluidised mass of sand, Fig 27.

The distinguishing feature of the core-shooter flow is the fact that the core-box is filled and the sand compacted at one and the same time. However, Geller and Poplavskii(69,80), discovered that the core is formed in two stages. The high speed cine photographs revealed that, the core-box is first filled with sand ejected from the blow hole, and at the end of this stage it appears to be completely full. There is, however, still a substantial amount of sand left in the reservoir sleeve. In the second stage the box continues to take sand, and the core is compacted by the pressure exerted by the fresh arrivals, under the action of the difference

between the air pressures in the reservoir and the core-box. At the end of this stage the core is completely formed and compacted, leaving in the reservoir only a small residue of loose sand. The core is, thus, compacted at the end of the second stage(80).

In summary, Geller and Poplavskii(69)(80) demonstrated that, other things being equal, the degree of compaction achieved in the core-box is a function of the size and shape of the sand squeezing lump in the reservoir sleeve, which in turn are determined by the air pressure when the lump is being formed. The conditions should, therefore, be adjusted so that the pressure when the lump is being formed is as high as possible. Accordingly those conditions, under which the box is filled by a continuous feeding process, are the optimum(69)(80).

In 1970. Khurtov, Chernykh, Kurdryashev, Denisov and Utenkov(70) carried out experiments on a core-shooter with different blow holes. The results revealed that the sand-air stream flow pattern depends on the number, size and shape of the blowing orifices. The best results are obtained with blow-holes which produce highly concentrated sand streams, as indicated by low compressed air consumptions. The wear on the core-boxes is usually below average when such blow holes are used(70).

The flow pattern of sand in the stream depends on the area of the slots in the sleeve and at each setting in this respect there is a minimum blowing orifice area below which the stream rapidly becomes less uniformly concentrated and the entire performance consequently

falls off. Streams produced by several blow holes are less concentrated than when a single orifice of equivalent area is provided.

Khurtov⁽⁷⁰⁾ explains that as compressed air passes through the layers of sand in the sand sleeve, it gives rise to the production of a fluidised zone of sand above the blowing orifice.

Extension of this fluidised zone in the sand column lies at the basis of flow in the core-shooter process. The way the zone extends depends on the pressure distribution, since it will tend to move in the direction of maximum change in the pressure gradient. When the air is admitted at the top of the reservoir, the maximum gradients occur in the axial regions and the fluidised zone will move upwards. The air supply to the sand column from the sides is clearly insufficient. The fluidised zone here will tend to spread too far towards the side walls if the maximum pressure gradient occurs around the edges of the sand column, Fig 28⁽⁷⁰⁾. The differences in the distances between adjacent isobars clearly increase when there is a zone of reduced sand concentration present. This indicates that once the fluidised zone has formed it spontaneously tends to spread preferentially in one direction. By regulating the amounts of air admitted to the sand from the top and sides of the sleeve it is possible to optimise the initial form of the flow of air through the sand so that the fluidised zone will extend equally in all directions⁽⁷⁰⁾. The situation is complicated by the fact that any given ratio of resistances between the different air admission zones

applies solely to a sand column of a given height. As the column height decreases (i.e. as sand flows out of the reservoir), the probability of the fluidised zone extending preferentially in one direction increases again.

In practical conditions the fluidised zone spreads extremely irregularly, since the sand in the reservoir invariably contains local regions where the density differs from the average. Hence, when the pressure distribution militates against the uniform extension of the fluidised zone, the latter usually degenerates into a channel extending from the blowing orifice either to the side surface of the sand column or to its free top surface. In both cases the sand concentration is reduced and the performance of the equipment becomes much poorer(70).

Some of the relatively recent research in the core-shooting/blowing processes has been carried out by Pelczarski(81) and Danko(82,83).

In the early 1970's Pelczarski and Danko(81,82) carried out investigations on the process of filling the core-box and core densening. For the investigations a bench blower was used in which a container with double walls, perforated from the inside was substituted for the shooting sleeve. Both the container and the core-box had front walls of clear plastic. On account of the great dynamics of the phenomena taking place during the process of evacuating the shooting chamber and filling the core-box with sand, the observations were recorded by a multi-

speed camera at a rate of 2000 and 3000 frames per second respectively.

Pelczarski and Danko agreed with several other authors⁽⁸⁰⁾⁽⁸⁴⁾⁽⁸⁵⁾ that the kinetic energy of the sand stream was most essential for the magnitude of core densening. To define the kinetic energy it is necessary to know the true speed of aggregation of sand grains falling on the layer already in the core-box. To define this speed two methods were applied⁽⁸¹⁾.

The first consisted of introducing into the core-sand contrasting larger grains of a foreign matter, the motion of which could easily be observed during the projection and analysis of the film, Fig 29. This made it possible to measure the speed of the stream during the period of filling the core-box of 0.5 secs. This speed obtained a maximum magnitude of 20m/sec and its variations are illustrated in Fig 30⁽⁸¹⁾.

The second possibility of defining the stream speed was obtained from the investigation carried out on a horizontal core blower. Where the course of the stream was horizontal the gravitational force did not interact with the initial speed of the stream as was the case in a vertical blower, but deflected the stream downwards. The shape of the central line of the stream makes it possible to define the horizontal component V_H of the speed of the true motion of the stream, Fig 31. The horizontal component V_H corresponds to the speed of the sand outflow from the blowing hole under the sole influence of the energy of the compressed air and may be calculated from the following formulae⁽⁸¹⁾:

$$\frac{S_1}{S} = \tan \alpha$$

$$\frac{V_v}{V_H} = \tan \alpha \implies V_H = \frac{V_v}{\tan \alpha} = V_v \cdot \frac{S}{S_1}$$

$$V_w = \sqrt{V_v^2 + V_H^2} = \sqrt{V_v^2 + \left(V_v \cdot \frac{S}{S_1}\right)^2}$$

$$V_w = V_v \sqrt{1 + \text{Cotg}^2 \alpha}$$

where:

S_1 - path of free fall of the particles during time

S - plane of the path of the particles during time

V_H - horizontal component of the stream speed

V_v - vertical component of the stream speed

V_w - the resultant speed of the stream.

The action of the kinetic energy of the sand stream may be observed by checking the distribution of the core densening in the section perpendicular to the direction of the stream, in particular when blowing holes which are small in relation to the core-box section are used. In such a case the stream impinging along the core-box axis directly transfers its kinetic energy to the layer building up in the core-box and, by its long lasting dynamic action, increases the density of the sand considerably more at the point where the stream falls than on the periphery of the core section(81,82). The results of the core-densening measurements along the

height and width of the core-box are illustrated in Fig 32.

It should be noted that the results illustrated in Fig 32 were obtained for the case in which only the kinetic energy of the stream was acting on the densening of the core sand. Elimination of the action of pressure of compressed air on the layers of sand in the core-box, and the influence of air filtrating on the core densening, was obtained by moving the core-box away from the head by which means atmospheric pressure always prevailed above the forming core(81,82).

Studies of the films taken during the experiments showed that, with a small stream speed at the moment of its approaching the bottom of the core-box, the free surface falls from the centre downwards (Fig 33a), and then levels out in the form of a liquid level (Fig 33b) at a slightly higher stream speed. As the box fills, the dynamic rapid impact of the falling stream forms a concave free surface, Fig 33c.

Further experiments on core shooting were carried out by Danko(83) using unconventional methods of producing cores of layered structure.

The sand in the shooting chamber, consisting of dark and light layers, for better observation, was shot into a core-box and the whole process filmed. This showed that the layers of sand in the shooting chamber undergo three distinct movements(83), Fig 34:-

- 1) Short period of uniformly accelerated movement to which every layer of sand is subject to a different degree, depending on its location in the chamber.

- 2) A period of steady movement of constant velocity.
- 3) A period in which the layers after reaching the region of the blow hole, become accelerated again which lead to an increased porosity of the area in the shooting chamber.

Observations of filling the core-box indicated the possibilities of two different filling patterns, depending on the conditions of the shooting parameters. For straight cores shot through a single blow hole of relatively large diameter (30mm), stable filling in by the mass of sand was seen and as a result a layered core was produced. Shooting through a smaller blow hole of 16mm in diameter caused the sand jet to circulate intensively and the sand layers were mixed up. In the case of 30mm blow hole there were voids and areas of lesser density in parts of the shot core. Using the 16mm blow hole improved the situation by eliminating the voids as a result of increased movement of the sand. This was due to an increased pressure of air which caused the directing of the sand towards the vents(83).

The application of the concept of two layered cores is based on simultaneous shooting of two different sand masses, one which fills the centre of the core, and the other forms the external profile. The centre mass can consist of less bonded sand almost without binder which will create a layer in the middle of the core of increased permeability. Furthermore, the lack of sufficient binder results in the reduction of strength in this section which enables easier removal of cores out of castings.

Danko(83) constructed a shooting chamber consisting of two cylinders which were filled with respective sand masses. The flow mechanism of the two sand masses, illustrated in Fig 35, were observed to be similar to that of a typical shooting chamber, except that there was simultaneous movement of both sand masses towards the common blow hole.

3.8. Flow of sand mixture in core blowing and shooting

Early publications(65-67)(72-74) on core-blowing and shooting consisted mainly of, recommendations and suggestions on different factors involved in the blowing/shooting processes. These recommendations were largely based on the working observations of the authors involved, and included; positioning of cores within core-boxes, number, sizes, and arrangements of core-box vents and blow-holes.

Gade(75) investigated the influence of blow hole diameter, vent area and air pressure on core-weight. His data neither confirmed nor conflicted Lincoln's(66) contention that a small blow hole will increase the "throwing power" of the sand. Gade(75) showed that vents could be used to direct sand to reach portions of the core-box difficult to fill.

Other authors(64)(68) emphasised that the performance of a core-blower or shooter was largely determined by the performance of the sand reservoir. Extensive research(64)(68-70)(80) on this subject resulted in guide lines for better transfer and introduction of air from the air reservoir to the sand magazine.

As far as the mechanisms of sand flow and sand compaction in the core-boxes are concerned, views are many and varied.

Lesnichenko(68) confirms, as established by other authors(76-79), that compaction is due to combined influence of kinetic energy of the sand injected into the box, and the pressure drop in the core-box due to the passage of air through the sand layers.

Geller & Poplavskii(69)(80) demonstrated that the degree of compaction achieved in the core, depends on the size and shape of the squeezing lump of sand in the sand magazine. It was suggested that the air pressure should be kept as high as possible when the squeezing lump was being formed. Under these circumstances a continuous feeding process in the core-box would be achieved.

Khurtov(70), however, showed that the sand/air stream flow pattern depends on the number, size and shape of the blow-holes. The best results were obtained with blow-holes which produce highly concentrated sand streams, as indicated by low compressed air consumptions.

Although different authors(68-70)(80-85) seem to show sufficient evidence to support their conclusions individually, it is almost impossible to draw solid parallels between them as a group. The only common ground, as confirmed by some of the most recent research(80)(84-85) in the field, is that the effect of kinetic energy of the sand stream is most influential for the magnitude of core densening. Furthermore, comparing the results of these authors, demonstrate that their conclusions are only valid for the custom built equipment

that they have employed. Other factors that have not been investigated include; binder content of the sand-binder mixture , and sand types. As the kinetic energy of the sand/air stream seems to be an important factor in determining sand flow and compaction, related variables such as different sands having different densities should be investigated.

It is, therefore, deemed necessary to carry out new investigations into the mechanisms of core blowing and core compaction exploring all the essential variables involved. In order to produce general rules governing the core blowing process, it is also necessary to use a variety of experimental equipment, for instance, different sizes and shapes of core-boxes and blow holes. These equipment should also resemble closely those used in the industry of core making.

A sequence of experiments to explore the effects of some key factors in the mechanism of sand flow into core-boxes was prepared.

The core blowing machine selected would be a batch type core blower as used in industry.

Finally, the variables to be studied include; core-box geometry, the blowing air pressure, the sand-binder mixture, the area and arrangements of core-box vents, and the blow hole shapes and areas.

4. EXPERIMENTAL
PROCEDURE

4. EXPERIMENTAL PROCEDURE

4.1. Introduction

The experiments were carried out in order to investigate the flow mechanism of sand inside core-boxes, and also to determine the effect of different control variables of the core-blowing process on the produced cores. These variables included the core-box geometry, the blowing air pressure, the sand-binder mixture, the area and arrangements of core-box vents and the blow hole shapes and areas.

4.2. Experimental equipment

The cores were blown using a batch type core-blower, illustrated in Fig 36. The blown cores were first weighed in box on a scale accurate to 0.1 of a gram and then hardened in an SO₂ gassing machine.

Three core-boxes were designed and manufactured in-house.

Core-box number one consists of a main body of cast iron and a front wall of perspex, Figs 37-42. The core-box cavity consists of a central channel and six side channels machined at 30°, 45° and 60° to the central channel, Fig 38. The cross section of the side channels is semi-circular on one side and rectangular (as is the central channel) on the other side, Fig 42. Provisions were made to allow for blockage of any channel, thus the core-box could be used partially. Furthermore, 107 slotted vents were incorporated in the core-box which could be blocked off or opened, by means of screws fitted to the back of the box, Fig 40, in order to allow for different venting arrangements.

Core-box number two, illustrated in Figs 43-45, was made of aluminium with a front wall of perspex. A smaller number of slotted vents (20) were incorporated in this core-box based on the experience obtained from experiments previously carried out on core-box number one.

A third core-box, illustrated in Figs 46 & 47, which is of much greater cavity volume in relation to the aforementioned core-boxes, was used to further investigate the flow of sand during the blowing process. This rectangular core-box contains a central shaft situated directly opposite and below the mouth of the core-box. Different shaped heads, illustrated in Fig 46, could be assembled on the top of this shaft in order to investigate the effect on the sand jet during the box filling process.

All three core-boxes were fitted with electronic light emitting and receiving devices at the mouth of the core-boxes, which were used to measure the time taken to fill the boxes. On arrival of sand at the mouth of the box a ray of light (a) would be broken and thus the timer would be started. Once the box was full, another ray of light (b) would be broken which in turn would cause the timer to stop. This is schematically illustrated in Fig 48. The timer used was accurate to 0.01 sec.

A series of blow holes of different shapes and areas were used for the experiments carried out, Fig 49. These were; a range of circular blow holes of 5, 10, 15, 20, 25 and 30mm in diameter, an equilateral triangular blow hole of 20mm each side and an area of 173.2mm^2 , and two

rectangular blow holes of widths 12mm and 9mm and length 26mm and 19.5mm respectively. The areas of these blow holes are 312mm^2 and 175.5mm^2 respectively.

In order to investigate the flow mechanism inside the core-boxes, a high speed camera was used to film the process of filling the boxes at 64 frames per second. The films taken could then be used to observe the flow of sand in the boxes at lower speeds. The films also provided another method of measuring the time taken for sand to fill a core-box in this case to an accuracy of 0.016 sec.

The sand mixer used for the experiments was a batch type mixer of up to 30kg capacity. The sand was mixed with the appropriate amount of the furan resin binder for a period of three minutes initially, followed by a further period of two minutes after the addition of methyl ethyle ketone peroxide (M.E.K.P.). The mix would then be transferred to the sand hopper of the core-blower.

Two types of sand were used, namely zircon and silica. The grain distribution of these sands and their AFS numbers (American Foundry Society number) are given in the Appendix.

4.3. Experimental groups

4.3.1. Group 1: Investigation of the sand flow mechanism

This group of experiments were carried out in order to investigate the sand flow mechanisms inside core-boxes. The experiments consisted of blowing the zircon-sand already mixed with 0.7% and 0.245% by weight of resin and M.E.K.P. respectively into the three core-boxes at an approximate air pressure of 6 bars. Different blowing conditions involving a range of blow hole shapes and areas together with different core-box venting arrangements were employed.

The process of filling the core-boxes was filmed throughout these experiments. The time taken for the sand to fill a given core-box was later determined by counting the number of frames showing the filling process.

The blowing cycle for each experiment was as follows;

1. The sand magazine was filled with the sand mix from the hopper (i.e. the sand magazine was always full before blowing a core).
2. The core-box vents were cleaned by blowing pressurised air (~ 6 bars) through them and also by using a vent cleaning tool.
3. The core-box was positioned on the blowing table.
4. The sand magazine fitted with the appropriate blow hole was transferred under the air reservoir and above the core-box.
5. The table was raised thus clamping the core-box to the sand magazine and this in turn to the air reservoir.

6. The core was blown.
7. The table was lowered.
8. The core-box was removed.
9. The blown core was weighed in box.
10. The core was hardened.
11. The core was stripped from the box and checked for soundness.

4.3.2. Group 2: Blowing air pressure and blow hole area vs core-weight, using core-box no. 2

These experiments were carried out in order to determine the effects of blowing air pressure, and blow hole area on core-weight and soundness. The cores produced were blown using the same sand-binder mix as that used in the previous group. Core-box number two was used together with a range of blow holes. The blowing air pressure range used was approximately between 2.41 - 5.86 bars (35-85 psi). The blowing cycle was the same as that employed in the previous group. Depending on the weight consistency of the blown cores three to six cores were blown at a given blowing condition (i.e. set air pressure and set blow hole) and the average weight and range of weights were recorded.

The experiments in this group were not carried out in any specific order in terms of blow holes, the blow holes used were chosen at random. Nor were the sand batches specific to any series of experiments. Sand-mix was added to the hopper as and when needed. The experiments were carried out in such a random and casual manner in order to simulate the production in industries.

These experiments were also carried out as preliminary experiments for group three, and were used to plan the experiments in this group.

Based on the results obtained from these experiments additional vents were incorporated in box number two increasing the number of vents in this core-box from 20 to 30.

4.3.3. Group 3: Further investigations of the effect of air pressure and blow hole area on core-weight

These experiments were carried out in order to investigate the effects of blowing air pressure and blow hole area on the weight and soundness of the cores.

Core-boxes one and two were used to produce cores from the same sand/binder mix as that used in the previous groups. This sand-binder mix was added to the magazine after every blow to ensure that the sand magazine was full prior to each blowing operation. The air pressures used were 2.76 - 5.52 bars (40-80 psi) for core-box number one and 2.41 - 5.86 bars (35-85 psi) for core-box number two. The blow-holes used were all circular and were 20, 15, 10 and 5mm in diameter for box number one and 30, 25, 20, 15, 10 and 5mm in diameter for box number two. All the vents of both boxes were thoroughly cleaned before starting this group of experiments. They were then cleaned by blowing with compressed air for a duration of one to two seconds between individual blows.

The order of experiments carried out was such that the air pressure was set at its lowest value. The experiments involving different blow holes were then

carried out using the largest blow hole first followed by the rest in order of decreasing size. This was then repeated for increasing values of air pressure.

4.3.4. Group 4: The effect of binder level on core-weight

These experiments were carried out to investigate the effect of the binder level in the sand-binder mix on the weight and soundness of the cores. Zircon sand mixed with 0.35%, 0.7% and 1.05% binder was used.

Core-boxes one and two were used to produce cores at air pressures of 2.76 - 5.52 bars (40-80 psi) for box one and 3.1 - 5.86 bars (45-85 psi) for box two. The blow holes used for box one were 20, 15 and 10mm in diameter and those used for box two were 25, 20, 15 and 10mm in diameter. The vents of both boxes were thoroughly cleaned before starting the experiments and then cleaned by blowing with compressed air between individual experiments.

The order of the experiments carried out on box one was the same as that described in the previous group. These experiments were carried out with the sand-binder mix containing 1.05% binder followed by 0.35% binder at a given air pressure.

The order of experiments carried out on box two is illustrated in Fig 50.

4.3.5. Group 5: Further investigations of the effect of binder level on core-weight

These experiments were carried out to further investigate the effect of the binder level in the sand-binder mix on the blown cores.

Zircon sand mixed with 0.35%, 0.7% and 1.05% binder was used. The blowing air pressures were 3.10 - 5.86 bars (45-85 psi). Core-box two together with blow holes of 25, 20, 15 and 10mm in diameter were used to produce the cores.

The experiments carried out here were divided into three series:-

- (i) sand-binder mix containing 0.35% binder
- (ii) sand-binder mix containing 0.7% binder
- (iii) sand binder mix containing 1.05% binder

Before each series of experiments the core-box and its vents were thoroughly cleaned. The vents were then cleaned by blowing with compressed air between individual experiments within the series. Furthermore, the sand-binder mix in the sand magazine and the hopper was changed for each air pressure setting. The order in which the experiments were carried out is illustrated in Fig 51.

4.3.6. Group 6: Core blowing using silica sand

These experiments were carried out to investigate the effects of the blowing air pressure, the blow hole area, and the binder level in the sand-binder mix on the blown cores using silica sand. Three different binder levels were employed. These were 0.75%, 1.5% and 2.25% by weight of the sand, due to the lower density of silica sand in relation with that of zircon sand. These ratios were chosen to give equivalent volumes of binder to silica sand as those used with zircon sand.

The experiments were carried out on core-boxes one and two. The air pressures used were 2.76 - 5.52 bars

(40-80 psi) for core-box one and 3.10 - 5.86 bars (45-85 psi) for core-box two. The blow holes used were 20, 15 and 10mm in diameter for core-box one, and 25, 20, 15 and 10mm in diameter for core-box two.

As in the previous group, the experiments carried out on each of the core-boxes were divided into three series depending on the binder level of the sand-binder mixture. The core-boxes and their vents were thoroughly cleaned before each series of experiments. The vents were then cleaned by blowing with compressed air between individual experiments within the series. The sand-binder mixture in the magazine and the hopper was also changed for each air-pressure setting.

The order of experiments carried out on core-box one is illustrated in Fig 52. The order of experiments carried out on core-box two was the same as that illustrated in Fig 51 with the exception of different binder levels.

5. RESULTS

5. RESULTS

5.1. Group 1: Investigation of the sand flow mechanism

This group of experiments, carried out in order to investigate the sand flow mechanism inside the core-boxes, was subdivided into two sub-groups a and b.

5.1.1. Group a

These experiments were all carried out on core-box number one, Fig 53. Preliminary experiments included blowing the sand-binder mix through blow holes of 5, 10, 15 and 20mm in diameter at an approximate air pressure of 6 bars with different core-box venting arrangements. The cores produced were weighed and the values obtained are tabulated in Fig 54 and plotted against blow hole area in Fig 55. It can be seen from this graph that the heaviest cores and the most consistent cores in terms of core-weight were produced when the core-box venting was reduced to only one vent at the end of each channel. These cores were also the best quality in terms of soundness as they did not contain any voids except when the smallest blow hole of 5mm in diameter was used. Cores produced using this blow hole contained small voids in channels 4 and 5. It can also be seen from this graph that the core-weights obtained with this venting arrangement increase at a rate of 0.39 gm per mm² of blow hole area. This rate and the rates given hereafter are calculated without taking into account the values obtained when blowing through the 5mm diameter blow hole, as this blow hole gave rise to unsteady filling of the box and unsound cores in all cases.

The second best cores in terms of core-weight, consistency and also core soundness were produced when the central row of vents in all channels were opened. The graph of core-weight against blow hole area plotted for this case runs almost parallel to that of the previous case. The core-weight in this case increases at a rate of 0.29 gm/mm^2 .

In the case of opening all the vents, the rate of change in core-weight is 0.41 gm/mm^2 . Again the graph plotted for this case runs almost parallel to that of the first case, but only in the region between blow holes of 10 and 20mm in diameter. In the region between $\phi 5\text{mm}$ and $\phi 10\text{mm}$ blow hole there is a relatively large increase in the core-weight of 148.6 gm as opposed to 38.3 gm and 48.4 gm respectively in the previous cases. The cores produced with this venting arrangement were all good quality sand cores except when the $\phi 5\text{mm}$ blow hole was used.

In the final test, the vents were only open above 1' (see Fig 53). The cores produced here were inconsistent in weight except when using the $\phi 20\text{mm}$ blow hole. These cores were relatively unsound and contained voids. These voids could be seen, in all channels when using $\phi 5\text{mm}$ blow hole, in channels 4, 5, 6 and 7 when using the $\phi 10$ and $\phi 15\text{mm}$ blow holes. The voids in channels 4 and 6 were slightly larger than those seen in channels 5 and 7. The core-weight increased at a rate of 0.74 gm/mm^2 .

Having studied the results obtained from the preliminary tests, 8 blow holes of different shapes and areas together with seven different venting arrangements

were employed to carry out 15 experiments. The process of filling the box in each experiment was filmed and the films later used to calculate the time taken to fill the box. The results are given in Fig 56.

In experiment number 1 the sand/air jet reached the bottom of channel 1 after 0.06 sec. It then filled up channel 1 up to level 3' after 0.26 sec, when it divided up into two subjects curving into channels 6 and 7, Fig 57. As more sand arrived the subjects were first formed and then broke off and travelled towards the end of channels 6 and 7. This action gave rise to filling these channels with channel 7 filling slightly faster than channel 6, Fig 58. The sand level in the box then rose up to level 2' after 1.47 sec, when subjects were again formed which in turn proceeded to fill channels 4 and 5 as illustrated in Figs 59-60. Channel 5 was filled slightly faster than channel 4 as more sand was pushed into it. Once the channels 4 and 5 were filled the sand level rose up to level 1' after 2.89 sec. Here subjects were formed as before and proceeded to fill channels 2 and 3 with 3 filling slightly faster than 2, Figs 61-63. It can be seen from these Figures that there are small voids in channels 2, 4 and 5. The box was filled after 4.17 sec. The overall filling process was unsteady as the sand/air jet was pulsating periodically, spraying the sand into the core-box, and at times only air was entering the core-box.

In experiment number 2, the overall filling process was steady. In this case the sand level in the box reached level 3' after 0.07 sec, where the main sand/air

jet split into two subjets in the shape of a V, Fig 64. These subjets on collision with the top walls of channels 6 and 7 thickened along these walls towards the bottom of the channels and thus gave rise to filling them as shown in Figs 65-66. It can be seen from these Figures that channel 7 was filled slightly faster than 6. Once these channels were filled the sand level steadily rose up to level 2' after 0.34 sec. Subjets were then formed as before and filled channels 4 and 5 as illustrated in Figs 67-71. Channel 5 was filled slightly faster than channel 4, this is clearly seen in Fig 70.

The sand level in the box then steadily rose up to level 1' after 0.59 sec. The sand/air jet then divided up into two subjets which in turn filled channels 2 and 3 as illustrated in Figs 72 and 73. The box was eventually filled after 0.9 sec, Fig 74.

In experiment number 3, once the sand level reached 3', subjets were formed at approximately 90° to the main sand/air jet. These subjets, on collision with the top walls of channels 6 and 7, expanded towards the bottom of the channels, and thus filling them, Figs 75 and 76. The sand level in the box then steadily rose up to level 2' after 0.16 sec. Subjets were again formed here that gave rise to filling channels 4 and 5, with channel 5 filling slightly faster than channel 4, Figs 77-79. The sand level then steadily rose up to level 1' after 0.28 sec. At this level subjets were formed at approximately 90° to the main sand/air jet and flew into channels 2 and 3 as more sand was supplied from the main jet, Fig 80. The box was eventually full after 0.41 sec, Fig 81.

In experiment number 4, the sand/air jet expanded to take the full width of channel 1 as it reached the bottom of this channel, Fig 82. This kind of expansion of the jet front occurred to a smaller degree in the previous cases and it was only quite apparent in this case. The subjects in this experiment were formed at a larger angle to the main sand/air jet with respect to those in the previous case. Furthermore, these subjects collided with top walls of the side-channels at a point further in the channels. Channels 3 and 5 were filled faster than channels 2 and 4 respectively, Figs 83-85. The box was full after 0.24 sec, Fig 86.

In experiment number 5, the venting of the box was reduced to only one vent at the end of each channel. This experiment, with respect to experiment number 3 where the same blow hole of $\phi 15\text{mm}$ was used, produced a slightly longer filling time of 0.48 sec. The expansion of the jet front, as seen in Fig 87, is more apparent than that seen in experiment number 3. The subjects formed here similarly hit the side channels, however, some sand was bounced back up the central channel as illustrated in Figs 88 and 89. Here, although channel 5 was filled slightly faster than 4, Figs 90 and 91, the difference was not as apparent as in experiment 3. Channels 2 and 3 were filled simultaneously, Fig 92.

In experiment number 6 a tapered blow hole was used. This blow hole was tapered from a larger diameter of 42mm to 15mm, Fig 49. The results obtained here were similar to those seen in the previous experiment. However, the box was filled in a slightly shorter time of 0.44 sec.

In experiment number 7, the box was filled in 0.5 sec. Here the triangular blow hole gave rise to a sand/air jet that became wider as it travelled down the central channel, Fig 93. Once the sand level in the box reached 3', subjects were formed which travelled in the direction of channels 6 and 7 thus filling them, Fig 93. Channel 7 filled slightly faster than channel 6. On arrival of more sand, the sand level in the box steadily rose up to 2' where subjects were formed and flew directly towards the bottom of channels 4 and 5, Fig 94. It can be seen from this Figure that channel 5 was filling faster than channel 4. The sand level then steadily rose up to 1' where subjects were formed from the main sand/air jet. These flew along the top walls of the side channels 2 and 3, filling them as illustrated in Fig 95.

The results obtained in experiment number 8 were similar to that observed in the previous experiment. The subjects here collided with the top walls of the side channels slightly further in and flew down the channels to fill them. The box was filled in 0.47 sec.

The time taken for the sand level to reach levels 3', 2' and 1' were approximately the same in the previous three experiments.

In experiment number 9, the rectangular blow hole equivalent in area to that of the $\phi 20\text{mm}$ blow hole was used. The time taken for the sand level in the box to reach levels 3', 2' and 1' and finally the overall filling time were approximately the same as that obtained in experiment number 4, where $\phi 20\text{mm}$ blow hole was used. The filling pattern, however, was slightly different in

this case. The subjects formed at a larger angle to the main sand/air jet colliding with the top walls of the side channels further down the channels, Figs 96-98. These angles of deflection were at their largest when the sand level was at 1'. At this level the subjects flew directly towards the bottom of channels 2 and 3, Fig 98.

Experiment numbers 10-15 were carried out to investigate the effect of the venting arrangement of the box on the filling process.

In experiment number 10 where the vents were blocked up to level 2' and in channel 4, the sand/air jet filled up the box in a similar manner to that seen in experiment number 1, where the same blow hole of 05mm was used. The time taken for the box to be filled up to different levels and the overall filling time was also approximately the same. The only exception was that channel 5 clearly filled faster than channel 4. Channel 5 was full when channel 4 was only half full. The filling process at different stages can be seen in Figs 99-103.

In experiment number 11, the same venting arrangement as that used in the previous experiment was used together with $\phi 15$ mm blow hole. The filling pattern and times here were similar to that seen in experiment number 3 where the same blow hole was used. Channel 5 filled relatively faster than channel 4 in this case when compared with that in experiment number 3. However, compared with the previous experiment (i.e. 10), filling of channel 4 did not lag as long behind channel 5. The process of filling the box at different stages can be seen in Figs 104-108.

Experiment number 12 was a repeat of experiment number 10 with a new venting arrangement (i.e. vents blocked up to 1'). The filling times were similar to that in experiment numbers 1 and 10. However, the filling pattern was different. The overall filling process was more unsteady and the sand/air jet was continuously pulsating. Channels 5 and 7 were filled faster than channels 4 and 6 respectively. Compaction in these channels was not as much as that in experiment number 1. These channels contained relatively large voids which became smaller as the box was filled up, Figs 109-113.

Experiment number 13 employed the same venting arrangement as that used in the previous experiment, together with a blow hole of 15mm in diameter. The time taken for the sand to reach different levels and finally to fill the box were approximately the same as that in the previous cases where the same blow hole was used (i.e. experiment numbers 3,5 and 11). The filling pattern, however, was somewhat different. The main sand/air jet front clearly widened and formed the shape of an arrow, Fig 114, as it reached the bottom of channel 1. Subjets were formed as before at levels 3', 2' and 1' which gave rise to filling the side channels. Channel 5 filled slightly faster than channel 4, Figs 115-116, but not as fast as in the previous cases where the same blow hole was used. Voids could be seen in channels 6 and 4 during the filling process. These voids later filled up as sand reached a higher level of 1'. Channels 2 and 3 filled simultaneously.

The final two experiments in this group were carried out to further investigate the effect of the venting arrangement on the filling process. The $\phi 15\text{mm}$ blow hole was used in both experiments.

In experiment number 14, where only the vents in channels 2, 4 and 6 were opened, the subjects formed at level 2' filled channel 4 faster than channel 5. Furthermore, voids could be seen in channel 5 which later became smaller and eventually disappeared as sand level in the box rose to fill it. Figs 117-123 illustrate the filling process at various stages.

In experiment number 15, where the vents in channels 3, 5 and 7 were opened, the subjects formed at levels 3', 2' and 1' gave rise to clearly faster filling of channels 7, 5 and 3 as opposed to 6, 4 and 2 respectively. This is illustrated in Figs 124-128. Voids could be seen in channel 4 at the end of the experiment. The time taken for the sand to reach different levels in the box were approximately the same as in the previous experiments where the same blow hole was used.

A selection of cores produced from the above experiments are illustrated in Figs 129-135.

In summary, as blow hole area was increased, the time taken to fill the box decreased by the same factor, Fig 136. Also the angle at which the subjects were formed to the main sand/air jet increased. This latter effect could also be seen as the blow hole shape was changed from circular to triangular to rectangular, all having the same area. For a given blow hole area, changing the shape of the blow hole did not considerably change the

time taken to fill the box. Furthermore, changing the venting arrangement for a given blow hole area did not considerably change the filling times. Slight changes in the filling times observed could be attributed to pulsating sand/air jets. For a given blow hole area, reducing the vents to one per channel resulted in relatively uniform filling of the box (i.e. both sides filling at the same time) when compared with all vents open. Blocking the vents on one side of the box gave rise to that side filling slower than the opposite side and also containing voids.

5.1.2. Group b

This group of experiments was carried out on box number 2, Figs 45, 46 and 137. Preliminary experiments included blowing the sand/binder mix through 5, 10, 15, 20, 25, and 30mm in diameter, the triangular and the rectangular blow holes equivalent in areas to that of $\phi 15\text{mm}$ blow hole, at an approximate air pressure of 6 bars with all vents open. The core-weights obtained increased as blow hole area was increased, Fig 138. The core-weights obtained when the triangular and the rectangular blow holes were used, were approximately the same as that obtained when the $\phi 15\text{mm}$ blow hole was used. The time taken to fill the box when using the latter three blow holes was also the same, 0.53 sec. Overall the time taken to fill the box decreased as the blow hole area was increased. However, a clear relationship between these two variables was not apparent.

The filling mechanism in all cases were similar. The main sand/air jet arrived at the bottom of the box after

0.05 sec, where it spread along the bottom of the box travelling towards the side walls as more sand arrived. Around 0.06 sec later an explosive type phenomenon gave rise to the sand in the box being thrown in all directions. This then usually continued until the horizontal section of the box (i.e. section 2, Fig 137) was filled. In some cases the filling process steadied after the initial explosive action and arriving sand moved over the layers of sand already in the box to fill it. The filling action in the neck of the box (i.e. section 1, Fig 137) on the whole was steady. The aforementioned sequences can be seen in Figs 139-140 where $\phi 10\text{mm}$ blow hole was used and Figs 141-143 where $\phi 15\text{mm}$ blow hole was used, with all vents open.

The intensity of the explosive phenomenon increased as blow hole diameter was increased from 5mm to 20mm. However, when blowing through $\phi 25\text{mm}$ and $\phi 30\text{mm}$ blow holes the greater incoming sand/air jet seemed to overcome the explosive phenomenon and give rise to a steady filling of the box. This is illustrated in Figs 144-146 where the $\phi 30\text{mm}$ blow hole was used. On the other hand, the unsteady filling was seen when the $\phi 5\text{mm}$ blow hole was used. The sand/air jet here was pulsating at times, allowing only air into the box, which gave rise to turbulent filling. This is illustrated in Figs 147-151.

A series of experiments were then carried out to investigate the effect of the venting arrangement on the filling process. For this purpose the blow hole size was kept constant (i.e. $\phi 15\text{mm}$). The results obtained from these experiments are illustrated in Fig 152.

It can be seen from the results of experiments 9-11 that the core weight increased as the venting was moved from the bottom three vents on section 2 of the box to the top three. Experiments 12-14 which were repeats of experiments 9-11 with the addition of the vents on section 1 of the box showed an increase in the core-weights. Addition of the vents on section 1 of the box also eliminated the voids seen in the cores produced in experiments 9-11. Cores produced in experiments 15 and 16 contained large voids on the side where vents were closed. Experiments 17 and 18 which were repeats of experiments 15 and 16 with the addition of extra vents in section 1 of the box showed an increase in the core-weight and a decrease in the size of the voids seen. Finally, relatively more turbulent filling and larger voids were observed in experiments 19 and 20 where only the vents on section one of the box were opened. The core-weight obtained here after the first blow (i.e. experiment 19) was the lowest compared with those obtained from the previous experiments. The filling process observed in experiment 19 is illustrated in Figs 153-156. A series of cores produced from the above experiments are illustrated in Figs 157-163.

5.2. Group 2: Blowing air pressure and blow hole area vs core-weight, using core-box no. 2

This group of experiments were carried out on box number two as preliminary experiments for group three. Blow holes of 5, 10, 15, 20 and 30mm in diameter were employed with an air pressure range of 2.41 - 5.86 bars (35-85 psi). The air pressure was set at its highest

value, a blow hole was then chosen at random and experiments were carried out for decreasing values of air pressure. This was then repeated with another blow hole chosen at random. The final order of blow holes chosen was $\phi 15\text{mm}$ blow hole followed by $\phi 10\text{mm}$, $\phi 20\text{mm}$ and $\phi 30\text{mm}$. The results obtained are tabulated in Fig 164. From these results graphs of core-weight against blow hole area and air pressure are plotted in Fig 165 and 166 respectively. No results were obtained when using the $\phi 5\text{mm}$ blow hole as it was not possible to fill the box with one blow at any of the pressure settings. It can be seen from the graphs that for a given blow hole area, increasing the blowing pressure increased the core-weight, however, for a given blow pressure setting, increasing the blow hole area did not always give rise to an increase in the core-weight. It can be seen from Fig 165 that under all air pressure settings except in the case of 2.41 bars (35 psi), the core weight initially increased as the blow hole area was increased from 76.8mm^2 ($\phi 10\text{mm}$) to 176mm^2 ($\phi 15\text{mm}$). The core-weight then gradually decreased for increasing values of blow-hole area. This gradual decrease in the core-weight is relatively less at higher values of blowing pressure. Fig 166 shows that in the region of 3.10 - 5.86 bars (45-85 psi) the heaviest cores were obtained when using the $\phi 15\text{mm}$ blow hole followed by $\phi 20\text{mm}$, $\phi 10\text{mm}$ and $\phi 30\text{mm}$ blow holes respectively. Furthermore, for a given blow hole the core-weights increased sharply at the initial stages of increasing air pressure (i.e. 2.41 - 3.79 bars (35-55 psi)) and then only increasing by relatively small

amounts, tending to level at the highest value of the air pressure setting. The cores produced in this group were all of 'good quality' except when the air pressure was at its lowest value of 2.41 bars (35 psi). The cores produced under the latter blowing condition were spongy and contained voids in the top corners of section 2 of the cores (see Fig 137).

5.3. Group 3: Further investigations of the effect of air pressure and blow hole area on core-weight

This group of experiments were carried out to further investigate the effect of the blowing air pressure and the blow hole area on the weight and soundness of the cores, and on the core-box filling time. These experiments were carried out on box number one, group a, and on box number two, group b. Additional vents were incorporated in box number two and positioned based on the results obtained from group number two. These vents are shown with dotted circles in Fig 137 on section 2 and 3 of the core-box. The order of experiments carried out on both core-boxes was such that the air pressure was set at its lowest value. The experiments involving different blow holes were then carried out using the largest blow holes first followed by the rest in order of decreasing size. This was then repeated for increasing values of air pressure. All vents were left open in all experiments.

5.3.1. Group a

The time taken for the sand-binder mix to fill the box was measured using apparatus previously described, Fig 48, and the results obtained were tabulated in Fig

167. It was observed that the values obtained were not always reliable. In some experiments sand bouncing around in the box would break the ray of light b (see Figs 55) used for stopping the timer before the box was actually full. However, reasonably accurate results were obtained when blow holes of 20 and 15mm in diameter were employed. Based on the relationship previously derived between the filling time and the blow hole area, the graph of filling time against blowing pressure was plotted, Fig 168, for $\phi 20\text{mm}$ blow hole. It can be seen from this graph that decreasing the air pressure by 1.38 bars (20 psi) results in an increase in the filling time of 25%.

The cores produced in these experiments were weighed and the values obtained used to plot graphs of core weights against blow hole area, Fig 169, and blowing air pressure, Fig 170. It can be seen from these graphs that the heaviest cores and the most consistent cores in terms of core-weight were obtained when the higher air pressure settings and blow hole area were employed. Fig 169 shows that for a given air pressure setting there are sharp increases in the core-weight as the blow hole area is increased from 19.6mm^2 ($\phi 5\text{mm}$) to 78mm^2 ($\phi 10\text{mm}$). Increasing the blow hole area from this point-on results in a relatively smaller and steadier climb in the core-weight. The steepest climb is seen at the lowest air pressure setting of 2.79 (40 psi). Fig 170 shows that for a given blow hole area, larger increases in the core-weight are obtained in the lower region of air pressure settings (i.e. 2.76 - 4.14 bar (40-60 psi)) relative to those obtained in the higher region of air pressure

settings (i.e. 4.14 - 5.52 bar (60-80 psi)). The graphs plotted for $\phi 20\text{mm}$ and $\phi 15\text{mm}$ blow holes run almost parallel to each other with the latter producing the lighter cores. The steeper climbs in the core-weight were observed when smaller blow holes of 5mm and 10mm in diameter were used. It was not possible to produce any cores at the lowest air pressure setting of 2.76 bar (40 psi) together with the lowest blow hole of 5mm in diameter. The variation of core-weights obtained at a given blowing condition was relatively less when higher values of air pressure setting and/or higher values of blow hole area were employed. Furthermore, the quality of the cores was poor when cores were produced under the lowest value of air pressure setting and/or when the smallest blow hole was used. The cores produced under the latter blowing conditions contained voids in some channels and/or were spongy in others.

5.3.2. Group b

It was not possible to measure the filling times in this group of experiments. This was due to the rather turbulent manner of filling, described, in group 1, which resulted in stopping the timer before the box was full. However, cores were produced under the different blowing conditions and the weights recorded. The results were tabulated in Fig 171. Graphs of the core-weights against the blow hole area and air pressure setting were plotted, Fig 172 and Fig 173 respectively. It can be seen from these graphs that, in general, core-weight increased as blowing pressure on blow hole area was increased. The variation in the core-weight seems to be relatively

larger in the lower region of air pressure setting (i.e. 2.41 - 3.79 bars (35-55 psi)) and when smaller blow holes of 5 and 10mm in diameter were used. Rather smaller increases in the core-weights and relatively steadier increases can be observed in the higher region of air pressure setting (i.e. 3.79 - 5.86 bars (55-85 psi)) and when larger blow holes of 15, 20, 25, and 30 mm in diameter were employed. Furthermore, the cores produced under the latter blowing conditions were the heaviest and the most consistent in terms of their weights. The cores produced were all sound cores except when the lowest pressure setting of 2.41 bars (35 psi) was used. Cores produced at this air pressure setting were all spongy and contained voids in sections 2 and 3 of the cores (Fig 137).

At the end of each series of experiments under different blowing conditions, some earlier experiments within the series were repeated. The core-weights obtained compared to the previous values obtained under the same blowing conditions were found to be between 10 to 30 gm lighter.

5.4. Group 4: The effect of binder level on core-weight

This group of experiments were carried out in order to investigate the effect of the resin binder content of the sand-binder mix on the weight and soundness of the cores produced under different blowing conditions. These different binder levels were 0.37%, 0.7% and 1.05% by weight of the sand. The experiments were sub-divided into two groups; those carried on box number 1, group a, and those carried on box number 2, namely group b.

5.4.1. Group a

These experiments consisted of blowing the sand-binder mix containing 1.05% and 0.35% binder level at different blowing conditions. The order of experiments carried out was as follows;

1. The air pressure was set at its lowest value.
2. Sand-binder mix containing 1.05% binder was transferred to the sand magazine and the hopper of the core-blower.
3. Experiments involving different blow holes were then carried out using the largest blow hole first followed by the rest in the order of decreasing size.
4. Any remaining sand was removed from the blower and a new batch of sand containing 0.35% binder was transferred to it.
5. Steps 2-4 were then repeated for increasing values of air pressure.

The time taken to fill the box was measured during each experiment, using the timer previously described. However, the values obtained were not always correct as during most of the experiments the timer was triggered to stop, as a result of the turbulent flow of the sand, before the box was truly full. Some of the results obtained were reasonably accurate and these, to an extent, seem to support the relationships previously derived between the filling time, the blow hole area, and the air pressure setting.

The overall results obtained are tabulated in Figs 174 and 175. From these results graphs of core-weight

against blow hole area and air pressure for different binder levels were plotted, Figs 176-179. It can be seen from these graphs that, generally, for a given binder level increasing the blowing air pressure and/or increasing the blow hole area result in an increase in the core-weight. On the whole, the rates of increased in the core-weight as a result of increases in the blowing air pressure or the blow hole area are seen to be steady. Furthermore, these rates seem to be very similar.

It can also be seen from the results that for a given blowing air pressure and/or given blow hole area, increasing the binder level in the mix results in a decrease in the core-weight. The soundness of the cores produced were also, generally, better when the mix containing the lower level of binder was used. However, the core produced from the mix containing 1.05% binder were stronger.

All the cores produced using the mix with the higher binder content were spongy and contained voids in different side channels except when the pressure setting was at 5.52 bar (80 psi) and the blow hole diameter was 20mm. The degree of the sponginess of the cores and the size of the voids decreased as the blowing air pressure and/or the blow hole area was increased. In the case of the 0.35% binder level, cores produced were only spongy or contained voids when the smallest blow hole of 10mm in diameter was used.

5.4.2. Group b

These experiments using core box number 2 consisted of blowing the sand-binder mix containing 0.36%, 0.7% and

1.05% binder level at different blowing conditions. The order of the experiments carried out here was the same as that in group a with the exception of the order in which the binder levels were employed at a given air pressure setting. The sand-binder mixes containing different levels of binder were chosen at random. The final overall order of the experiments carried out is shown in Fig 50.

The results obtained were tabulated in Fig 180 and graphically represented in Figs 181-186. It can be seen from these graphs that for a given binder level increasing the air pressure and/or increasing the blow hole area result in increases in the core-weight. For a given blow hole, the average rates of increases in the core-weight as a result of increases in the air pressure are the smallest in the case of 0.35% binder level. These rates seem to be similar to each other in the cases of 0.7% and 1.05% binder levels, with the latter case showing slightly larger rates than the former. For a given air pressure setting, the average rate of increase in the core-weight resulting from increases in the blow hole area is the highest in the case of the 1.05% binder level. These rates seem to be similar to each other in the remaining binder level cases. In general, for a given blowing condition (i.e. given air pressure and blow hole area) increasing the binder content in the mix gave rise to an increase or no significant change in the core-weights. The only exceptions were in the experiments where 5.52 (85 psi) together with $\phi 10\text{mm}$ blow hole and 4.48 bar(65 psi) together with $\phi 15$ and $\phi 10\text{mm}$ blow holes were used. In these experiments increasing the binder

level beyond 0.7% resulted in small decreases in the core-weight. Overall, increases in the core-weight as a result of increases in the binder level seem to be larger in the region of 0.35%-0.7% compared to those seen in the region of 0.7%-1.05% binder levels. Furthermore, these increments in the core-weights seem to be relatively larger when the highest pressure setting and/or the highest blow hole diameter were employed.

All the cores produced were found to be sound with the exception of those produced at the lowest air pressure setting of 3.10 bar (45 psi) and using the sand-binder mix containing 1.05% binder. These cores showed wrinkles on section 3 of the cores. The cores also became stronger as the binder content in the mix was increased under all blowing conditions.

5.5. Group 5: Further investigations of the effect of binder level on core-weight

These experiments were carried out on box number 2 to further investigate the effect of the binder level in the sand-binder mix on the blown cores. These experiments were essentially the same as those carried out on box number 2 in the previous group. The exceptions here were that the order in which different binder levels and air pressure settings were employed were predetermined and different to those seen in the previous group. The three binder levels involved were employed individually to form their own series of experiments. The core-box was also thoroughly cleaned and all the vents were cleaned out at the start of these series of experiments. Experiments

involving different blowing conditions within the series were then carried out, with the air pressure set at its highest value first. A set of experiments involving different blow holes were then carried out using the largest blow hole first and the rest in the order of decreasing size. This was then repeated for decreasing values of air pressure within the series. Furthermore, different sand batches were used for different air pressure settings. A summary of the order of the experiments carried out is shown in Fig 51. The results obtained were tabulated in Fig 187 and graphically represented in Figs 188-193. It can be seen from these graphs that for a given binder level increasing the blowing air pressure and/or increasing the blow hole area result in increases in the core-weight. Within the range of blow holes used the average rates of increases in the core-weight as a result of increases in the air pressure can be seen to be the smallest in the case of the 0.7% binder level and the highest in the case of the 1.05% binder level with the remaining case laying in between. Within the range of pressures employed, the average rates of increases in the core-weight resulting from increases in the blow hole area seem to be the smallest in the case of the 0.35% binder level and the highest in the case of the 1.05% binder level with the remaining case laying in between. For a given blowing condition, increasing the binder level in the mix from 0.35% to 0.7% did not result in any significant changes in the core-weights obtained, except when the lowest air pressure setting of 3.10 bar (45 psi) was employed. The core-weights obtained here

increased as the binder level was increased to 0.7%. Increasing the binder level from 0.7% to 1.05% resulted in increases in the core-weights obtained for all blowing conditions except when the pressure setting of 3.10 bar (45 psi) was employed. The core-weights obtained using this pressure setting decreased as a result of the increase in the binder level.

In the case of the 0.35% binder level, good, sound cores were, generally, produced except that lines of sand were missing on section 3 of the cores leading to the vents on this section of the box. Furthermore spots of sand were missing on section 2 of the cores opposite the vents on this section of the box. These defects decreased in area as the blowing air pressure and or the blow hole area were decreased.

All the cores produced using the sand-binder mix containing 0.7% binder were good and sound. Very small spots of sand on section 2 and small lines of sand on section 3 of the cores were seen to be missing when the lowest air pressure setting of 3.10 (45 psi) was employed.

The cores produced when using the sand-binder mix containing 1.05% binder were all good and sound. Only a very small amount of sand was seen to be missing on section 2 of the cores when the highest pressure of 5.86 bar (85 psi) together with the largest blow-hole of 25mm in diameter were used.

Overall, the strengths of the cores produced increased as the binder level in the sand-binder mix was increased.

5.6. Group 6: Core blowing using silica sand

This group of experiments was carried out in order to investigate the effects of the blowing air pressure, the blow hole area, and the resin binder content of the sand-binder mix on the blown cores using silica sand. Sand-binder mix containing 0.75%, 1.5% and 2.25% binder by weight of sand was used. These ratios were chosen to give equivalent values of binder to silica sand as those used for zircon sand.

The experiments were sub-divided into two groups; those carried out on box number 1, (group a), and those carried out on box number 2 (group b). As in the previous group different batches of sand-binder mix were used for each blowing air pressure setting. The core-boxes and their vents were also thoroughly cleaned before the start of each series of experiments involving different binder levels.

5.6.1. Group a

The order in which these experiments were carried out is illustrated in Fig 52. The results obtained from the experiments are tabulated in Fig 194 and graphically represented in Figs 195 and 196. The time taken for the sand-binder mix to fill the box was measured using the timer previously described and the results obtained can be seen in Fig 194. These values are not all accurate as in most cases the timer was made to stop, due to the turbulent flow of the sand, before the box was full.

It can be seen from Figs 195 and 196 that for a given binder level increasing the blowing air pressure and for increasing the blow hole area result in an

increase in the core-weight. Furthermore, the overall rates of increases in the core-weight resulting from increases in the blowing air pressure or the blow hole area are similar. The results also show that, for a given blowing condition, increasing the binder content in the sand-binder mix resulted in decreasing the core-weights produced. Generally, the rates of decreases in the core-weights resulting from increases in the binder level seen in the region of 0.75%-1.5% are smaller than those seen in the region of 1.5%-2.25%. The only exception to the above are when the lowest pressure setting of 2.76 bar (40 psi) was employed together with blow holes of 20 and 15mm in diameter. The aforementioned rates of change in the core-weights under these conditions are, overall steady, and relatively larger within the region of 0.75%-1.5% when compared with the results obtained under other blowing conditions within the same region.

All cores produced using the sand-binder mix containing 0.75% binder were sound. These cores were only slightly spongy in the side channels when the smallest blow hole of 10mm in diameter together with the lowest pressure setting of 2.76 (40 psi) were employed.

The cores produced using the mix containing 1.5% binder appeared much stronger than those produced from the mix with the lower binder level. All the cores produced under a blowing pressure setting of 5.52 (80 psi) within the range of blow holes used and all the cores produced under 4.14 bar (60 psi) together with blow holes of 20 and 15mm in diameter were sound and of good quality. The soundness of the cores produced beyond this

point deteriorated as the blowing air pressure and/or the blow hole area was decreased. The cores became slightly more spongy in the side channels.

All the cores produced using the mix with 2.25% binder content were spongy and contained small voids in different side channels. The only exceptions were the cores produced under a blowing air pressure setting of 5.52 bar (80 psi) together with blow holes of 20 and 15mm in diameter. The core produced under the latter blowing conditions were sound and of good quality. Overall, the quality of the cores deteriorated with decreasing values of air pressure settings and/or decreasing values of blow hole area.

Generally, the cores produced increased in strength as the binder level in the mix was increased.

5.6.2. Group b

The order of the experiments carried out in this group was the same as those carried out on box number 2 in group 5, Fig 51. However, it should be noted that the binder levels used in these experiments are 0.75%, 1.5% and 2.25% and not those illustrated in Fig 51, which apply only to zircon sand-binder mixes.

The results obtained are tabulated in Fig 197 and graphically represented in Figs 198 and 199. It can be seen from the results that for a given binder level in the mix increasing the blow hole area within the range of blowing air pressures used result in small increases in the core-weight. The average rates of change in the core-weight resulting from changes in the blow hole area are similar in the case of 0.75% binder level for all blowing

air pressure settings. In the case of 1.5% binder level, the above rates steadily increase as air pressure is increased. In the case of 2.25% binder level the above rates increase as the blowing air pressure is increased from 3.10 bar (45 psi) to 4.48 bar (65 psi) and then remains constant for increasing values of the blowing pressure.

The average rates of change in the core-weight resulting from changes in the blowing pressure for a given blow hole area are similar and relatively steady in the case of 2.25% binder level. In the case of 1.5% binder level, the above rates are also similar for all blow holes, however, the rates seen in the region of 3.10 bar (45 psi) to 4.48 bar (65 psi) are smaller than those seen in the region of 4.48 bar (65 psi) to 5.86 bar (85 psi). In the case of 0.75% binder level the above rates are similar. These are also larger than those in the previous cases of binder level in the region of 3.10 bar (45 psi) to 4.48 bar (65 psi). Increasing the blowing pressure beyond 4.48 bar (65 psi) did not show any considerable effect on the core-weight for any blow hole in this particular case.

For a given blowing condition, increasing the binder level did not show any significant change in the core-weights obtained at 5.86 bar (85 psi). At 4.48 bar (65 psi) the core-weights continuously decreased as the binder level was increased. The decreases in the core-weight were larger in the region of 0.75% to 1.5% binder levels than those seen in the region of 1.5% to 2.25%, at the latter blowing pressure. At 3.10 bar (45 psi), the

core-weights obtained slightly increased as the binder level was increased from 0.75% to 1.5%. Increasing the binder content in the mix to 2.25% resulted in a decrease in the core-weights obtained.

All the cores produced showed no evidence of poor compaction. The strength of the cores increased as the binder level in the mix was increased.

5.7. Summary of results

Group numbers	Core-box number one	Core-box number two
	<p>This core-box was primarily designed and used to study the sand flow mechanism and sand compaction during core blowing. The box was later used to study the effects of, air pressure, blow hole area and shape, the area of the box vents and their arrangement around the box, the binder level in the sand/binder mix, and the type of sand on core; weight, soundness, and compaction.</p>	<p>This box was designed to enable the rapid production of cores. The box was used to investigate the effects of different variables governing core blowing on the production of cores. These variables included; air pressure, blow hole, core-box vents, type of sand, and binder level in the sand/binder mix.</p>
<p>Group 1. Sand flow mechanism</p> <p>Zircon sand</p>	<p>The experiments carried out on this box revealed that different sand flow patterns were produced according to different blowing conditions which gave rise to different sand compaction within the box. The venting arrangements in the box could be used to direct sand to selected areas of the box and thus affect the filling time and compaction of such areas. The filling time of the box was found to be related to the blow hole area and the blowing air pressure. The compaction of the core was observed to take place under two stages; a primary compaction resulting from the influence of the kinetic energy of the sand/air jet entering the box and, a secondary compaction resulting from the passage of air through the mass of sand already in the box.</p> <p>The weight of the cores produced increased as the air pressure or the blow hole area was increased. The rate of increase in the core-weight, however, decreased as the optimum values of blow hole area and air pressure were approached.</p>	<p>The filling mechanism for this box was similar for all values of air pressure and blow hole area. An explosive type phenomenon occurred shortly after the arrival of the sand/air jet at the bottom of the box. This then continued until the horizontal section of the box was filled. The intensity of the explosion generally increased as the blow hole area was increased. However, the greater sand/air jets resulting from 25 and 30 mm in diameter blow holes seemed to give rise to steady filling of the box.</p> <p>Different shaped blow holes of the same area gave rise to similar filling times for the same blowing condition.</p> <p>The venting arrangements within the box was used to alter the core weight and soundness. Better quality cores and heavier cores were produced as the venting of the box was moved higher on the horizontal sections of the box.</p>

Group numbers	Core-box number one	Core-box number two
<p>Group 2. Preliminary experiments on blow hole area and air pressure vs core-weight</p> <p>Zircon sand</p>	<p>NOT USED</p>	<p>The cores produced were all of good quality except when the lowest value of air pressure (35 psi) was employed. For a given blow hole area the core-weight increased as the air pressure was increased, however, for a given air pressure the core-weight did not always increase with increasing values of blow hole area.</p>
<p>Group 3. Blow hole area and air pressure vs core-weight</p> <p>Zircon sand</p>	<p>The filling time of the core-box increased for decreasing values of air pressure. The average core-weight increased as the blow hole area and/or the air pressure increased.</p>	<p>Higher values of core-weight were recorded as a result of incorporating more vents at suitable positions. The core-weight increased as the blow hole area and/or the air pressure were increased.</p>
<p>Group 4. Binder level vs core soundness and weight</p> <p>Blowing conditions varied randomly</p> <p>Zircon sand</p>	<p>For a given blowing condition; the filling times recorded were similar for the different binder levels employed, the average core-weight increased as the binder level was decreased. The cores produced from the mix containing 0.35% binder were sounder than the cores from the mix of 1.05% binder content.</p>	<p>For a given blowing condition; comparatively heavier cores were produced using the mix with 1.05% binder level. However, the same cores were not as sound as cores produced using the lower binder levels of 0.35% and 0.7% in the mix.</p>
<p>Group 5. Binder level vs core soundness and weight</p> <p>Blowing conditions varied in a predetermined manner</p> <p>Zircon sand</p>	<p>NOT USED</p>	<p>For a given blowing condition, no significant core-weight differences were recorded in the cores produced from mixes containing 0.35% and 0.7% binder. The cores produced from the mix containing 1.05% binder; were heavier than those produced from the mix with 0.35% binder when the highest values of blow hole area and air pressure were employed, and lighter when the lowest values of air pressure and blow hole area were employed.</p>
<p>Group 6. Repeating the experiments carried out in the above groups using silica sand</p>	<p>The relationships between blow hole area, air pressure and core-weight were confirmed. Increasing binder level in the mix led to the production of lighter and poorer quality cores. Silica sand showed better flowability than zircon sand.</p>	<p>For a given blowing condition, increasing the binder content in the mix either did not result in any significant changes in the core-weight or gave rise to small decreases in them. Compared to box number one, this box showed less sensitivity to binder content in the mix.</p>

6. DISCUSSION

6. DISCUSSION

6.1. Introduction

The core-blowing process of core-making can be divided into several stages which take place separately in different parts of the core-blower, these being the air reservoir, the sand magazine, the blow holes, and the core-box.

Primarily, compressed air is admitted into the sand magazine via a valve from the air reservoir. This results in an immediate decrease of the air pressure in the air reservoir and an increase of the air pressure in the sand magazine. Since air rapidly flows through the sand in the magazine a pressure distribution is set up, the structure of which determines the force exerted by the air on the sand. As the air approaches the blow hole, this being a smaller diameter than the sand magazine, its velocity is increased sufficiently to tear sand loose from the mass and carry it into the core-box. The cavity left in the sand magazine becomes progressively larger until it fails to support the sand above, causing it to drop and lower the sand in the magazine.

This results in the production of a sand/air jet being injected into the core-box. The size and shape of the jet is determined by the geometry of the blow holes.

The sand/air jet on arrival at the bottom of the core-box spreads to produce subjects which are forced towards the sides of the core-box as more sand and air are supplied from the sand magazine via the blow holes. This results in layers of sand being built up in the core-box which eventually fill it.

The filling process can take place under different filling patterns governed by the air pressure, the size and shape of the blow holes and the amount and arrangement of the venting in the core-box, for a given system (i.e. core-blower and core-box).

The sand being deposited in different areas of the core-box is continuously compacted by two mechanisms. The factors involved in the two mechanisms of compaction are the kinetic energy of the sand/air jet and subsequently the kinetic energy of the subjects formed, and the passage of air through the sand resulting from a pressure distribution set up in the core-box by the incoming compressed air.

The velocity of the air flowing through the sand in the core-box is increased in the near vicinity of the vents as it escapes through them onto atmosphere. This could be sufficiently large to tear the smaller sand particles from the mass and carry them outside the core-box leaving behind small craters in the core.

Consequently the detailed understanding of the core-blowing process requires an appreciation of each stage. Each stage interacts with others, but they can be explained in detail separately. The interaction between stages occurs because the air/sand flow rate is governed by the most resistive orifice to flow. This can be anywhere in the system (i.e. between the reservoir and magazine, at the blow holes or in the venting in the core-box). During blowing the controlling orifice may change as sand flows into the core-box thus producing transitory effects.

6.2 Sand magazine

The behaviour of the sand particles in the sand magazine is governed by the flow of the compressed air through them. At the start of the blowing cycle compressed air is suddenly introduced to the top of the sand in the magazine from the air reservoir through a perforated plate. Observations of this plate after the end of the blowing cycle revealed that some sand was stuck to the plate around the holes in it and also on the rubber ring situated around the perimeter of the plate which is used for sealing purposes. This suggests that at the start of the blowing cycle the compressed air on meeting the top layer of sand in the magazine disturbs it. The sand particles on the top of the mass of sand are thrown about as streams of air entering through the holes of the air reservoir plate permeate the mass in a turbulent manner.

The expansion of the compressed air in the magazine and the continuous arrival of more compressed air from the air reservoir increases the air pressure in the magazine and sets up a pressure distribution. Measurements of the air pressure in different parts of the sand magazine by several authors(68-70)(83)(86) experimenting under similar conditions have shown that the air pressure in the magazine initially rises and then gradually decreases as sand and air flows from the magazine into the core-box. Fig 200 shows the air pressure measured by Geller(69) in air reservoir and on top of the mass of sand in the magazine. Within the particular experiment carried out, the air was admitted

on top of layered sand in the magazine and the movement of them observed. The layers of sand were compacted in the reservoir forming a depression on the free surface of the mass, and when the mass started to move it underwent longitudinal compression and compaction. A crater was formed in the mass of sand and flow ceased. During this latter stage Geller recorded that the pressure in the centre of the mass of sand greatly exceeded that on the side walls.

Fig 201 illustrates the pressure-time curves inside a sand magazine produced from the experiment carried out by Lesnickenko(86). Curve 1 shows the variation of the air pressure for the flow of sand from the sand magazine through a 37mm diameter blow hole, whereas, Curve 2 represents the variation of the air pressure for the flow of sand through a blow hole of 110mm in diameters.

These results show that the flow of sand from the magazine takes place as a result of a pressure distribution set up in the magazine. This is brought about by the air filtering through the mass of sand and finally escaping through the blow hole. It is therefore clear that all the phenomena associated with sand flow from the sand magazine are caused by the filtration of air through the sand. Sand flow starts from the near vicinity of the blow hole where particles of sand are carried away into the core-box, causing a reduction in the local sand concentration behind them. The increased porosity lowers the air pressure and increases the pressure gradient across the sand mass. This in turn promotes increased air filtration rates which leads to

increased interaction forces between the air and the sand. Thus sand particles start to be carried away from this layer and the process can now be seen to be continuous. A zone of sand of lower concentration than its immediate surroundings extends up from layer to layer. The lower concentration of this area leads to its increased flowability and as a result sand within the zone flows into the core-box. These events leave behind a channel in the sand magazine observed throughout the experiments carried out in the above work. When a stable channel is formed, sand flow ceases but collapse of the channel may then occur and the process of channel formation starts again.

There are situations in which a channel does not form completely through the sand mass but collapses before it reaches this stage. The flow of sand from the magazine to the core-box does not show a pulsating effect but appears under these circumstances to be continuous.

The pulsating sand/air jets experienced when blowing through a blow hole of 5mm in diameter are observed when channelling occurs through the entire mass of sand. The cross-sectional area of a channel formed in the sand magazine is determined by the cross-section of the area of the blow hole employed. Examination of the sand magazine after a series of experiments involving different size blow holes revealed that larger channels were produced when larger blow holes were used.

Within the experiments carried out in the present work it was observed that when a blow hole of 5mm in diameter, together with core-box number 1 was used, the

resultant sand/air jet was pulsating throughout the filling of the core-box, and at times only air entered the box carrying no sand with it. The situation was improved when a blow hole of 10mm in diameter was used in that, pulses were reduced to one or two during which time the sand/air jet took a spraying form as opposed to the usual column form. The pulsating and spraying effect of the jet was completely non-existent as larger blow holes were used. This could be explained by using the pressure time curves produced by Lesnichenko⁽⁸⁶⁾, Fig 201. These curves show that sand flow from the magazine took place under significantly higher air pressures when the smaller blow hole of 37mm in diameter was used. The presence of the higher air pressures in the magazine give rise to the sand in it being more compacted and as a result when a channel is formed, it will be harder for the air flowing through it to tear sand away from the walls of the channel. However, when larger blow holes are used the sand in the magazine is not as compacted and as a result easier to collapse while a channel is being formed during sand flow from the magazine.

6.3. Sand/air jets

The size and shape of the sand/air jets produced is governed entirely by the size and shape of the blow holes employed. The speed of the jet and the rate of its flow through the blow hole is governed by the air pressure in the magazine. However, for a given blowing pressure the size of the blow hole affects the speed and resultant flow rate of the jet as this determines the variation of the blowing pressure in the magazine during the blowing process.

The experiments carried out in group one on box number one showed that different size and shape sand/air jets could be produced by employing appropriate blow holes. Of these, jets produced using the smallest blow holes were not stable during the filling for reasons associated with the phenomena occurring in the sand magazine previously described.

The fronts of jets undergo a widening effect as they approach the bottom of the core-box. This is pronounced with jets of larger cross-sectional area. As sand and air enter the core-box, the pressure of the air in the core-box is increased. This gives rise to back pressure against the front of the incoming jet. Furthermore, the air in front of the jet is compressed forming an air cushion under the jet which promotes the widening effect of the jet front. The pronounced widening effect observed with larger jets is brought about due to the larger cross-section of the jets occupying more of the centre channel and, consequently, reducing the area left in the

channel for the movement of the air away from the incoming jet.

On collision of the sand/air jet with the bottom of the core-box, both sand and air are bounced off and pushed to the sides to fill the cavities in the core-box.

The sand/air jet flowing via a circular blow hole forms a cone of sand on the bottom of the box or on the layers of sand already in the core-box. Studies of the films taken during the experiments show that the base of this cone increases in area as the area of the blow hole is increased. Once a cone is formed the sand particles in the centre of the cone come to rest, whereas the particles of sand on the outer surface of the cone slip down and on collision with other sand particles supplied by the jet are pushed away from the centre of the cone. This was confirmed by observations during a series of experiments carried out involving a range of blow holes using zircon and silica sands with binder levels 50% lower than the recommended levels. A film of resin had previously built up on the bottom plate of core-box number two as a result of using the sulphur dioxide-furan (SO_2) process in hardening the cores. Cores were then blown using the core-blower and the removal of the film opposite the blow hole observed. It was observed that a film spot of a several mm in diameter representing the exact centre of the jet was left, whereas a ring of the film build-up exceeding the diameter of the sand/air jet was removed, Fig 202. The above phenomenon was observed with silica sand showing that the speed of the sand particles on the outer regions of the sand cone are

greater and promote sand blasting effects on the layer of film build-up. Similar experiments with zircon sand did not result in the removal of the film build-up. The results showed some sand sticking onto the layer of film opposite the blow hole, Fig 203. This evidence demonstrates that the faster flow of sand particles on the outer layer of the cone is responsible for embedding the sand particles in the layer of film in the fashion shown. However, it also shows that the lighter sand particles of silica sand blown under the same blowing conditions have acquired higher velocities. In both cases the effects seen are pronounced with a decreasing area of the blow hole which shows that higher jet speeds are achieved via smaller blow holes. This is to be expected given the high pressure in the magazine with smaller blow hole size, Fig 201.

The subjects formed as a result of sand particles flowing away from the sand/air jet, once it has collided with the bottom of the box or existing sand layers in the core-box take different forms according to the size and shape of the blow hole and the speed of the jet.

With a small blow hole of 5mm in diameter the subjects formed are comparatively small in size which curve into the side channels and then break off, Figs 57, 60 and 62. At this stage although the speed of the sand/air jet is the highest compared with those produced by other blow holes, the mass flow rate is the lowest and as a result only a small amount of sand is available for the formation of the subjects. Figs 61 and 62 also show the subjects flowing into the side channels in a manner

resembling that of a wave. This is because the speed of the sand particles on the top layer of the subject is higher due to less resistance to their movements. Therefore, for a given time the top surface of the subjects travel a greater distance.

The subjects formed when using a blow hole of 10mm in diameter are somewhat larger as the flow rate of the jet is now about four times that of the flow rate achieved through the 5mm diameter blow hole, (this factor is based on the experimental relationships calculated from the filling times). The speed of the sand/air jet is sufficiently high for the jet to pierce the layers of sand already in the box, Fig 64. As more sand and air are supplied by the jet, the sand particles are bounced upwards and sideways towards the side channels to form subjects. The front of these subjects on collision with the top walls of the side channels spread and try to run along these walls in all directions. However, the gravitational forces and more significantly forces exerted on the subjects by the incoming air flowing towards the vents at the bottom of the side channels pushes the subjects down towards the bottom of the side channels, Figs 63, 64, 67 and 72.

Some sand particles flow along the top walls of the side channels in an upward direction and eventually end in travelling up the sides of the main central channel. This is caused by the air which travels up the main central channel. As the lower parts of the core-box are filled with sand, and the vents in these regions are blocked off, the flow of the air through the sand and the

lower vents is made more difficult. It is therefore easier for the air to escape from the unblocked vents in the higher parts of the core-box and as a result an air flow towards these vents is set up that carries some particles of sand with it.

As larger blow holes are used, the base of the cone of sand produced by the sand/air jet becomes bigger and the angles of the side walls of the cone less steep. This results in the subjects formed flowing at a larger angle to the direction of the main sand/air jet, Figs 75 and 83.

6.4. Core-box venting

The vents in the core-box play an important part in the filling of the core-box with sand. For a given blowing air pressure, the rate of change of pressure in the core-box and consequently, the pattern of air flow and its rate of flow out of the core-box are governed by the open area of the vents and also the location of the vents in the core-box. One could even compare the core-box with the sand magazine and the vents with the blow holes.

At the start of the blowing process, the air pressure in the core-box increases as sand and air are pushed into it from the sand magazine. A pressure distribution is set up in the core-box according to the area of the venting and the position of the vents around the box. This pressure distribution gives rise to a particular air flow pattern, the structure of which determines the forces exerted by air on the sand⁽⁸⁰⁾. At first, the increased air pressure in the box gives rise to a similar rate of flow of air through all the vents, given that the effective open areas of the vents are the same. As the box is filled with sand and consequently, some vents are blocked, air flow favours those vents which are not yet blocked. The escaping air will take the least resistant route out of the core-box as the pressure gradient between the entry point (the blow hole) and the unblocked vents will be the greatest.

Experiments carried out in group one on venting arrangements revealed that, the air in the core-box could be persuaded to flow in a particular path and as a result

direct the sand flow in that path. The results obtained from core-box number one showed that when all the vents in the core-box were left open, channels 3, 5 and 7 were filled faster than their counterparts, channels 2, 4 and 6, respectively, Fig 53. This is due to channels 3, 5 and 7 having approximately three times as many vents as their opposite channels. This faster filling is a pronounced effect since channels 3, 5 and 7 are approximately twenty percent larger in volumes than channels 2, 4 and 6 respectively. Conversely, when all the vents in channels 3, 5 and 7 were blocked off and the vents in channels 2, 4 and 6 were left open, faster filling occurred in the latter channels. More symmetrical filling of the core-box was achieved by opening only one vent at the end of each channel.

Experiments carried out during the hardening cycle (gassing cycle) of the core-making process revealed more evidence confirming the fact that gases entering the core-box will flow on out through the quickest and least resistant of the routes. Gassing the cores while all the vents in the box were left open only resulted in hardening around thirty percent of the sand in the higher regions of the core-box, while the rest of the core was left uncured. The hardness of the cured portions of the cores decreased with increasing distance from the mouth of the core-box. Complete gassing of the cores was achieved by having only one vent open at the end of each channel.

Experiments on venting arrangements carried out on core-box number two also revealed that more air flow and

consequently, more sand flow was directed towards those sections of the core-box with comparatively more venting. One sided venting of the core-box gave rise to that side being filled with more sand than the other. However, employing the same area of venting with different positioning gave different results in terms of the flow of air and sand in the core-box. For instance, by opening the same number of vents in the bottom, the middle or the top row of section two of the core-box, Fig 137, cores of different weight and soundness were produced.

6.5. Compaction

Sand compaction in core-boxes by the core-blowing process results from the kinetic energy of the sand injected into the core-box, and also from the pressure distribution (gradient) in the core-box due to the passage of air through the sand. In the practical sense, it is virtually impossible to periodically separate the effects of the two factors on compacting the sand in the core-box during the filling process. However, in order to enable the discussion of the mechanisms of compaction resulting from the two separate factors, the compaction resulting from the former factor will be referred to as Primary Compaction, and that resulting from the latter factor referred to as Secondary Compaction.

The films taken during the experiments made it possible to observe the process of filling the core-box at a rate 64 times slower than real time. Observations thus carried out enabled a closer knowledge of the mechanism of the motion of the sand particles in the core-box. It may be observed that the sand/air jet entering the core-box behaves like a quasi-fluid during its motion. The sand/air jet on collision with the bottom of the core-box or with layers of sand already in the box, spreads to the sides like a jet of liquid when filling the core-box. Thus the shape of the upper surface of the core-sand building up may assume various shapes, giving rise to subjects of different character. This makes it possible to put forward a hypothesis concerning the motion of the sand particles in the direction of the flow

of the sand/air jet as well as to the sides of the core-box which is essential for defining the sand motion and its densening during filling the core-box.

Primary compaction of the sand in the core-box results from the kinetic energy of the sand/air jet being injected from the sand magazine via the blow hole. The magnitude of the kinetic energy of the sand/air jet (in particular sand particles that make up the jet) depends on the speed of the sand particles and their masses.

When a sand/air jet arrives at the bottom of a core-box it spreads out and the sand particles travel towards the sides of the core-box at an angle of 90° to the direction of the flow of the incoming sand/air jet. This was the initial motion of any sand/air jet irrespective of its size and speed within the experiments carried out.

The experiments illustrating this particular phenomenon were carried out on core-box number three, when a rectangular head was assembled on top of the central shaft within the core-box. Sand/air jets produced via blow holes of 10, 20 and 30mm in diameter under a blowing air pressure of 6 bars all behaved similarly, Figs 204-208.

However, when a sand/air jet falls on a layer of sand already in the box, the outcome will be rather different according to its size and speed, since it is now able to penetrate the presented media on collision and deform it. When a series of sand particles of given kinetic energy impacts a sand layer, the resulting forces are transferred onto the nearest grains in their path, Fig 209. The impact of any individual sand particle may

be resolved into two components; a vertical component and an horizontal one. The vertical component exerts a densening effect on the layers of sand laying beneath, while the horizontal component causes the sideways motion of the sand particles receiving the impact. The horizontal components originating from the impact of the sand particles inside the jet will cancel each other out, only the sand particles on the outer layer of the jet falling onto the layer of sand will displace the surface grains with more freedom of movement from it and shift them to the sides. The shifted grains thus frees the neighbouring sand particles within the jet which are then also able to move freely outwards. This motion may be transferred onto the following sand particles laying nearer to the axis of the jet, the motion being restricted by the dynamic action of the jet(81).

Considering the mechanism of sand motion, the phenomenon of the various shapes of the subjects and their angle of projection from the direction of the flow of the main jet observed during the filling of core-box number one may now be discussed.

A sand/air jet on collision with the layer of sand already in the box will penetrate the surface of it. Consequently, this surface will assume a concave shape. The sand particles in the jet form a cone, and those in the centre of the cone come to rest, thus building up the layers of sand beneath. Those sand particles on the outer surface of the cone will slip sideways and travel in the path presented to them by the concave surface of the layer of sand already in the box, Fig 210.

Smaller blow holes give rise to comparatively higher speeds of the jet and smaller ratio of the cross-section area of the jet to the cross-section area of the cavity of the box being filled. The higher speeds produce deeper impressions and a more concave surface on the layers of sand and the resultant subjets flow at a more acute angle to the direction of the flow of the incoming jet.

Slower speeds of the bigger jets produce a shallower impression and a less concave surface on the layer of sand in the box. The resultant subjets, therefore, flow at a larger angle to the direction of the incoming jet. Furthermore, the ratio of the cross-section area of the main jet to the cross-section area of the cavity of the box being filled is comparatively greater. This results in more of the sand particles on the outer surface of the main jet colliding with those sand particles already moving upwards on the concave surface of the layer of sand. The kinetic energy of the incoming particles are higher than those moving upwards. The resultant collective motion of the sand particles which form the subjets will be at an even larger angle to the direction of the incoming jet.

Secondary compaction takes place simultaneously with the primary compaction and also after the primary compaction has come to an end. The flow of the air in the core-box and its rate of flow out of the box is governed by the vents. The air flows towards the vents and in doing so assists primary compaction as well as giving rise to secondary compaction. The flow of the subjets is partially directed by the air flow in the core-box.

The subjets, on formation, travel towards the sides of the core-box under the influence of their kinetic energies. However, the air entering the box will biasly push the subjets in the direction of its flow towards the vents. If this partial change of direction of the subjets is towards those cavities of the core-box furthest away from the main sand/air jet, then one could safely say that the air flow is assisting primary compaction. The concave shapes of the surfaces of the subjets nearer to the main sand/air jet seen in Figs 90, 91 and 115 illustrate this effect.

Filtration of air through the sand results in the secondary compaction. This takes place during the entire filling process. In the initial stages of the filling process sand is compacted as a result of both the kinetic energy of the sand particles and the air pushing them in the direction of its flow. At later stages, when the higher portions of the core-box are being filled, sand movements in the lower already filled parts are still apparent. This is due to the air still flowing through these parts of the core-box and pushing the sand particles in its direction.

Observations of the cores after the gassing also confirmed that a significant amount of compaction can be achieved via the secondary compaction. Cores containing voids in some parts of the channels of core-box number one as a result of poor compaction during the filling process were hardened in the usual manner, previously described. After the gassing cycle it was observed that the voids had been eliminated and the level of the sand

in the central channel has gone down. This drop in the level of sand increased when gassing cores of comparatively lower weight containing larger voids due to poorer compaction. Similar observations were noted during the production of cores using core-box number two.

6.6. Discussion of results

6.6.1. Group 1. Investigations of sand flow mechanism

6.6.1.1. Group a

The preliminary experiments carried out in this group on core-box number one clearly showed that for a given blow hole, the best results in terms of core-weight and core soundness were achieved as a result of reducing the venting to one vent at the end of each channel. As core-box venting was increased to vents along the centre of all channels being open and finally all vents open, the resultant core-weights obtained decreased, accordingly. This effect is due to the reduction of secondary compaction caused by excess venting in the core-box. Each vent, when cleaned and unblocked by sand, provides an air passage area of approximately 4.0mm^2 . It must also be noted that venting is also provided along the parting line between the perspex front and the cast iron body of the core-box, since the pressure in the box during the blowing cycle pushes the perspex front away and provides a very small gap at the parting line. However, this situation occurs under all blowing conditions, and therefore the effect of different venting arrangements could still be compared.

When blowing of a core is carried out while the vents at the end of each channel only are open, the incoming air has to flow through the mass of sand already in the box in order to escape via the vents. In doing so, it promotes secondary compaction on its path. The same phenomenon occurs during the hardening cycle, when the gases used are made to flow to the end of the channels,

compaction occurring prior to the polymerisation reaction. Alternatively, when all the vents are open, the incoming air will escape via those unblocked vents in the higher region of the box as the vents in the lower regions are partially blocked off with sand. Thus the volume of air flowing through those parts of the channels containing sand is comparatively less than the case when only vents at the end of the channels are open. Therefore, the work done by the air in terms of compacting the sand (a better term may be rearranging the sand particles) along the channels (secondary compaction) is less.

In the case of having only vents above the level 1' in the core-box open, the cores produced contained voids in channels 4, 5, 6 and 7, Fig 53. This result further illustrates the importance of secondary compaction. Since all the vents in those channels were blocked off, secondary compaction was virtually non-existent in them, and compaction of the sand in these channels was entirely achieved under the influence of the kinetic energy of the subjects flowing into them (Primary compaction). Thus, if the incoming sand/air jet does not produce sufficient kinetic energy, as in the cases of 5, 10 and 15mm diameter blow holes with this venting arrangement, compaction in the aforementioned channels is poor and voids can be seen. During the hardening cycle, when the venting was always provided by one vent at the end of each channel, the voids were filled and the level of sand in the central channel of the core-box was lowered. The resultant compaction during this stage is entirely

achieved by the flow of the gasses used through the mass of sand (secondary compaction).

Within the series of experiments carried out in this group, the first four clearly showed that there is a direct relationship between the filling time and the area of the blow hole used, Figs 56, 136. This relationship suggests that the average mass flow rate of the sand/air jet is largely governed by the area of the blow hole for a given blowing condition, and thus the effect of different speeds of the jets resulting from different blow holes, on the average mass flow rate of the sand/air jets (and consequently the filling time) is not significant when this core-box is concerned.

The core-weights obtained during these experiments show that for a given blowing condition, increasing the blow hole area results in increasing the core-weights, Fig 55. Increasing the blow hole area results in increasing the mass flow rate of air and sand from the sand magazine into the core-box. Increased flow rate of sand promotes more primary compaction as the jet carries more kinetic energy. Increased flow rate of air promotes more secondary compaction as well as assisting primary compaction.

The results obtained from experiment numbers 5 to 9 further support the above arguments, in that the filling times resulting from different shaped blow holes of the same area were similar. However, the filling patterns were different in that the subjects formed at comparatively larger angles to the main sand/air jet when the triangular or the rectangular blow holes were used,

as opposed to the circular blow holes. Larger angles of the subjects to the main sand/air jet gives rise to these subjects flowing comparatively more in the direction of the side channels, which enhances primary compaction in them. Thus the size and shape of the blow hole can be used to control the formation of the subjects and direct these in such a manner as to aid primary compaction in those areas of the core-box where the primary jet has no influence on.

Experiment numbers 10 to 15 showed that different venting arrangements could also be used to control the behaviour of the subjects. One sided venting of the core-box gives rise to easier flow from that side which results in greater flow of air and sand to that side. This in turn enhances both primary and secondary compaction in that side. The resultant cores produced in this way were clearly better compacted on the side with the vents open.

6.6.1.2. Group b

The preliminary experiments carried out in this group on core-box number two revealed an explosive type phenomenon occurring during the filling process when blow holes of 5, 10, 15 and 20mm in diameter were used. This was also observed when the triangular or the rectangular blow hole (equivalent in area to that of ϕ 15mm blow hole) were used. In all cases this phenomenon occurred approximately 0.1 sec after the start of sand flow into the core-box. This situation may arise from two different conditions.

The sand/air jet on arrival at the bottom of the core-box spreads and as more sand arrives a pile of sand is built up, Fig 139. It is reasonable to assume that the speed of the jet during this time is not at its highest, since the air pressure in the magazine would still be increasing to its peak. Once the air pressure in the magazine reaches its peak, the sand/air jet can attain its highest speed. If this is sufficiently high for the jet to penetrate the pile of sand already in the box and reach the bottom of the core-box, a unique situation arises. On collision with the bottom of the core-box the sand particles in the jet will bounce and travel at different angles to the main jet according to their kinetic energies. In doing so, they will collide with other sand particles in their paths and thus push them away as illustrated in Figs 139-143. Observations of a similar phenomenon were noted during experiment number seven of group a, where a triangular blow hole was used, Fig 93.

Alternatively, the concentration of sand in the main sand/air jet could decrease while the concentration of air in it could increase as a result of channelling in the magazine. In the extreme case a channel forms through the entire mass of sand in the magazine, at which time a jet of only air enters the core-box. The jet of air could then penetrate the pile of sand already in the core-box to reach the bottom of it. The air on collision with this section turns towards the vents in order to escape, and thus pushes the pile of sand away towards the vents. This

is illustrated in Figs 149-150, where a blow hole of 5mm in diameter was used.

Comparison of the results obtained from experiment numbers 3, 7 and 8, Fig 138, shows that changing the shape of the blow hole while its area is kept constant does not affect the filling time when blowing under the same blowing conditions. These results again suggest that the average mass flow rate of sand into the core-box is dependent on the area of the blow hole. Furthermore, changing the blow hole shape did not result in any advantages or disadvantages in terms of the core-weights and soundness. Since the pattern of filling with all three blow holes were similar, the same overall compaction of the cores is achieved and, therefore, the core-weights are the same.

Experiment numbers 9 to 20 showed the effect of the venting arrangement on the sand flow in the core-box, the filling time, and the core-weight, Fig 152. When blowing is carried out with all vents open, sufficient venting of the core-box is apparently present and incoming air is easily exhausted from the box leaving sand behind. The resultant core is a sound well compacted one. However, when the venting area in the core-box is reduced to a level insufficient to exhaust the volume of the incoming air, a back pressure is set up in the box during the blowing process. This leads to a reduction of the pressure gradient between the mouth of the magazine and the core-box. Consequently, the flow rate of air and sand from the magazine is reduced, this can be seen from the longer filling times obtained, Figs 138 and 152.

This, in turn, results in poorer compaction, lower weights and voids seen in the cores.

The experiments also revealed that venting in the higher regions of section two of the core-box, Fig 137, produced better results in terms of compacting the cores than venting in the lower regions of this section. This is due to a build up of back pressure in the core-box which takes place comparatively earlier when the venting is provided in the lower regions of the core-box (i.e. as soon as layers of sand block off the vents and restrict air flow out of the core-box). Also, when the venting is provided in the higher regions of the core-box, compaction of the sand in these regions can take place by the secondary route as well as by primary compaction. Venting in the lower regions of the core-box gives rise to core defects in the form of small voids, in the highest regions of the core-box, Figs 159-161, as these are now devoid of secondary compaction and may also have insufficient primary compaction due to pressure build up in the box.

6.6.2. Group 2. Preliminary experiments on blow hole area and air pressure vs core-weight

The results of this group of experiments show that for a given blow hole increasing the blowing pressure gives rise to increases in core-weight. This is due to increased flow rates of sand and air from the magazine into the core-box. However, there are optimum values of the blowing pressure beyond which significant improvements in compacting the cores cannot be achieved.

Increasing the blow hole area may be expected to increase the compaction of the cores and their weights. However, the results of this group of experiments showed that the heaviest cores were produced when the $\phi 15\text{mm}$ blow hole was used and the lightest cores were produced when the $\phi 30\text{mm}$ blow hole was used, Fig 166. This is due to the order in which these experiments were carried out. The blow hole of 15mm in diameter was used at the start of this series of experiments. As cores are produced, the vents in the core-box gradually are blocked with sand and binder. This gives rise to a continual reduction of the available venting area in the core-box, which in turn results in continual reduction of both primary and secondary compaction. It is important to note that the negative effect on compaction resulting from decreased venting area can overcome the positive effect resulting from increased area of the blow hole. The sand/air flow rates are thus governed by the smallest area in the system.

6.6.3. Group 3. Blow hole area and blowing air pressure vs core-weight

The results of these experiments confirm that for a given blowing condition increasing the blowing pressure and/or increasing the blow hole area result in increasing the overall compaction of the cores, produced, Figs 169-170, 172-173.

The results obtained from the experiments carried out in sub-group a, on filling times as the blowing pressure was changed, confirm that the flow rates of sand and air are decreased as the blowing pressure is decreased. This is established from the longer filling times recorded at lower blowing air pressures, Figs 167-168.

The results of the experiments carried out in sub-group b show that higher core-weights are obtained as a result of incorporating more vents (suitably positioned) in core-box number two. These vents are shown with dotted circles in Fig 137 on sections 2 and 3 of the core-box. The extra venting in the core-box promotes both primary and secondary compaction in the manner previously described.

6.6.4. Group 4. Binder level vs core-weight and soundness

The results of the experiments carried out in this group on core-box number one show that for a given blowing condition heavier cores were produced when the binder level was at 0.35%. Furthermore, the cores were comparatively much sounder than those produced from a sand binder mix containing 1.05% binder. The latter cores were either spongy or contained voids at the end of the side channels and/or around the middle of these channels on the bottom walls. It must be noted that these areas are not in the direct paths of the subjects during the filling process.

In explaining the compaction problems experienced when the higher binder level was used, primary and secondary compaction must be considered separately.

Comparison of the filling times, show that the average flow rates of sand from the magazine into the core-box are similar for the two binder levels, (as the filling times recorded under the same blowing conditions are similar). Therefore, the kinetic energy of the jets in both cases are similar which gives rise to approximately the same primary compaction force. However, the mix containing 1.05% binder was noticeably stickier than that containing 0.35% binder. This extra stickiness can cause a reduction in the flowability of the sand in the box and consequently a reduction in the effect of primary compaction.

The re-occurrence of the voids seen, when the mix contained 1.05% binder, at those areas where densening is largely the resultant of secondary compaction indicates

that the sand particles in these areas have been rearranged to, comparatively, a lesser degree by the flow of air through them. This is because the concentration of resin at the inter-particle contact points within this mass of sand/binder mix is greater, Fig 211, giving rise to comparatively higher capillary forces between the sand particles. It is also reasonable to assume that the mix containing 1.05% binder will be less permeable than the mass of partially resin coated sand particles in the mix containing 0.35% binder. Lower permeability of a mass of sand reduces the flow rate of air through it which in turn results in the reduction of secondary compaction.

The results obtained using core-box number 2 show that at times comparatively heavier cores were produced using a sand-binder mix of 1.05% binder level. These cores also contained voids and spongy areas, whereas the cores produced under the same blowing conditions using a sand-binder mix of 0.35% or 0.7% binder levels were sound. Such results indicate that a core can be compacted to a high weight as a result of sufficient primary compaction and still contain voids and spongy areas as a result of insufficient secondary compaction.

The above experiments were carried out in a random order and the core-box vents were not thoroughly cleaned before the start of each series of experiments. It, therefore, follows that it is not possible to directly compare the results obtained from different binder levels. It has already been established that compaction within this core-box is highly sensitive to the area and position of its vents, and the results obtained here

confirm that these effects can outweigh the effect of increased binder content.

In order to enable the direct comparison of the results obtained according to different binder levels in the mix experiments in group 5 were carried out.

6.6.5. Group 5. Further investigations of the effect of binder level on core-weight and soundness

Comparison of the core-weights obtained from using sand binder mixes containing 0.35% and 0.7% binder did not show any significant differences. Comparison of the cases of 0.35% and 1.05% binder levels revealed that, at the highest value of the blowing air pressure and the highest value of the blow hole area, slightly heavier cores were produced with the 1.05% binder level. The difference in the core-weights obtained (0.5% to 0.8%) from the two cases gradually decreased with decreasing values of air pressure and blow hole area until ultimately the cores produced from the mix containing 1.05% binder became lighter than those produced from the mix containing 0.35% binder level. This is due to the variation of primary and secondary compaction according to different blowing conditions.

A jet produced via a large blow hole and under a high blowing air pressure will have a high value of kinetic energy. For instance, the sand/air jet produced via the $\phi 25\text{mm}$ blow hole at a blowing pressure of 5.86 bars (85 psi) has the highest kinetic energy within the experiments carried out, since it gives rise to the fastest filling time and the heaviest core. Under such conditions when primary compaction forces are high capillarity does not hinder sand flow in the core-box. Since the overall compaction in core-box number two is largely achieved via primary compaction, it is possible to produce cores of similar weights using sand/binder mixes containing the different binder levels. The

percentage increases in the core-weight recorded when using the mix containing 1.05% binder are approximately the same as the percentage increase in the binder level.

Alternatively, when the blowing pressure is at its lowest and the smallest blow hole is used, the resultant sand/air jet is a comparatively weak one having the lowest kinetic energy. Under such conditions, where the subjects do not travel far from the main sand/air jet and the primary compaction forces are low, capillarity can affect sand flow within the core-box. It, therefore, follows that the mass of sand containing 0.35% binder will be more compacted under both primary and secondary compaction forces. Consequently, comparatively sounder and heavier cores are produced as indicated by the results.

6.6.6. Group 6. Core blowing using silica sand

The results of the experiments carried out on core-box number one shows that the core-weight obtained decreased as the binder level in the mix increased. Furthermore, the soundness of the cores, particularly in those areas that are not in the direct paths of the subjects, deteriorated as the binder level in the mix increased. The deterioration of the cores was pronounced in the case of 2.25% binder level as the blow hole area and/or the blowing pressure were reduced. These results further confirm that decreasing the binder content enhances the flowability of the sand-binder mix and increases secondary compaction of the mass in the core-box.

The results obtained from the experiments carried out using core-box number 2 also confirm the above. For any blowing condition, increasing the binder level either did not result in any significant changes in the core-weights or gave rise to small decreases in them, Fig 212.

Some sand spraying out of the vents was observed during the blowing process. This occurs as the sand layers in the box reach the vents. The smaller sand particles closest to the vents are carried out by the escaping air. This phenomenon also occurs after the air reservoir valve has been shut, due to the residue of compressed air in the sand magazine which continues to flow through the mass of sand in the magazine and the core-box and is finally exhausted via the vents. Sand spraying was largely apparent in the case of the lower

binder level (0.75%), since the mass of sand particles are less bound together.

Such observations were also recorded during similar experiments using zircon sand. The sand spraying in these experiments was also largely apparent in the case of the lowest binder level of 0.35% and virtually non-existent in the case of 1.05% binder level. The amount of sand spraying also decreased as the blow hole area and/or the blowing pressure was decreased. This is due to the comparatively lower volumes of air entering the core-box under the above blowing conditions. It is the occurrence of this phenomenon during the blowing process and also during the hardening cycle that gives rise to lines and pockets of sand seen missing on section 3 and 2 of core-box number two respectively. The amount of sand missing decreased as the binder level was increased. Also, the amount of sand missing seen when using zircon sand was more than that seen when using silica sand. This could be attributed to the finer grains of zircon compared with the coarser grains of silica used.

Overall, comparison of the results obtained when using silica sand with those when using zircon sand revealed that better flowability and compactability were achieved when using the former sand.

Comparison of the two core-boxes revealed that core-box number one is more sensitive to binder level than core-box number two. This is due to comparatively more of the overall compaction in core-box number two resulting from primary compaction.

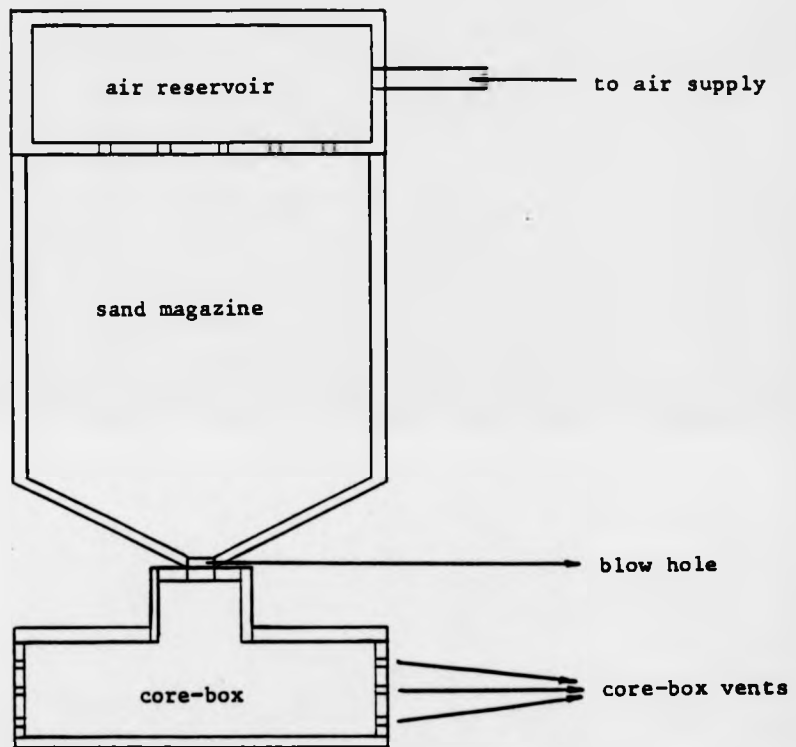
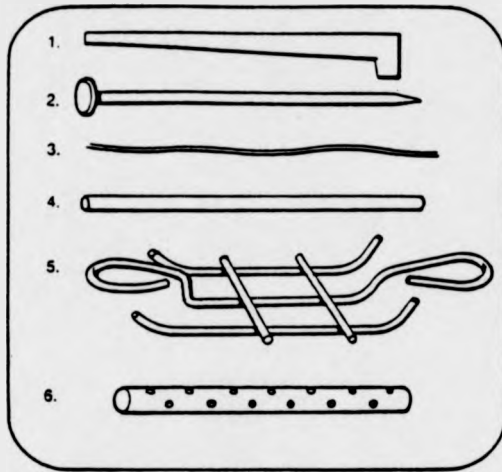


Fig 1. Section through core blower and core-box



- 1) sprigs
- 2) nails
- 3) wire
- 4) rod
- 5) rod grid construction
- 6) perforated tube

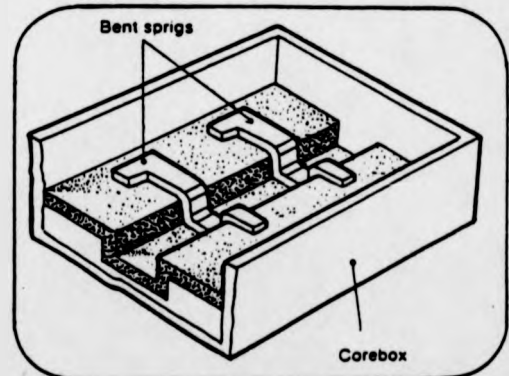
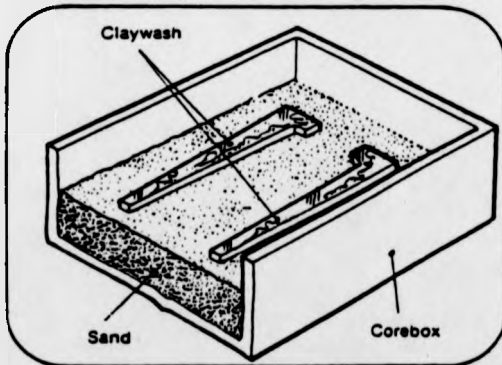
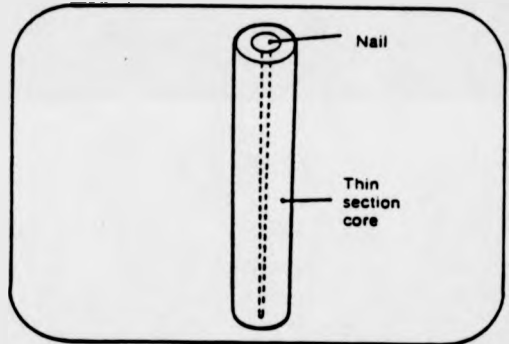
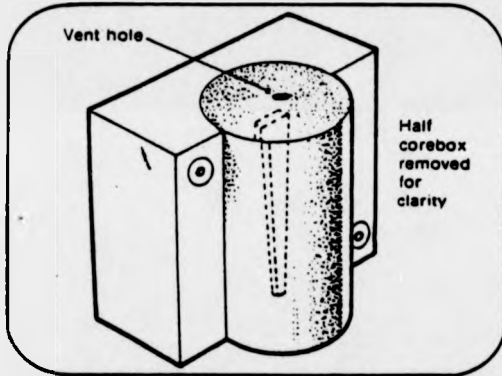


Fig 2. Core reinforcement, EITB publications⁽²⁾

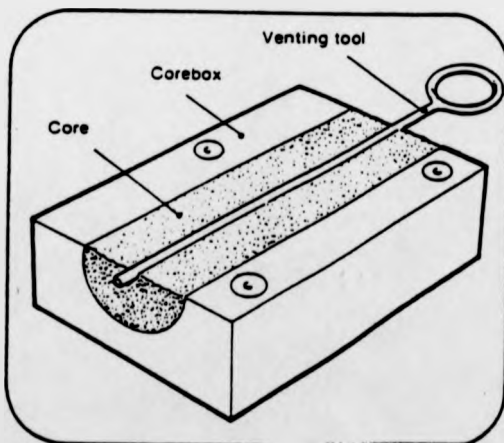
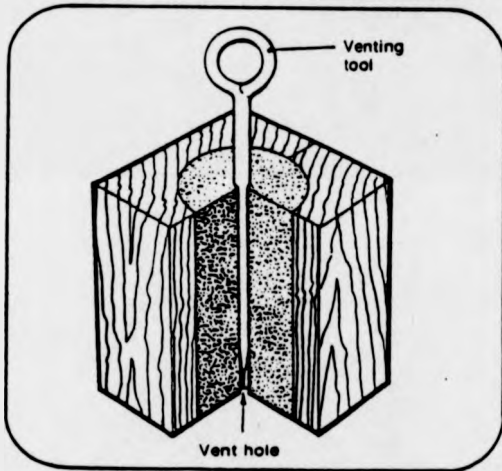
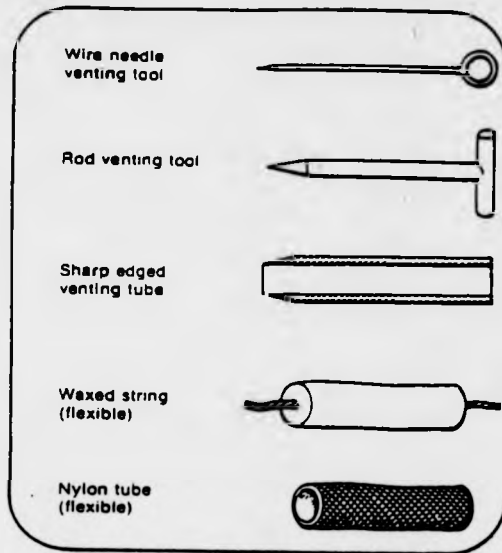
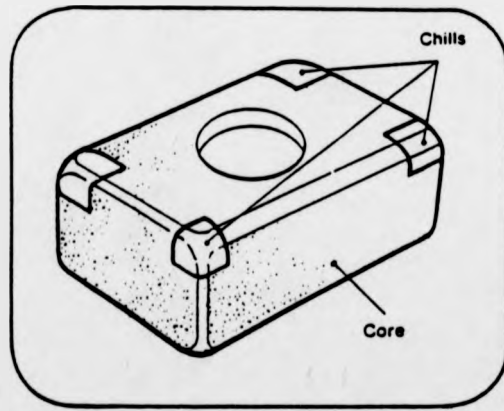
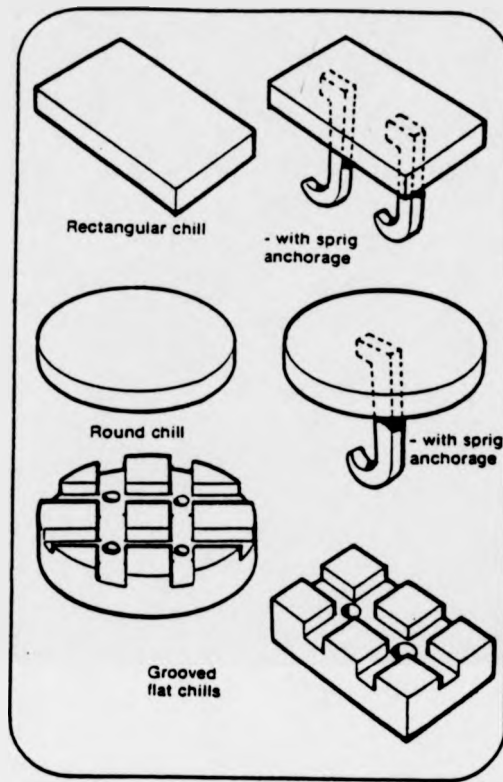
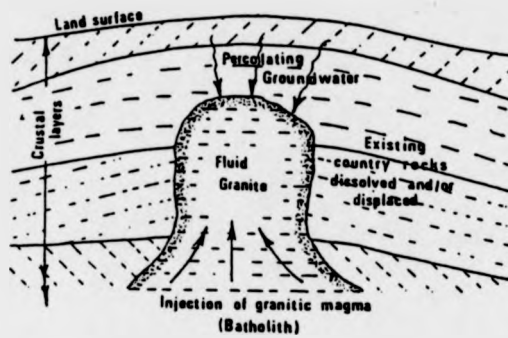


Fig 3. Core venting tools, EITB publications⁽²⁾

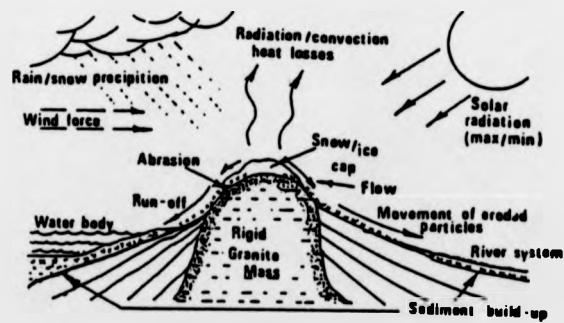


Core with corner chills

Fig 4. Core chills, EITB publications(2)



Initial source of silica-bearing rock mass



Erosion and transport of the granitic rock

Fig 5. Sedimentation processes, Webster(5)

Name	Location	Origin	Type	GF No	Type of Grading	GRAB Shape	GRAB Surface	cm ² /g Sp. Surface	SiO ₂	Al ₂ O ₃	Fe ₂ O ₃	Alk	Clay	% exp ¹ 1,550°C C-2-1 Retractormess
Messingham	Lincoln	Recent	Silica	64	1	S/a		140	95	2.3	0.2	1.2	0.9	5.3
Southport	Lancs	Recent	Silica	70	1	r-S/a		126	93	2.3	0.9	1.1		
Irvine	Ayrshire	Recent	Silica	70	1	r-S/a		90	90	3.7	2.2	1.6		
Chelford	Cheshire	Glacial	Silica	47	1	S/a	abraded	98	96	1.5	0.2	0.9	0.3	7.7
Windsor Ross	Cheshire	Glacial	Silica	68	1	S/a		133	96	1.6	0.6	1.9	0.2	3.7
Coalgaton	Cheshire	Glacial	Silica	63	1	S/a		123	96	2.0	0.3	1.0	0.9	3.9
Erith	Kent	Tertiary	Nat Bond	170	2	S/a							10.0	
Southampton	Hants	Tertiary	Nat Bond	100	2	S/a		(240)	87	3.6	4.1	2.8	15.8	
Calve	Wilt	Tertiary	Silica	60	1	S/a		(140)						
Erith	Kent	Cretaceous	Silica	60	1	S/a		128	99		0.6	0.1	nil	6.4
Redhill	Surrey	(Lower Greensand)	Silica	131	1	S/a-a	abraded + corroded	260	99	0.2	0.1	Tr	0.6	5.9
Reigate	Surrey	(Lower Greensand)	Silica	35	1	S/a		(70)	99	0.1	0.1	Tr	nil	
King's Lynn	Norfolk	(Lower Greensand)	Silica	70	1	S/a	abraded + lobed	153	98	1.0	0.1	0.5	0.3	5.8
Leighton Buzzard	Beds	(Lower Greensand)	Silica	60	1	r-S/a		140	98	0.4	0.2	0.2	1.0	5.7
Pickersing	Yorks	Jurassic	Nat Bond	105	2	S/a		(240)	90	4.5	1.4	2.0	24.0	slumped
Devon	Wilt	Jurassic	Nat Bond	105	2	S/a								
Wimborng	Northants	Jurassic	Silica	90	1	S/a	abraded lobed faceted	200	97	1.0	0.6	0.6	0.4	3.0
Bromsgrove	Worce	Triassic (Blunier)	Nat Bond	110	2	S/a		(260)	87	7.5	1.4	2.3	12.0	
Manafield	Notts	Triassic (Blunier)	Nat Bond	130	2	S/a			78	10.1		3.2	14.0	
Kinnerton	Cheshire	Triassic (Blunier)	Nat Bond	54	2	S/a			90	4.5	1.3		6.2	
Manafield	Notts	Triassic	Silica	54	1	S/a		(110)	93	4.1	0.4	1.9	nil	
Levenson	Leamk	Carboniferous	Silica	55	1	Se-a		130	99	0.5	0.1	0.1	0.4	6.0
Levenson	W Lothian	Carboniferous	Silica	116	3	1		301	97	1.9	0.2	0.6	—	
Milngava	Dumbaron	Carboniferous	Silica	60	1	S/a-a			98	0.6	0.6	0.1	—	1.0
Dullatur	Dumbaron	Carboniferous	Nat Bond	40	3	S/a			90	5.7	0.9	1.4	17.0	
Scottish Rock	Leamk	Carboniferous	Nat Bond	73	3	S/a			84	7.2	2.1	0.2	15.2	
Tow Law	Durham	Carboniferous	Nat Bond	49	3	S/a-a		125	82	9.0	1.5	1.9	21.8	-1.7
Dursand	Durham	Carboniferous	Nat Bond	65	3	S/a-a			81	9.6	2.5	2.0	15.5	-6.6

(—) values approximate (r = rounded, S/a = sub-angular, a = angular).

Fig 6. U.K. silica sand deposits, Webster⁽⁵⁾

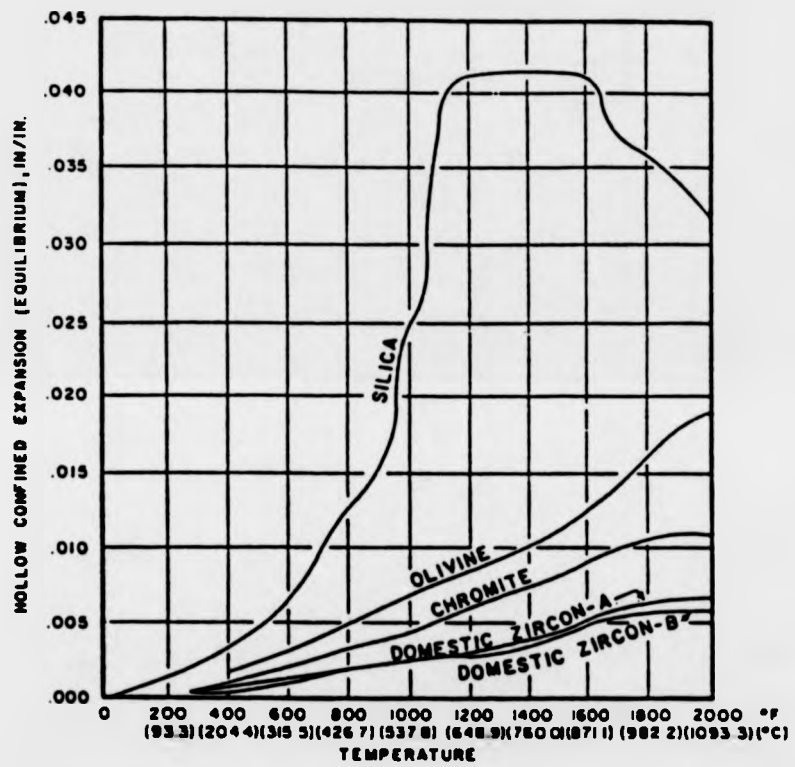


Fig 7. Thermal expansion curves for mineral sands, Garner⁽⁴⁾

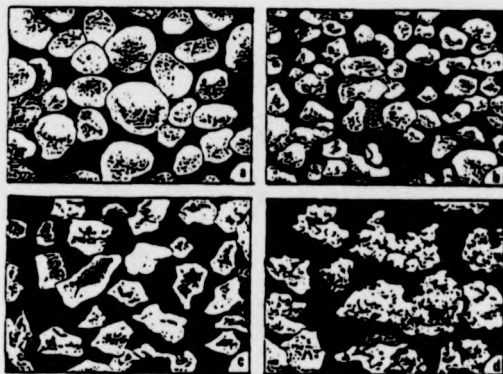


Fig 8. Basic shapes of sand grains: a. round, b. subangular, c. angular, d. compound, Webster⁽⁵⁾

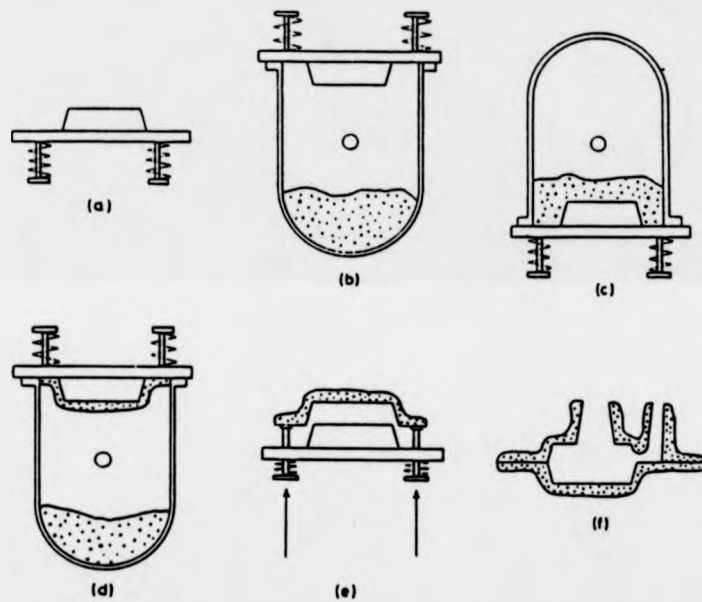


Fig 9. Basic production sequence in shell moulding: a. pattern plate, b. pattern plate mounted on dump box, c.,d. investment, e. ejection, f. shell assembly, Beeley⁽⁷⁾

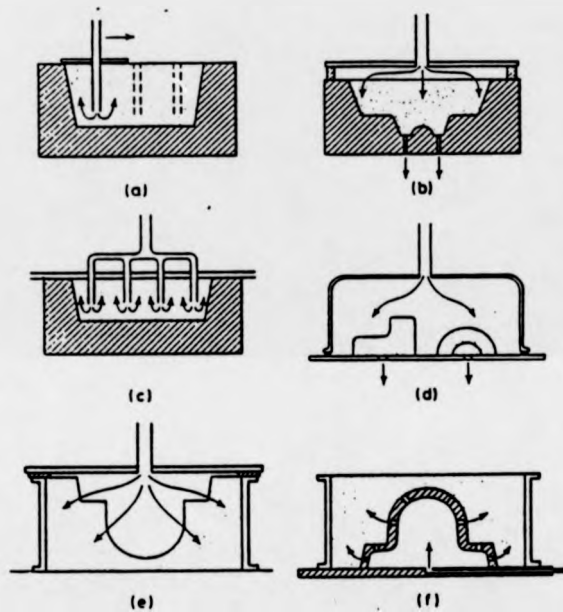


Fig 10. Examples of systems for carbon dioxide hardening of cores and mould parts: a. progressive treatment using single probe, b. cover board or hood, c. multiple probe, d. hood over previously stripped cores, e. treatment of mould after pattern draw, f. passage of gas through hollow pattern, Beeley⁽⁷⁾

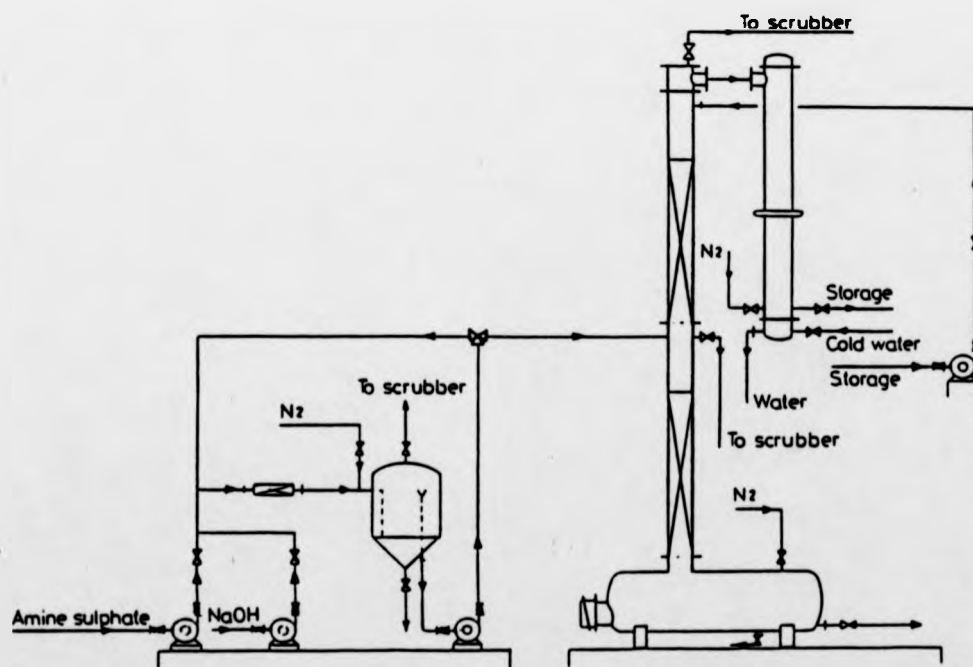
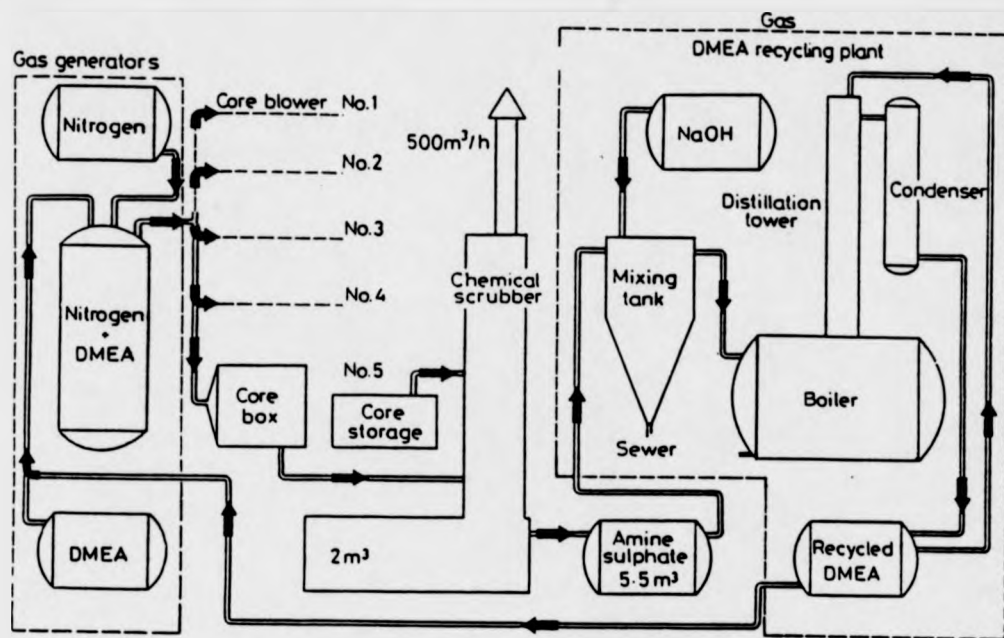


Fig 11. DMEA recycling plant, Kunsch⁽⁴⁸⁾

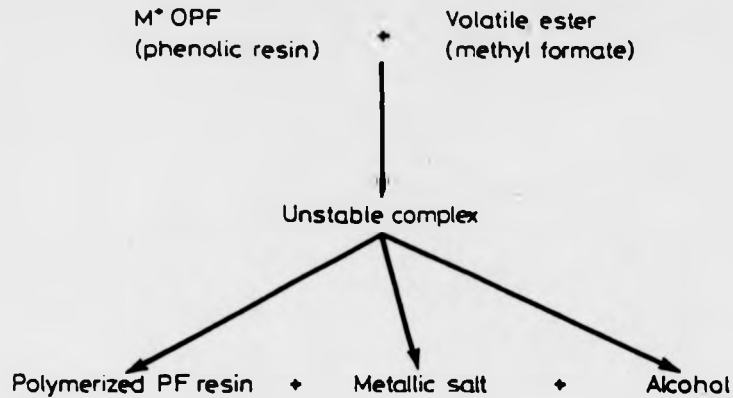


Fig 12. Schematic representation of the reaction mechanism of the Betaset process, Shephard⁽⁵¹⁾

Resin		Hardener	
Type -	Phenolic resole	Composition -	Methyl formate
Appearance -	Dark red	Appearance -	Clear, colourless low-viscosity liquid
Nitrogen content -	Negligible	Flash-point -	Below -20 °C
Viscosity (25°C) -	100 mPa.s (100 cP)	Boiling-point -	32 °C
Flash-point -	Above 65 °C	Latent heat of vaporization	481 kJ/kg
Free formaldehyde -	Less than 0.5%	Explosive limits	
Free phenol -	Less than 3.0%	(in air) -	5-23% v/v
Furfuryl alcohol -	Zero	Sulphur -	Zero
Isocyanates -	Zero	Recommended Limits:	
Relative density (20 °C) -	1.26	TWA-8h -	100 ppm
Storage (20°C) -	4 months	TWA-10min -	150 ppm
		Relative density (20 °C) -	0.97
		Storage life -	2 years

The properties of Betaset resin and hardener.

Magnesium	Stainless steel
Aluminium	High-alloy steels
Grey iron	High-conductivity copper
Nodular iron	Leaded gunmetal
Malleable iron	Manganese bronze
Ni-Hard	Aluminium bronze
Ni-Resist	Phosphor bronze
Carbon steel	Cupro-nickel
Manganese steel	Nickel-chrome

Fig 13. Alloys successfully cast with the Betaset process, Shephard⁽⁵¹⁾

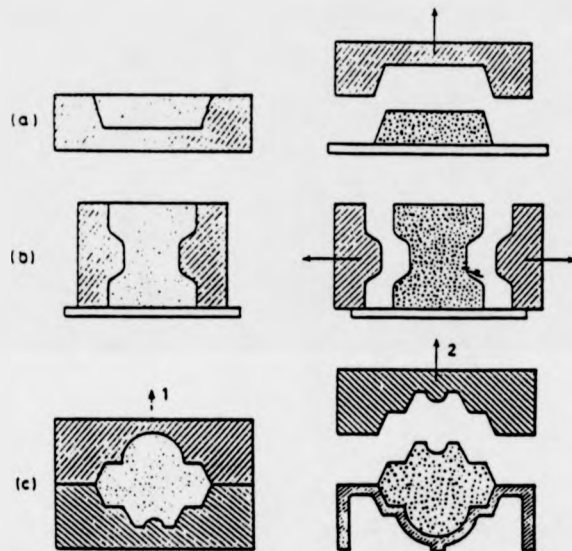


Fig 14. Core-box design: a. one piece open sided core-box, b. split core-box with vertical joints, c. split core-box, core turned out on to carrier, Beeley⁽⁷⁾

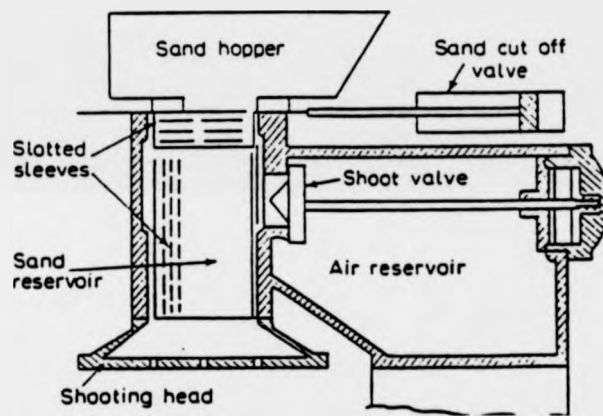


Fig 15. Section through coreshooter, Gardner(71)

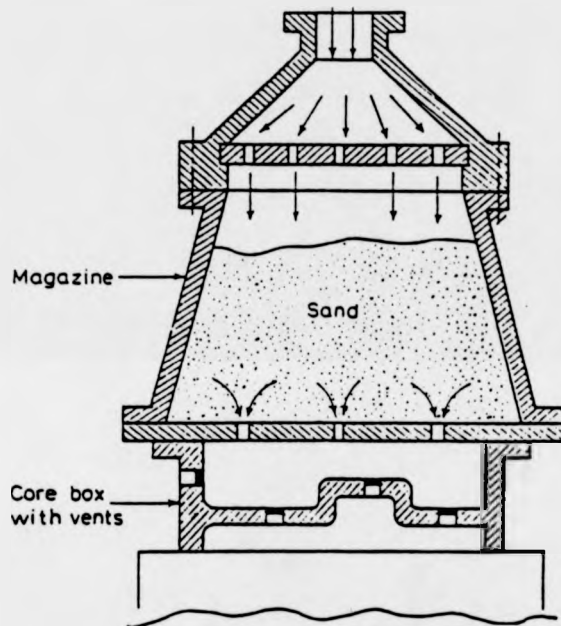
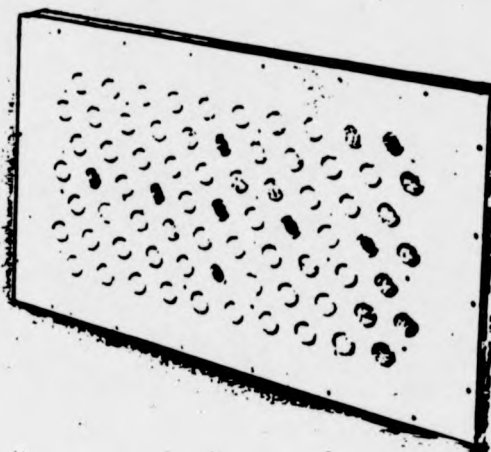
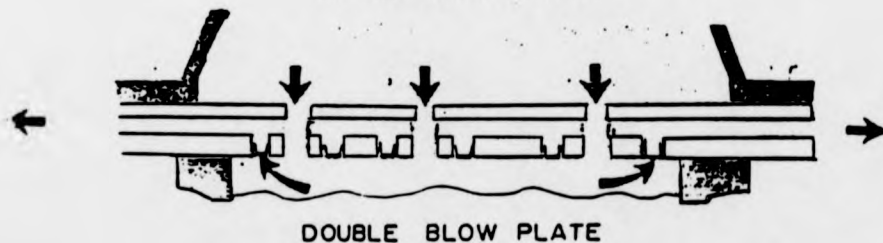


Fig 16. Section through coreblower, Gardner⁽⁷¹⁾

Universal plate permits versatile arrangement of tubes, vents.



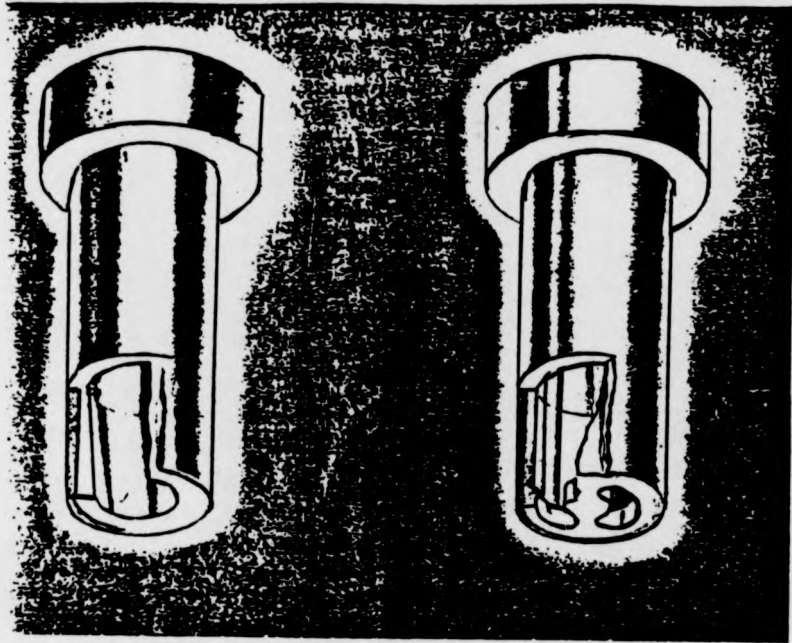
SINGLE BLOW PLATE



DOUBLE BLOW PLATE

The single blow plate seals the sand magazine and directs the sand into core box. The double plate provides more venting.

Fig 17. Universal, Single and Double blow plates, Clark⁽⁶⁴⁾



Blow holes may be round or slotted. They may be as large as possible without dumping the sand or small so as to spray sand.

Cross section showing three different blow tubes designed to break and clean at core line.

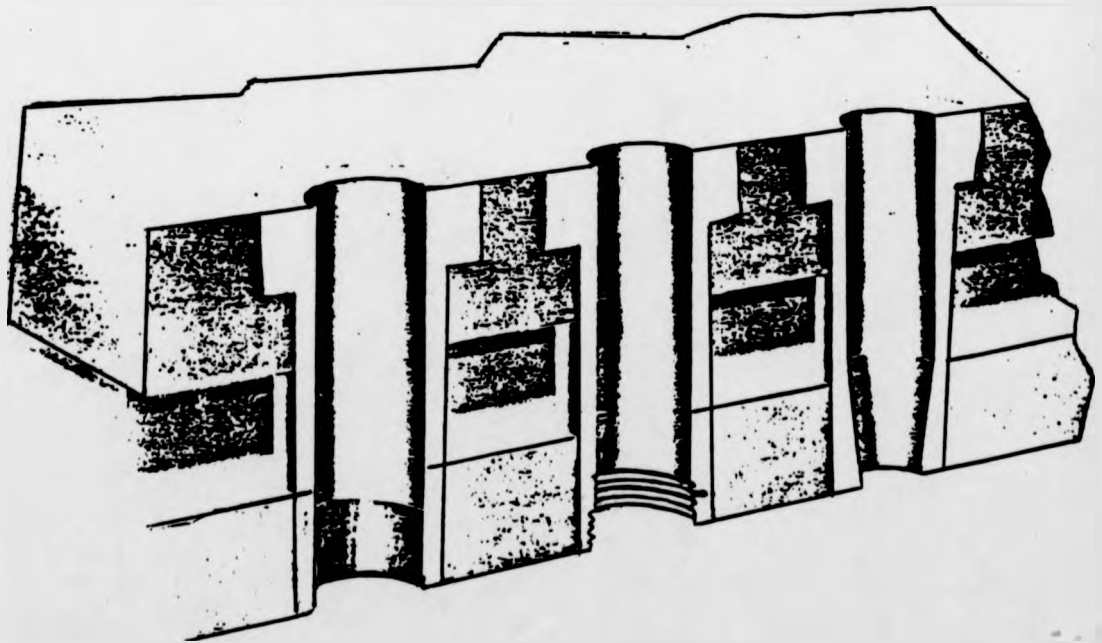


Fig 18. Various blow tubes, Clark⁽⁶⁴⁾

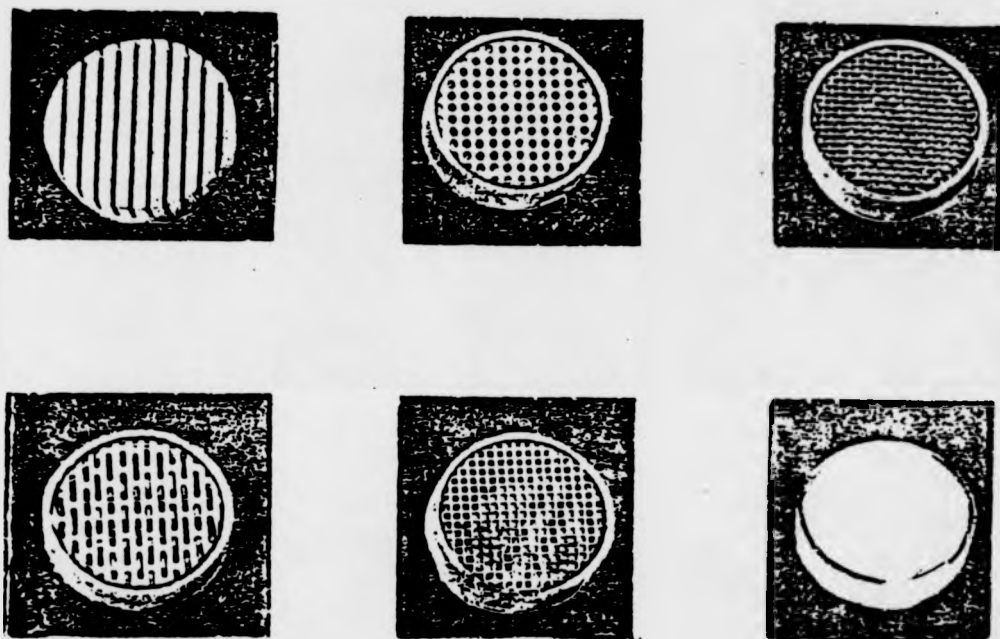


Fig 19. Various core-box vents, Clark⁽⁶⁴⁾

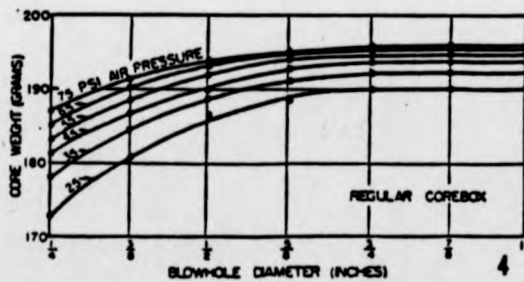
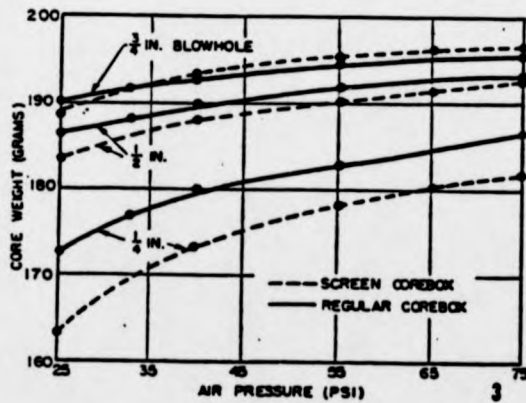
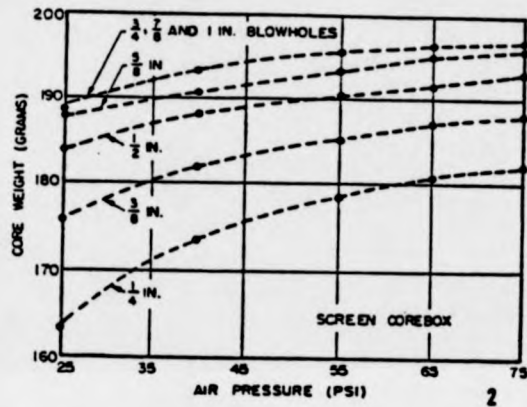
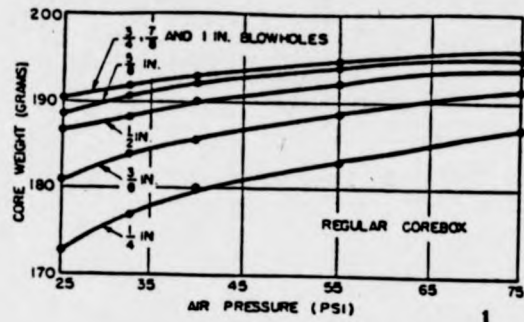


Fig 20. Variation of core weight according to different blow holes and air pressures, Gade⁽⁷⁵⁾

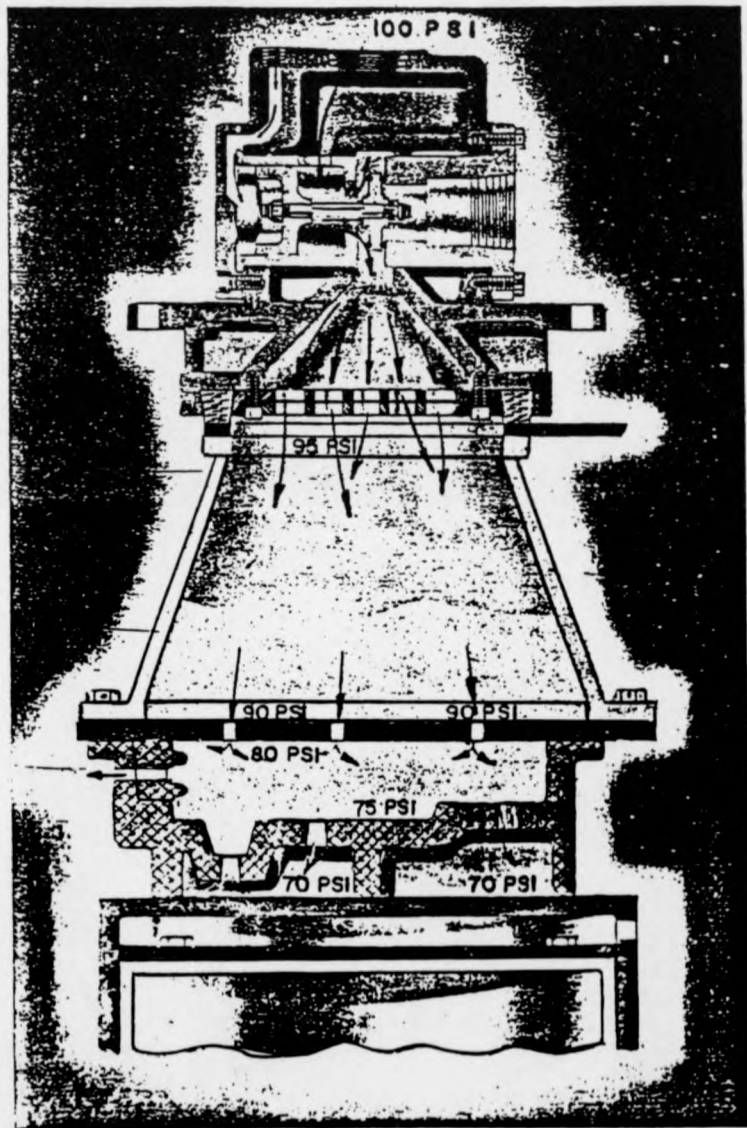


Fig 21. Satisfactory air pressure drop shown in diagram of core blower, Clark⁽⁶⁴⁾

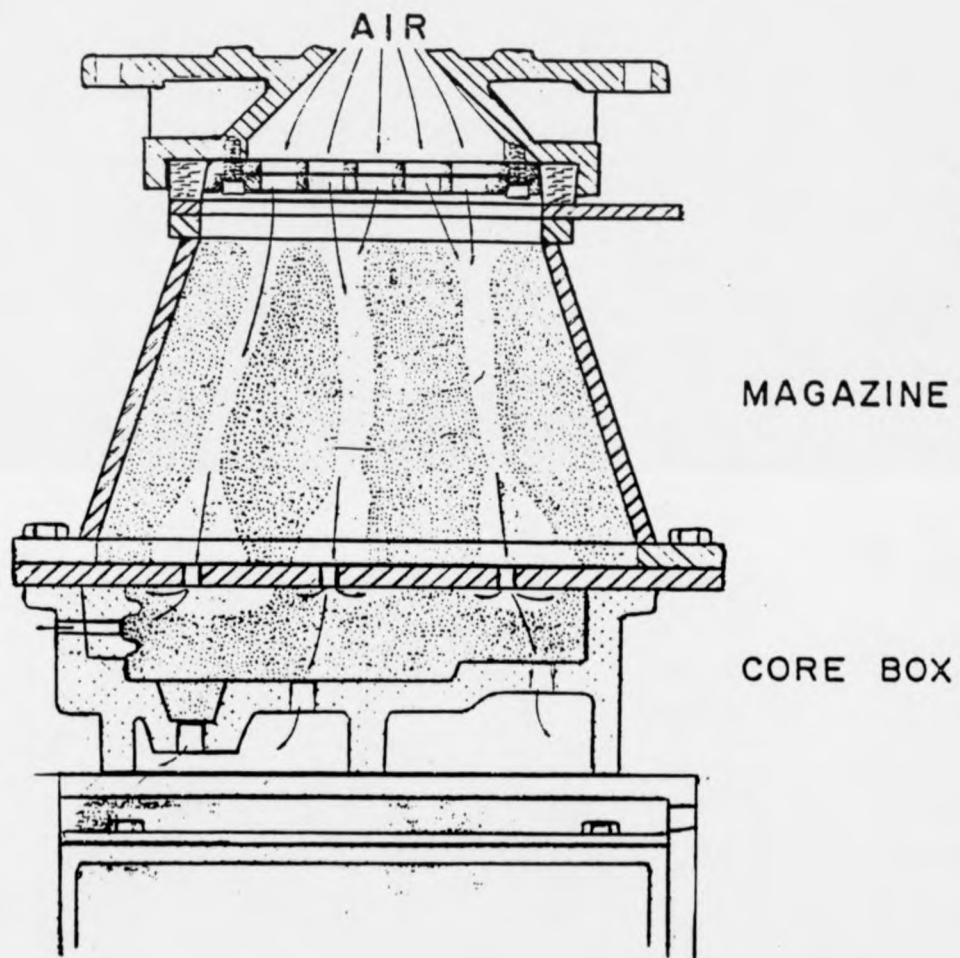
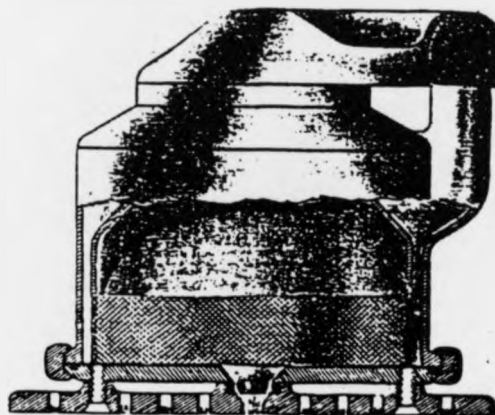
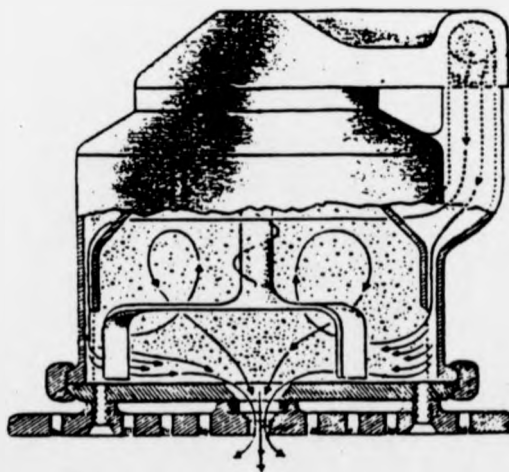


Fig 22. Formation of channels in sand magazine, Clark⁽⁶⁴⁾



Introducing air through screened liner reduces channeling by agitation in magazine.



Continuously rotating paddles may be used to break up channels and keep blow plate covered.

Fig 23. Techniques used to prevent channelling, Clark⁽⁶⁴⁾

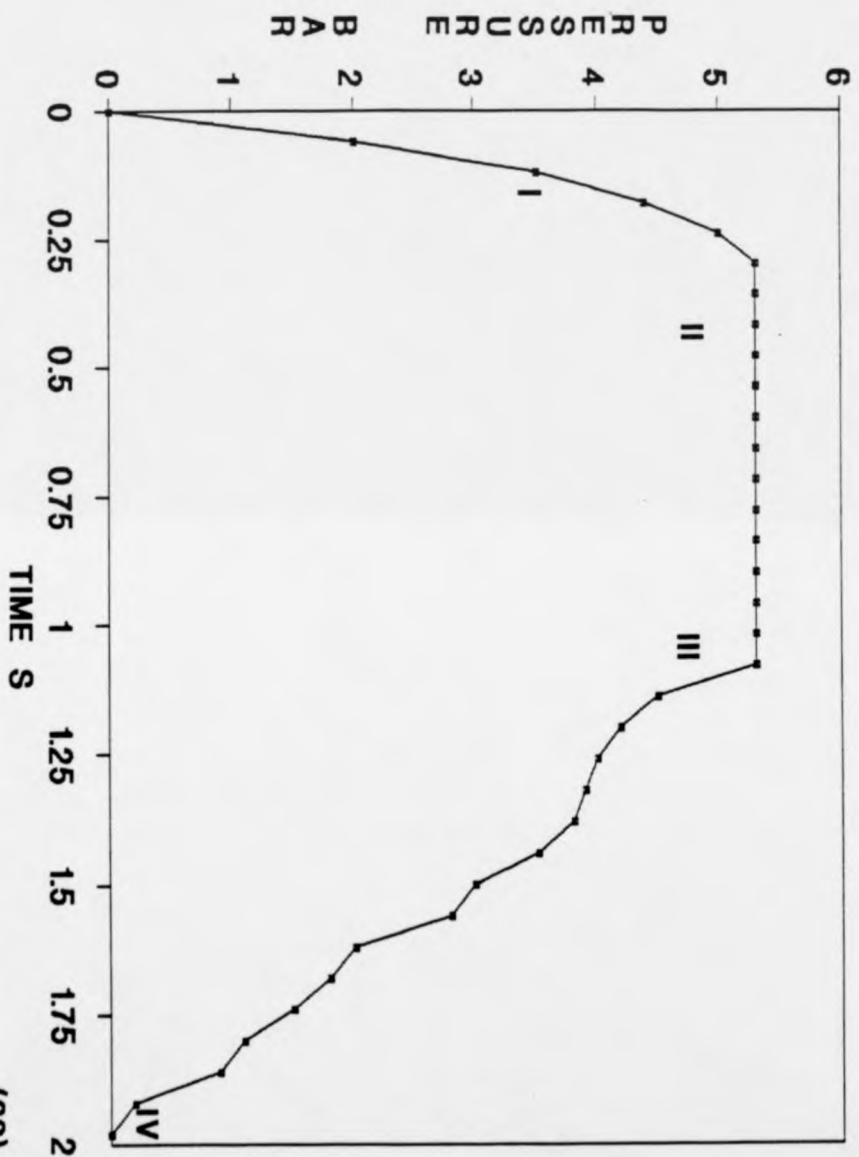


Fig 24(a). Pressure vs Time in the coreblower reservoir, Lesnichenko

(68)

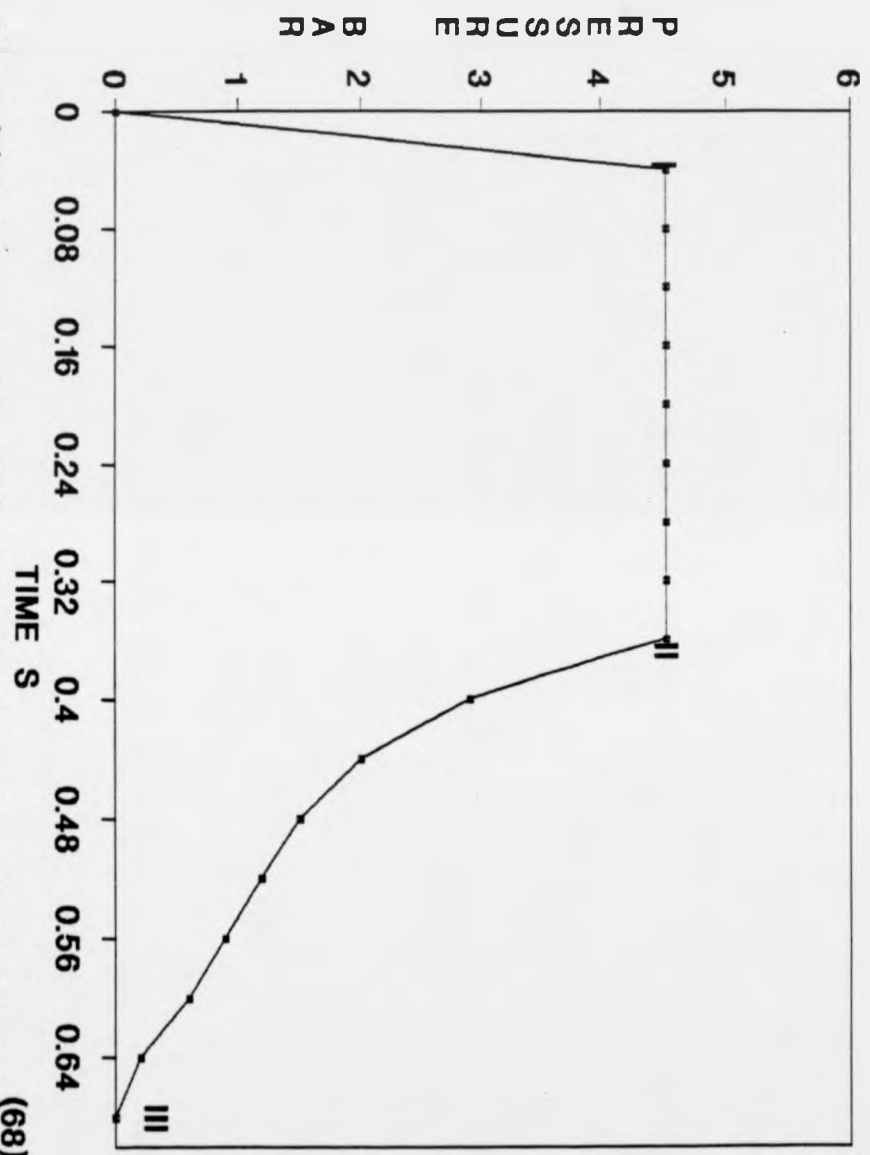


Fig 24(b). Pressure vs Time in the coreshooter reservoir, Lesnichenko (68)

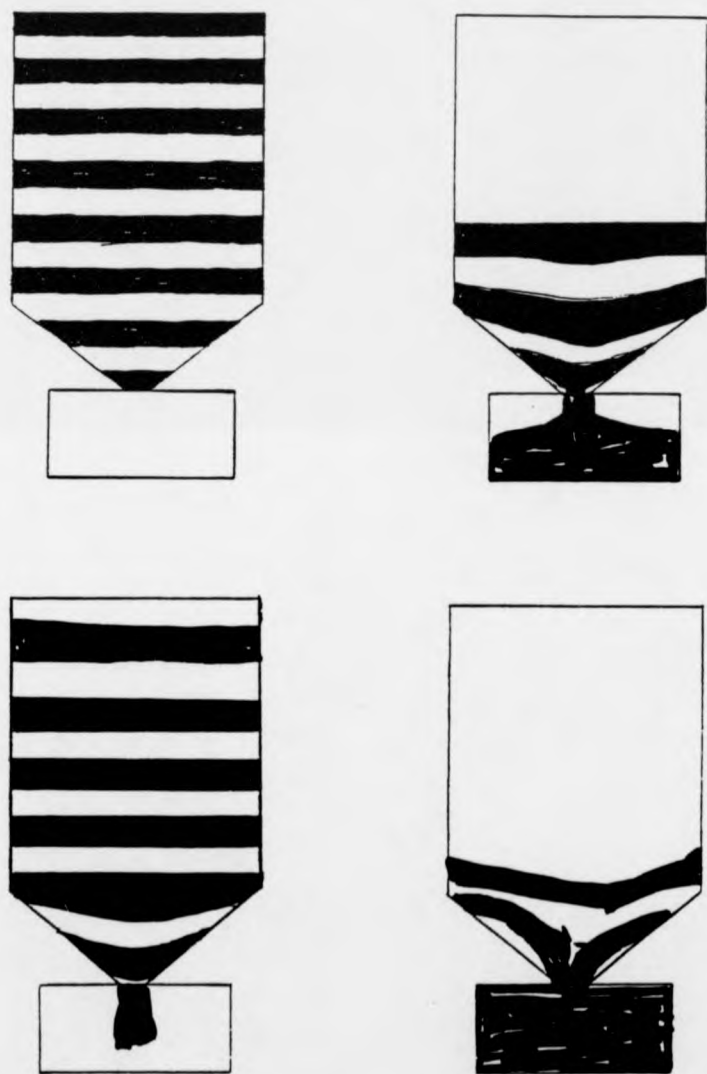


Fig 25. Movement of layered sand in sand sleeve, Geller⁽⁸⁰⁾

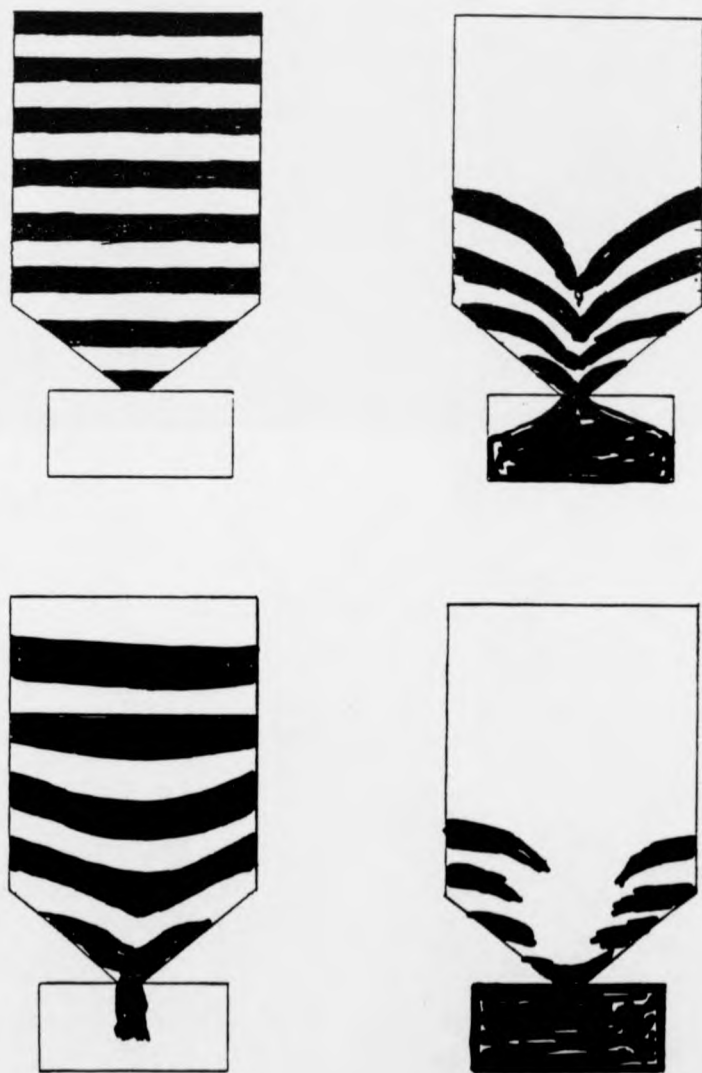


Fig 26. Movement of layered sand in sand sleeve, Geller⁽⁸⁰⁾

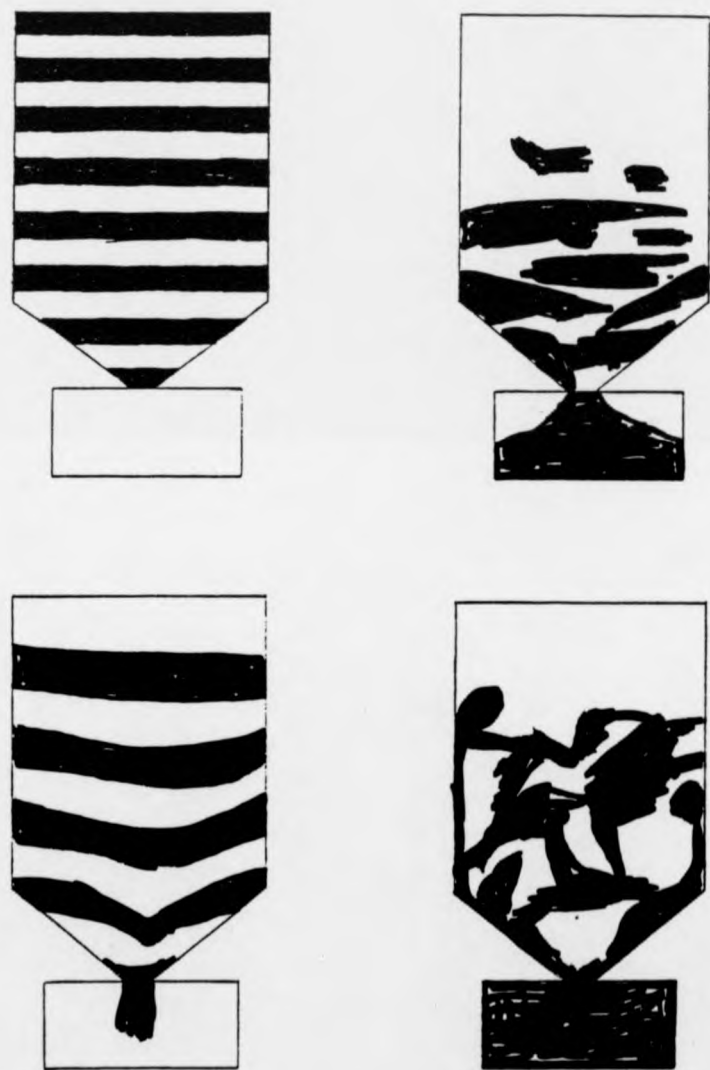


Fig 27. Movement of layered sand in sand sleeve, Geller⁽⁸⁰⁾

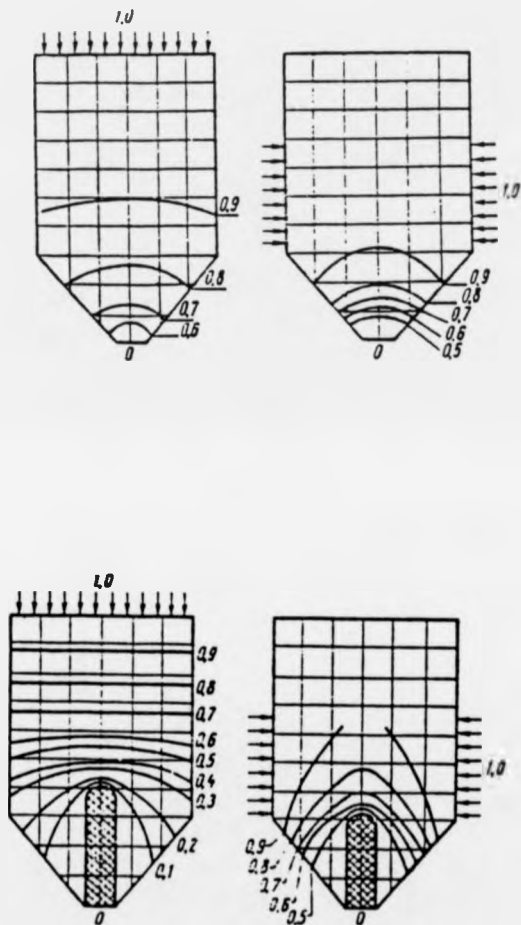


Fig 28. Air pressure variation in sand sleeve, Khurtov(70)

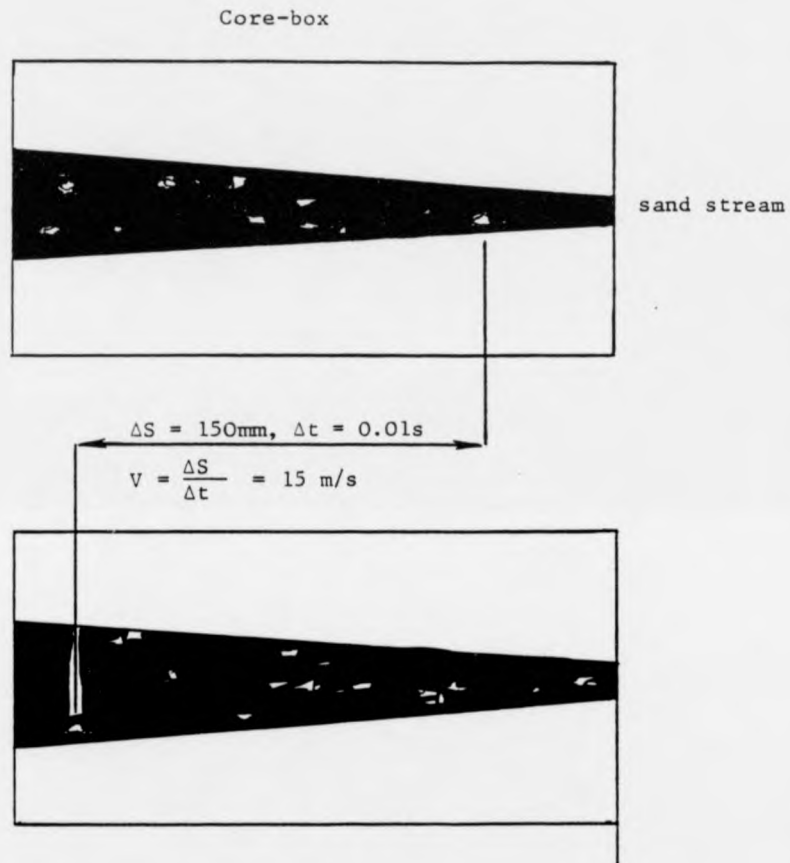


Fig 29. Movement of the contrasting substance in the sand stream, Pelczarski⁽⁸¹⁾

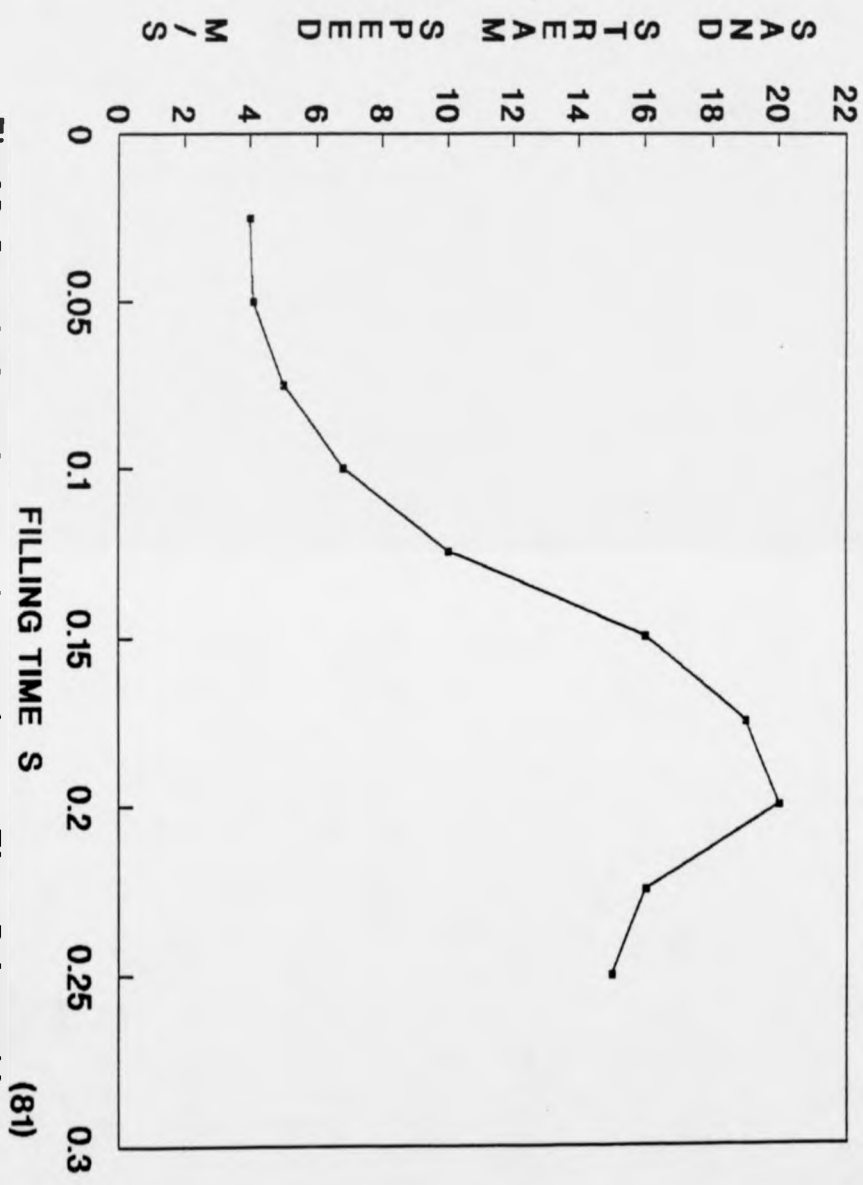


Fig 30. Speed of sand stream in core-box vs Time, Pelczarski

(81)

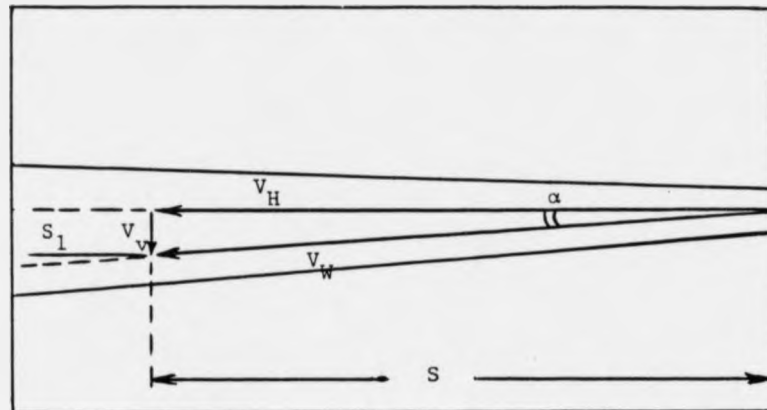


Fig 31. Determination of the horizontal component of the speed of the sand flow, Pelczarski⁽⁸¹⁾

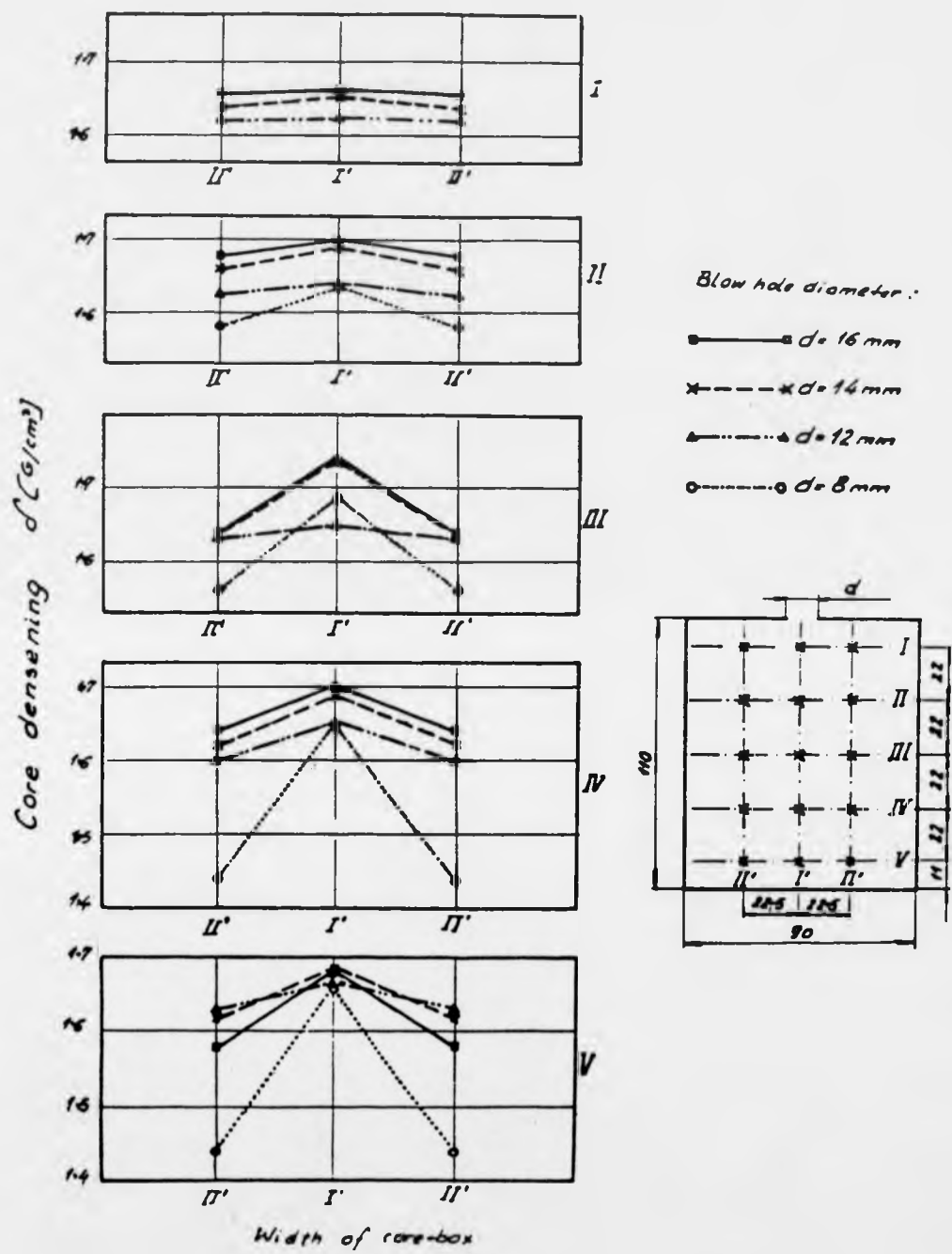


Fig 32. Variation of core density across and along the core-box, Pelczarski⁽⁸¹⁾

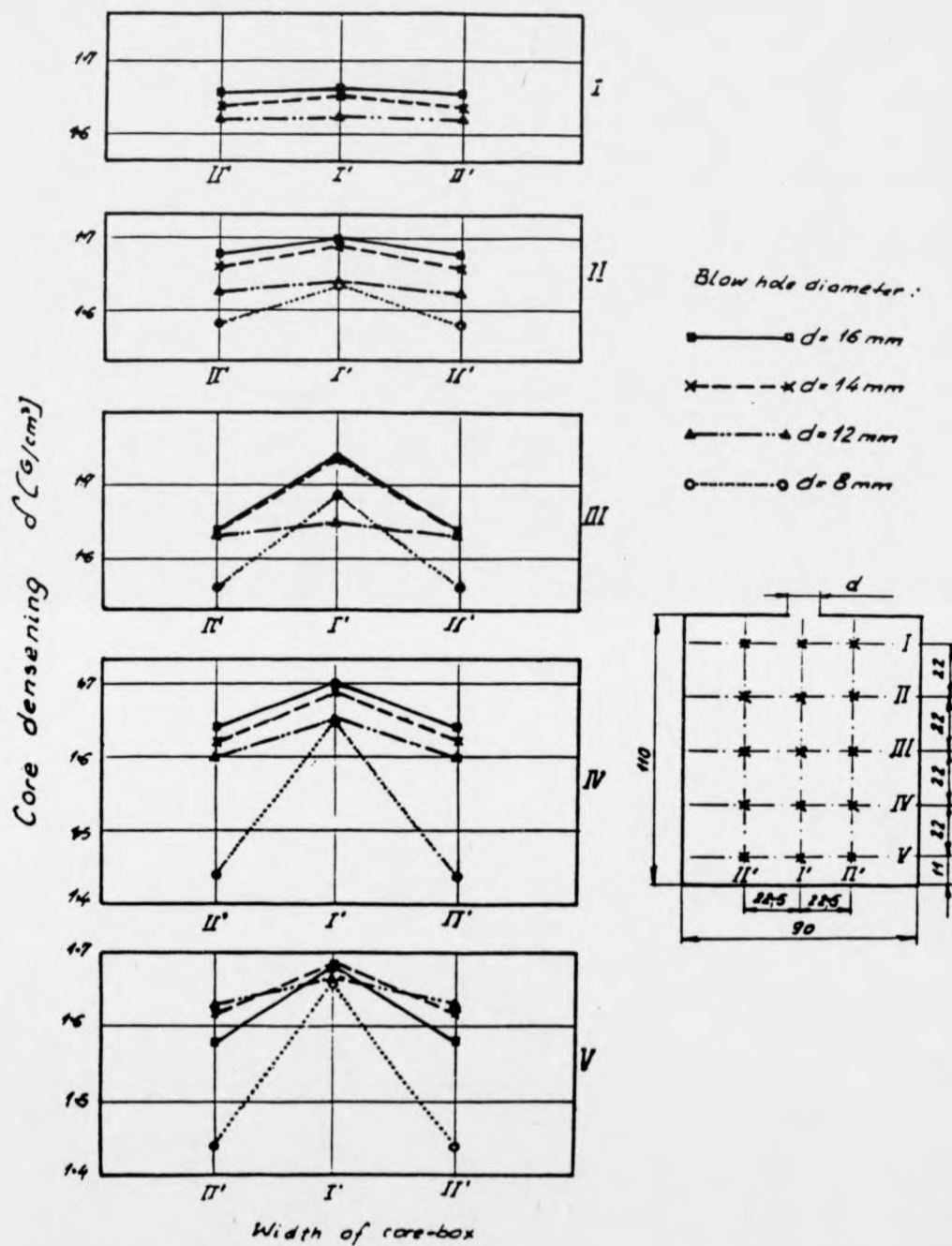


Fig 32. Variation of core density across and along the core-box, Pelczarski⁽⁸¹⁾

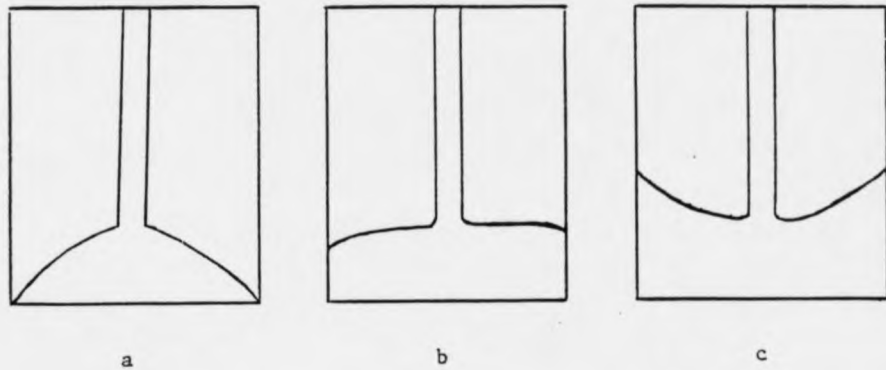


Fig 33. The shape of the free surface when filling the core-box with sand, Pelczarski⁽⁸¹⁾

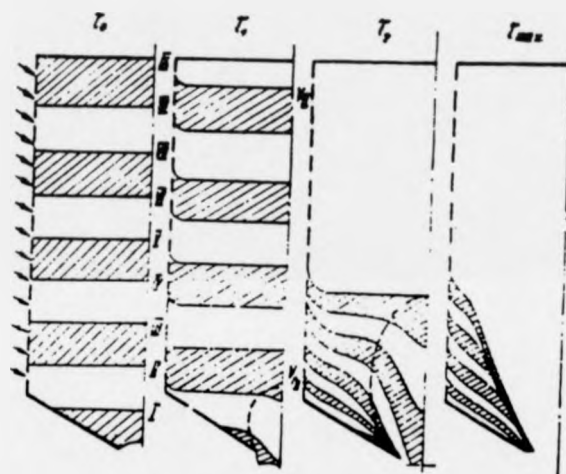


Fig 34. Movement of layered sand in sand magazine, Danko⁽⁸³⁾

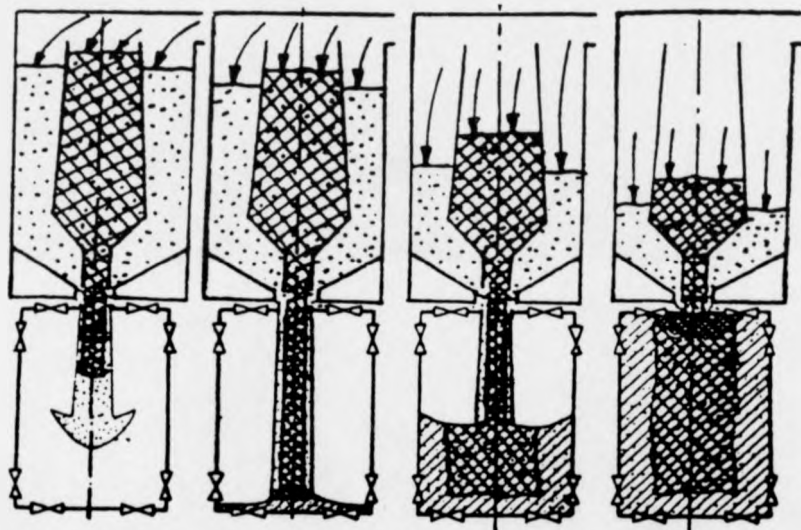


Fig 35. Core-box filling by two different sands, Danko⁽⁸³⁾



Fig 36. Core blower

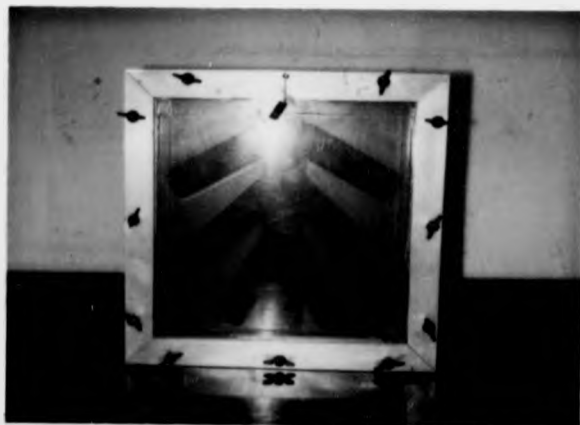


Fig 37. Core box number one

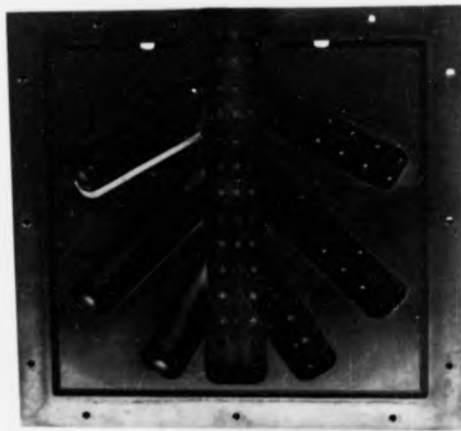


Fig 38. Main body of core box number one

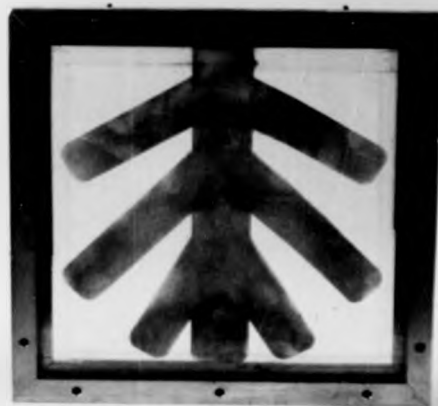
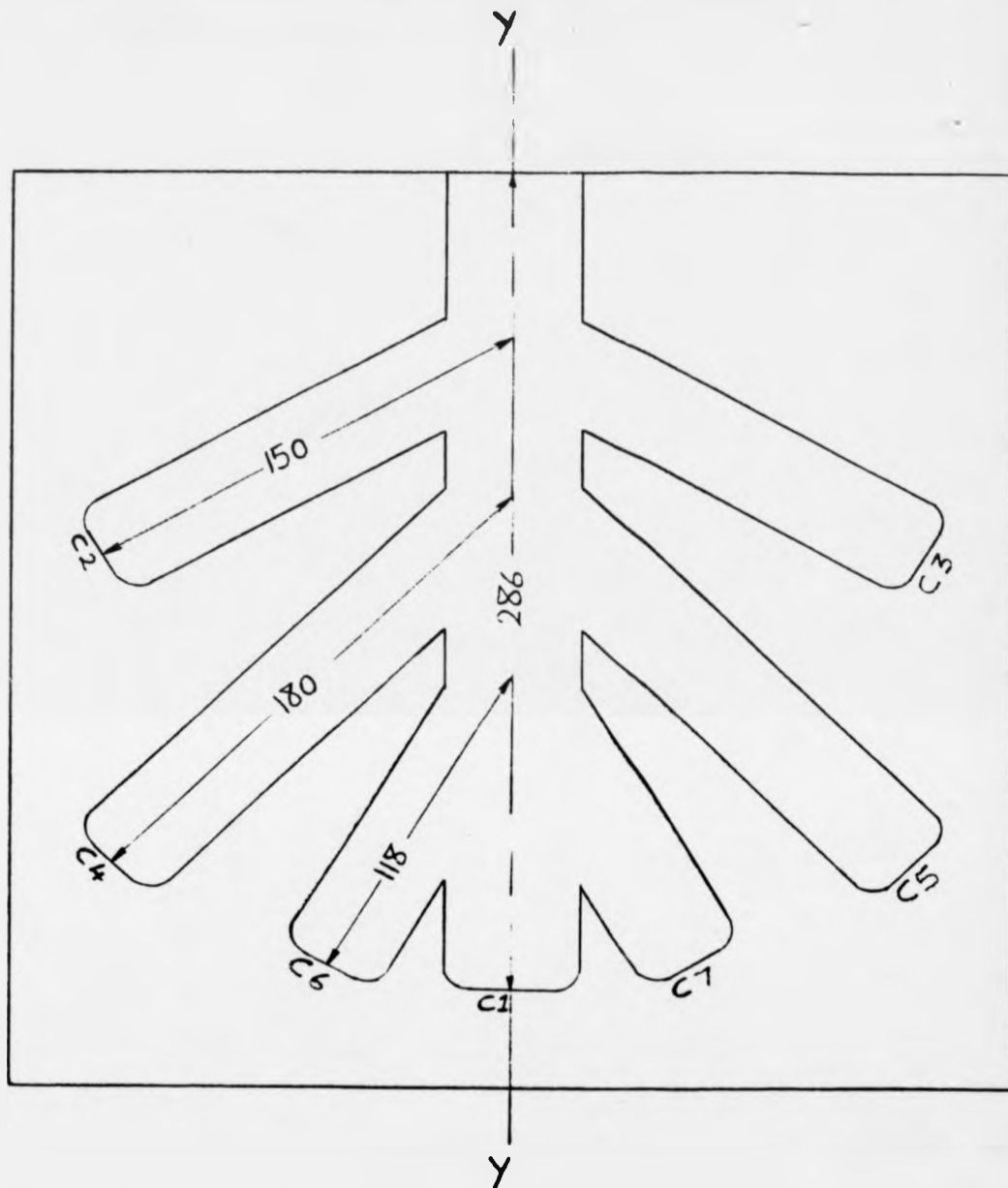


Fig 39. Perspex front of core box number one

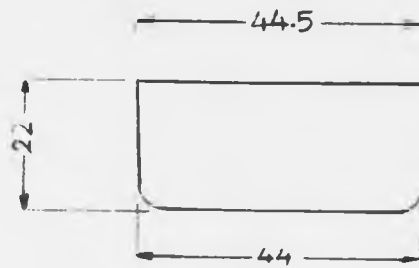


Fig 40. Back of core box number one

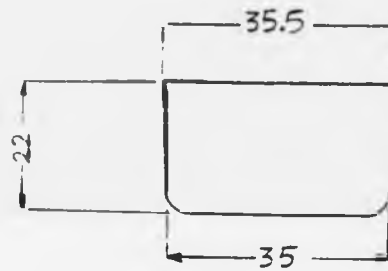


SCALE 1 : 0.5
 DIMENSIONS MM
 SYMMETRICAL ABOUT YY
 "C" CHANNEL

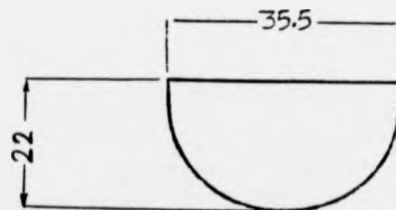
Fig 41. Front view of core-box number one



a. Cross section of channel one



b. Cross section of channels 3, 5 and 7



c. Cross section of channels 2, 4 and 6

SCALE 1 : 1
 DIMENSIONS MM

Fig 42. Cross sections of different channels of core-box number one

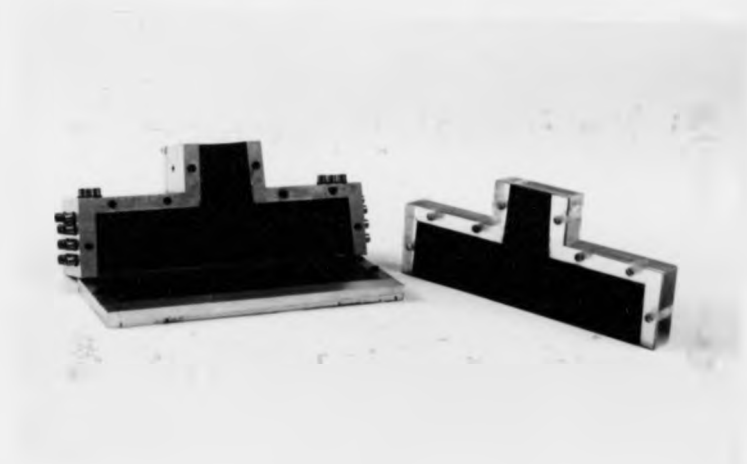


Fig 43. Core box number two

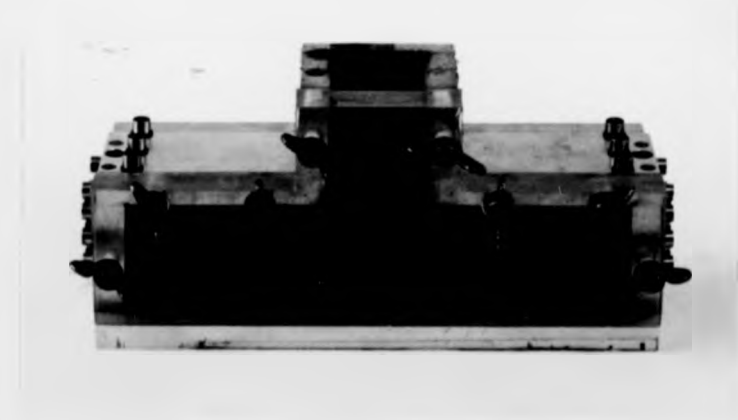
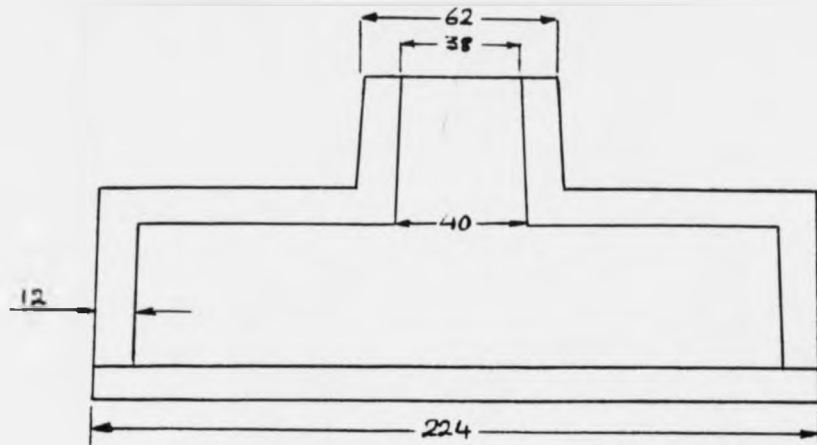


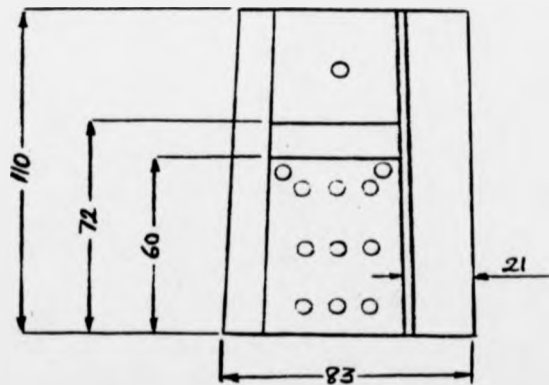
Fig 44. Core box number two



a. Front view



b. Plan view



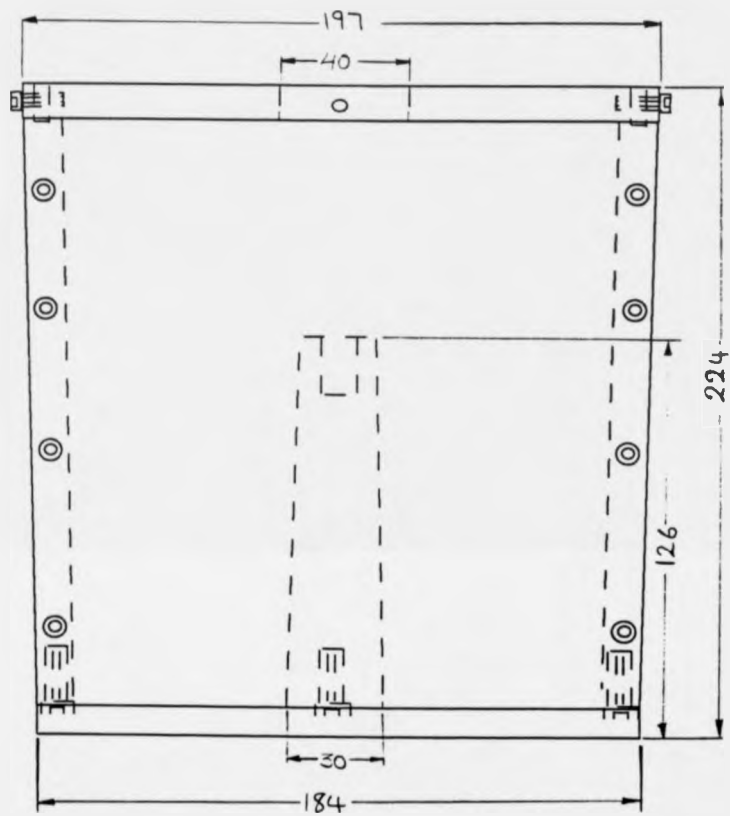
c. Side view

SCALE
DIMENSIONS 1 : 0.5
MM

Fig 45. Core-box number two

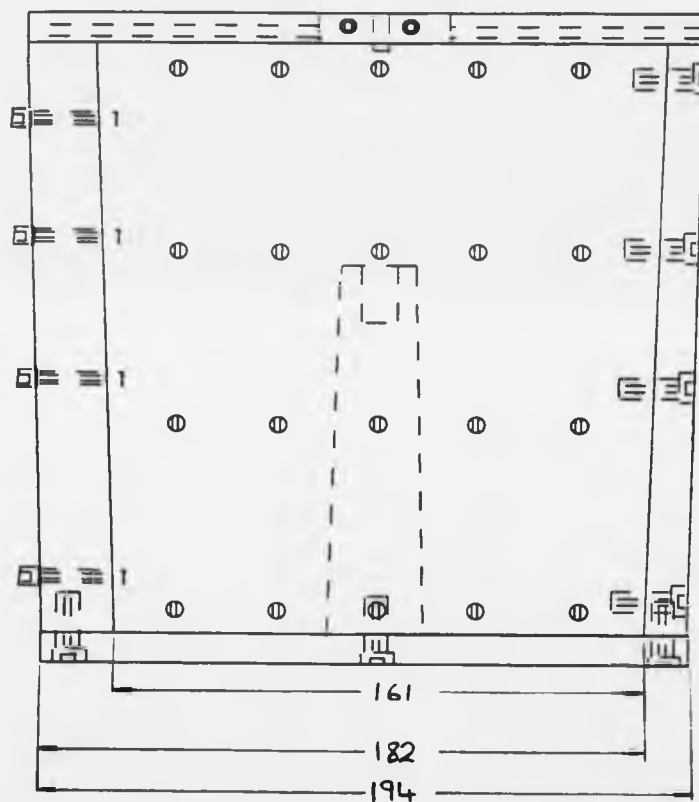


Fig 46. Core box number three



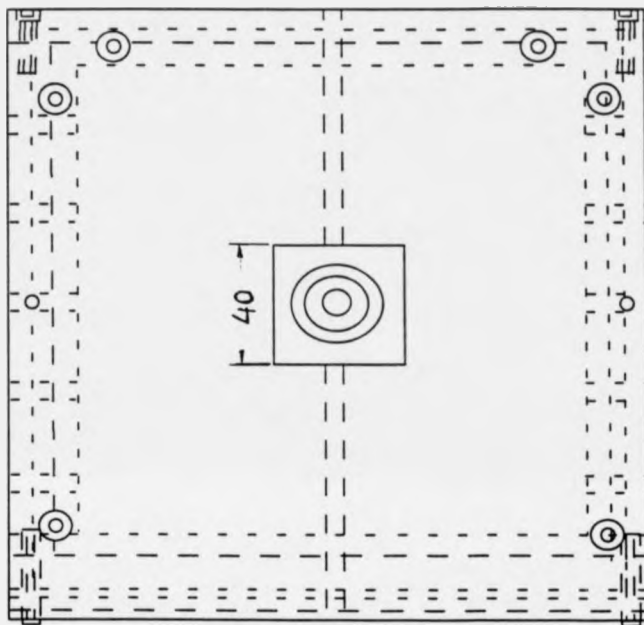
SCALE 1 : 0.5
 DIMENSIONS MM

Fig 47a. Front view of core-box number 3



SCALE 1 : 0.5
 DIMENSIONS MM

Fig 47b. Side view of core-box number 3



SCALE 1 : 0.5
DIMENSIONS MM

Fig 47c. Plan view of core-box number 3

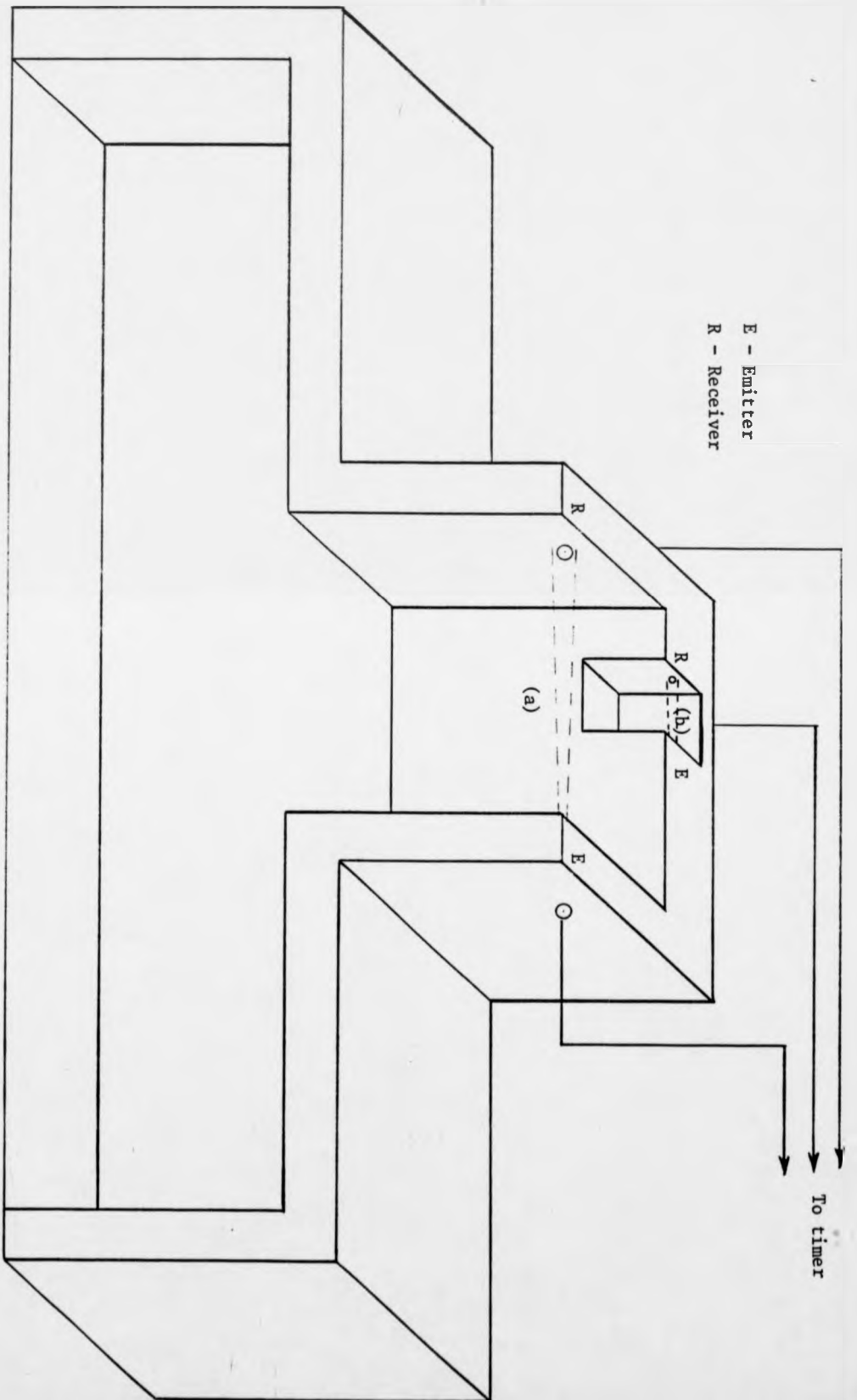


Fig 48. Schematic diagram of core box number 2 showing filling time measurement technique



Fig 49. Blow holes used in the experiments

Experimental Series	Air pressure psi	bars	Binder level %	Blow hole ϕ mm
1	45	3.10	0.35	25
				20
				15
				10
			1.05	25
				20
				15
				10
			0.70	25
				20
				15
				10
2	65	4.48	0.70	25
				20
				15
				10
			1.05	25
				20
				15
				10
			0.35	25
				20
				15
				10
3	85	5.86	0.35	25
				20
				15
				10
			0.70	25
				20
				15
				10
			1.05	25
				20
				15
				10

Fig 50. Order of experiments carried out on core box 2 in group 4. All vents open (a total of 30)

Experimental series	Binder level %	Air Pressure psi	Air Pressure bars	Blow hole ϕ mm	Sand batch number
(i)	0.35	85	5.86	25	1
				20	
				15	
(i)	0.35	65	4.48	10	2
				25	
				20	
(i)	0.35	45	3.10	15	3
				20	
				10	
(ii)	0.70	85	5.86	25	4
				20	
				15	
(ii)	0.70	65	4.48	10	5
				25	
				20	
(ii)	0.70	45	3.10	15	6
				20	
				10	
(iii)	1.05	85	5.86	25	7
				20	
				15	
(iii)	1.05	65	4.48	10	8
				25	
				20	
(iii)	1.05	45	3.10	15	9
				20	
				10	

Fig 51. Order of experiments carried out on box 2 in group 6. All vents open (a total of 30)

Experimental series	Binder level %	Air Pressure psi	Air Pressure bars	Blow hole ϕ mm	Sand batch number
(i)	0.75	80	5.52	20	1
				15	
				10	
(i)	0.75	60	4.14	20	2
				15	
				10	
(i)	0.75	40	2.76	20	3
				15	
				10	
(ii)	1.50	80	5.52	20	4
				15	
				10	
(ii)	1.50	60	4.14	20	5
				15	
				10	
(ii)	1.50	40	2.76	20	6
				15	
				10	
(iii)	2.25	80	5.52	20	7
				15	
				10	
(iii)	2.25	60	4.14	20	8
				15	
				10	
(iii)	2.25	40	2.76	20	9
				15	
				10	

Fig 52. Order of experiments carried out on box 1 in group 6. All vents open

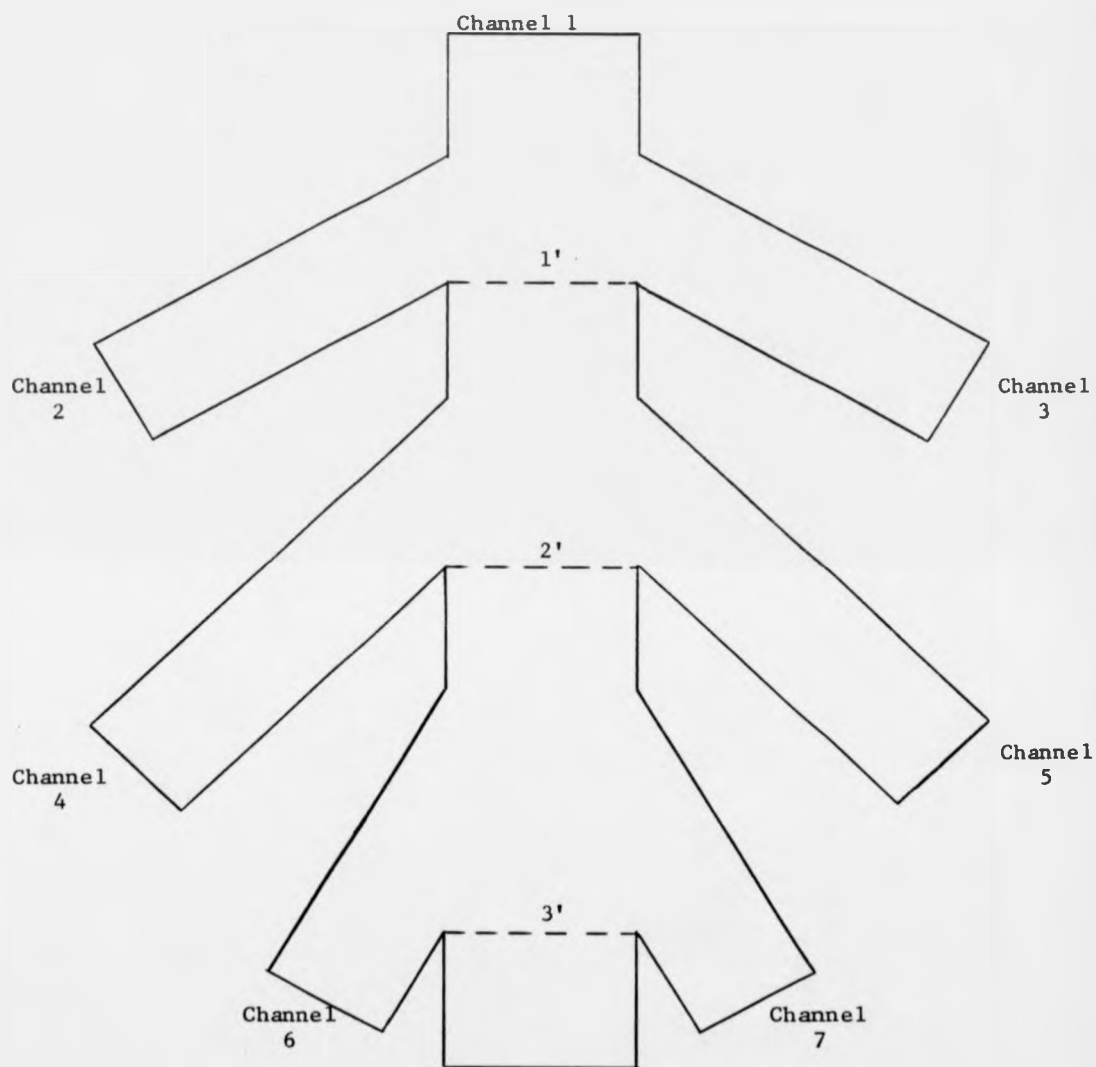


Fig 53. Schematic diagram of core-box number 1 showing the numbers of different channels and levels 1' to 3'

Blow hole φ mm	Core-box venting arrangement core-weight gms			
	All vents open	Central row of vents open in each channel	One vent open at the end of each channel	Vents open above 1'
5	1706.3 ¹⁷⁵⁹ ₁₆₅₀	1839.3 ⁴⁷ ₃₁	1861.9 ⁸² ₂₅	1730.2 ¹⁸¹⁹ ₁₆₄₂
10	1854.9 ⁶⁹ ₄₀	1887.7 ⁹⁴ ₈₁	1900.2 ¹⁹⁰⁵ ₁₈₉₄	1770.5 ¹⁸⁴⁰ ₁₆₄₂
15	1902.4 ¹⁹¹⁴ ₁₈₉₀	1910.3	1930.6 ³⁴ ₂₇	1818.4 ¹⁸⁰⁵ ₁₈₄₃
20	1952.5 ⁵³ ₅₀	1955.4 ⁵⁶ ₅₄	1991.6 ⁹³ ₉₀	1944.5 ⁹⁷ ₄₂

Blowing air pressure = 6 bars

Fig 54. Preliminary experiments carried out in sub-group a of group 1 on box 1

CORE-BOX 1
ZIRCON SAND
RESIN CONTENT = 0.7 %

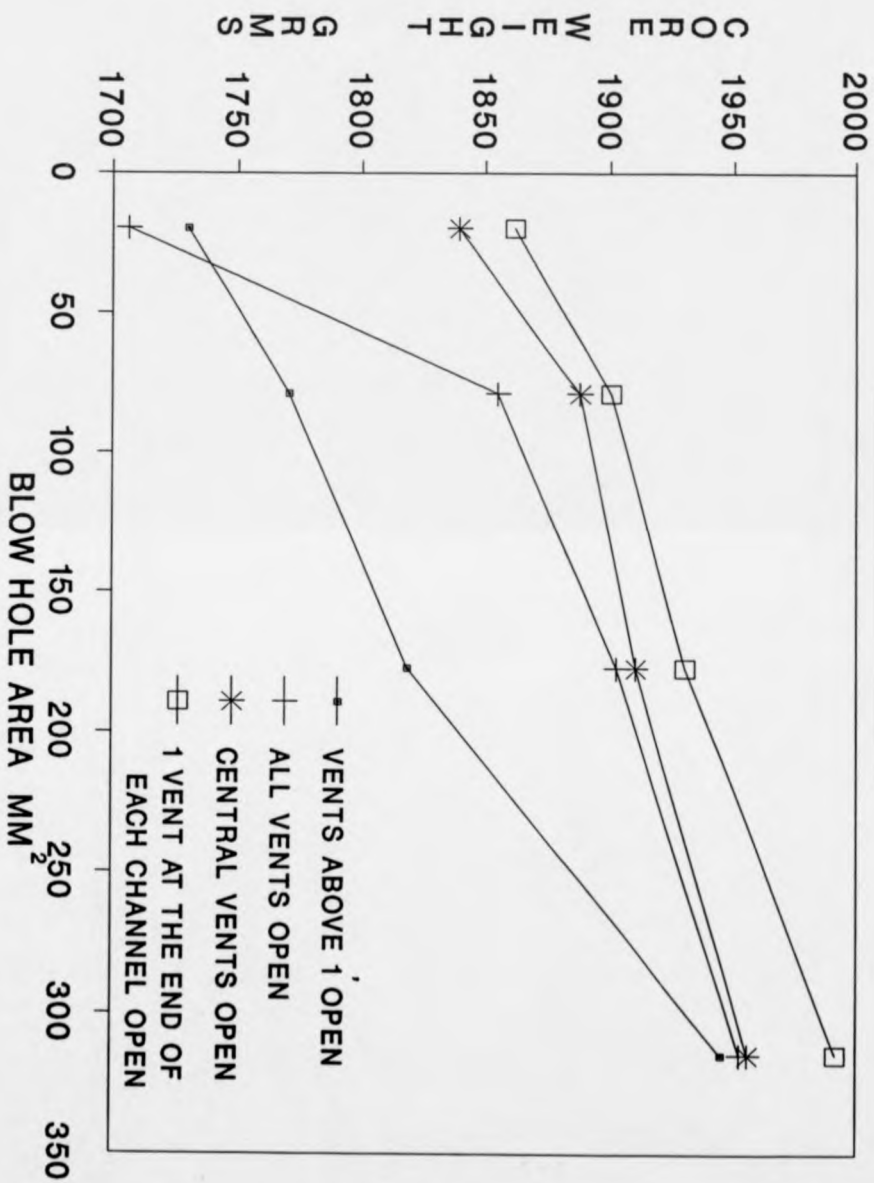


FIG 55. CORE-WEIGHT vs BLOW HOLE AREA

Experiment number	Blow hole	Core-box venting arrangement	Blow time 1 frame = 1/64 secs
1	φ5mm	All vents open	267 = 4.17
2	φ10mm	All vents open	57.5 = 0.90
3	φ15mm	All vents open	26.5 = 0.41
4	φ20mm	All vents open	15.5 = 0.24
5	φ15mm	One central vent open at the end of each channel	31 = 0.48
6	Tapered circular = φ15mm	" "	28 = 0.44
7	Triangular = φ15mm	" "	32 = 0.50
8	Rectangular = φ15mm	" "	30 = 0.47
9	Rectangular = φ20mm	" "	17 = 0.26
10	φ5mm	Vents blocked up to 2' & in channel 4	260 = 4.06
11	φ15mm	" "	26 = 0.41
12	φ5mm	Vents blocked up to 1'	262 = 4.09
13	φ15mm	" "	26 = 0.41
14	φ15mm	Vents in channels 2, 4 & 6 open only	31 = 0.48
15	φ15mm	Vents in channels 3, 5 & 7 open only	30 = 0.47

Blowing air pressure 2 bars

Fig 56. Experiments carried out in sub-group a of group 1 on box 1

Experiment number	Blow hole	Core-box venting arrangement	Blow time 1 frame = 1/64 secs
1	φ5mm	All vents open	267 = 4.17
2	φ10mm	All vents open	57.5 = 0.90
3	φ15mm	All vents open	26.5 = 0.41
4	φ20mm	All vents open	15.5 = 0.24
5	φ15mm	One central vent open at the end of each channel	31 = 0.48
6	Tapered circular = φ15mm	" "	28 = 0.44
7	Triangular = φ15mm	" "	32 = 0.50
8	Rectangular = φ15mm	" "	30 = 0.47
9	Rectangular = φ20mm	" "	17 = 0.26
10	φ5mm	Vents blocked up to 2' & in channel 4	260 = 4.06
11	φ15mm	" "	26 = 0.41
12	φ5mm	Vents blocked up to 1'	262 = 4.09
13	φ15mm	" "	26 = 0.41
14	φ15mm	Vents in channels 2, 4 & 6 open only	31 = 0.48
15	φ15mm	Vents in channels 3, 5 & 7 open only	30 = 0.47

Blowing air pressure \approx bars

Fig 56. Experiments carried out in sub-group a of group 1 on box 1

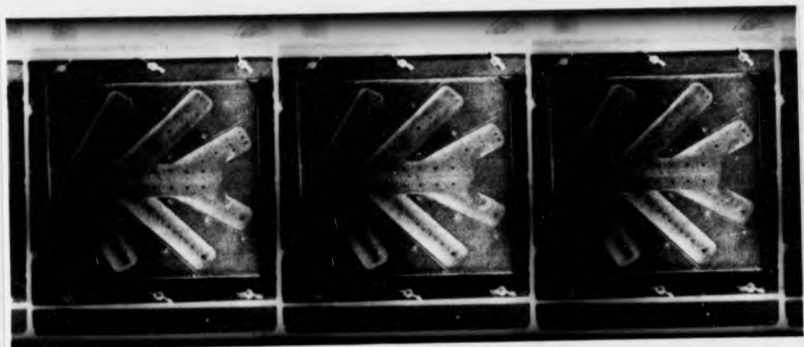


Fig 57. Φ 5 mm blow hole, all vents open

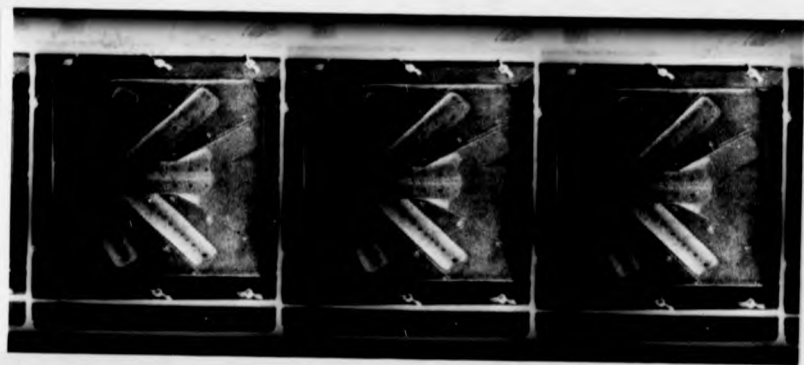


Fig 58. Φ 5 mm blow hole, all vents open



Fig 59. $\Phi 5$ mm blow hole, all vents open

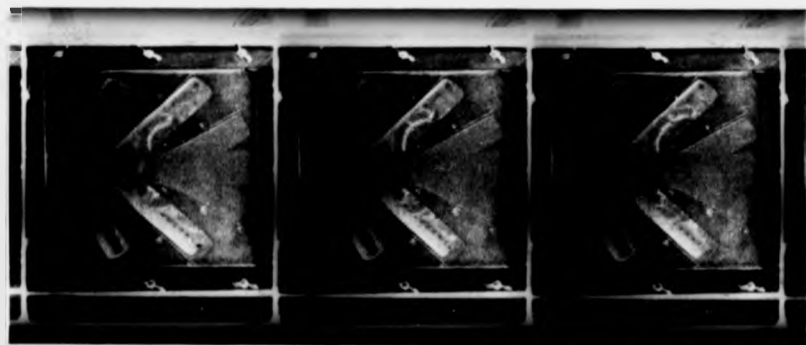


Fig 60. $\Phi 5$ mm blow hole, all vents open

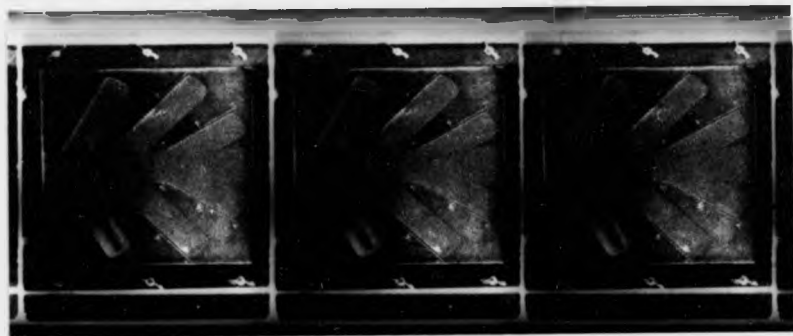


Fig 61. ϕ 5 mm blow hole, all vents open

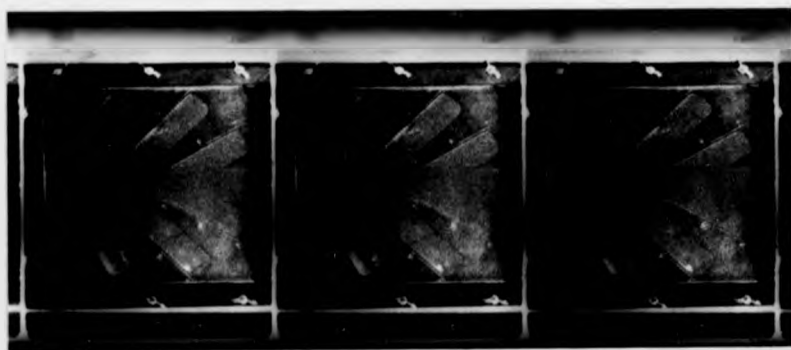


Fig 62. ϕ 5 mm blow hole, all vents open

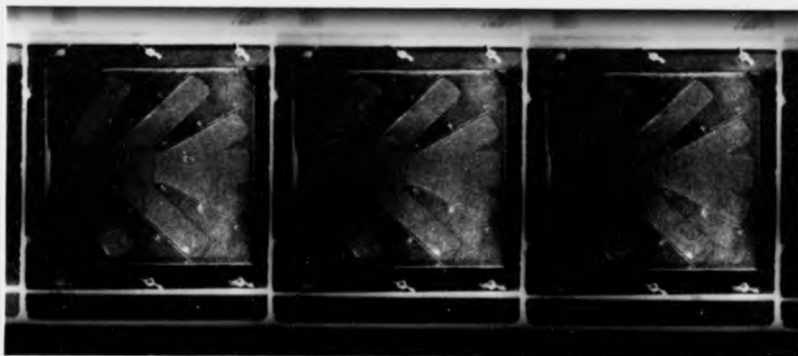


Fig 63. $\phi 5$ mm blow hole, all vents open

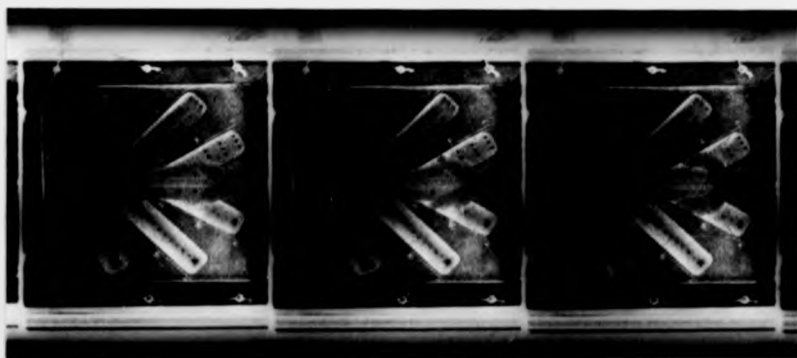


Fig 64. $\phi 10$ mm blow hole, all vents open

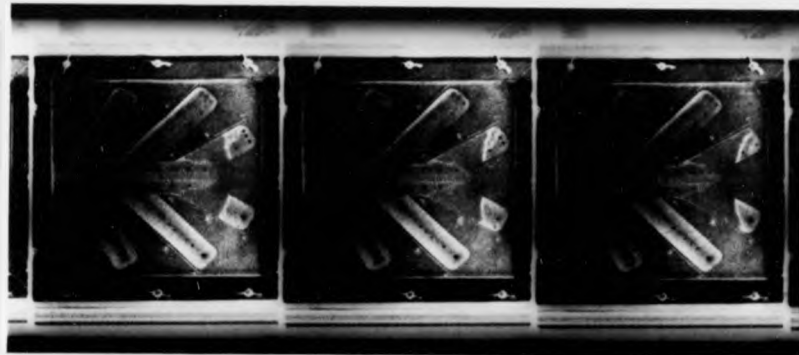


Fig 65. ϕ 10 mm blow hole, all vents open

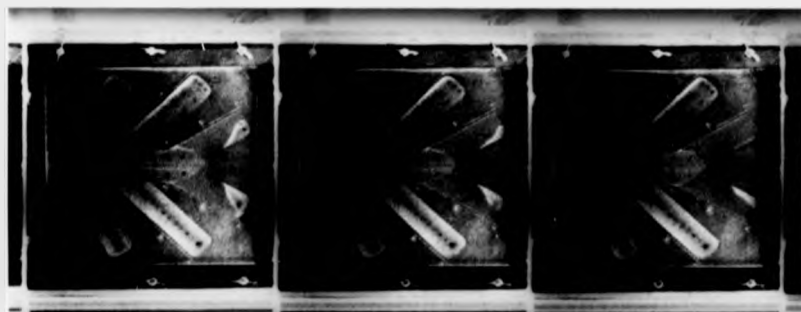


Fig 66. ϕ 10 mm blow hole, all vents open

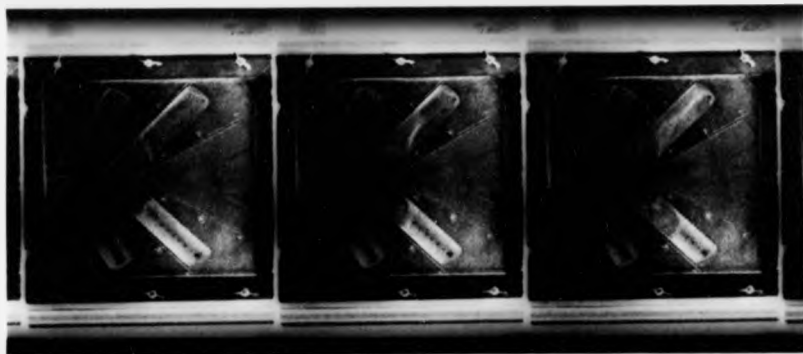


Fig 67. $\phi 10$ mm blow hole, all vents open

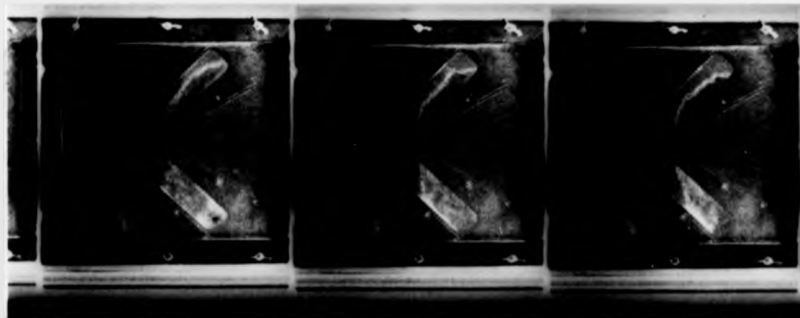


Fig 68. $\phi 10$ mm blow hole, all vents open

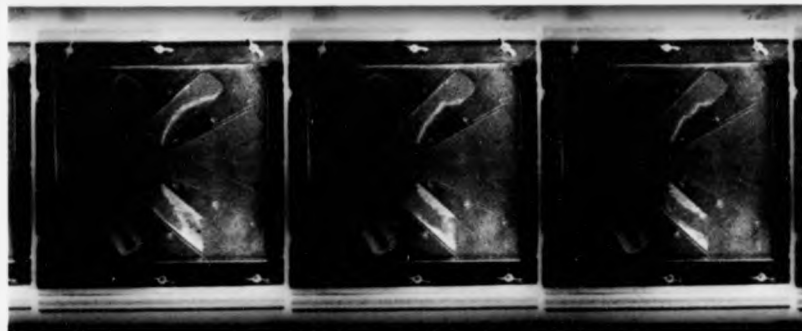


Fig 69. Φ 10 mm blow hole, all vents open

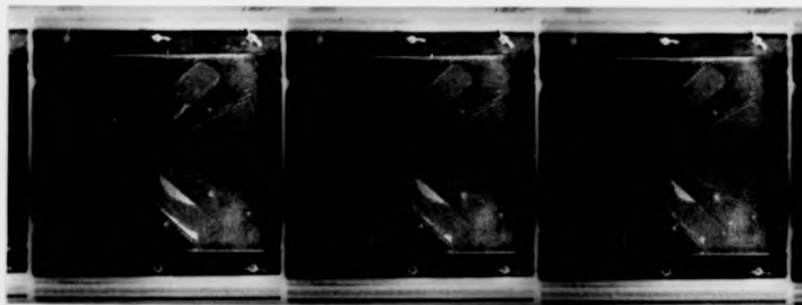


Fig 70. Φ 10 mm blow hole, all vents open

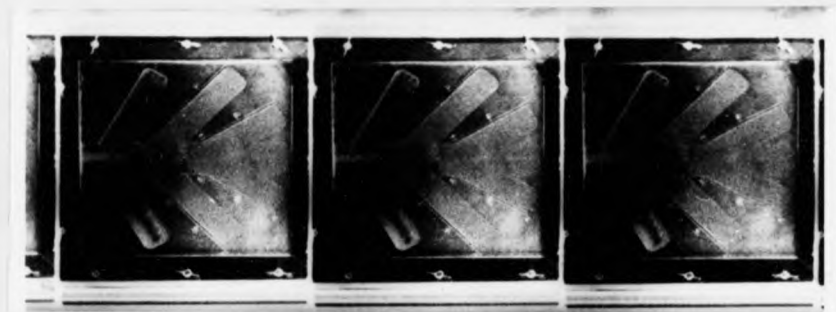


Fig 71. Φ 10 mm blow hole, all vents open

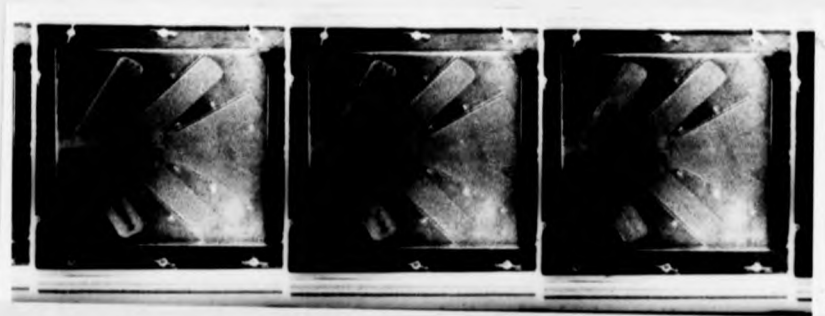


Fig 72. Φ 10 mm blow hole, all vents open



Fig 73. Φ 10 mm blow hole, all vents open

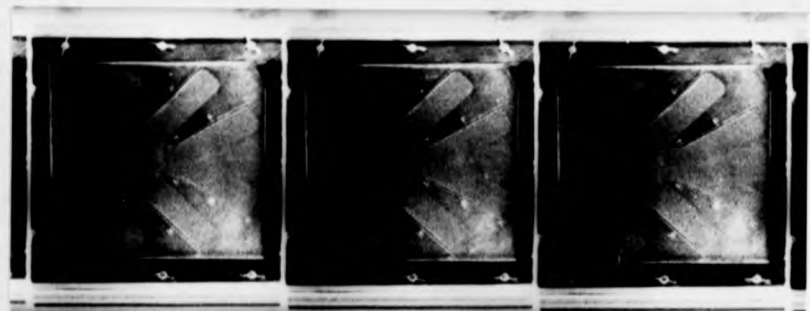


Fig 74. Φ 10 mm blow hole, all vents open

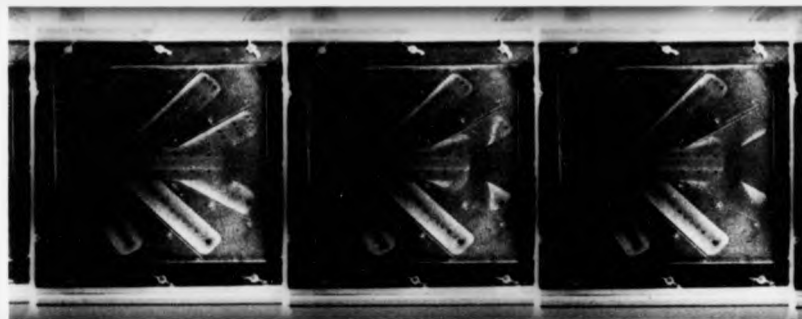


Fig 75. ϕ 15 mm blow hole, all vents open

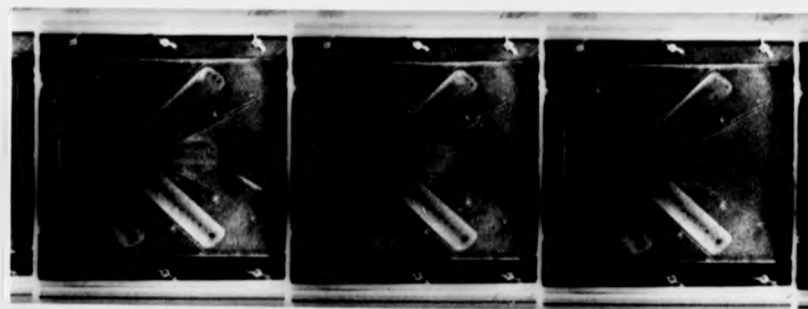


Fig 76. ϕ 15 mm blow hole, all vents open

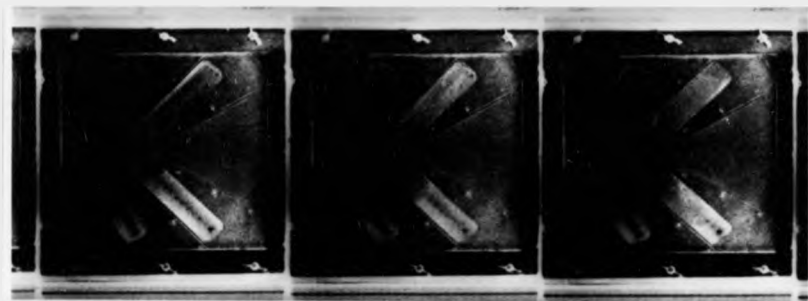


Fig 77. Φ 15 mm blow hole, all vents open

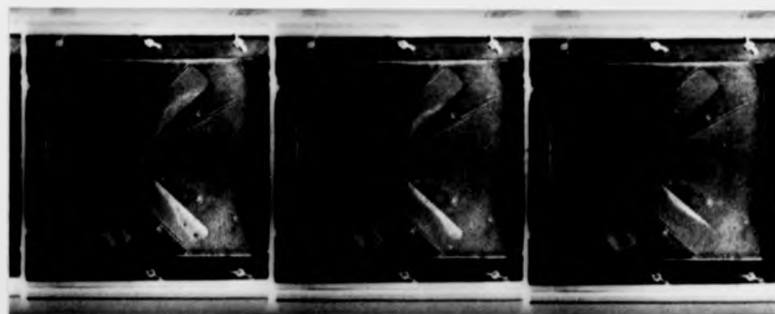


Fig 78. Φ 15 mm blow hole, all vents open

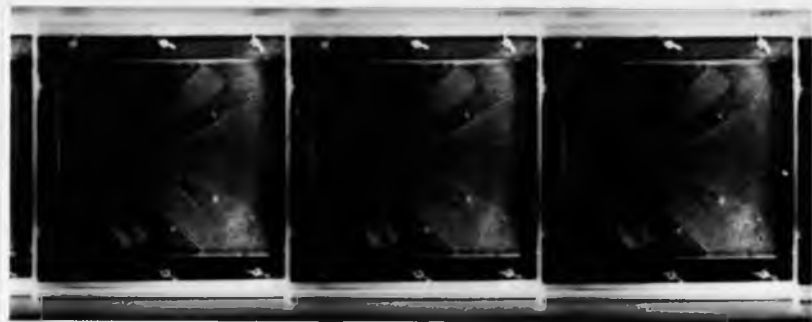


Fig 79. Φ 15 mm blow hole, all vents open

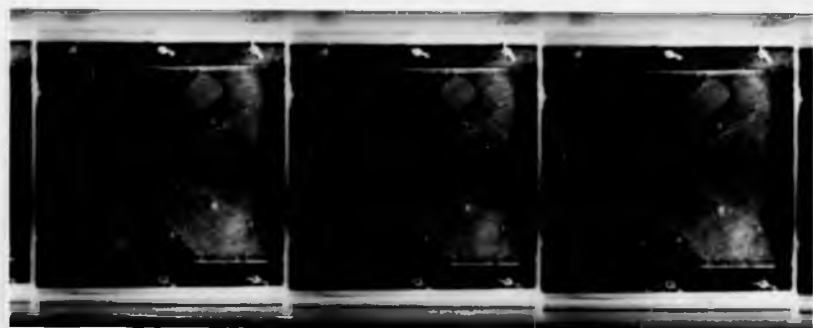


Fig 80. Φ 15 mm blow hole, all vents open

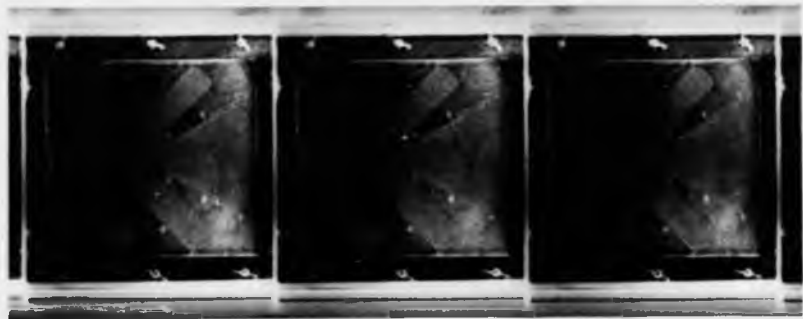


Fig 81. Φ 15 mm blow hole, all vents open

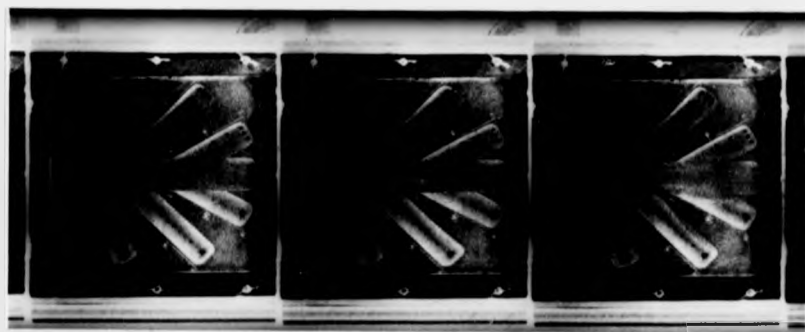


Fig 82. Φ 20 mm blow hole, all vents open

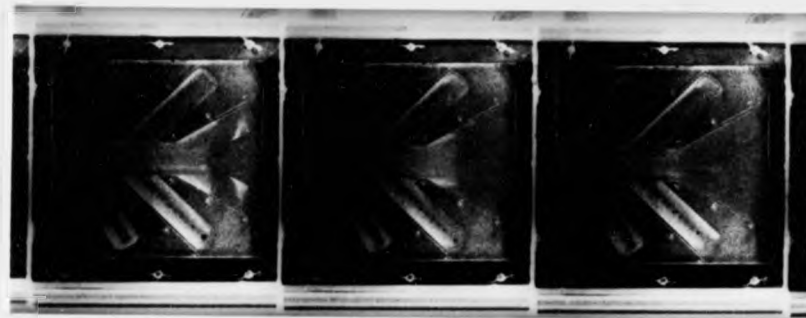


Fig 83. ϕ 20 mm blow hole, all vents open

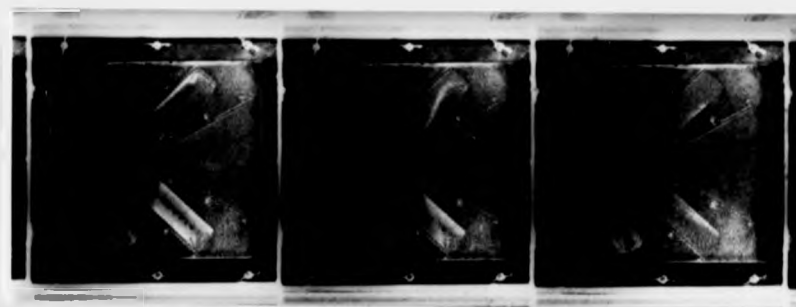


Fig 84. ϕ 20 mm blow hole, all vents open

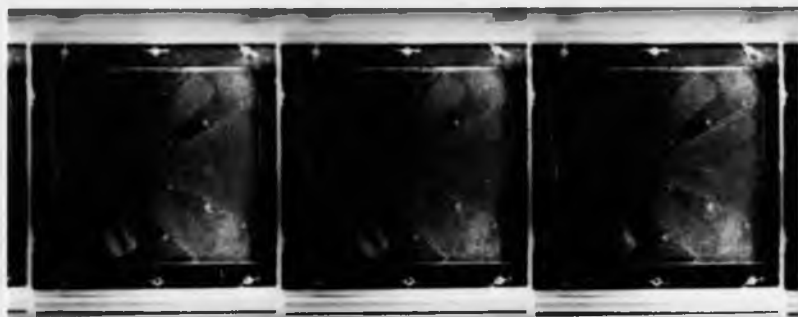


Fig 85. Φ 20 mm blow hole, all vents open

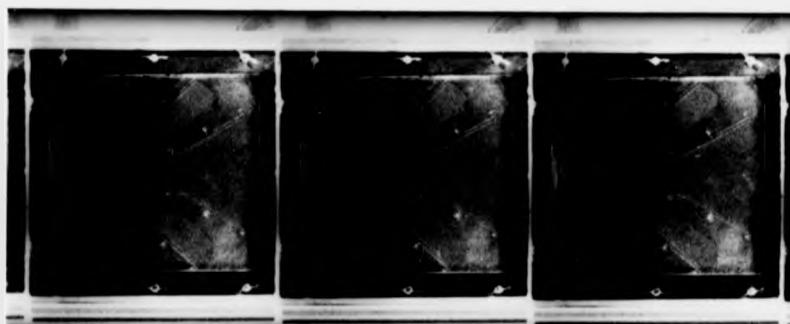


Fig 86. Φ 20 mm blow hole, all vents open

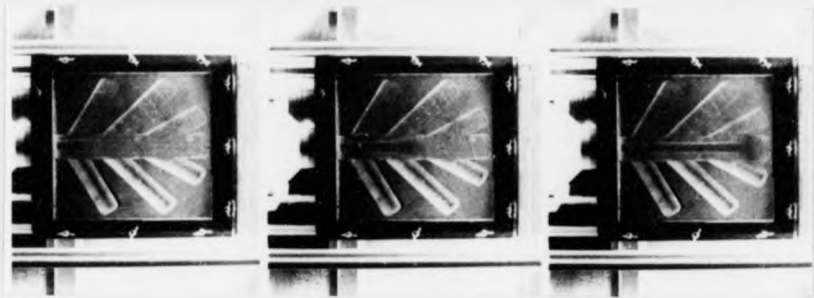


Fig 87. $\phi 15$ mm blow hole, one vent at the end of each channel open

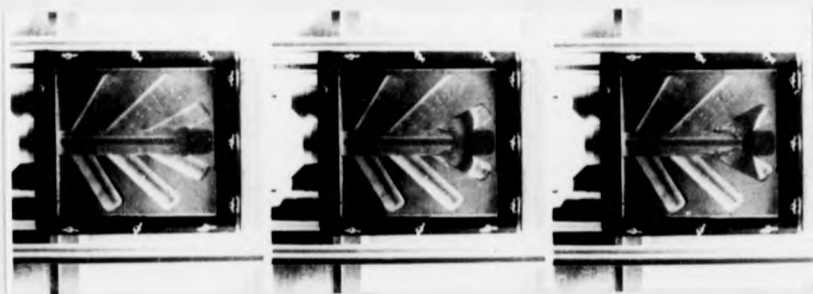


Fig 88. $\phi 15$ mm blow hole, one vent at the end of each channel open

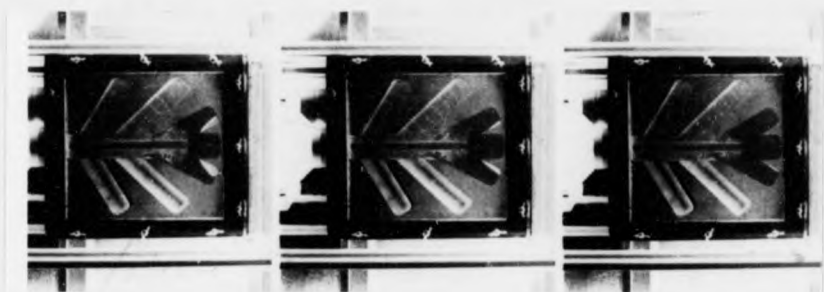


Fig 89. $\Phi 15$ mm blow hole, one vent at the end of each channel open

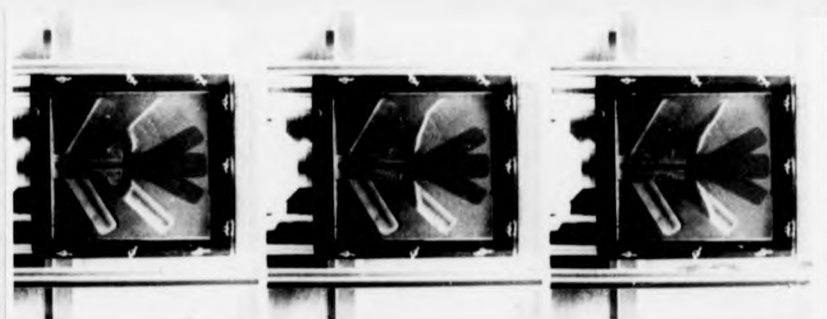


Fig 90. $\Phi 15$ mm blow hole, one vent at the end of each channel open

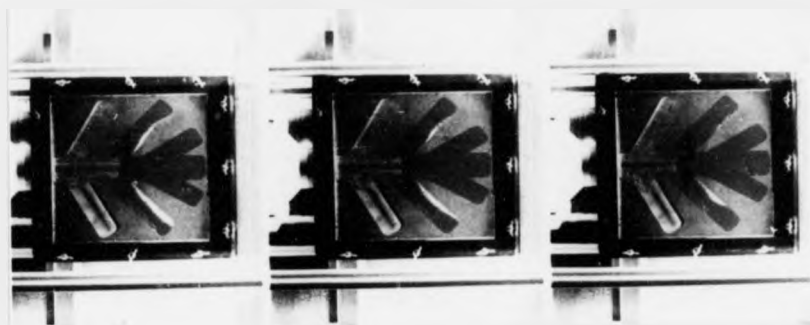


Fig 91. $\Phi 15$ mm blow hole, one vent at the end of each channel open

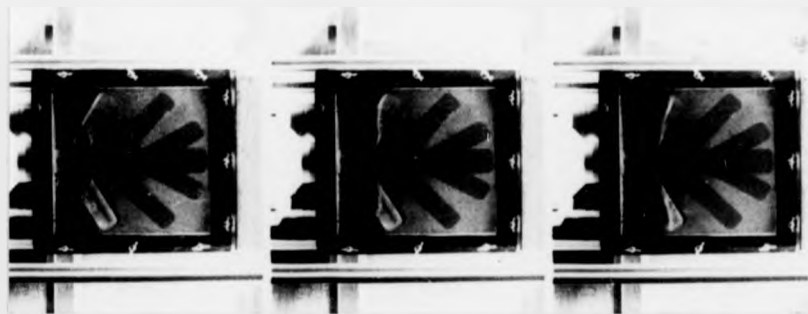


Fig 92. $\Phi 15$ mm blow hole, one vent at the end of each channel open

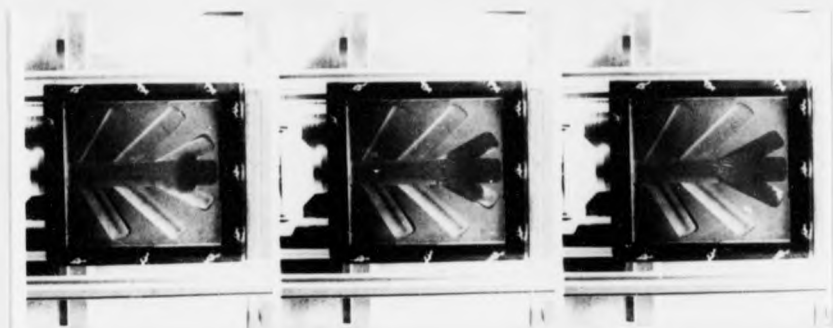


Fig 93. Triangular blow hole = $\Phi 15$ mm, one vent at the end of each channel open

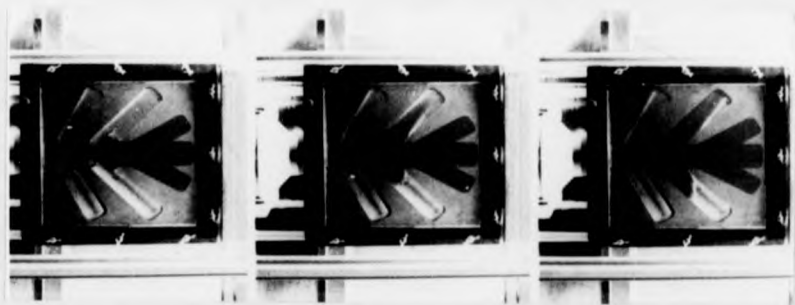


Fig 94. Triangular blow hole = $\Phi 15$ mm, one vent at the end of each channel open

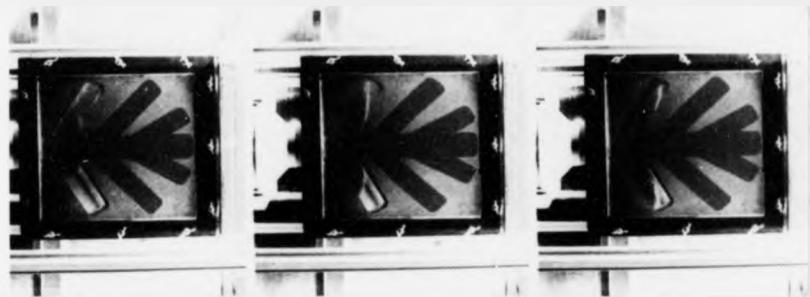


Fig 95. Triangular blow hole = Φ 15 mm, one vent at the end of each channel open

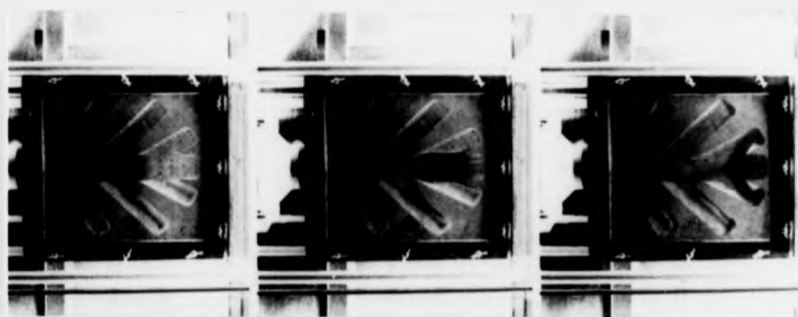


Fig 96. Rectangular blow hole = Φ 20 mm, one vent at the end of each channel open

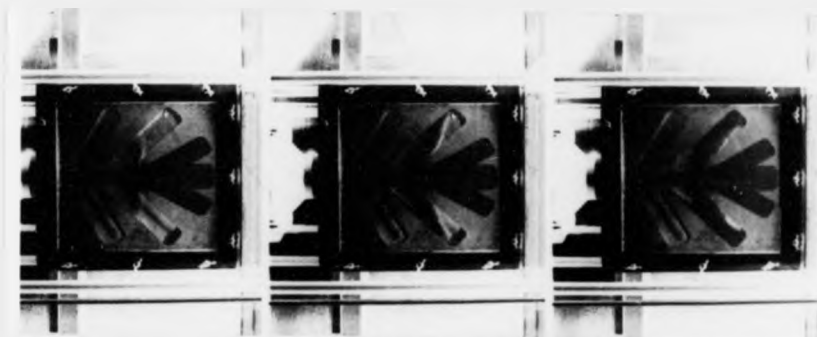


Fig 97. Rectangular blow hole = $\phi 20$ mm, one vent at the end of each channel open

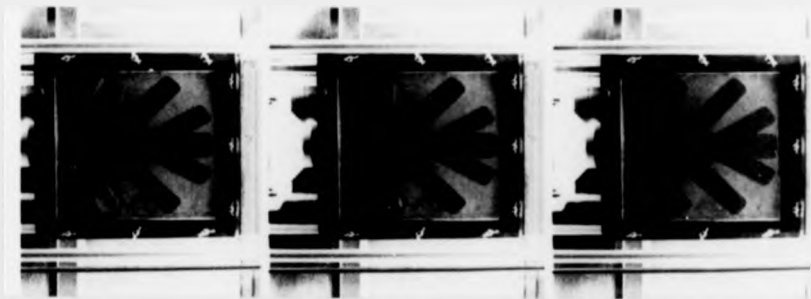


Fig 98. Rectangular blow hole = $\phi 20$ mm, one vent at the end of each channel open

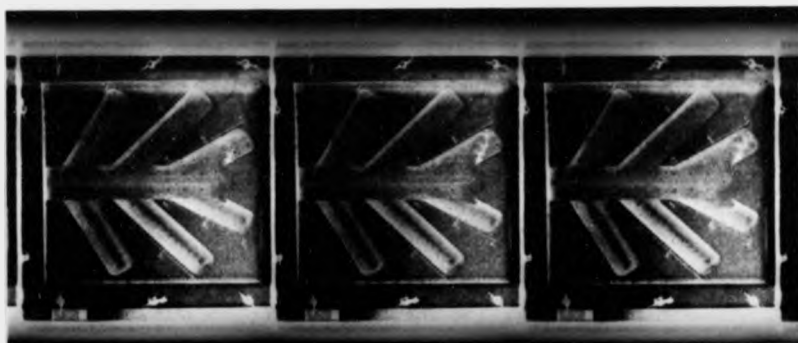


Fig 99. $\Phi 5$ mm blow hole, vents up to 2' and in channel 4 closed

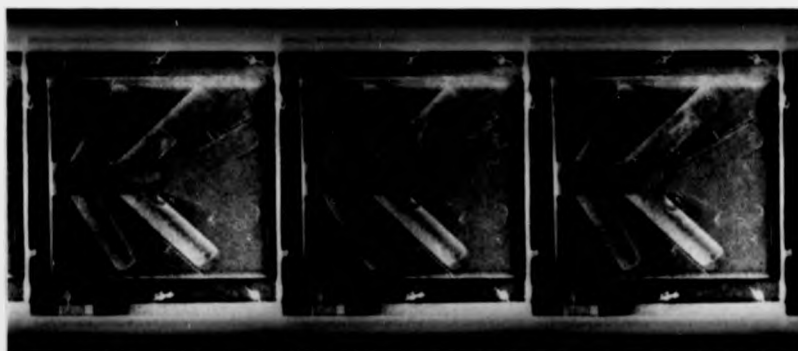


Fig 100. $\Phi 5$ mm blow hole, vents up to 2' and in channel 4 closed

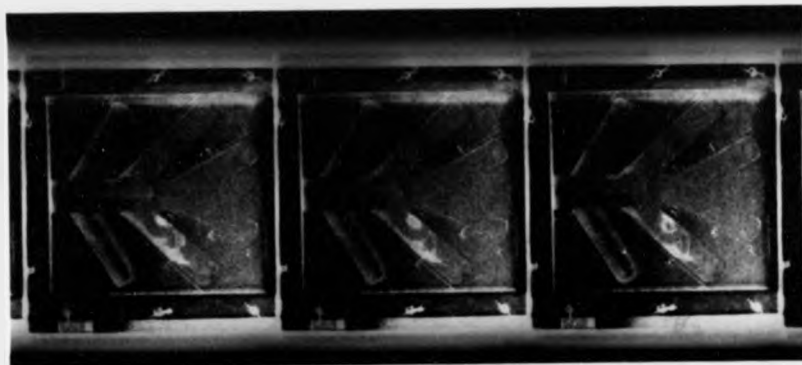


Fig 101. ϕ 5 mm blow hole, vents up to 2' and in channel 4 closed



Fig 102. ϕ 5 mm blow hole, vents up to 2' and in channel 4 closed



Fig 103. $\phi 5$ mm blow hole, vents up to 2' and in channel 4 closed

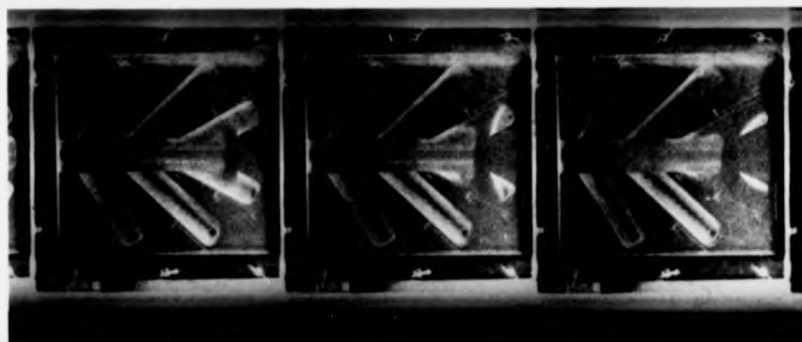


Fig 104. $\phi 15$ mm blow hole, vents up to 2' and in channel 4 closed

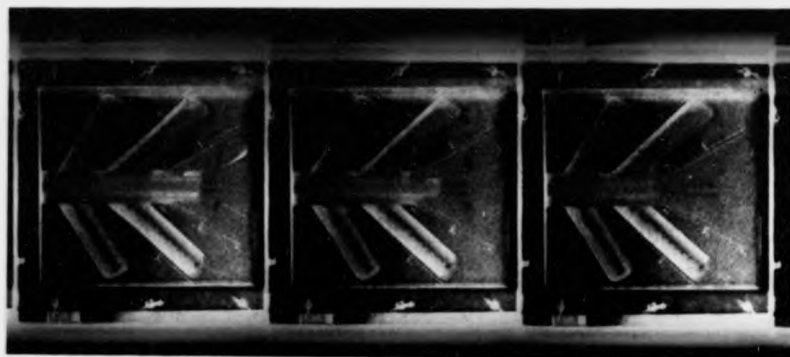


Fig 105. Φ 15 mm blow hole, vents up to 2' and in channel 4 closed



Fig 106. Φ 15 mm blow hole, vents up to 2' and in channel 4 closed



Fig 107. ϕ 15 mm blow hole, vents up to 2' and in channel 4 closed



Fig 108. ϕ 15 mm blow hole, vents up to 2' and in channel 4 closed

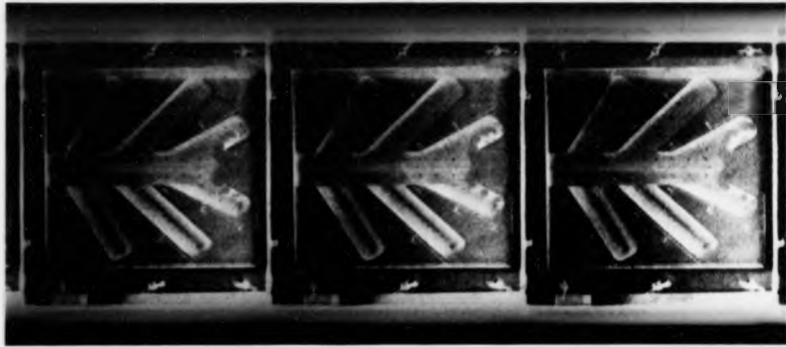


Fig 109. \varnothing 5 mm blow hole, vents up to 1' closed

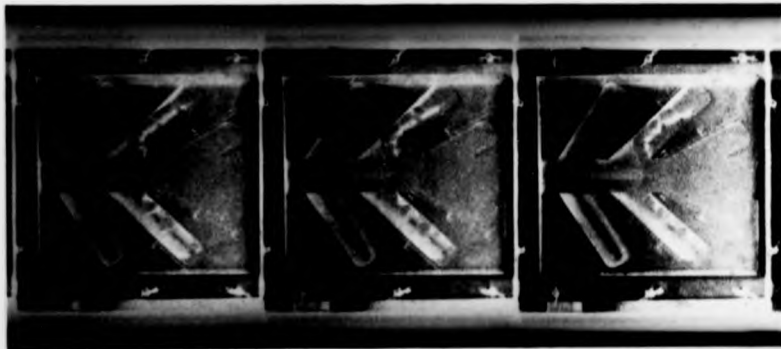


Fig 110. \varnothing 5 mm blow hole, vents up to 1' closed

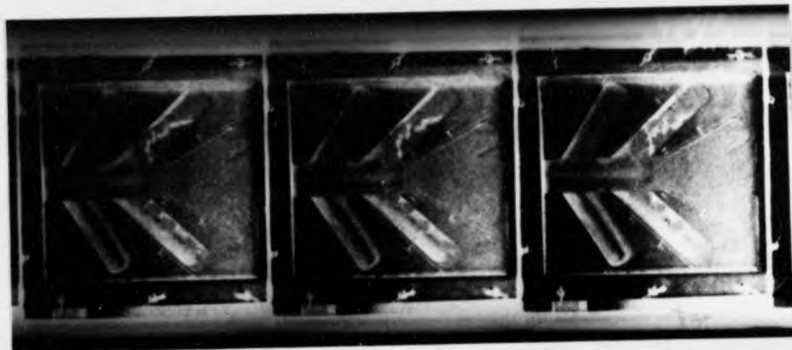


Fig 111. $\Phi 5$ mm blow hole, vents up to 1' closed

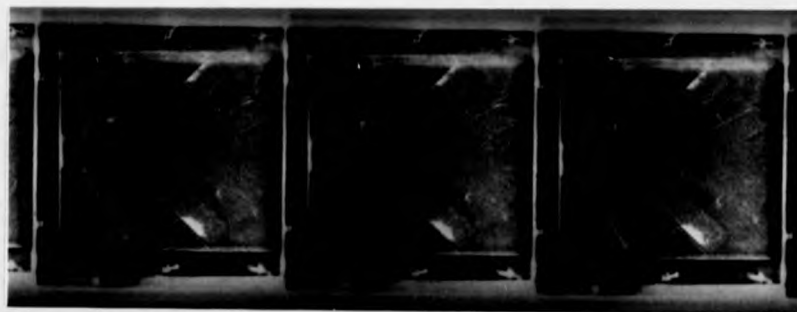


Fig 112. $\Phi 5$ mm blow hole, vents up to 1' closed

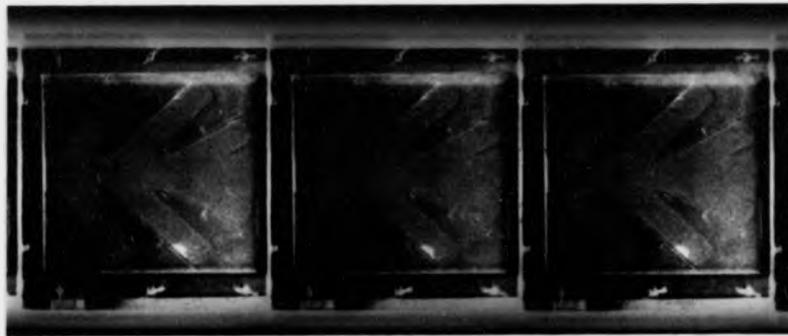


Fig 113. $\phi 5$ mm blow hole, vents up to 1' closed

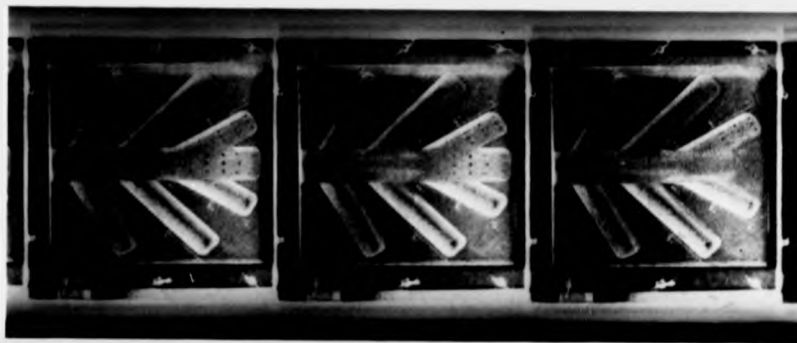


Fig 114. $\phi 15$ mm blow hole, vents up to 1' closed

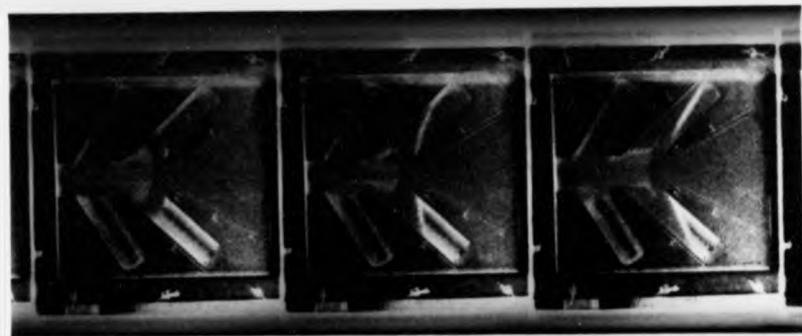


Fig 115. $\phi 15$ mm blow hole, vents up to 1' closed

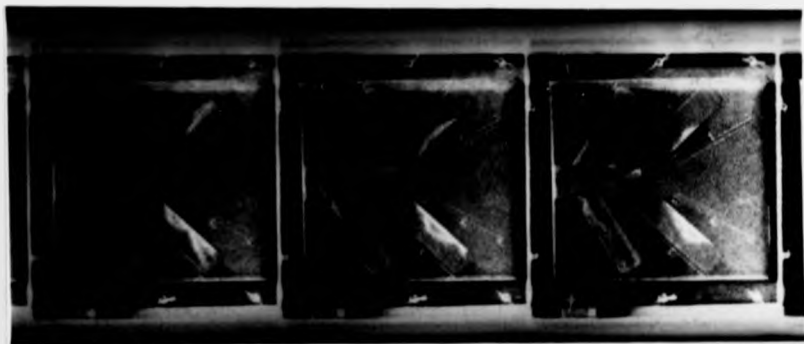


Fig 116. $\phi 15$ mm blow hole, vents up to 1' closed

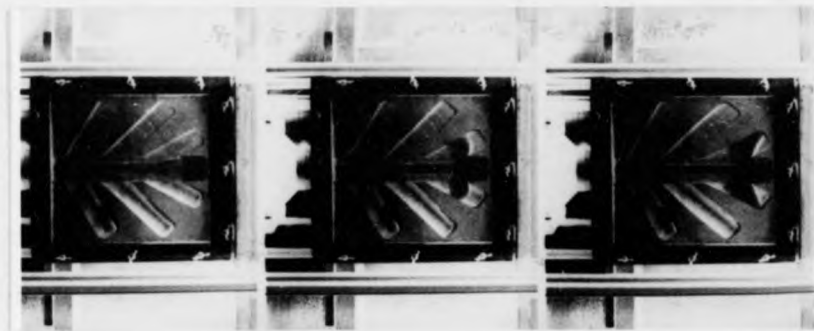


Fig 117. Φ 15 mm blow hole, vents in channels 2, 4 and 6 open

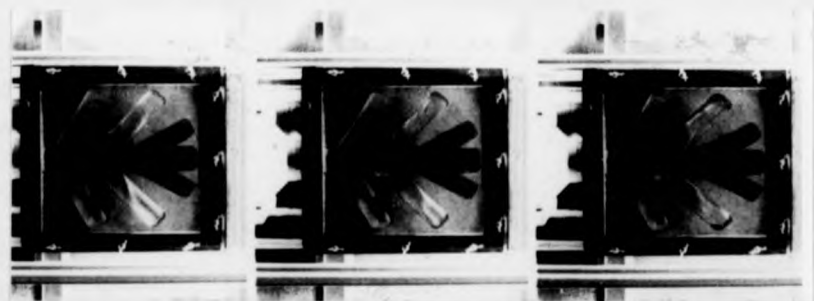


Fig 118. Φ 15 mm blow hole, vents in channels 2, 4 and 6 open

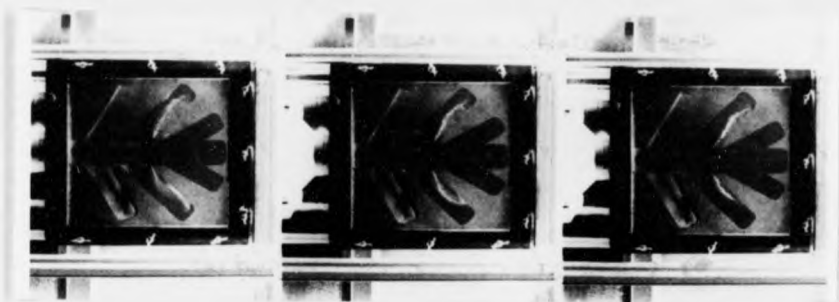


Fig 119. $\Phi 15$ mm blow hole, vents in channels 2, 4 and 6 open

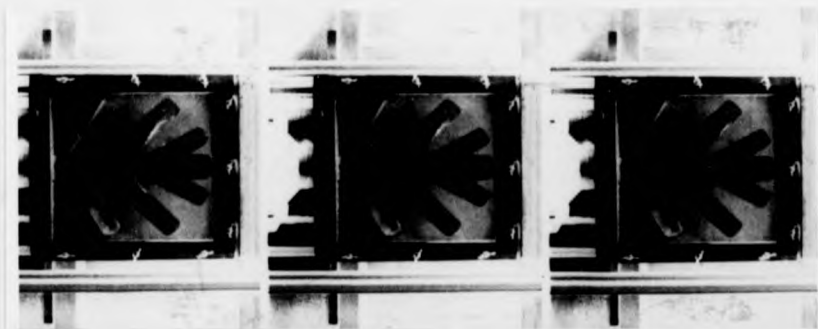


Fig 120. $\Phi 15$ mm blow hole, vents in channels 2, 4 and 6 open

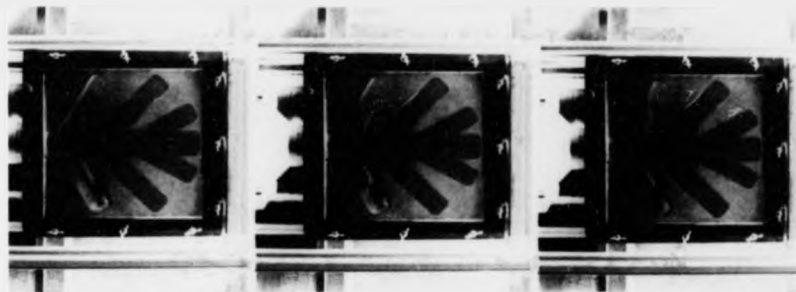


Fig 121. $\phi 15$ mm blow hole, vents in channels 2, 4 and 6 open

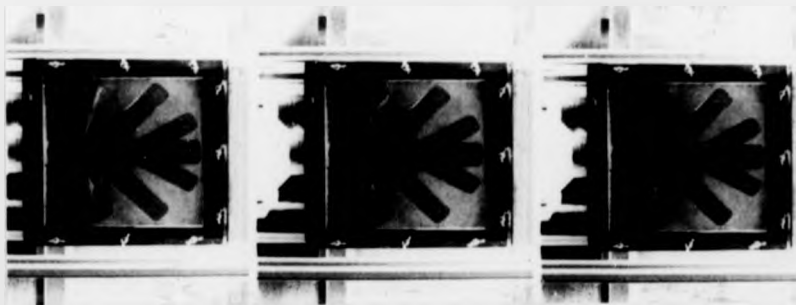


Fig 122. $\phi 15$ mm blow hole, vents in channels 2, 4 and 6 open

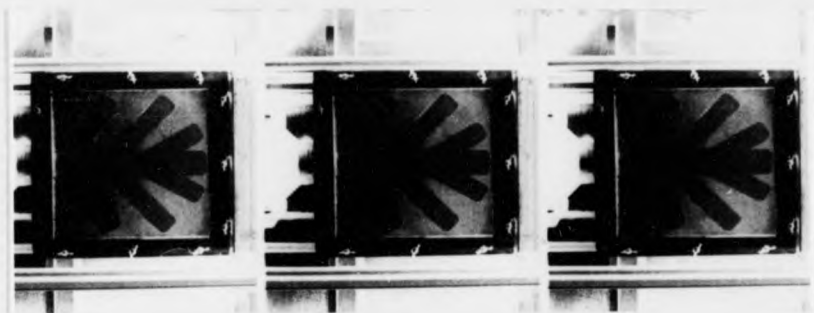


Fig 123. $\phi 15$ mm blow hole, vents in channels 2, 4 and 6 open

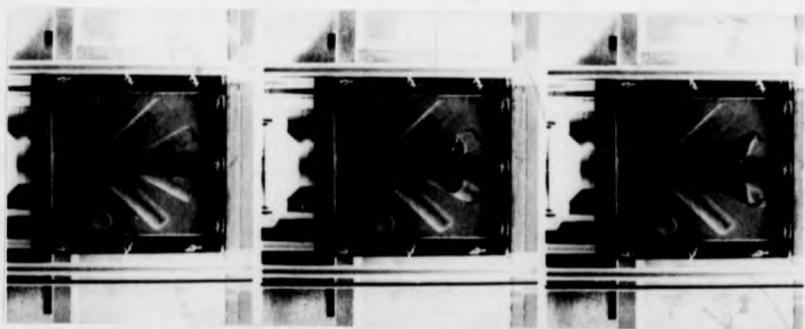


Fig 124. $\phi 15$ mm blow hole, vents in channels 3, 5 and 7 open

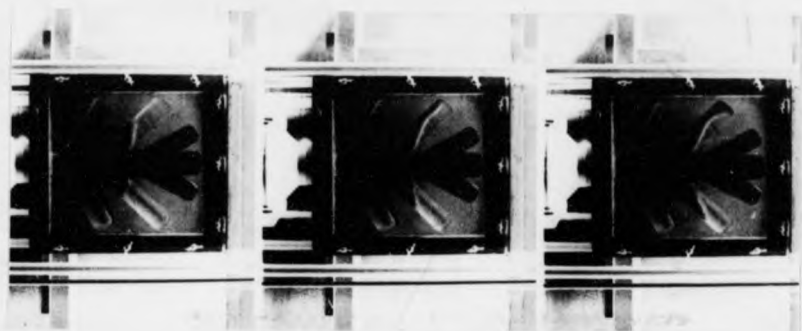


Fig 125. $\phi 15$ mm blow hole, vents in channels 3, 5 and 7 open

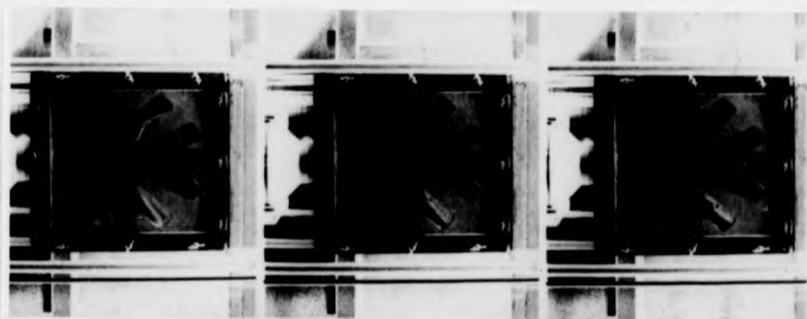


Fig 126. $\phi 15$ mm blow hole, vents in channels 3, 5 and 7 open

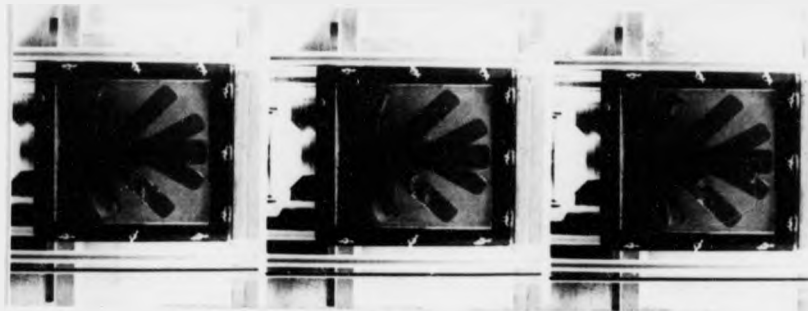


Fig 127. Φ 15 mm blow hole, vents in channels 3, 5 and 7 open

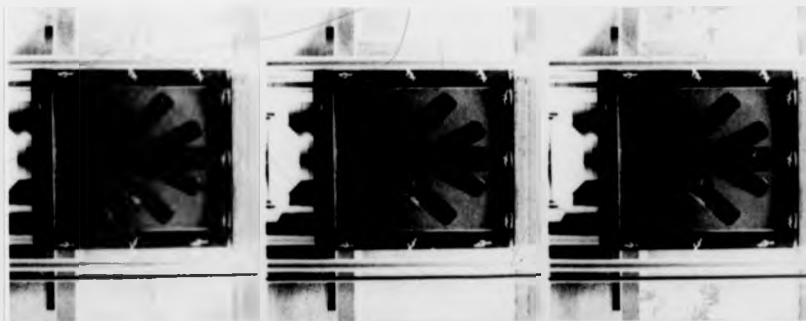


Fig 128. Φ 15 mm blow hole, vents in channels 3, 5 and 7 open



Fig 129. Sound core



Fig 130. Sound core



Fig 131. Core containing spongy areas



Fig 132. Core containing spongy areas



Fig 133. Core containing spongy areas

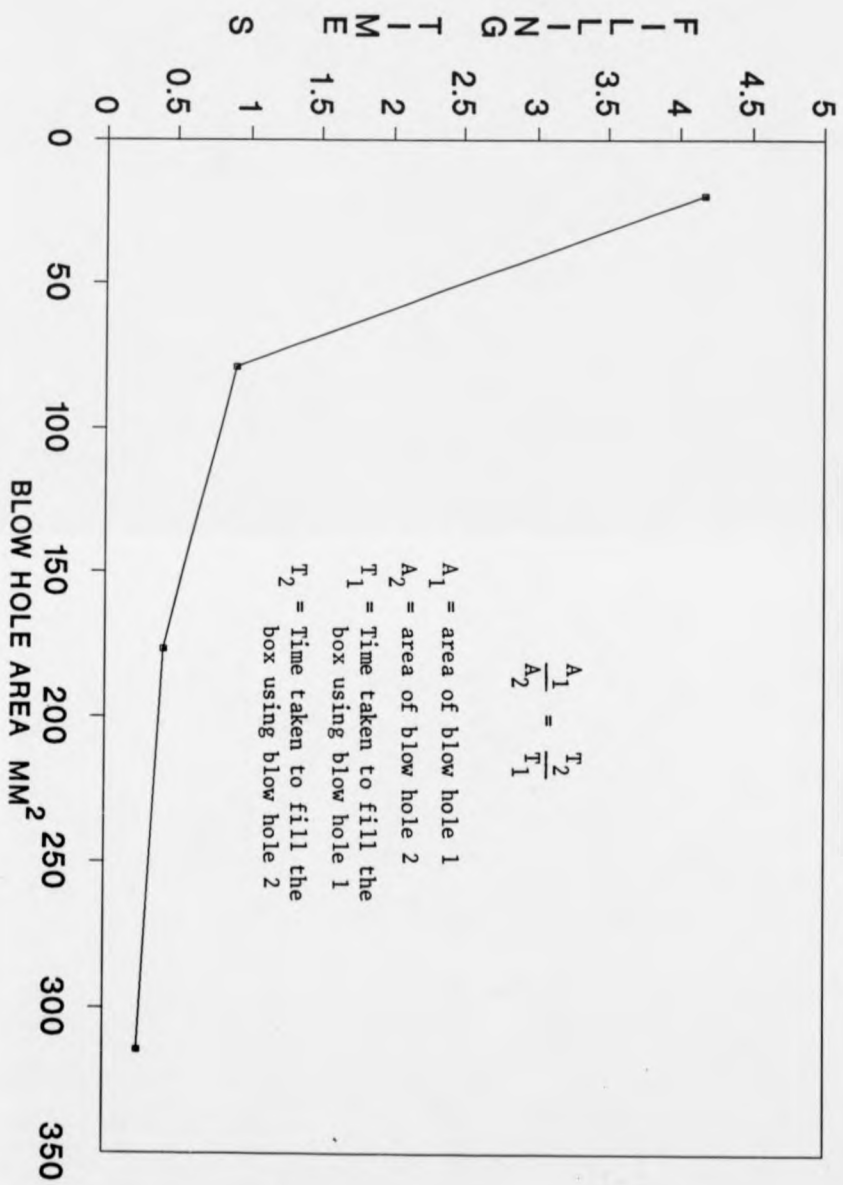


Fig 134. Core containing voids



Fig 135. Core containing voids

CORE-BOX 1
 ALL VENTS OPEN
 ZIRCON SAND
 RESIN CONTENT = 0.7 %



$$\frac{A_1}{A_2} = \frac{T_2}{T_1}$$

A₁ = area of blow hole 1
 A₂ = area of blow hole 2
 T₁ = Time taken to fill the box using blow hole 1
 T₂ = Time taken to fill the box using blow hole 2

FIG 136. FILLING TIME vs BLOW HOLE AREA

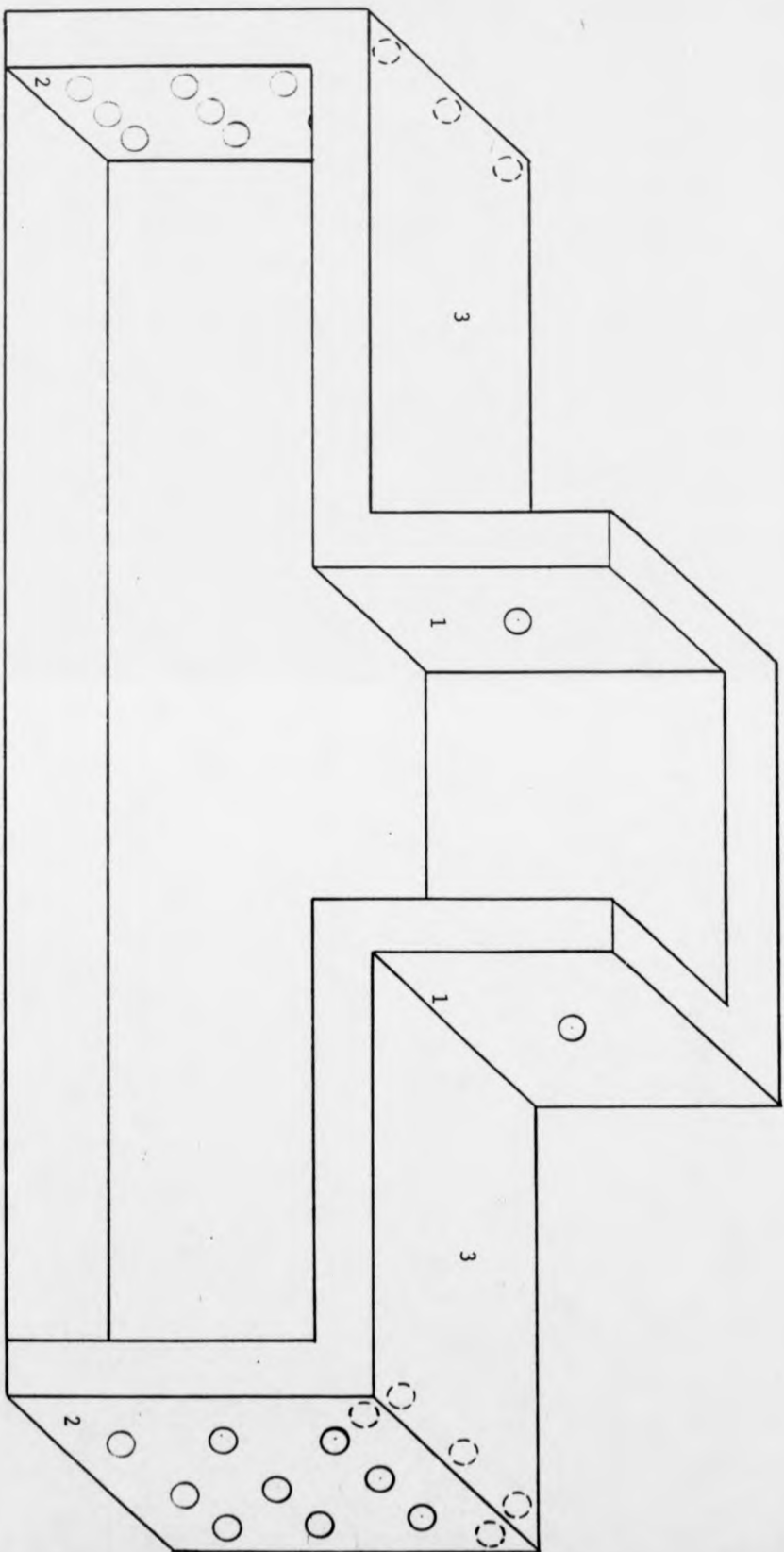


Fig 137. Schematic diagram of core-box number 2 showing the position of the vents and the number of different sections of the core-box

Experiment No.	Blow hole	Core-box venting arrangement	Core-weight gms	Blow time 1 Frame = 1/64 secs
1	φ5mm	All open (a total of 20)	1504 ¹⁵¹³ ₁₄₉₅	290 = 4.53
2	φ10mm	" "	1504 ¹⁵¹⁰ ₁₅₀₀	76 = 1.19
3	φ15mm	" "	1508 ¹² ₀₃	34 = 0.53
4	φ20mm	" "	1521 ²⁶ ₁₉	23 = 0.36
5	φ25mm	" "	1521 ²⁴ ₁₉	NOT MEASURED
6	φ30mm	" "	1523 ²⁵ ₂₂	12 = 0.19
7	φ15 = triangular	" "	1506 ¹¹ ₀₂	34 = 0.53
8	φ15 = rectangular	" "	1504 ¹³ ₀₀	34 = 0.53

Fig 138. Experiments carried out in sub-group b of group 1 on box 2

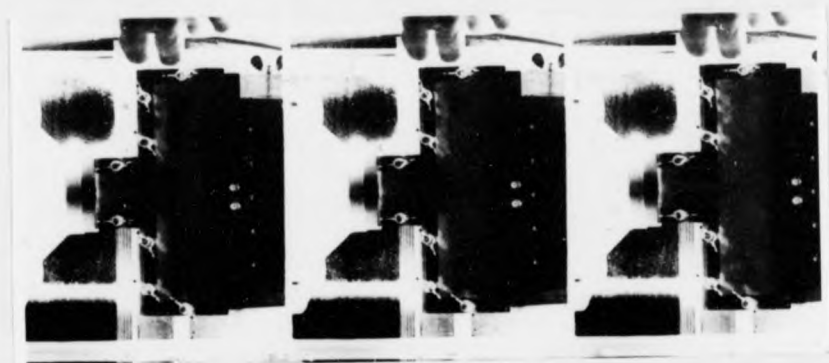


Fig 139. Φ 10 mm blow hole, all vents open

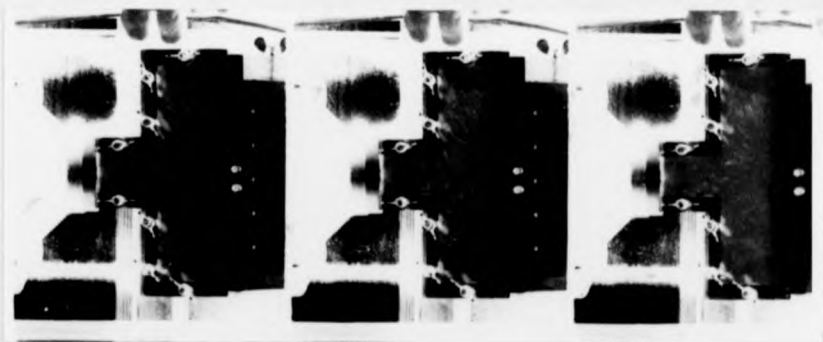


Fig 140. Φ 10 mm blow hole, all vents open

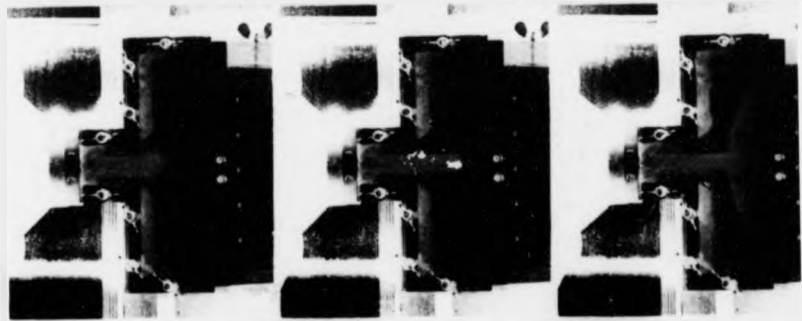


Fig 141. Φ 15 mm blow hole, all vents open

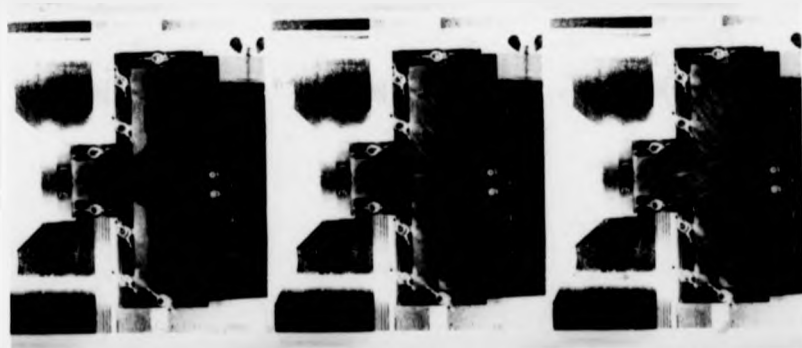


Fig 142. Φ 15 mm blow hole, all vents open

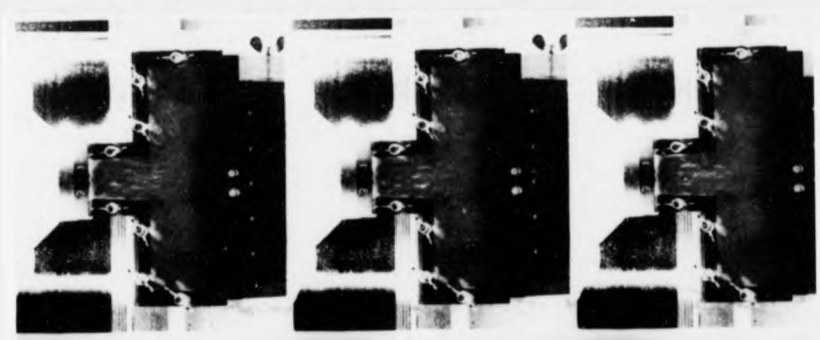


Fig 143. Φ 15 mm blow hole, all vents open



Fig 144. Φ 30 mm blow hole, all vents open

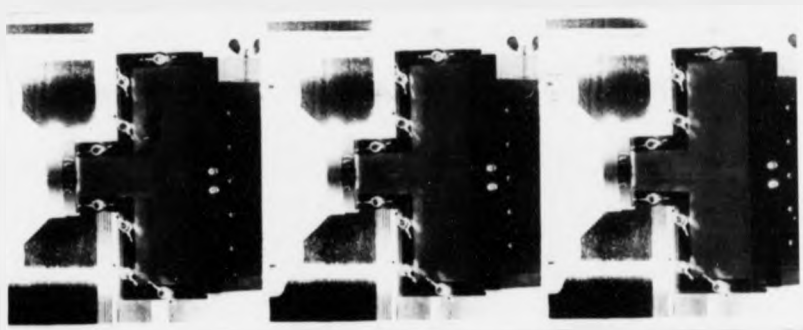


Fig 145. $\Phi 30$ mm blow hole, all vents open



Fig 146. $\Phi 30$ mm blow hole, all vents open

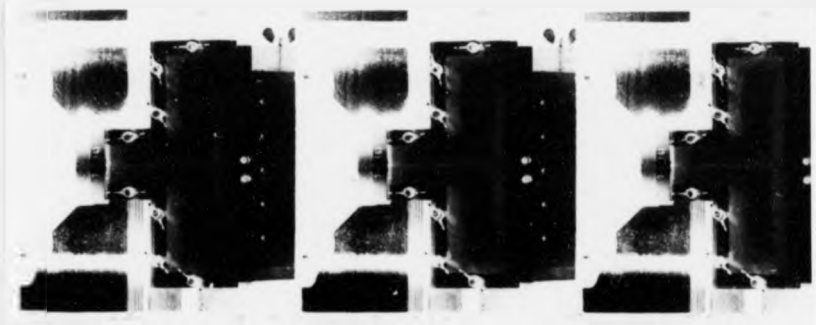


Fig 147. $\phi 5$ mm blow hole, all vents open

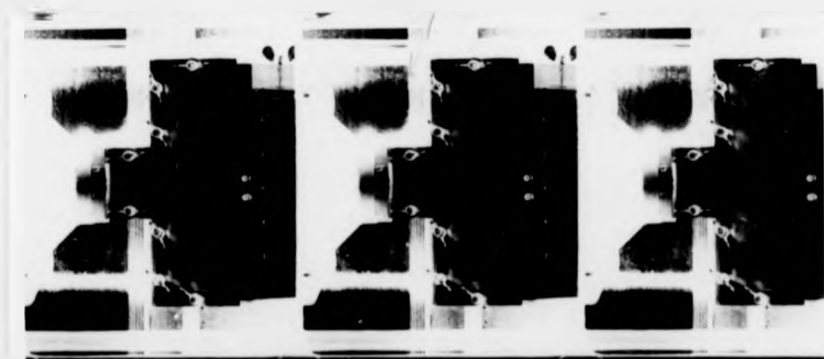


Fig 148. $\phi 5$ mm blow hole, all vents open

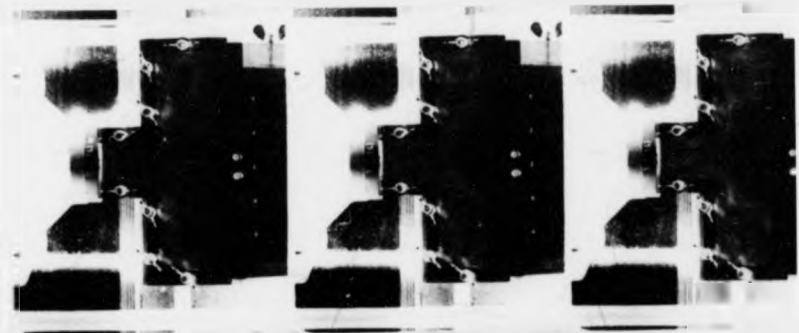


Fig 149. $\phi 5$ mm blow hole, all vents open

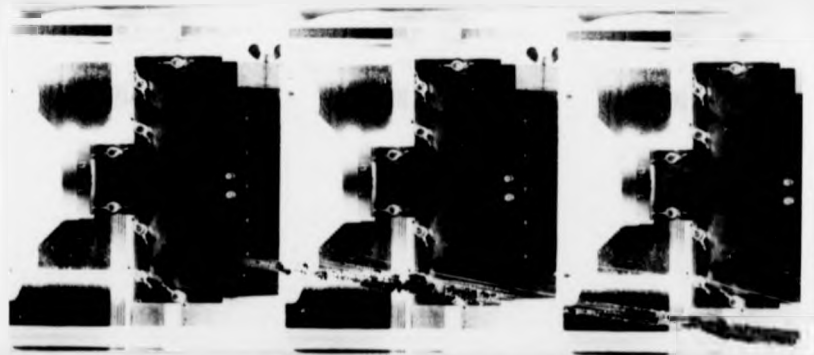


Fig 150. $\phi 5$ mm blow hole, all vents open



Fig 151. $\phi 5$ mm blow hole, all vents open

Experiment number	Core-box venting arrangement (Vents open)	Core-weight gms	Blow time secs	Comments
9	Bottom 3 vents of Section 2	1436 ⁴⁰ ₃₁	1.06	Voids on topcorners of section 2
10	Middle 3 vents of Section 2	1449 ⁵⁷ ₃₈	0.70	" (smaller)
11	Top 3 vents of Section 2	1458 ⁶⁴ ₅₂	0.70	" (smaller)
12	Bottom 3 vents of Section 2 & Section 1	1445	0.67	No voids
13	Middle 3 vents of Section 2 & Section 1	1457	0.64	No voids
14	Top 3 vents of Section 2 & Section 1	1468	0.62	No voids
15	Vents of Section 2 on L.H.S.	1407 ¹⁶ ₀₈	0.62	Large voids on R.H.S.
16	Vents of Section 2 on R.H.S.	1402 ¹⁴⁰⁸ ₁₃₉₂	0.62	Large voids on L.H.S.
17	Vents of Section 2 on L.H.S and Section 1	1420 ³⁴ ₁₁	Not measured	Voids on R.H.S.
18	Vents of Section 2 on R.H.S. and Section 1	1428 ³⁵ ₂₀	Not measured	Voids on L.H.S.
19	Vents of Section 1, First blow	1327 ¹⁴¹⁰ ₁₂₄₈	1.73	Large voids on both sides of Section 2
20	Vents of Section 1, second blow	1491 ¹⁵⁰⁰ ₁₄₈₄	Not measured	Smaller voids on both sides of Section 2

φ15mm blow hole at ~ 6 bars

Fig 152. Experiments carried out in sub-group b of group 1 on box 2



Fig 153. $\Phi 15$ mm blow hole, vents on section 1 open only



Fig 154. $\Phi 15$ mm blow hole, vents on section 1 open only

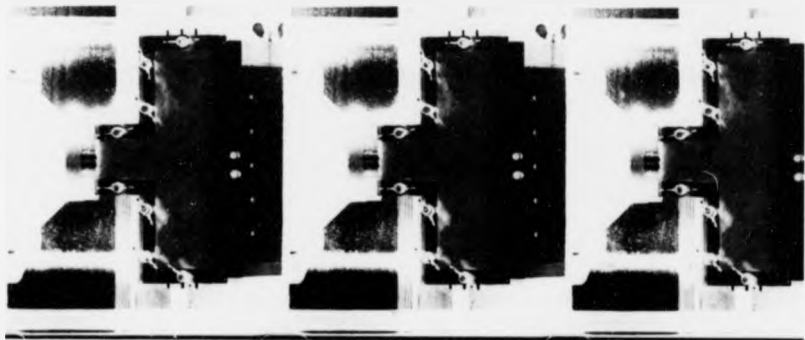


Fig 155. $\phi 15$ mm blow hole, vents on section 1 open only

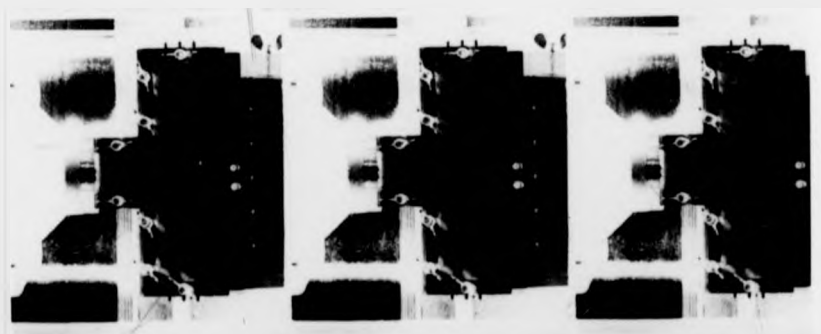


Fig 156. $\phi 15$ mm blow hole, vents on section 1 open only



Fig 157. $\phi 15$ mm blow hole, vents on section 1 open only



Fig 158. $\phi 15$ mm blow hole, vents on left side of the core-box open only

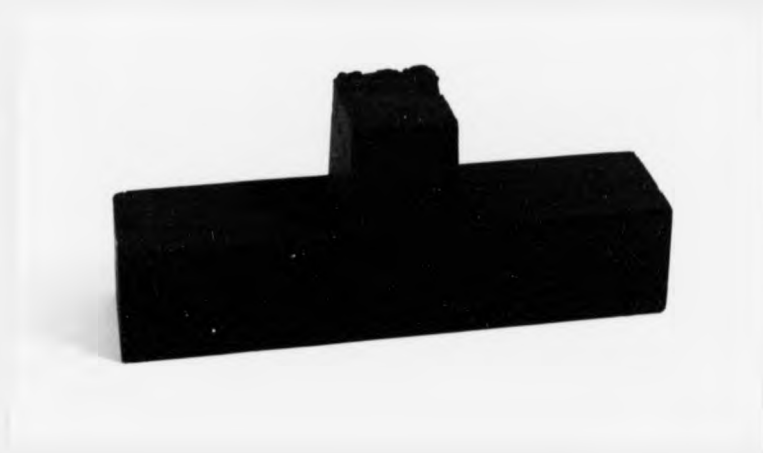


Fig 159. $\phi 15$ mm blow hole, top 3 vents on the right hand side and bottom 3 vents on the left hand side on section 2 of the core-box open only



Fig 160. $\phi 15$ mm blow hole, bottom 3 vents of section 2 and vents on section 1 of the core-box open only



Fig 161. ϕ 15 mm blow hole, middle 3 vents on section 2 of the core-box open only

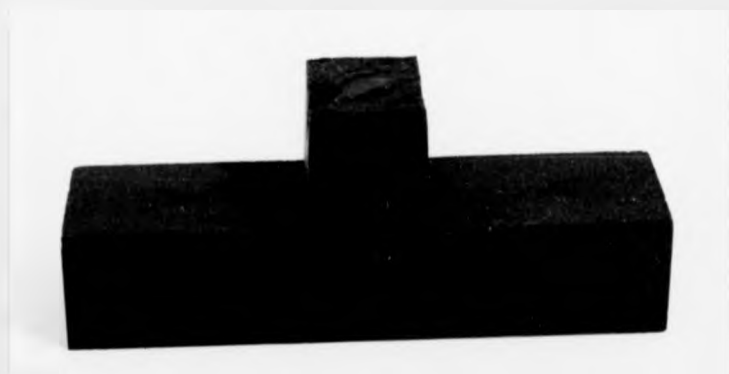


Fig 162. ϕ 15 mm blow hole, middle 3 vents on section 2 and vents on section 1 of the core-box open only



Fig 163. ϕ 15 mm blow hole, top 3 vents of section 2 and vents on section 1 of the core-box open only

Air pressure		Blow hole diameter mm			
psi	bars	10	15	20	30
85	5.86	1501	1508	1505 ¹³ ₀₀	1503 ⁰⁶ ₀₀
75	5.17	1497 ⁹⁹ ₉₆	1505 ⁰⁷ ₀₄	1501 ⁰⁴ ₁₄₉₉	1495 ⁹⁶ ₉₄
65	4.48	1486 ⁸⁹ ₈₄	1504 ⁰⁷ ₀₁	1492 ⁹⁶ ₈₉	1484 ⁸⁶ ₈₄
55	3.79	1485 ⁹¹ ₇₆	1496 ⁹⁷ ₉₃	1486 ⁸⁸ ₈₃	1476 ⁷⁸ ₇₄
45	3.10	1466 ⁷⁸ ₅₄	1478 ⁸² ₇₀	1469 ⁷¹ ₆₈	1462 ⁶⁴ ₆₀
35	2.41	1314 ⁷¹ ₁₂	1413 ³³ ₁₃₉₇	1448 ⁶⁵ ₃₂	1421 ²⁶ ₁₅

Core-weight gms

Fig 164. Experiments carried out in group 2 on box 2.
All vents open (a total of 20)

CORE BOX 2
 ALL VENTS OPEN (20)
 ZIRCON SAND
 RESIN CONTENT = 0.7 %

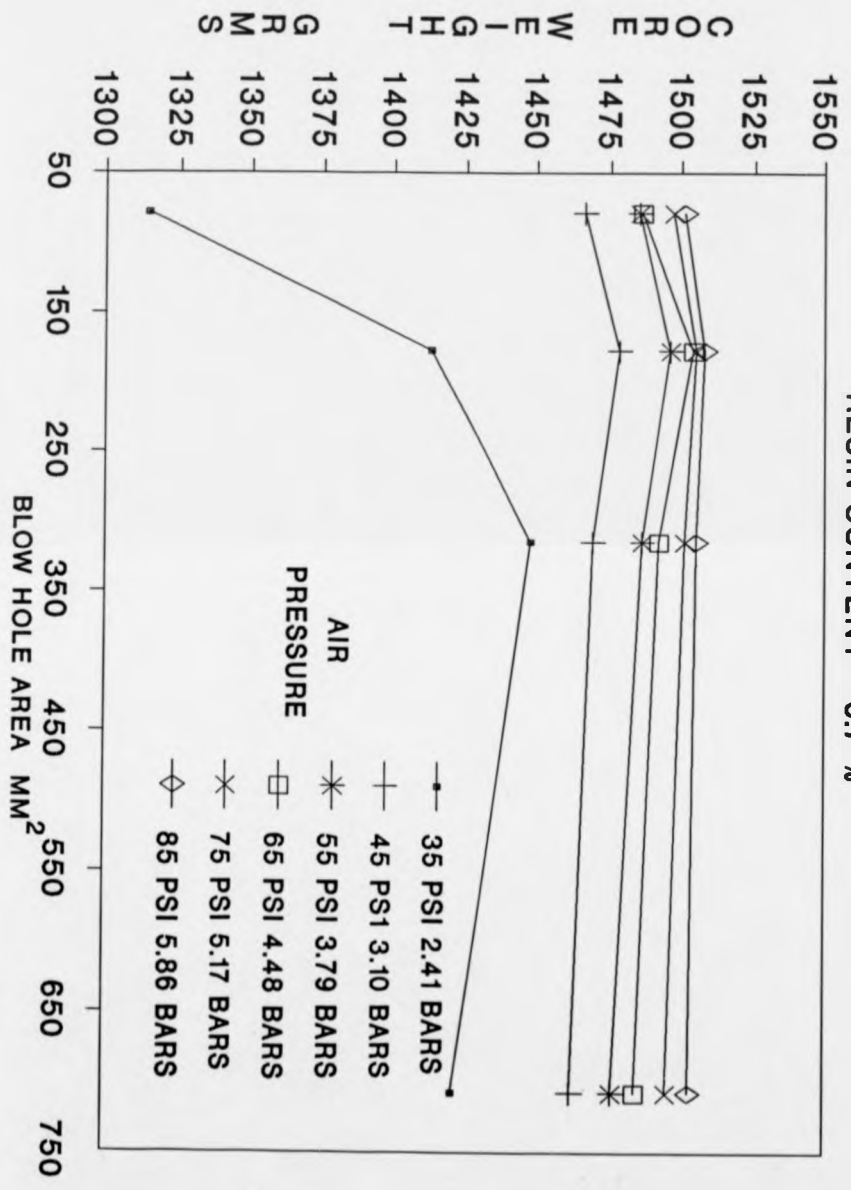


FIG 165. CORE-WEIGHT vs BLOW HOLE AREA

CORE-BOX 2
 ALL VENTS OPEN (20)
 ZIRCON SAND
 RESIN CONTENT = 0.7 %

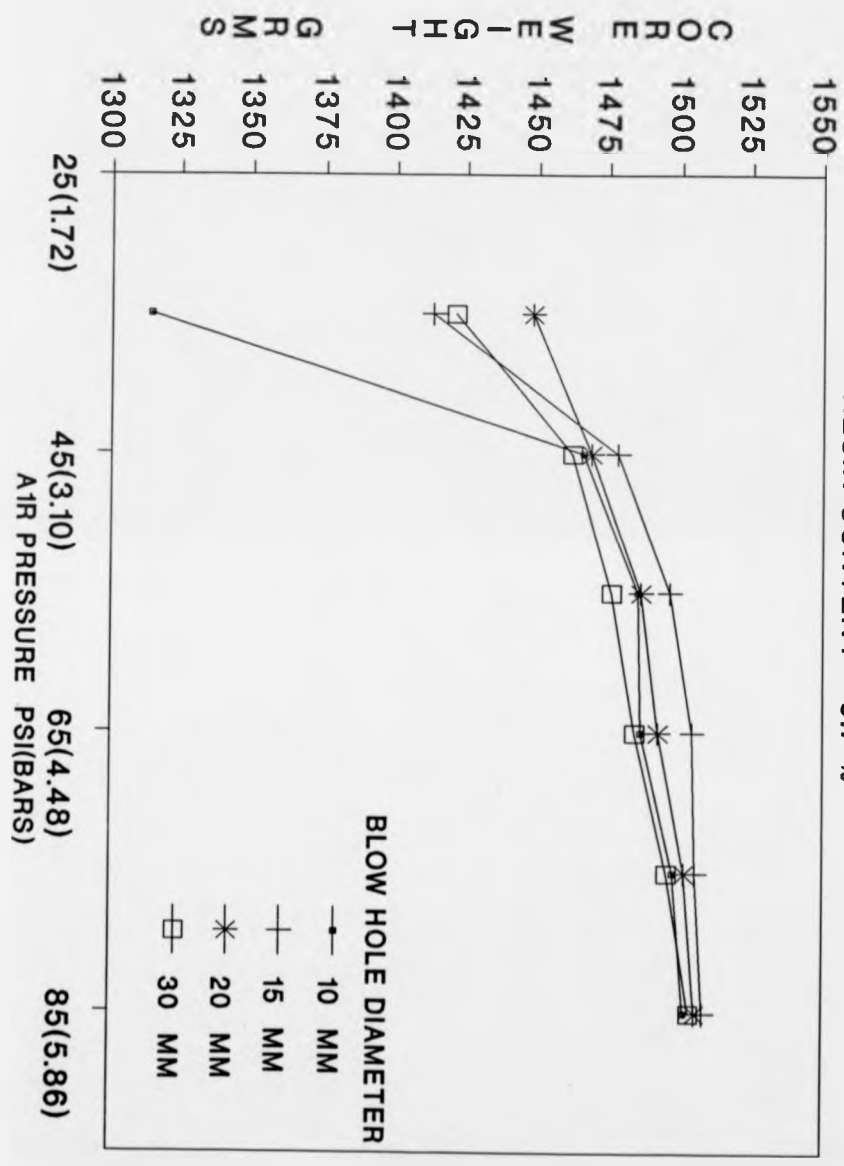


FIG 166. CORE-WEIGHT vs AIR PRESSURE

Pressure psi bars		Blow hole ϕ mm	AV Time sec	AV Core-weight grms
80	5.52	20	0.28 ^{0.30} _{0.27}	1933 ³⁶ ₂₉
80	5.52	15	0.49 ^{0.58} _{0.44}	1869 ⁹⁰ ₄₆
80	5.52	10	0.89 ^{0.93} _{0.85}	1833 ⁵³ ₀₅
80	5.52	5	5.50 ^{6.13} _{5.00}	1716 ¹⁷⁶⁶ ₁₆₅₃
60	4.14	20	0.35	1908 ¹⁰ ₀₆
60	4.14	15	0.59 ^{0.69} _{0.45}	1835 ⁴⁸ ₁₇
60	4.14	10	1.02 ^{1.07} _{0.96}	1793 ¹⁸²⁸ ₁₇₅₁
60	4.14	5	5.70 ^{6.25} _{4.97}	1674 ¹⁷⁷⁵ ₁₅₈₅
40	2.76	20	0.44 ^{0.42} _{0.46}	1855 ⁶⁰ ₄₉
40	2.76	15	0.75 ^{0.81} _{0.70}	1750 ⁶⁹ ₃₅
40	2.76	10	1.48 ^{1.56} _{1.35}	1642 ⁷⁷ ₁₆
40	2.76	5	NOT BLOWABLE	

Fig 167 Experiments carried out in sub-group a of group 3 on box 1 (All vents open)

CORE-BOX 1
 ALL VENTS OPEN
 ZIRCON SAND
 RESIN CONTENT = 0.7 %

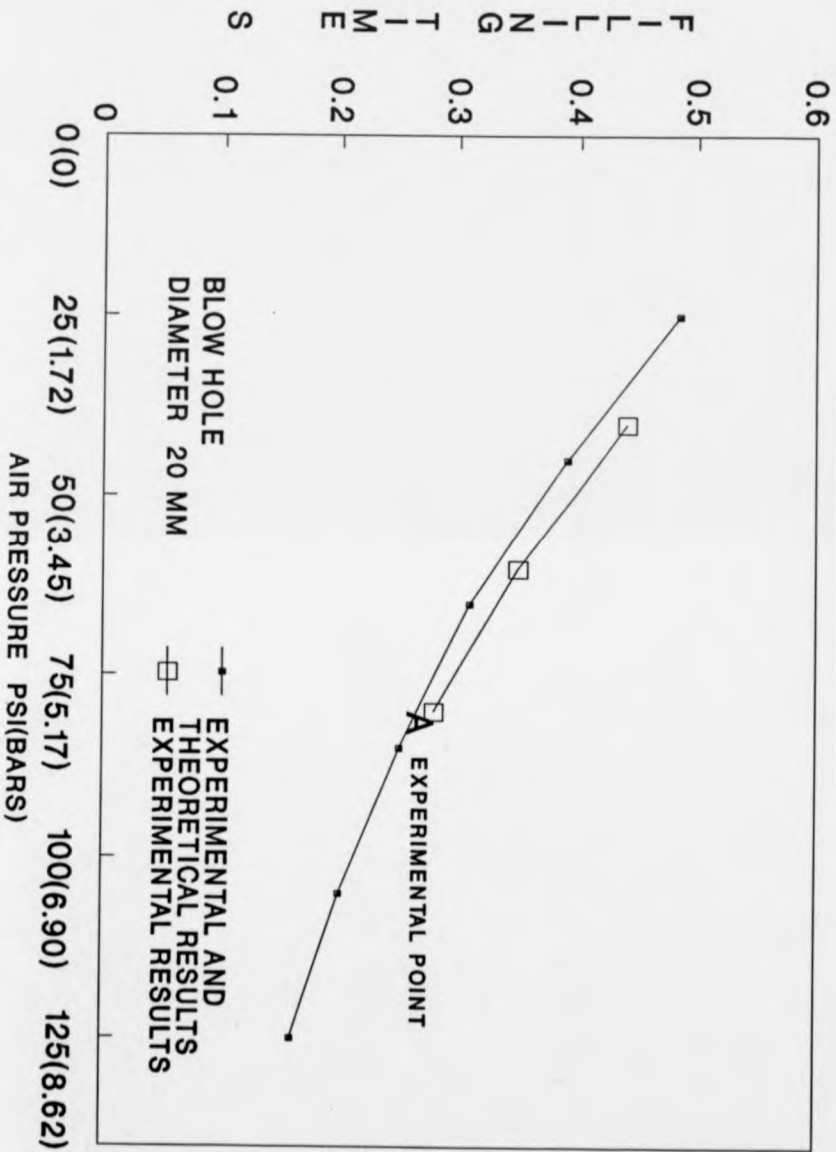


FIG 168. FILLING TIME vs AIR PRESSURE

CORE-BOX 1
 ALL VENTS OPEN
 ZIRCON SAND
 RESIN CONTENT = 0.7 %

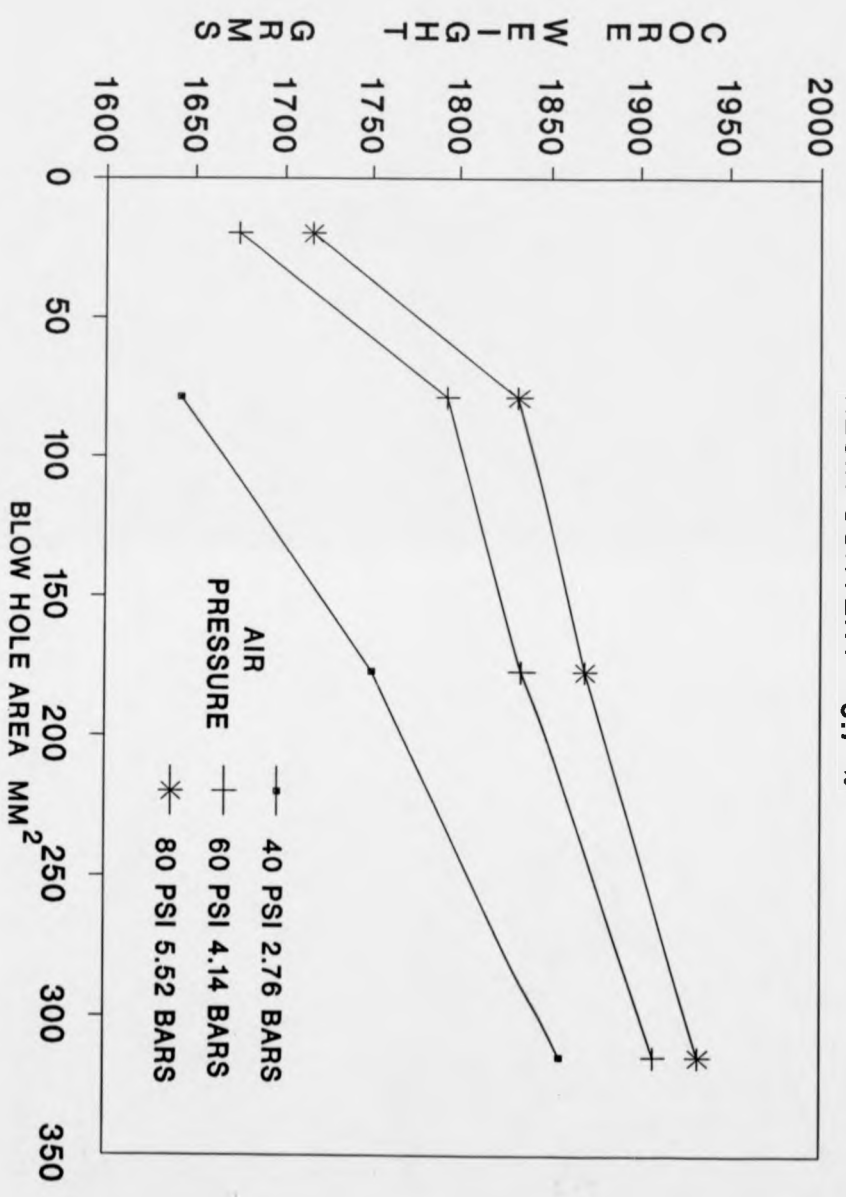


FIG 169. CORE-WEIGHT vs BLOW HOLE AREA

CORE-BOX 1
 ALL VENTS OPEN
 ZIRCON SAND
 RESIN CONTENT = 0.7 %

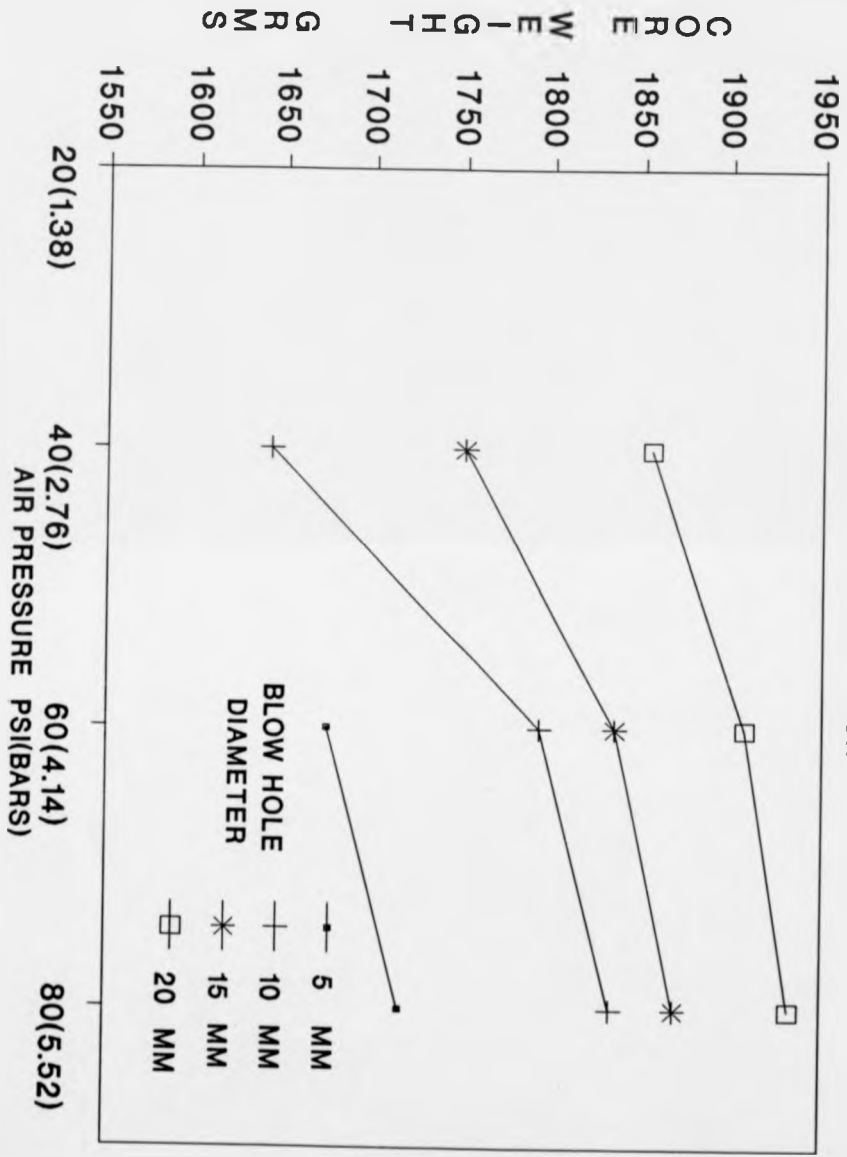


FIG 170. CORE-WEIGHT vs AIR PRESSURE

Pressure		Blow hole ϕ mm						Correct weight grms
psi	bars	5	10	15	20	25	30	
85	5.86	1495 ⁴⁶⁰ ₅₁₅	1508 ⁰⁴ ₁₃	1518.5	1524	1530	1537 ³⁵ ₃₈	
75	5.17	1489 ⁴⁶⁴ ₅₂₀	1502	1513 ¹¹ ₁₅	1520 ¹⁹ ₂₁	1523.5	1528	
65	4.48	1485 ⁴⁶⁵ ₅₀₁	1496.5	1509 ⁰⁸ ₁₀	1518	1522 ²¹ ₂₃	1527	
55	3.79	1472 ⁷⁰ ₇₄	1491 ⁹⁰ ₉₂	1503	1508	1518 ¹⁷ ₁₈	1527	
45	3.10	1431 ²⁶ ₃₆	1469.5 ⁶⁷ ₇₁	1483 ⁷⁹ ₈₄	1493.5 ⁹⁵ ₉₂	1502.5 ⁰⁴ ₀₁	1515 ¹⁶ ₁₄	
35	2.41	-	1432 ²⁷ ₃₉	1458 ⁵⁷ ₅₉	1469.5 ⁶⁹ ₇₀	1483.5 ⁸³ ₈₇	1502.5 ⁰⁰ ₀₅	

Fig 171. Experiments carried out in sub-group b of group 3 on box 2, all vents open (a total of 30)

CORE-BOX 2
 ALL VENTS OPEN (30)
 ZIRCON SAND
 RESIN CONTENT = 0.7 %

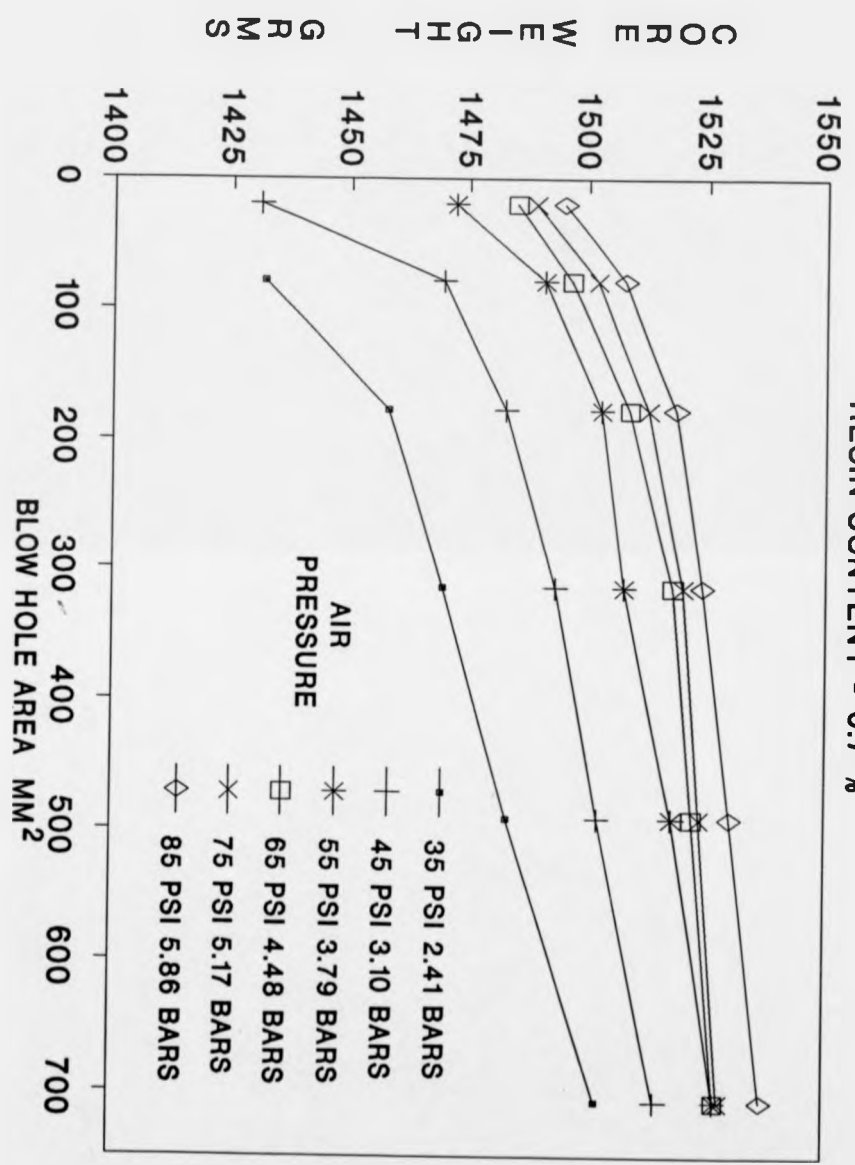


FIG 172. CORE-WEIGHT vs BLOW HOLE AREA

CORE-BOX 2
 ALL VENTS OPEN (30)
 ZIRCON SAND
 RESIN CONTENT = 0.7 %

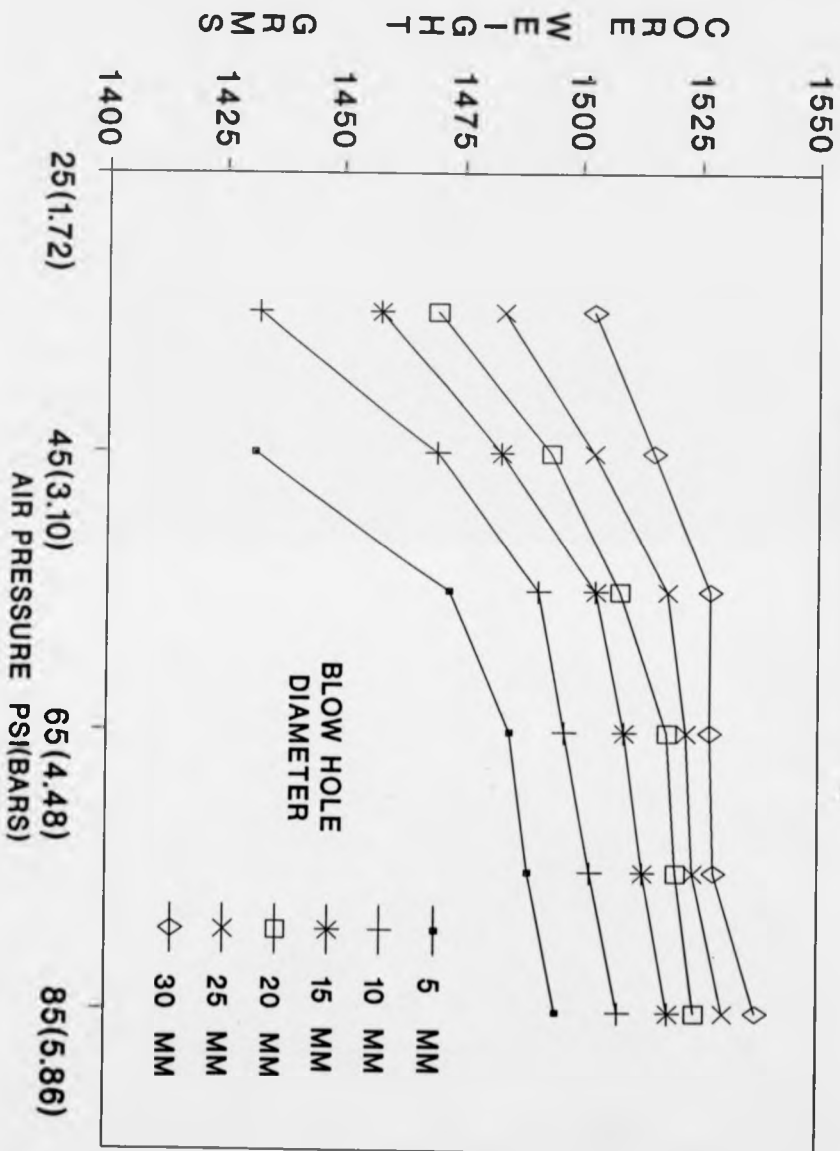


FIG 173. CORE-WEIGHT VS AIR PRESSURE

Pressure psi bars	Blow hole ϕ mm	AV Time sec	AV Core-weight grms
80 5.52	20	0.31	1921 ²⁵ ₁₉
80 5.52	15	0.48 ^{0.44} _{0.52}	1835 ⁴¹ ₃₀
80 5.52	10	0.93 ^{0.87} _{0.97}	1751 ⁸⁰ ₃₅
60 4.14	20	0.35	1882 ⁷³ ₉₀
60 4.14	15	0.64 ^{0.64} _{0.65}	1791 ⁹⁹ ₈₃
60 4.14	10	1.14 ^{1.30} _{1.02}	1693 ⁸⁸ ₉₈
40 2.76	20	0.44 ^{0.43} _{0.44}	1798 ¹⁸⁰¹ ₁₇₉₅
40 2.76	15	0.77 ^{0.85} _{1.82}	1733 ³⁶ ₂₈
40 2.76	10	1.70 ^{1.82} _{1.56}	1584 ⁸⁶ ₈₂

Fig 174 Experiments carried out in sub-group a of group 4 on box 1. Resin content = 1.05% (All vents open)

Pressure psi bars	Blow hole ϕ mm	AV Time sec	AV Core-weight grms
80 5.52	20	0.24 ^{0.24} _{0.25}	1924 ²⁷ ₂₃
80 5.52	15	0.43 ^{0.46} _{0.41}	1852 ⁵⁴ ₄₉
80 5.52	10	0.91 ^{0.98} _{0.85}	1790 ¹⁸¹⁸ ₁₇₆₈
60 4.14	20	0.34	1904
60 4.14	15	0.46 ^{0.47} _{0.46}	1813 ¹⁵ ₁₁
60 4.14	10	0.95 ^{0.99} _{0.91}	1412 ¹⁴ ₁₀
40 2.76	20	0.44 ^{0.47} _{0.41}	1836 ⁴³ ₃₁
40 2.76	15	0.79 ^{0.84} _{0.74}	1747 ⁵¹ ₄₃
40 2.76	10	1.30 ^{1.41} _{1.23}	1642 ⁵² ₂₉

Fig 175. Experiments carried out in sub-group a of group 4 on box 1. Resin content = 0.35% (All vents open).

CORE-BOX 1
 ALL VENTS OPEN
 ZIRCON SAND
 RESIN CONTENT = 1.05 %

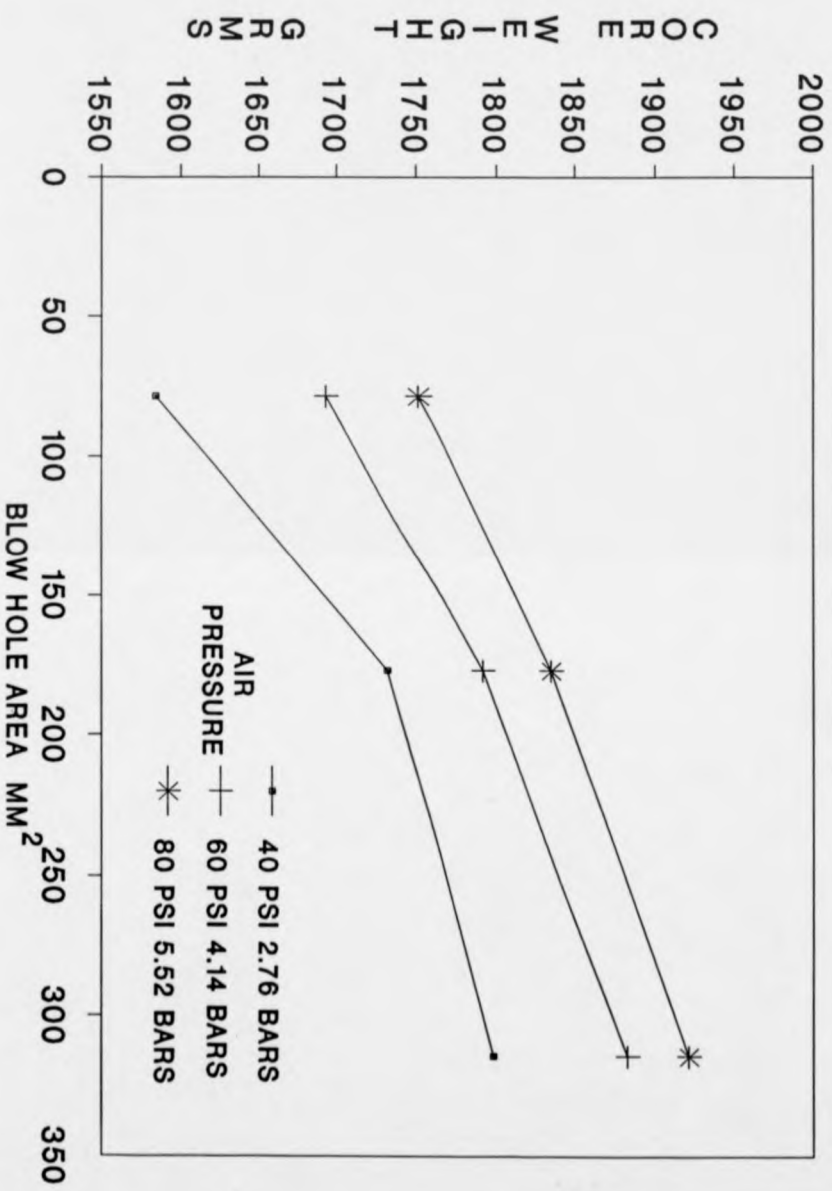


FIG 176. CORE-WEIGHT VS BLOW HOLE AREA

CORE-BOX 1
 ALL VENTS OPEN
 ZIRCON SAND
 RESIN CONTENT = 1.05 %

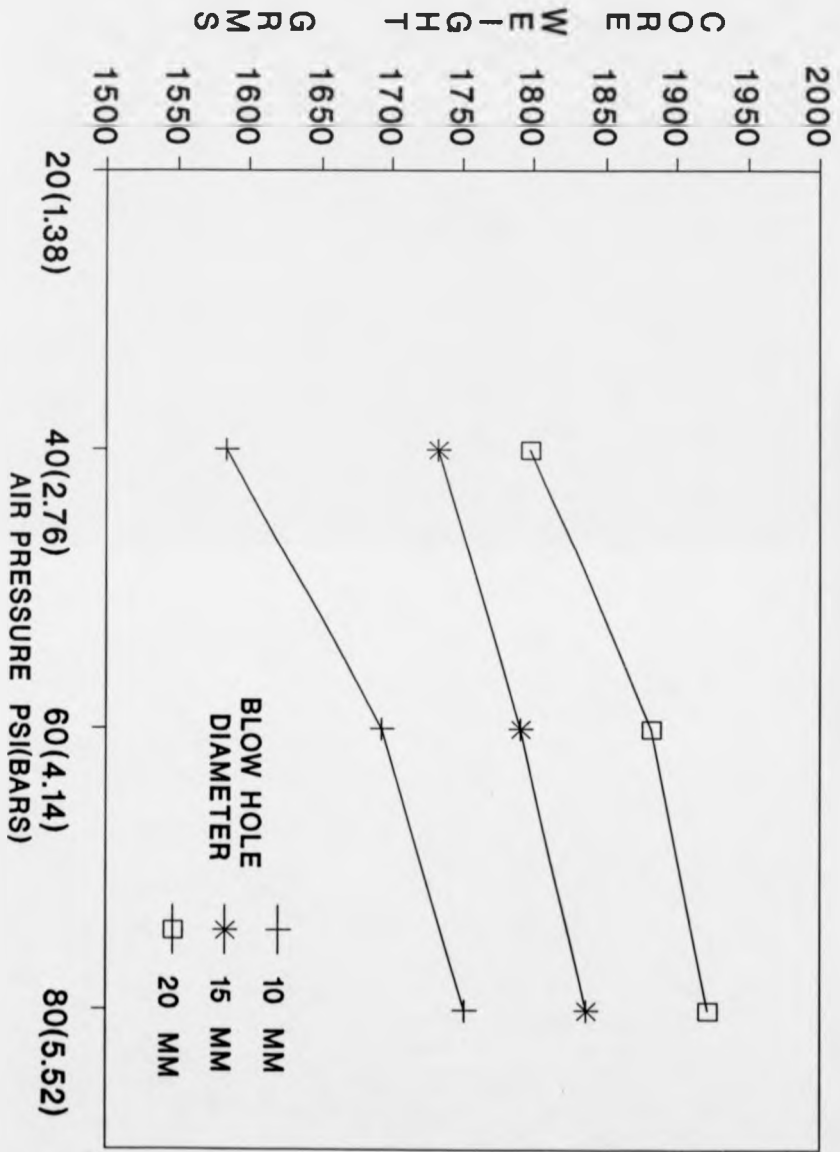


FIG 177. CORE-WEIGHT vs AIR PRESSURE

CORE-BOX 1
 ALL VENTS OPEN
 ZIRCON SAND
 RESIN CONTENT = 0.35 %

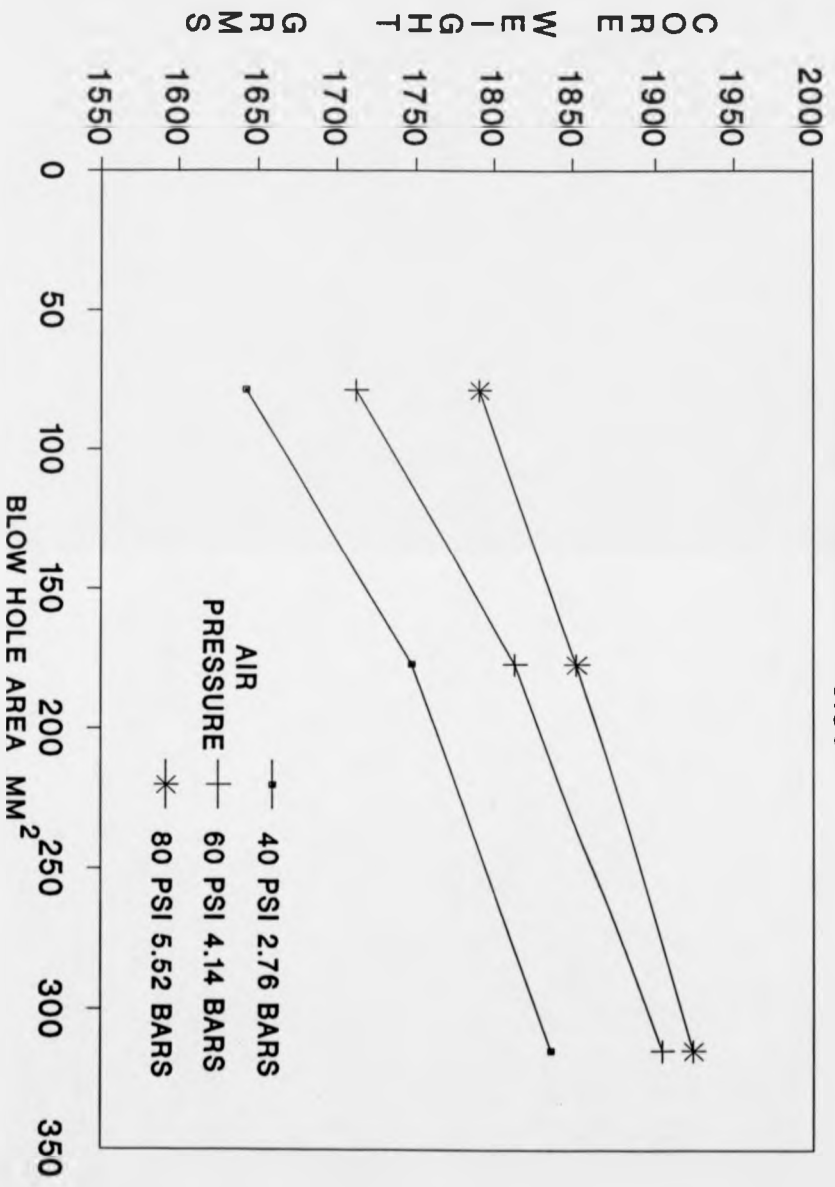


FIG 178. CORE-WEIGHT vs BLOW-HOLE AREA

CORE-BOX 1
 ALL VENTS OPEN
 ZIRCON SAND
 RESIN CONTENT = 0.35 %

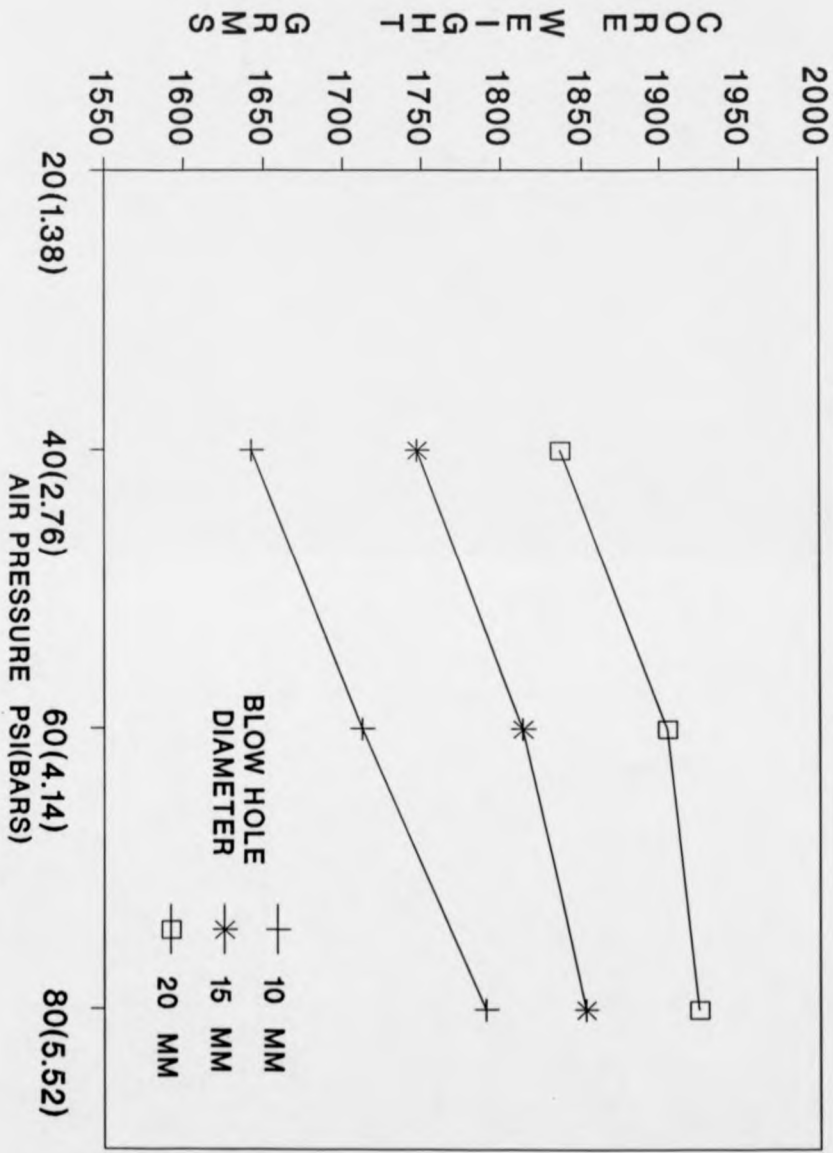


FIG 179. CORE-WEIGHT vs AIR PRESSURE

Pressure psi bars	Blow hole ϕ mm	Average core-weight/gms			
		RC = 0.35%	RC = 0.7%	RC = 1.05%	
85	5.86	25	1522 ²³ ₂₂	1539 ⁴⁰ ₃₈	1544 ⁴⁵ ₄₄
85	5.86	20	1512 ¹³ ₁₂	1532 ³³ ₃₁	1537 ³⁸ ₃₅
85	5.86	15	1508 ¹⁰ ₀₆	1526 ²⁷ ₂₅	1526 ²⁶ ₂₅
85	5.86	10	1505 ¹² ₀₀	1517 ²² ₁₂	1513 ¹⁸ ₀₈
65	4.48	25	1516 ¹⁷ ₁₅	1525 ²⁶ ₂₅	1528 ²⁹ ₂₇
65	4.48	20	1507	1517	1519 ²⁴ ₁₄
65	4.48	15	1496 ⁹⁷ ₉₅	1513 ¹⁵ ₁₀	1507 ¹⁴ ₀₂
65	4.48	10	1488 ⁸⁹ ₈₆	1508 ⁰⁹ ₀₇	1490 ⁹⁵ ₈₅
45	3.10	25	1512 ¹³ ₁₁	1514 ¹⁶ ₁₂	1519 ²¹ ₁₈
45	3.10	20	1504 ⁰⁵ ₀₃	1509 ⁰⁹ ₀₈	1511 ¹⁵ ₀₆
45	3.10	15	1494 ⁹⁶ ₉₃	1498 ⁹⁹ ₉₇	1498 ⁵⁰⁴ ₄₉₃
45	3.10	10	1479 ⁸¹ ₇₆	1480 ⁸⁴ ₇₅	1480 ⁸¹ ₇₈

Fig 180 Experiments carried out in sub-group b of group 4 on box 2. All vents open (a total of 30)

CORE-BOX 2
 ALL VENTS OPEN (30)
 ZIRCON SAND
 RESIN CONTENT = 0.35 %

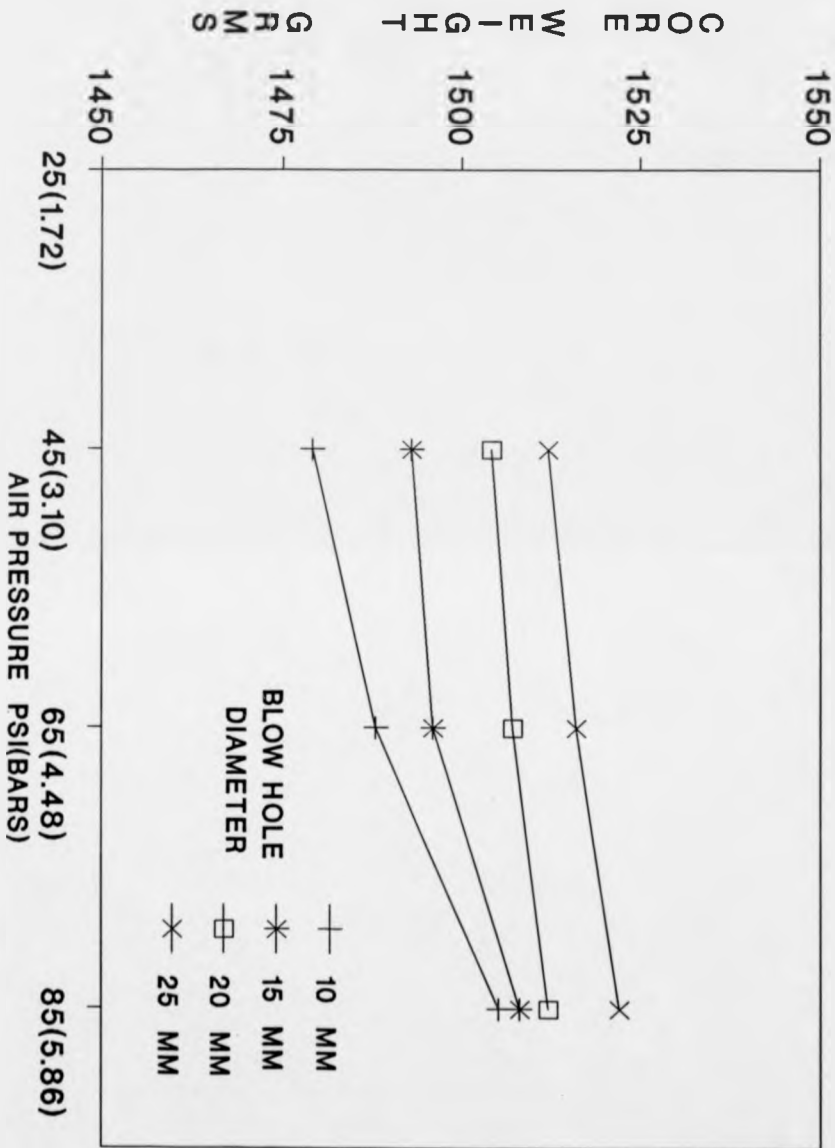


FIG 181. CORE-WEIGHT vs AIR PRESSURE

CORE-BOX 2
 ALL VENTS OPEN (30)
 ZIRCON SAND
 RESIN CONTENT - 0.7 %

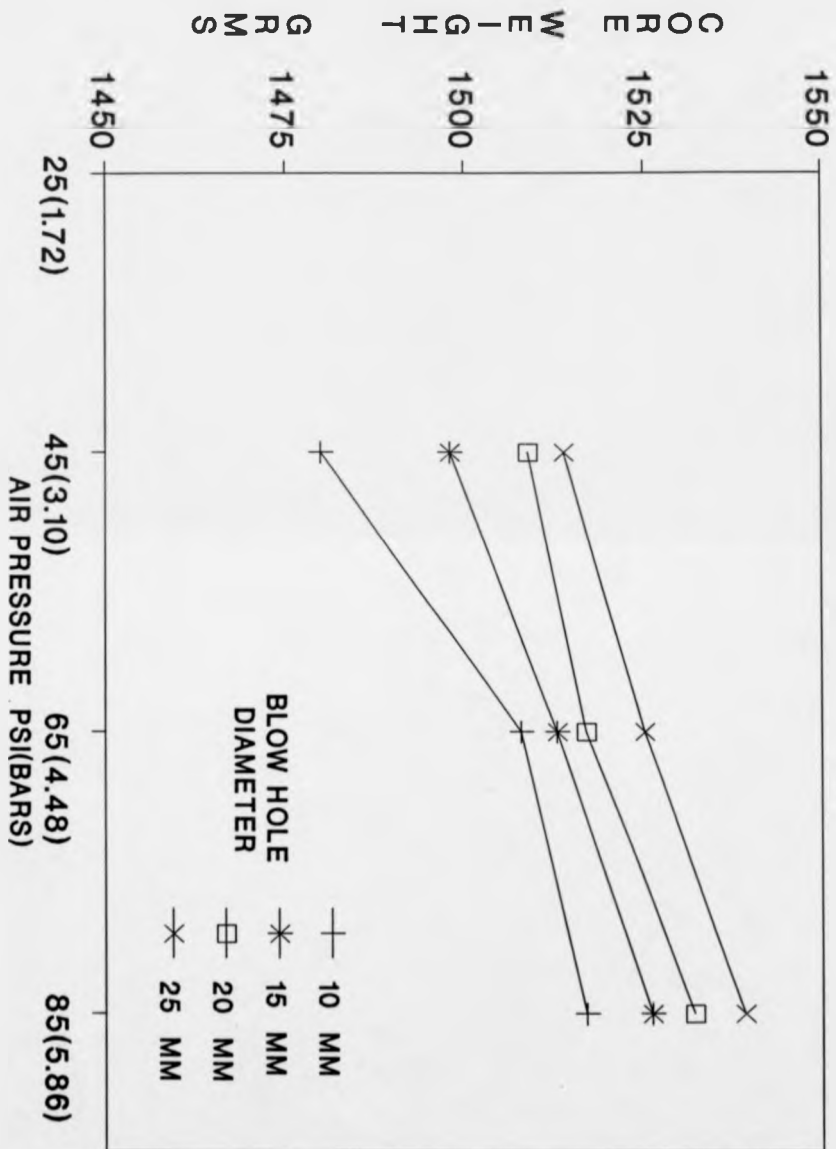


FIG 182. CORE-WEIGHT vs AIR PRESSURE

CORE-BOX 2
 ALL VENTS OPEN (30)
 ZIRCON SAND
 RESIN CONTENT - 1.05 %

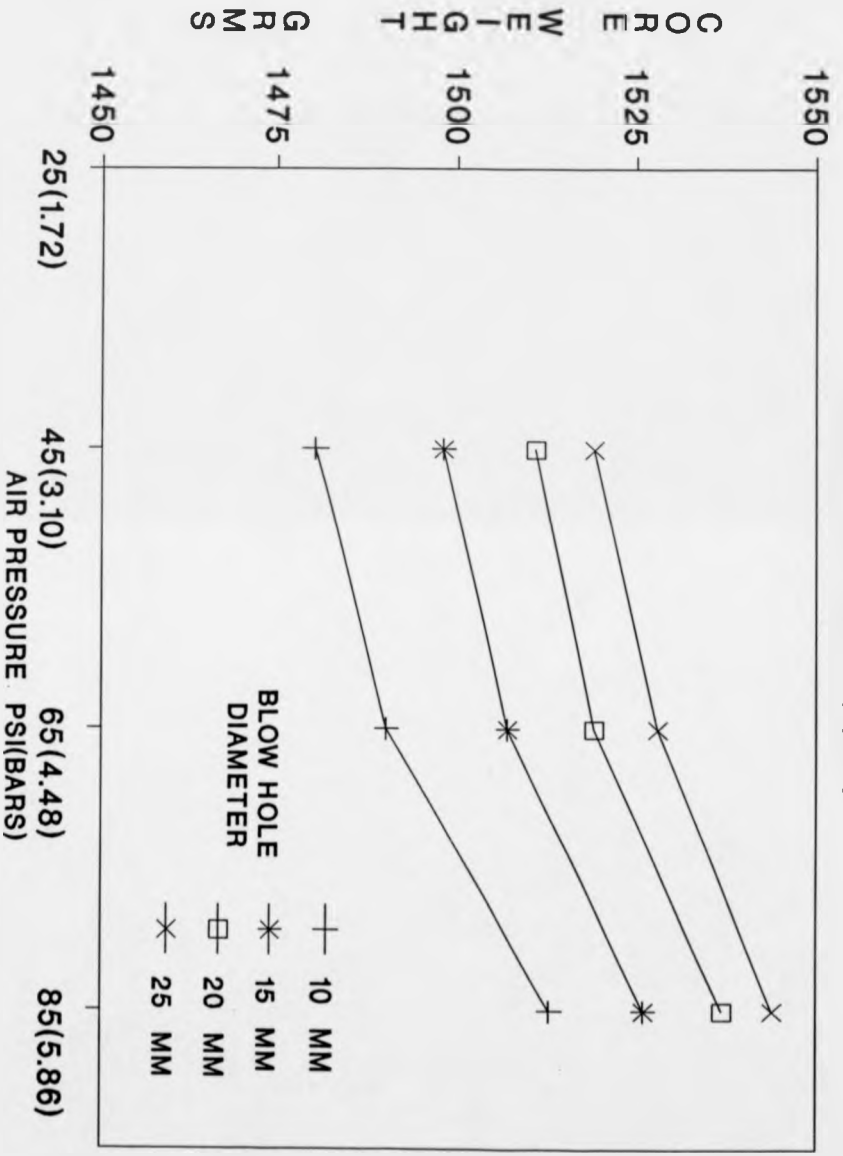


FIG 183. CORE-WEIGHT vs AIR PRESSURE

CORE-BOX 2
 ALL VENTS OPEN (30)
 ZIRCON SAND
 RESIN CONTENT = 0.35%

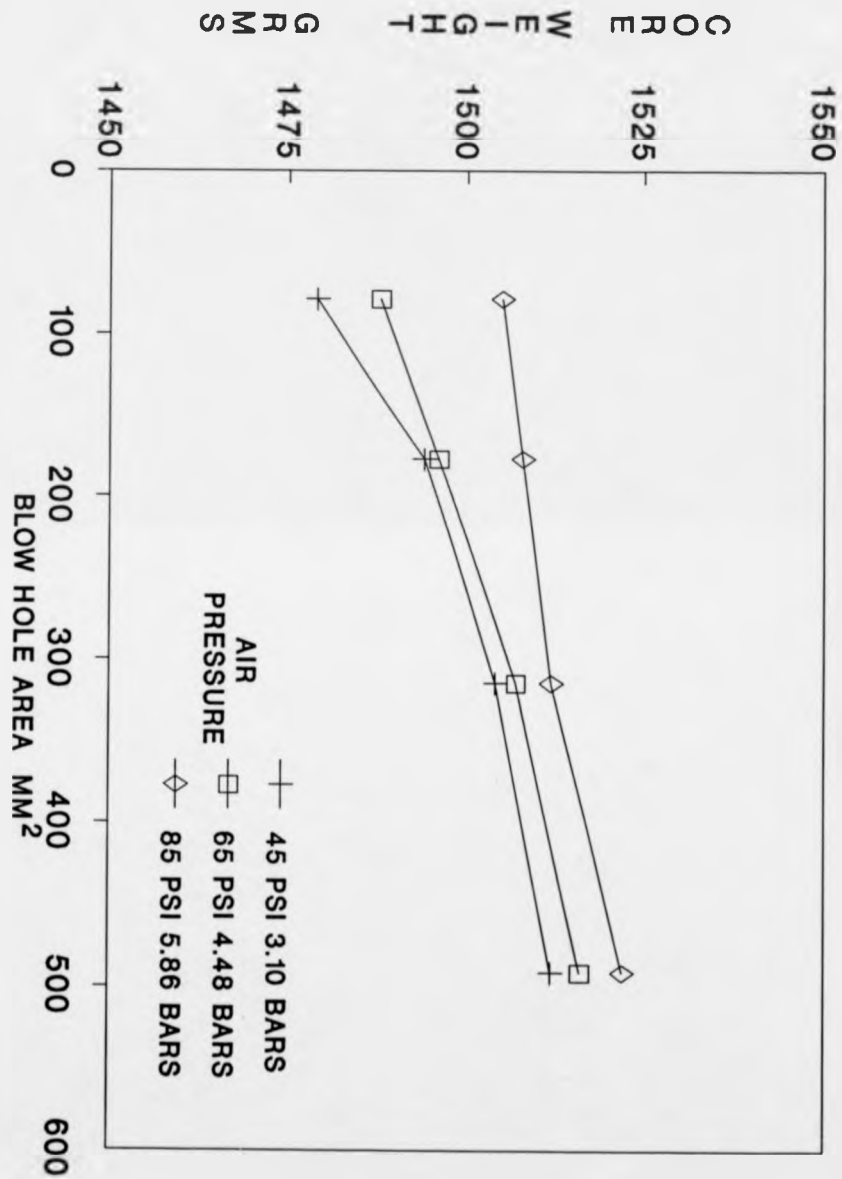


FIG 184. CORE-WEIGHT vs BLOW HOLE AREA

CORE-BOX 2
 ALL VENTS OPEN (30)
 ZIRCON SAND
 RESIN CONTENT = 0.7 %

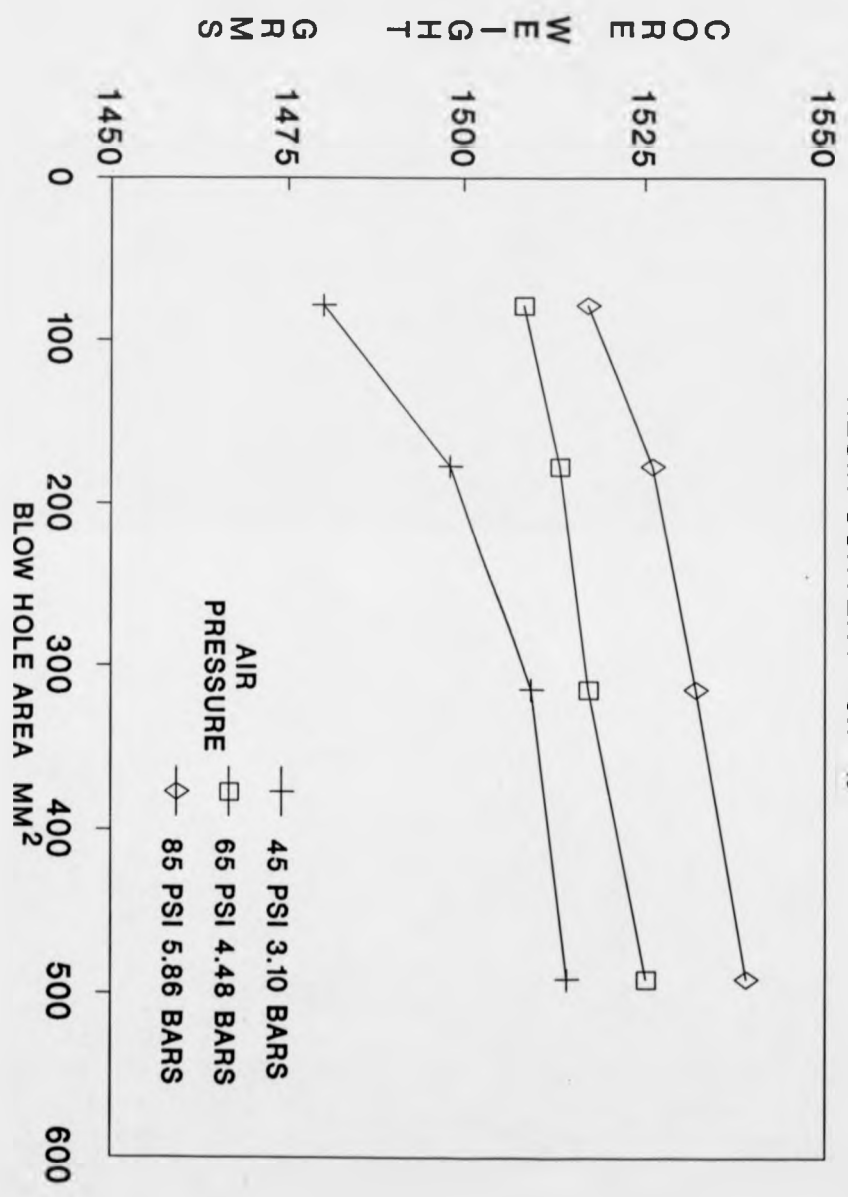


FIG 185. CORE-WEIGHT vs BLOW HOLE AREA

CORE-BOX 2
ALL VENTS OPEN (30)
ZIRCON SAND
RESIN CONTENT = 1.05%

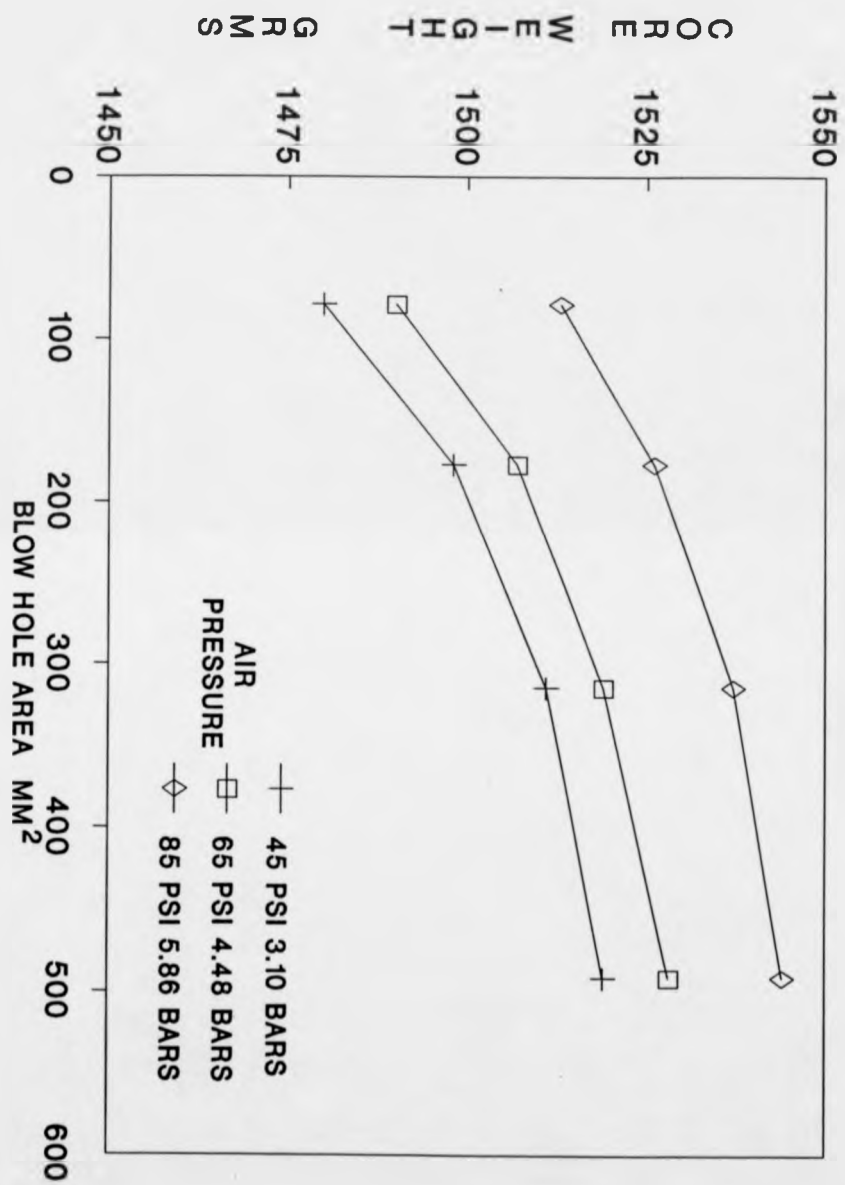


FIG 186. CORE-WEIGHT vs BLOW HOLE AREA

Pressure psi bars	Blow hole ϕ mm	Average core-weight/gms		
		RC = 0.35%	RC = 0.7%	RC = 1.05%
85 5.86	25	1530 ⁰⁰ ₀₀	1530 ³³ ₂₆	1543 ⁴⁴ ₄₃
	20	1520 ²¹ ₁₉	1519 ²¹ ₁₈	1534 ³⁶ ₃₃
	15	1513 ¹⁵ ₁₁	1512 ¹³ ₁₀	1523 ²⁴ ₂₃
	10	1504 ⁰⁵ ₀₃	1500 ⁰² ₄₉₅	1512 ¹⁴ ₀₉
65 4.48	25	1511 ¹² ₁₀	1509 ¹⁰ ₀₈	1519 ²⁰ ₁₉
	20	1499 ⁰¹ ₄₉₇	1500 ⁰¹ ₉₉	1502 ⁰⁵ ₀₀
	15	1494 ⁹⁶ ₉₃	1493 ⁹⁵ ₉₂	1497 ⁹⁹ ₉₆
	10	1486 ⁹¹ ₈₀	1486 ⁸⁸ ₈₃	1487 ⁸⁸ ₈₀
45 3.10	25	1485 ⁸⁶ ₈₃	1500 ⁰² ₉₉	1478 ⁷⁹ ₇₇
	20	1481 ⁸⁷ ₈₀	1497 ⁰⁰ ₉₄	1476 ⁷⁷ ₇₅
	15	1470 ⁷¹ ₆₈	1488 ⁹² ₈₄	1456 ⁷⁰ ₄₆
	10	1463 ⁷² ₅₈	1470 ⁷² ₆₇	1447 ⁵⁵ ₄₀

Fig 187 Experiments carried out in group 5 on box 2.
All vents open (a total of 30)

CORE-BOX 2
 ALL VENTS OPEN (30)
 ZIRCON SAND
 RESIN CONTENT = 0.35 %

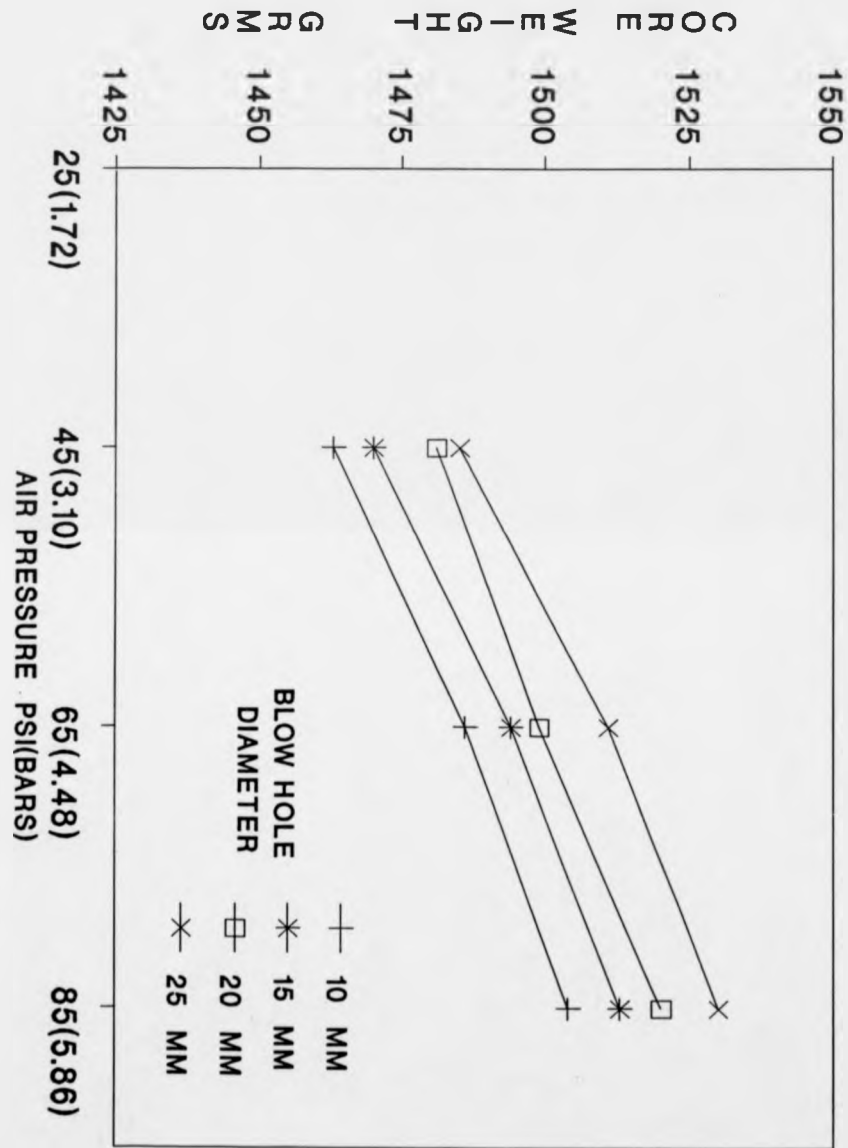


FIG 188. CORE-WEIGHT vs AIR PRESSURE

CORE-BOX 2
 ALL VENTS OPEN (30)
 ZIRCON SAND
 RESIN CONTENT = 0.7 %

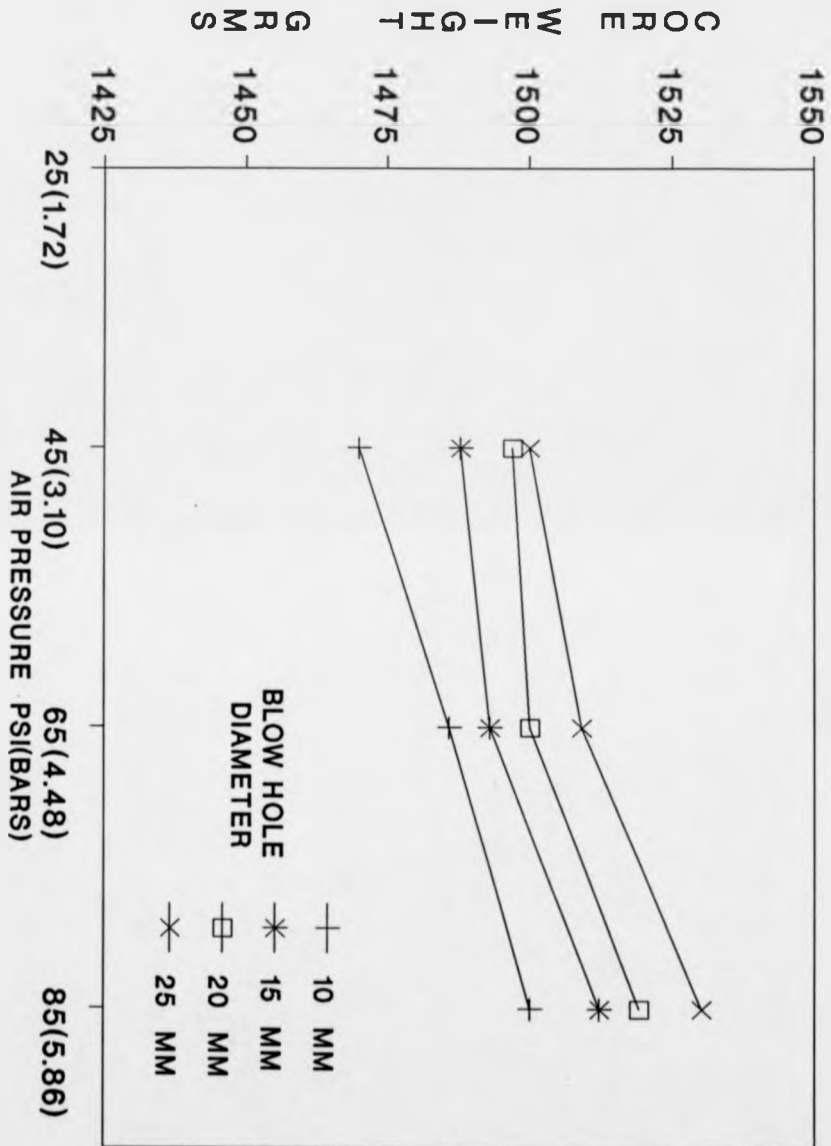


FIG 189. CORE-WEIGHT vs AIR PRESSURE

CORE-BOX 2
 ALL VENTS OPEN (30)
 ZIRCON SAND
 RESIN CONTENT = 1.05 %

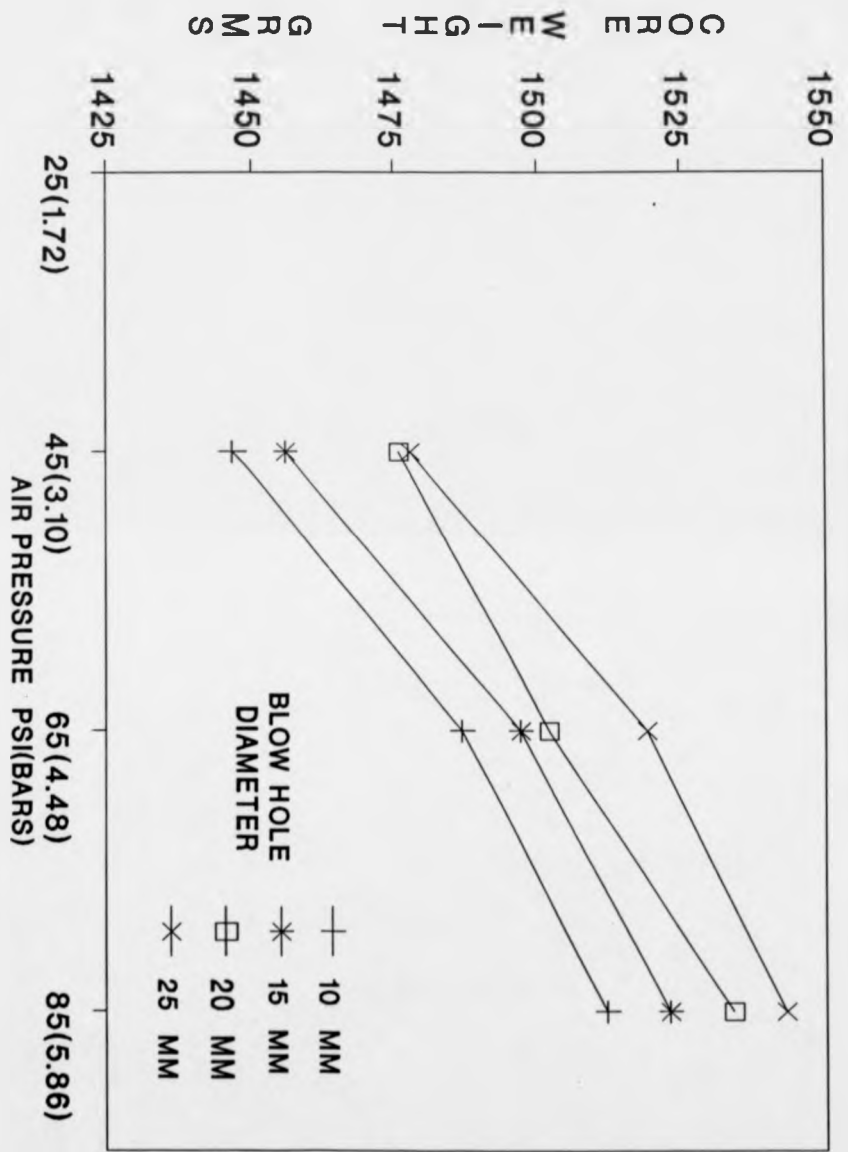


FIG 190. CORE-WEIGHT VS AIR PRESSURE

CORE-BOX 2
 ALL VENTS OPEN (30)
 ZIRCON SAND
 RESIN CONTENT = 0.35%

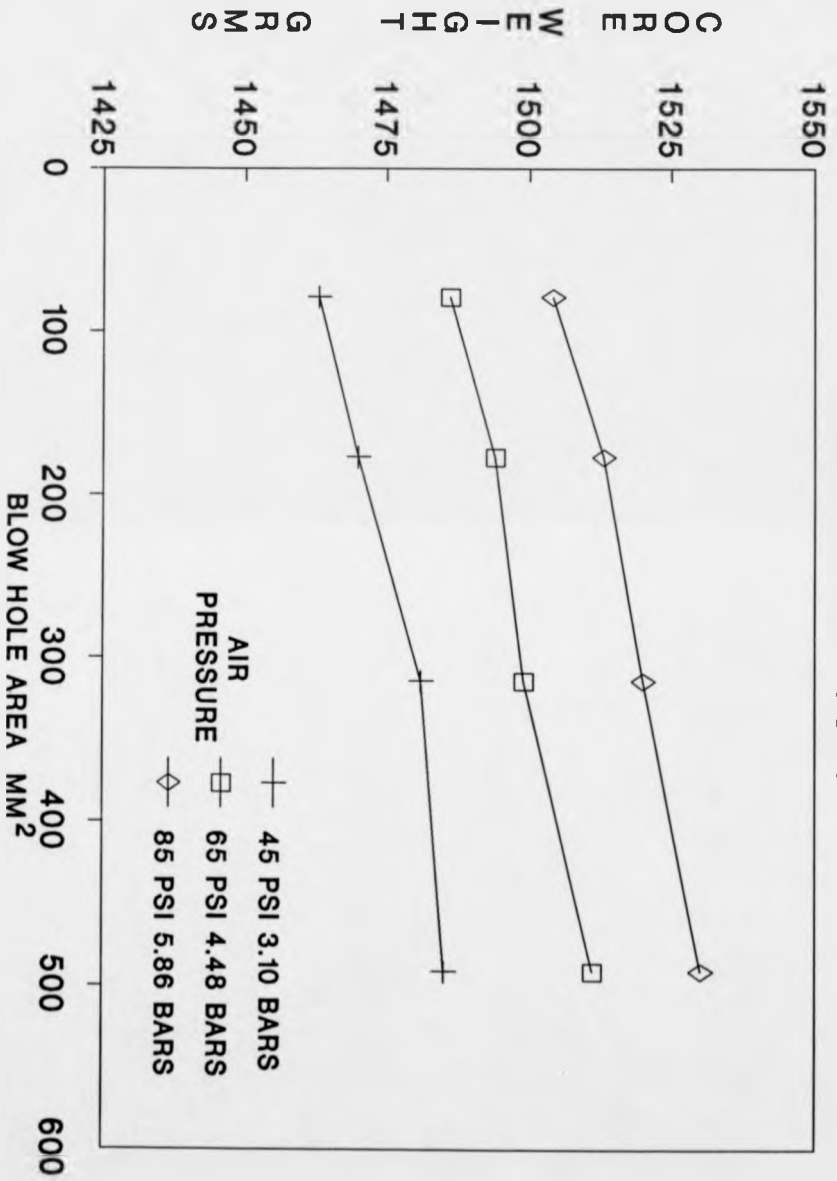


FIG 191. CORE-WEIGHT vs BLOW HOLE AREA

CORE-BOX 2
 ALL VENTS OPEN (30)
 ZIRCON SAND
 RESIN CONTENT = 0.7 %

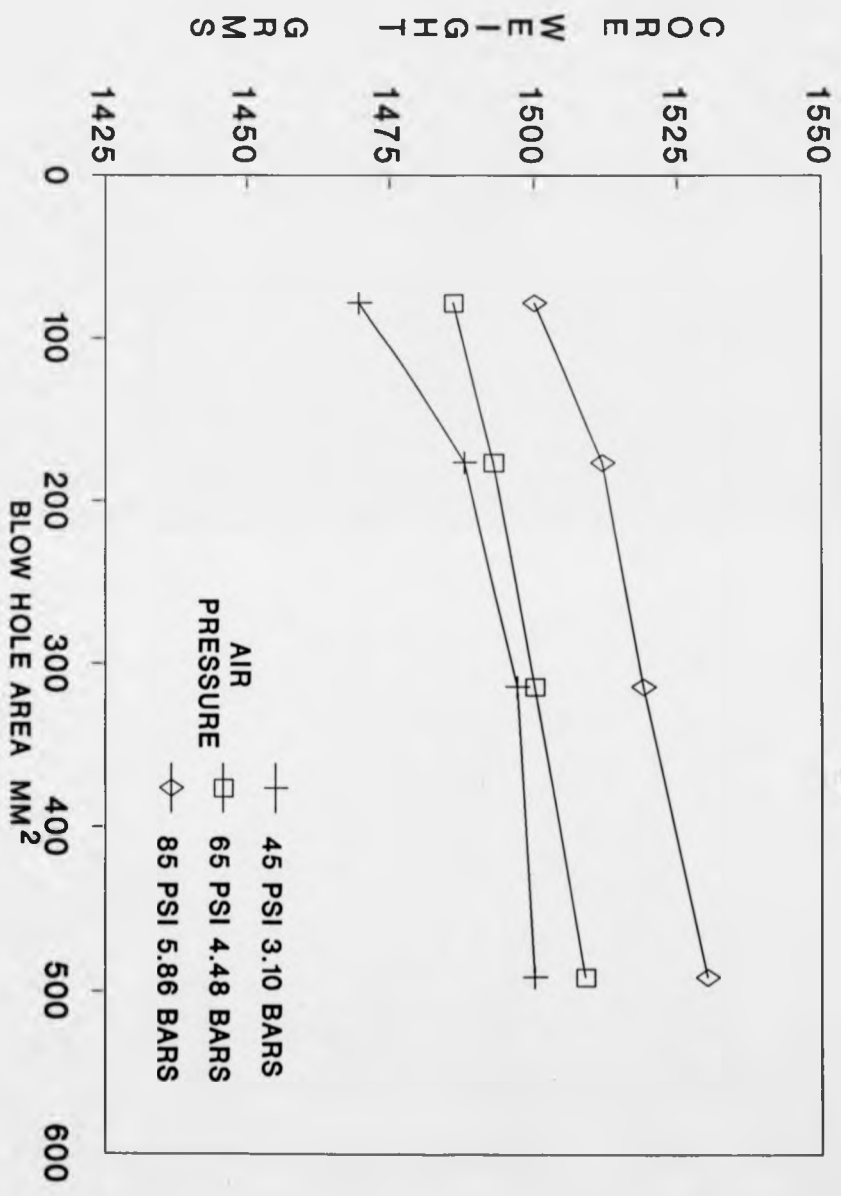


FIG 192. CORE-WEIGHT vs BLOW HOLE AREA

CORE-BOX 2
 ALL VENTS OPEN (30)
 ZIRCON SAND
 RESIN CONTENT = 1.05%

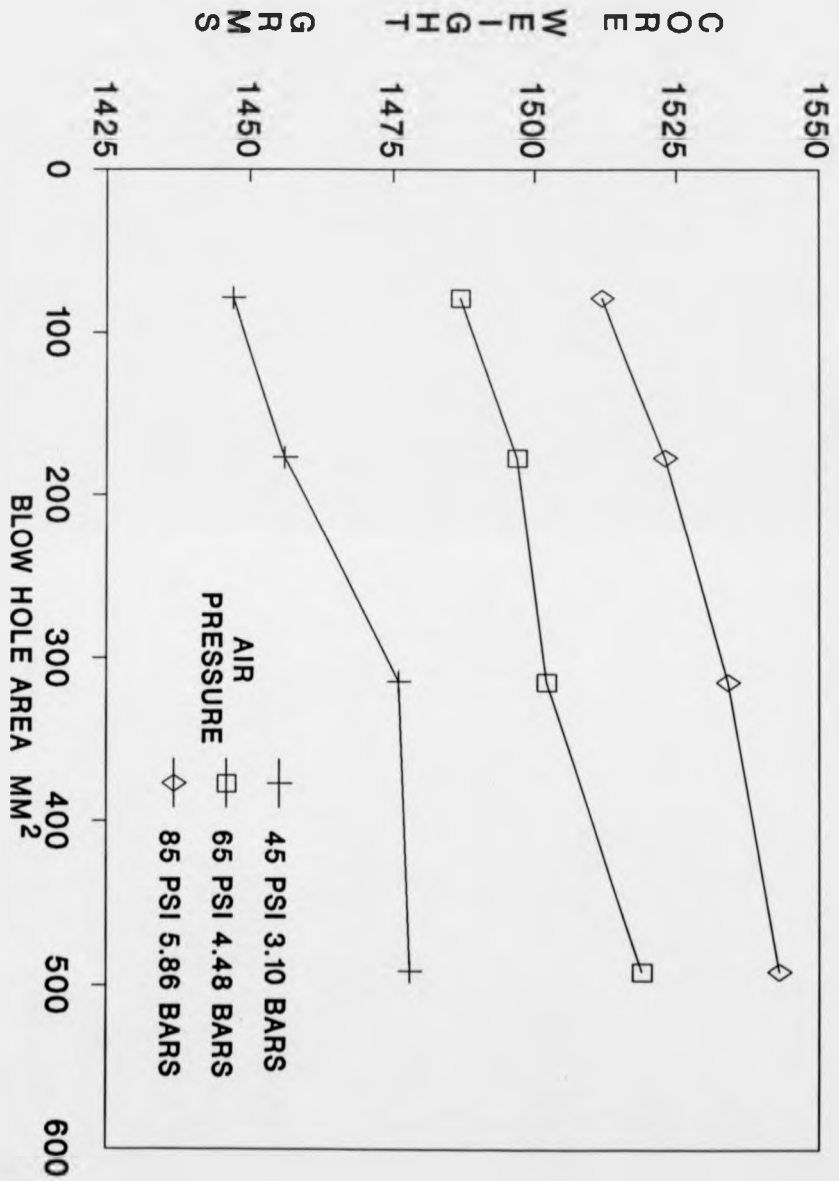


FIG 193. CORE-WEIGHT VS BLOW HOLE AREA

Pressure psi bars	Blow hole ϕ mm	Average core-weight/gms						
		RC = 0.75%		RC = 0.7%		RC = 1.05%		
		Time s	Time s	Time s	Time s	Time s	Time s	
80	5.52	20	0.23	1007 ⁰⁸ ₀₆	0.23	1001 ⁰³ ₀₀	0.23	977
80	5.52	15	0.39	985 ⁸⁶ ₈₄	0.38	977 ⁷⁷ ₇₆	0.39 ³⁹ ₃₈	948 ⁴⁹ ₄₈
80	5.52	10	0.62 ⁶³ ₆₁	939 ⁴³ ₃₅	0.69 ⁷⁰ ₆₈	935 ³⁹ ₃₀	0.63 ⁶² ₆₄	908 ¹⁰ ₀₆
60	4.14	20	0.27 ²⁷ ₂₆	994 ⁹⁶ ₉₃	0.26 ²⁶ ₂₅	989 ⁹¹ ₈₆	0.26 ²⁶ ₂₅	963 ⁶⁴ ₆₂
60	4.14	15	0.40 ⁴³ ₃₇	965 ⁶⁶ ₆₄	0.35	958 ⁵⁹ ₅₇	0.43	937 ⁴⁹ ₃₅
60	4.14	10	0.69 ⁷⁰ ₆₈	920 ²³ ₁₈	0.8	915 ²¹ ₀₉	0.68 ⁷³ ₆₅	884 ⁸¹ ₇₇
40	2.76	20	0.35 ³⁶ ₃₅	973 ⁷⁵ ₇₂	0.42	954	0.35 ³⁶ ₃₅	933 ³⁵ ₃₁
40	2.76	15	0.54 ⁵⁷ ₅₁	950 ⁵⁰ ₄₉	0.59	930	0.53 ⁵³ ₅₂	909 ¹¹ ₀₇
40	2.76	10	0.86 ⁸⁶ _{1.28}	894 ⁹⁸ ₈₉	1.15 ⁸² _{0.99}	880 ⁸² ₇₉	0.88 ⁸⁶ _{0.86}	850 ⁵² ₄₈

Fig 194 Experiments carried out in sub-group a of group 6 on box 1. (All vents open)

CORE-BOX 1
ALL VENTS OPEN
SILICA SAND
RESIN CONTENT = 0.75%

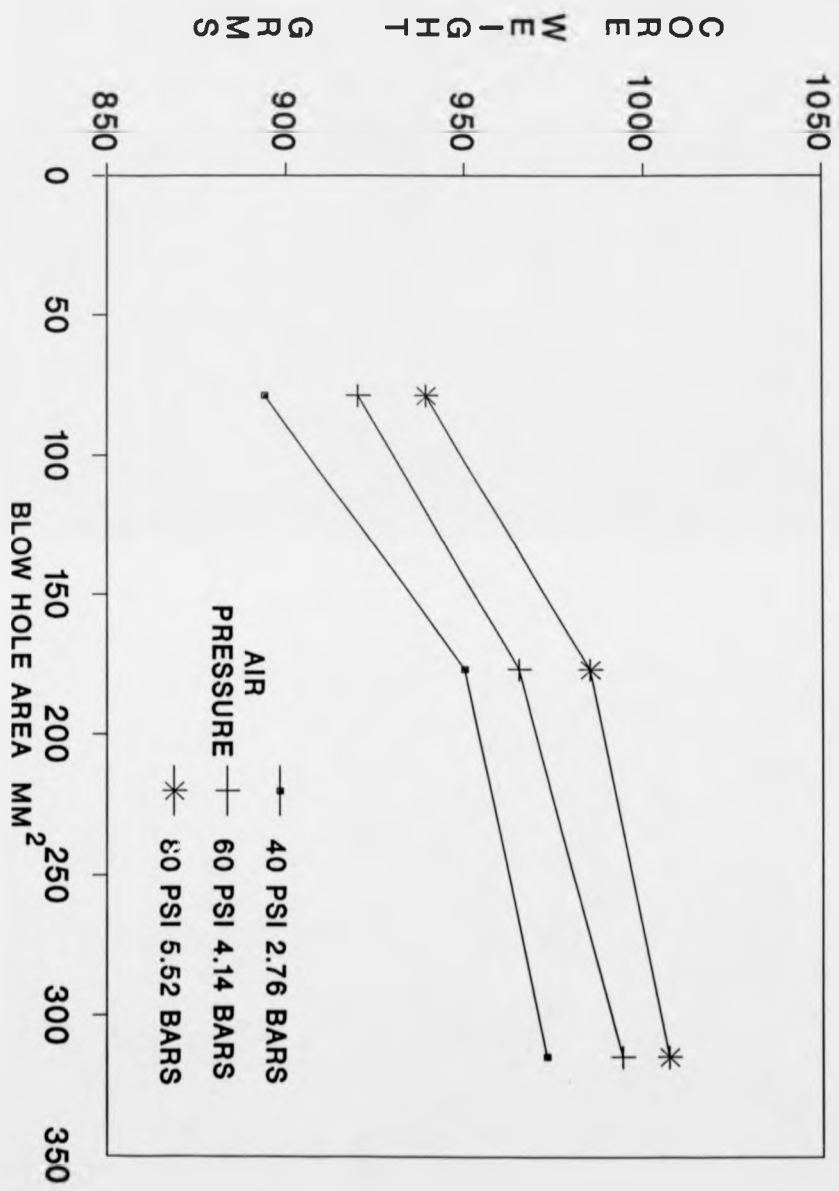


FIG 195 a. CORE-WEIGHT vs BLOW HOLE AREA

CORE-BOX 1
 ALL VENTS OPEN
 SILICA SAND
 RESIN CONTENT = 1.50 %

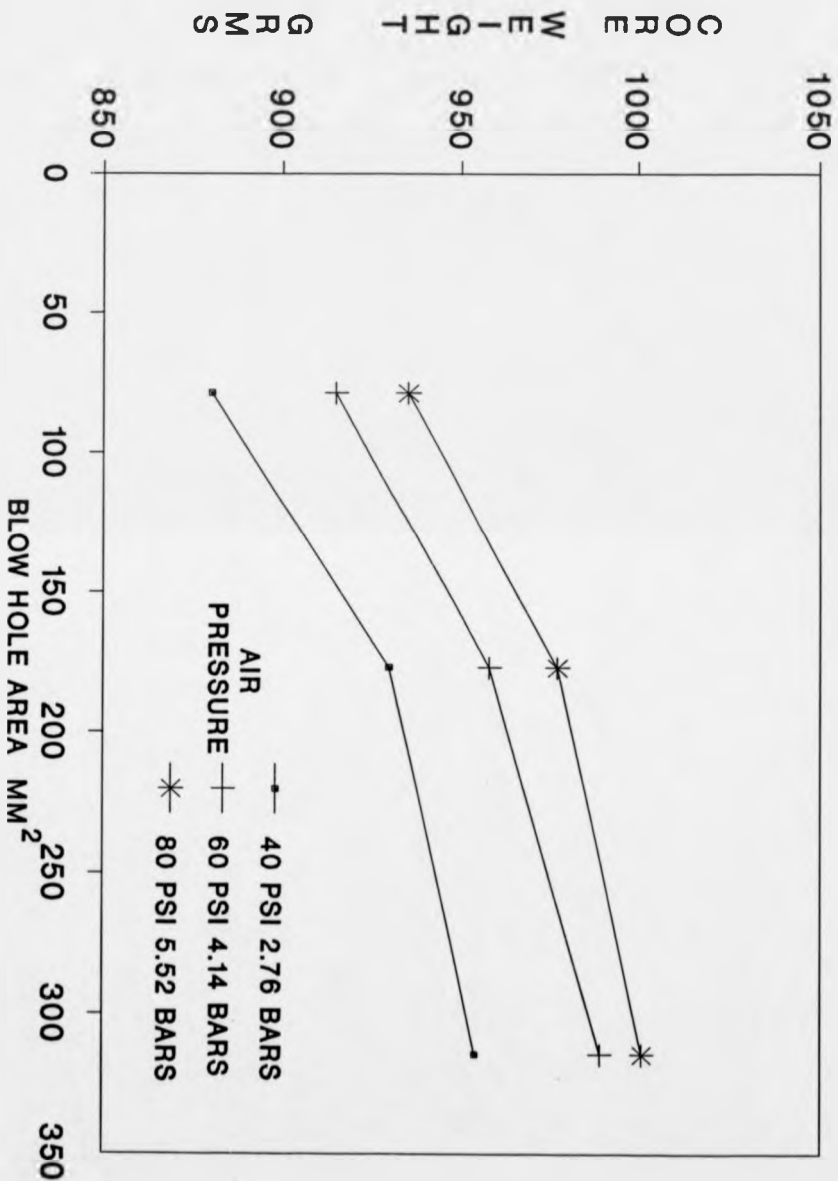


FIG 195 b. CORE-WEIGHT vs BLOW HOLE AREA

CORE-BOX 1
 ALL VENTS OPEN
 SILICA SAND
 RESIN CONTENT = 2.25%

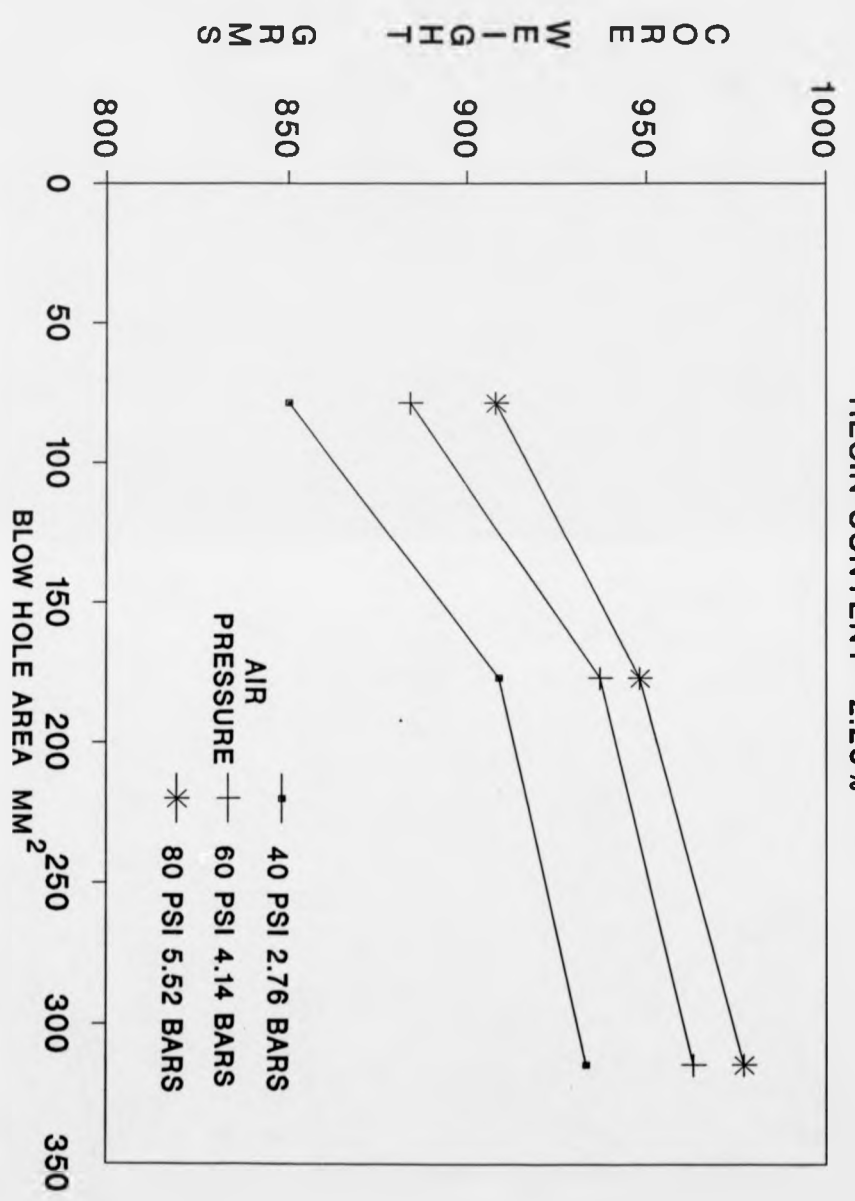


FIG 195 c. CORE-WEIGHT vs BLOW HOLE AREA

CORE-BOX 1
 ALL VENTS OPEN
 SILICA SAND
 RESIN CONTENT = 0.75 %

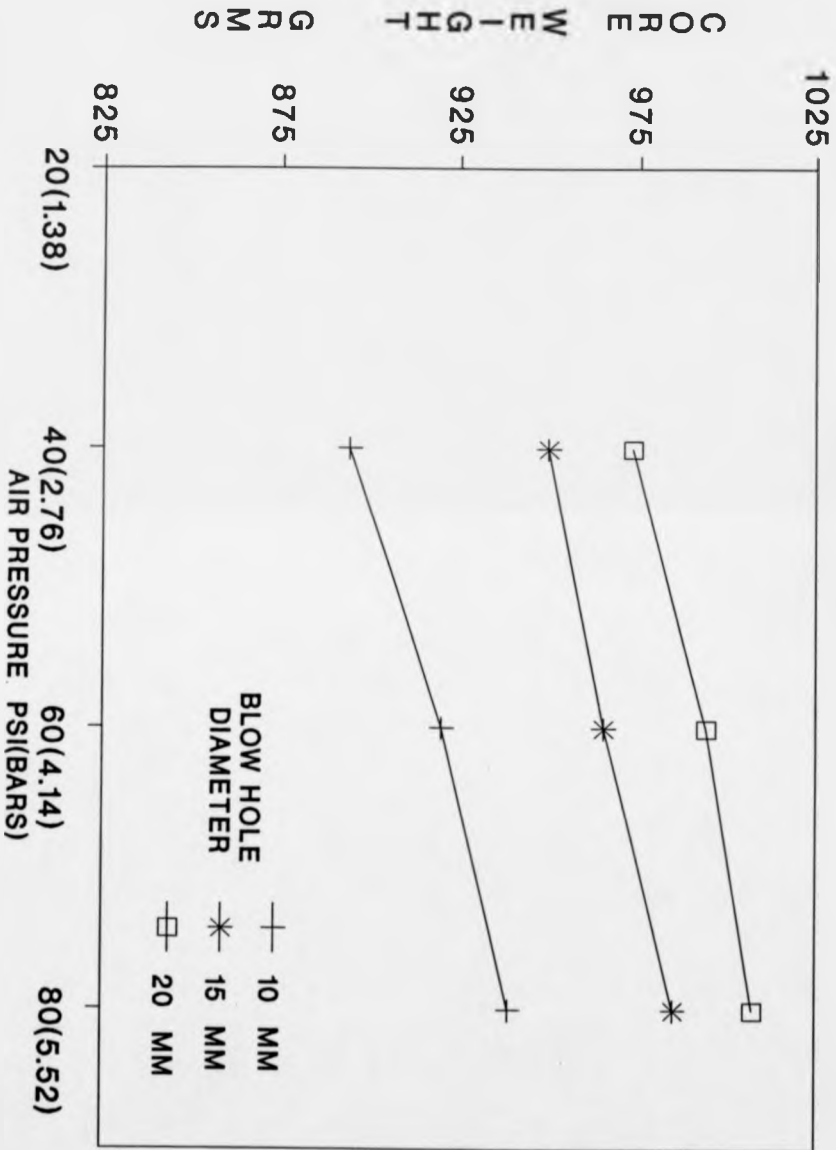


FIG 196a. CORE-WEIGHT vs AIR PRESSURE

CORE-BOX 1
 ALL VENTS OPEN
 SILICA SAND
 RESIN CONTENT = 1.50 %

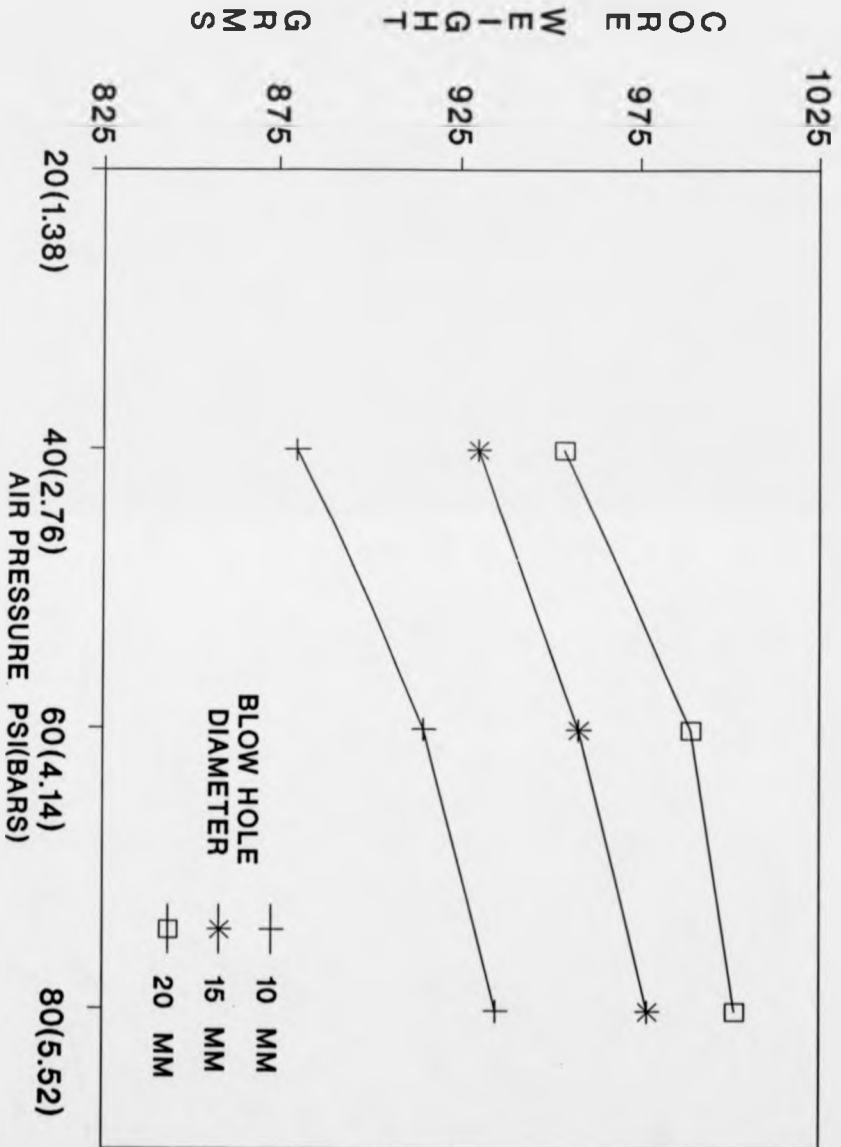


FIG 196b. CORE-WEIGHT vs AIR PRESSURE

CORE-BOX 1
 ALL VENTS OPEN
 SILICA SAND
 RESIN CONTENT = 2.25 %

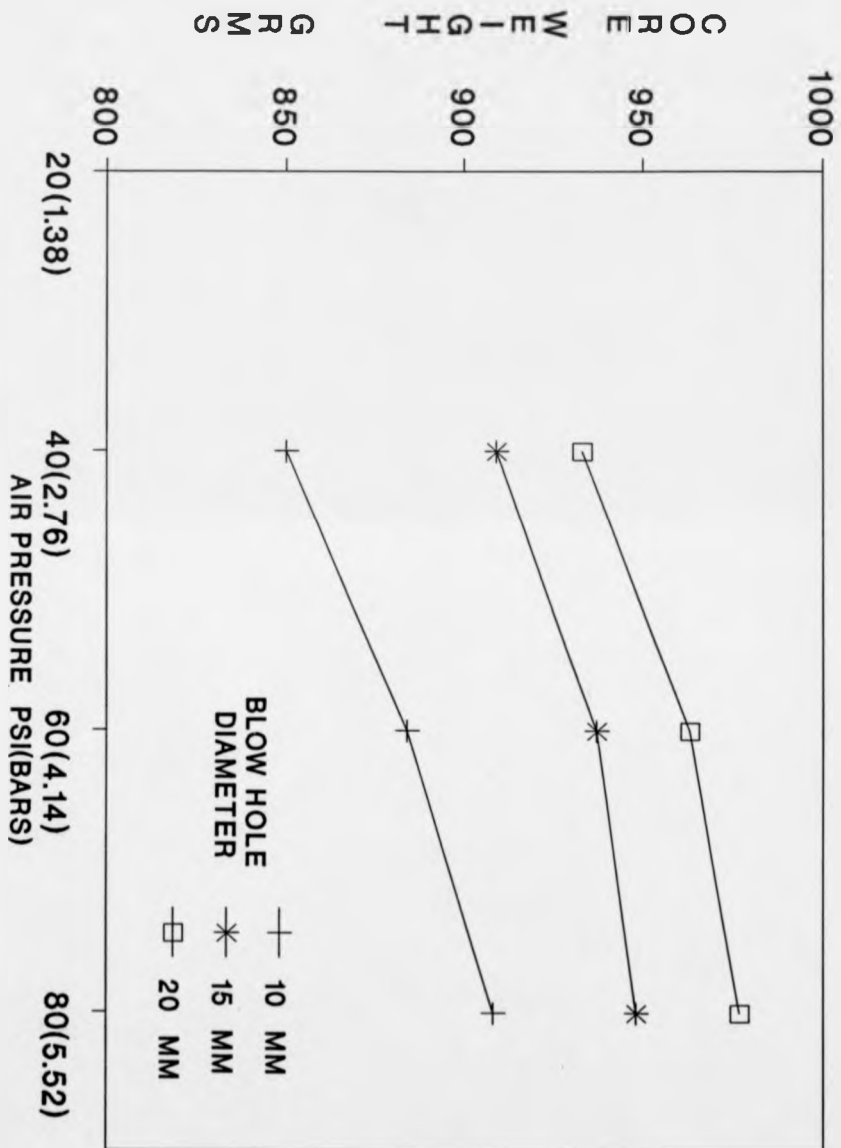


FIG 196c. CORE-WEIGHT vs AIR PRESSURE

Pressure		Blow hole ϕ mm	Average core-weight/gms		
psi	bars		RC = 0.75%	RC = 1.5%	RC = 2.25%
85	5.86	25	791 ⁹² ₉₁	794	794 ⁹⁵ ₉₃
85	5.86	20	790 ⁹⁰ ₈₉	790	790 ⁹¹ ₉₀
85	5.86	15	787 ⁸⁷ ₈₆	785	786
85	5.86	10	784	784	785 ⁸⁶ ₈₅
65	4.48	25	790 ⁹¹ ₈₉	781	778 ⁷⁸ ₇₇
65	4.48	20	788	777	775 ⁷⁵ ₇₄
65	4.48	15	787	774	772 ⁷³ ₇₂
65	4.48	10	784 ⁸⁴ ₈₅	773 ⁷³ ₇₄	769 ⁷⁰ ₆₈
45	3.10	25	770	772 ⁷³ ₇₁	763 ⁶³ ₆₂
45	3.10	20	769	770 ⁷¹ ₇₀	760 ⁶⁰ ₅₉
45	3.10	15	766 ⁶⁷ ₆₆	768 ⁶⁹ ₆₈	760
45	3.10	10	764 ⁶⁵ ₆₄	766 ⁶⁷ ₆₆	758 ⁶⁰ ₅₆

Fig 197 Experiments carried out in sub-group b of group 6 on box 2. All vents open (a total of 30)

CORE-BOX 2
 ALL VENTS OPEN (30)
 SILICA SAND
 RESIN CONTENT = 0.75%

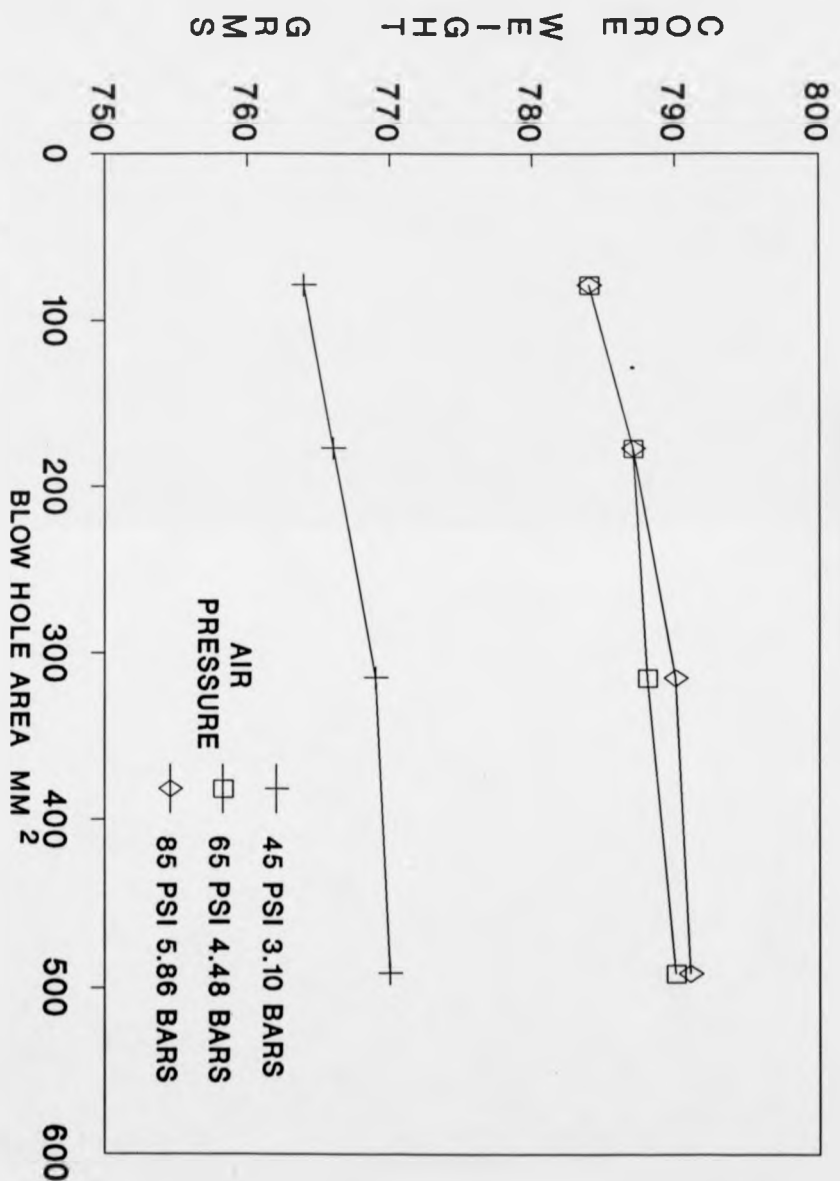


FIG 198 a. CORE-WEIGHT VS BLOW HOLE AREA

CORE-BOX 2
 ALL VENTS OPEN (30)
 SILICA SAND
 RESIN CONTENT = 1.50%

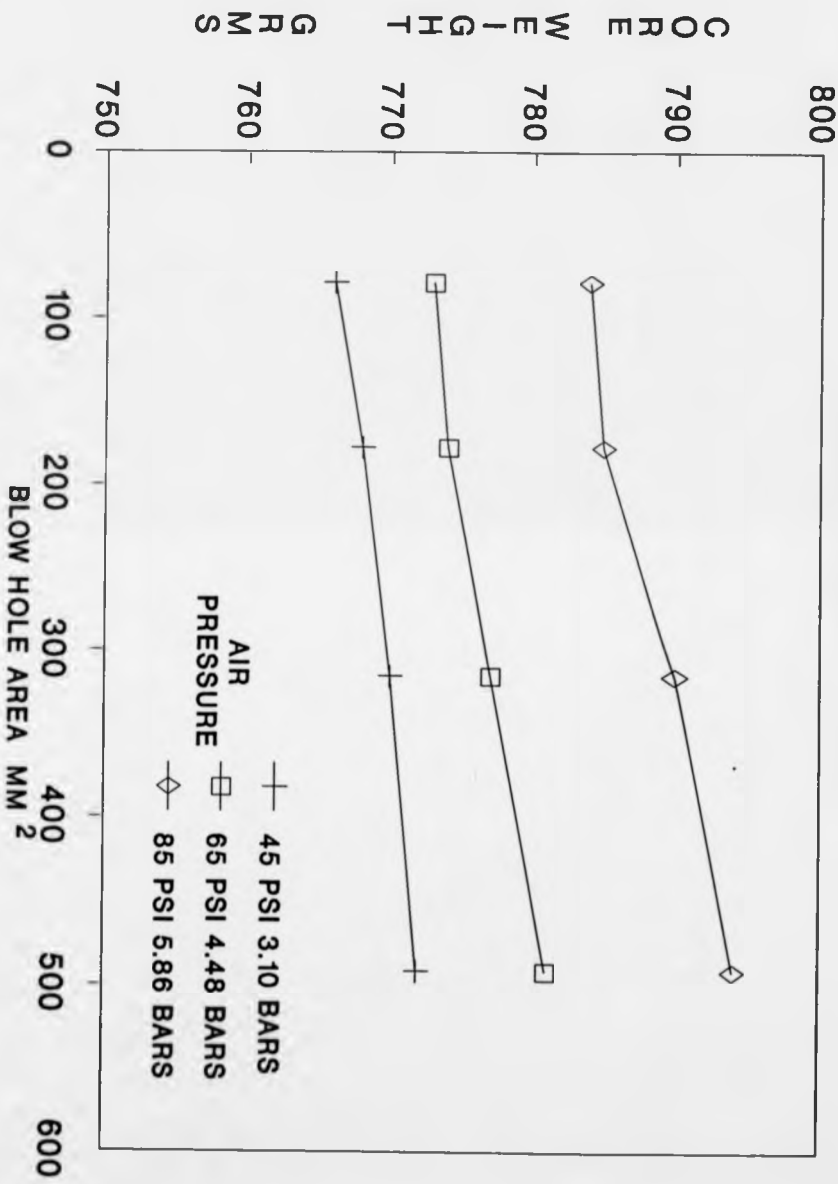


FIG 198 b. CORE-WEIGHT vs BLOW HOLE AREA

CORE-BOX 2
 ALL VENTS OPEN (30)
 SILICA SAND
 RESIN CONTENT = 2.25%

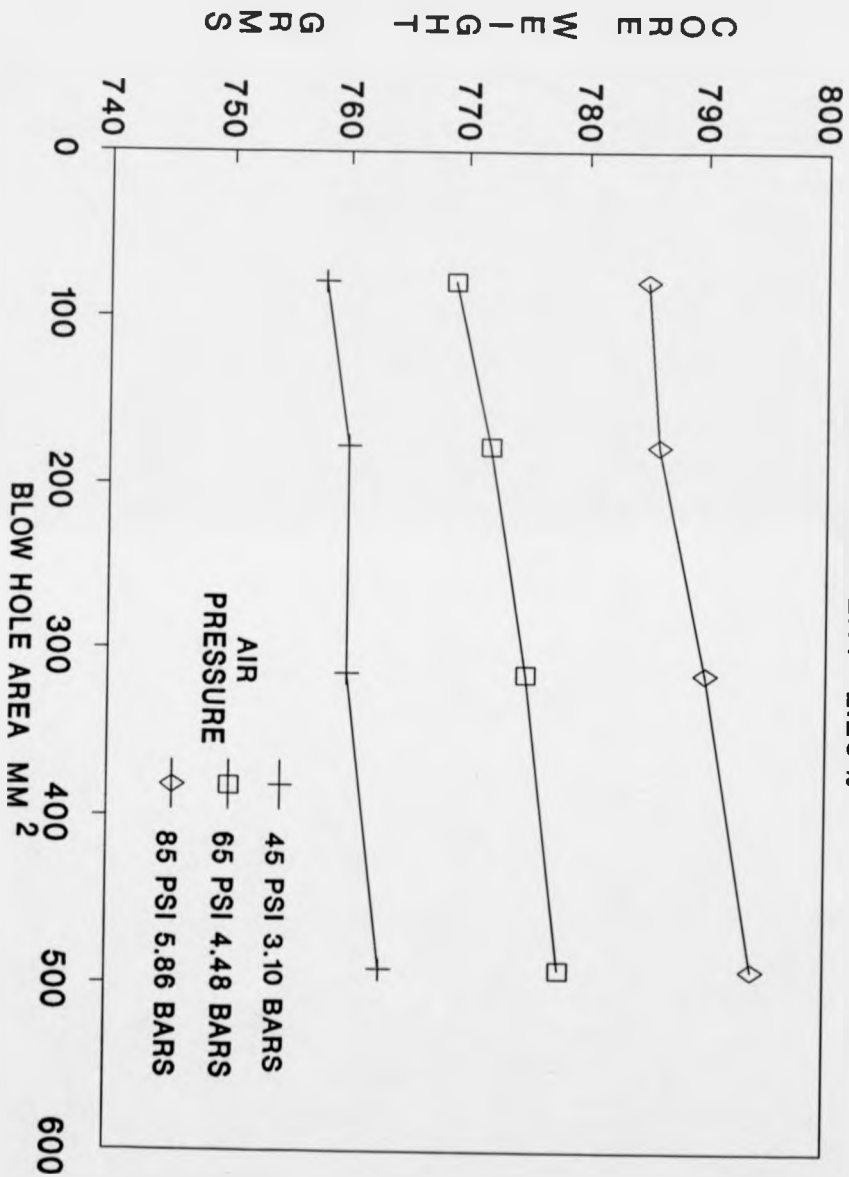


FIG 198 c. CORE-WEIGHT VS BLOW HOLE AREA

CORE-BOX 2
 ALL VENTS OPEN (30)
 ZIRCON SAND
 RESIN CONTENT = 0.75 %

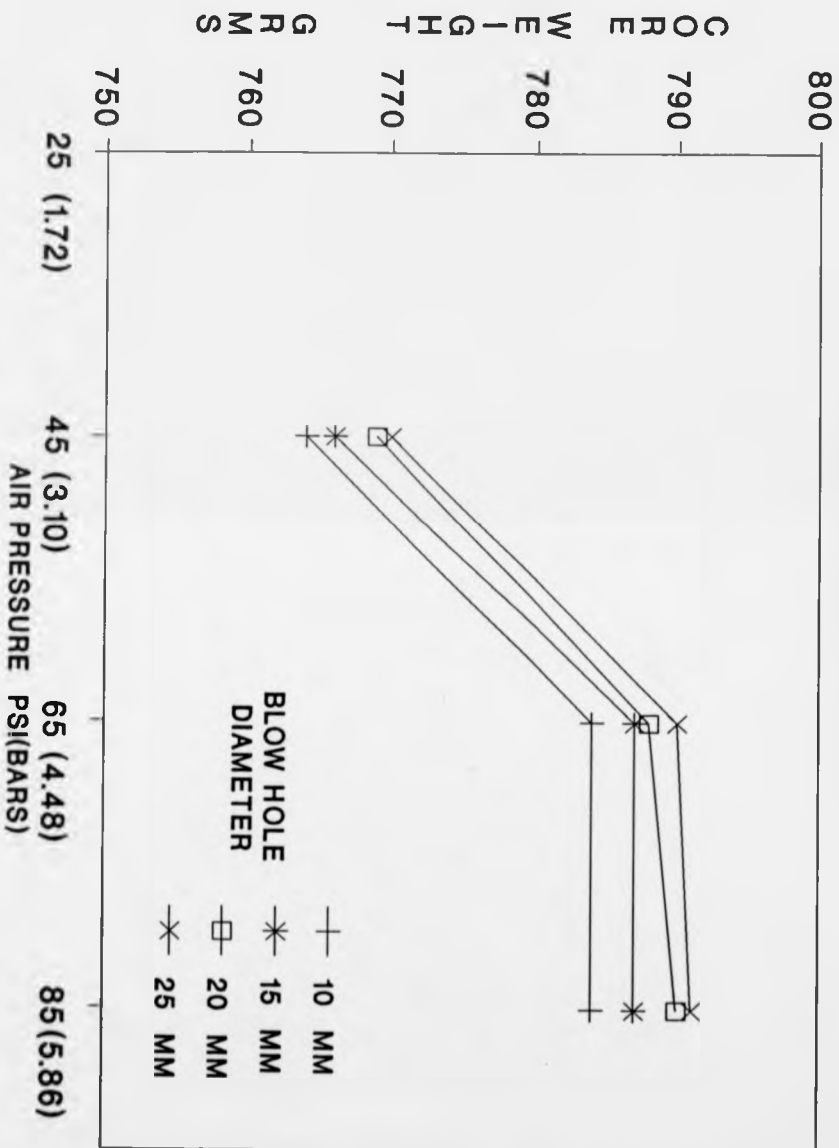


FIG 199 a. CORE-WEIGHT vs AIR PRESSURE

CORE-BOX 2
 ALL VENTS OPEN (30)
 ZIRCON SAND
 RESIN CONTENT = 1.50 %

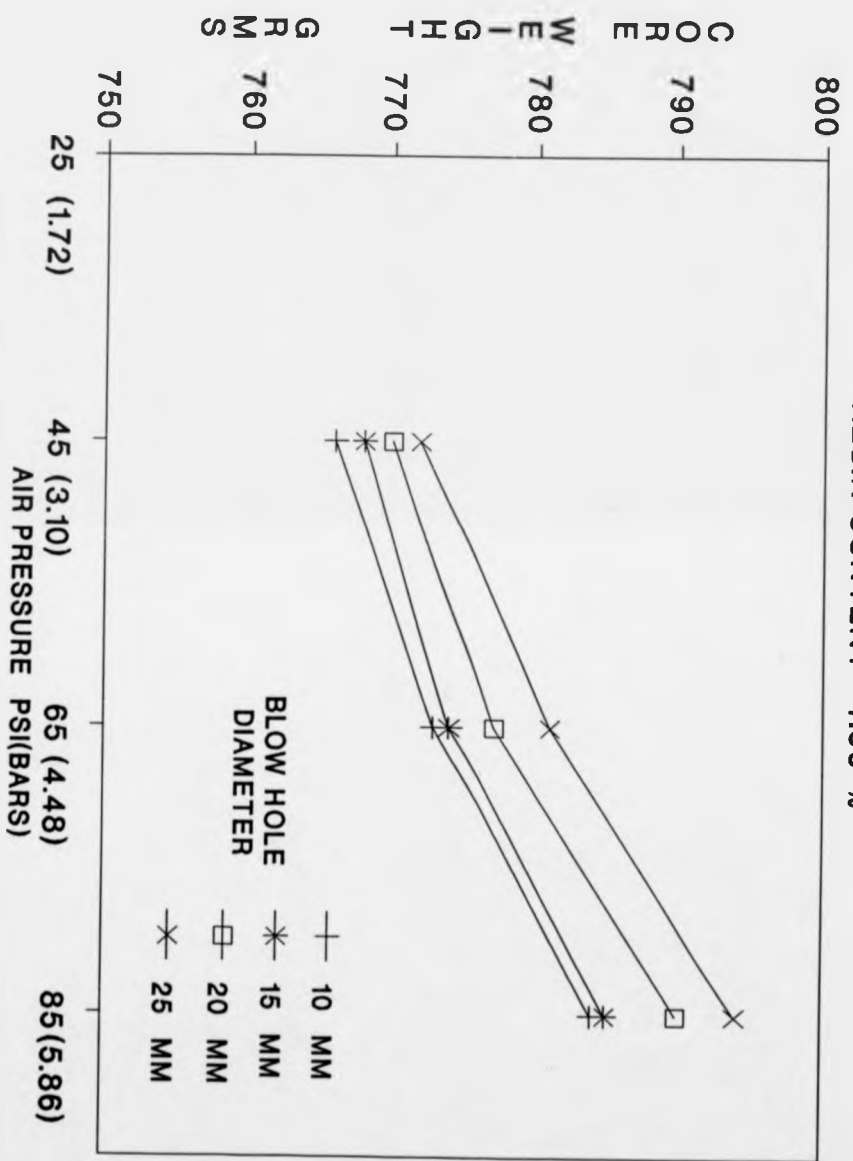


FIG 199 b. CORE-WEIGHT vs AIR PRESSURE

CORE-BOX 2
 ALL VENTS OPEN (30)
 ZIRCON SAND
 RESIN CONTENT = 2.25 %

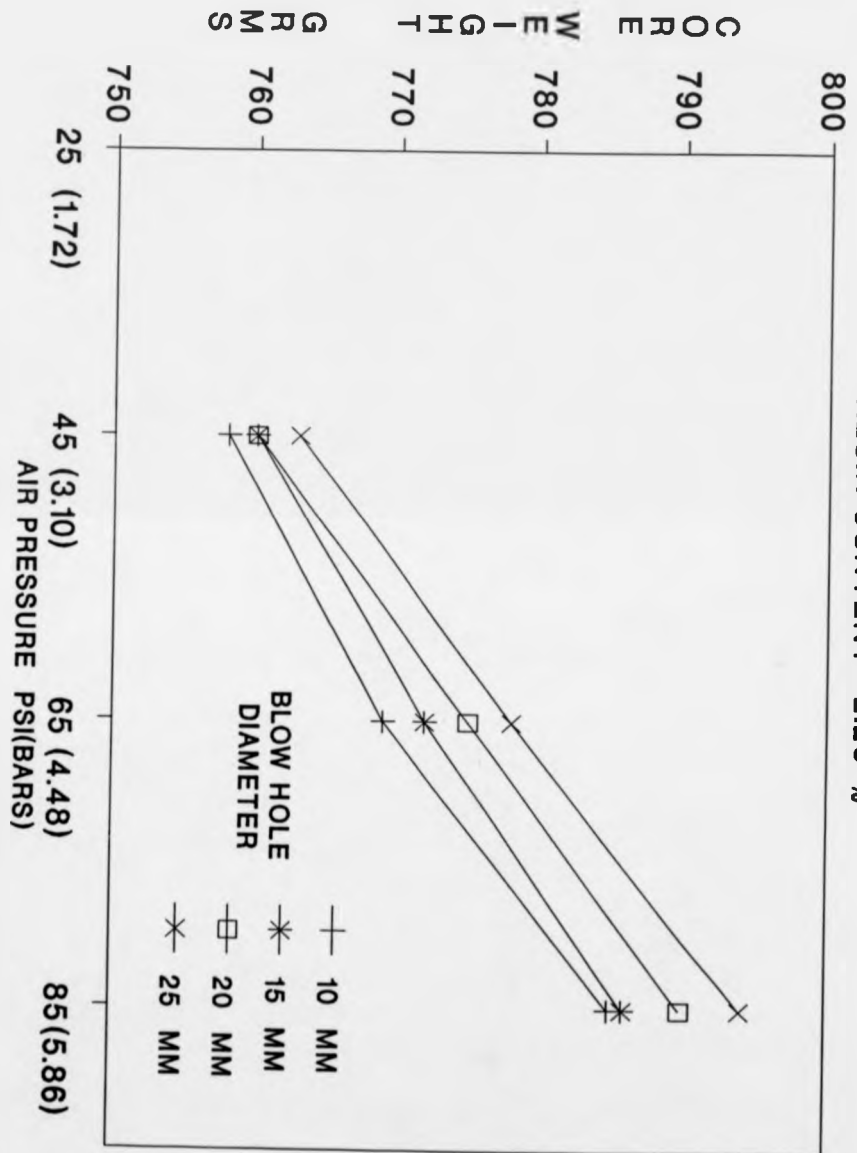


FIG 199 c. CORE-WEIGHT vs AIR PRESSURE

PRESSURE vs TIME

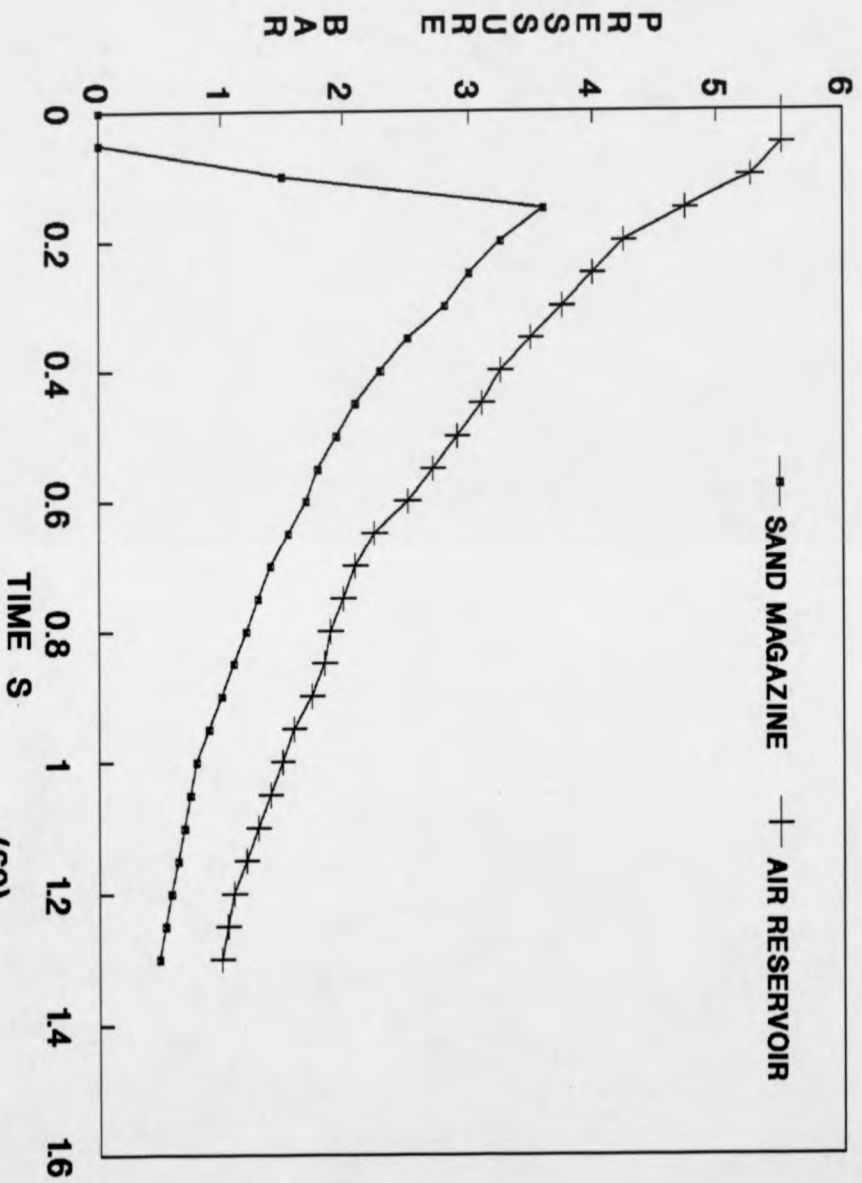


FIG 200. AFTER GELLER (69)

PRESSURE vs TIME
IN SAND MAGAZINE

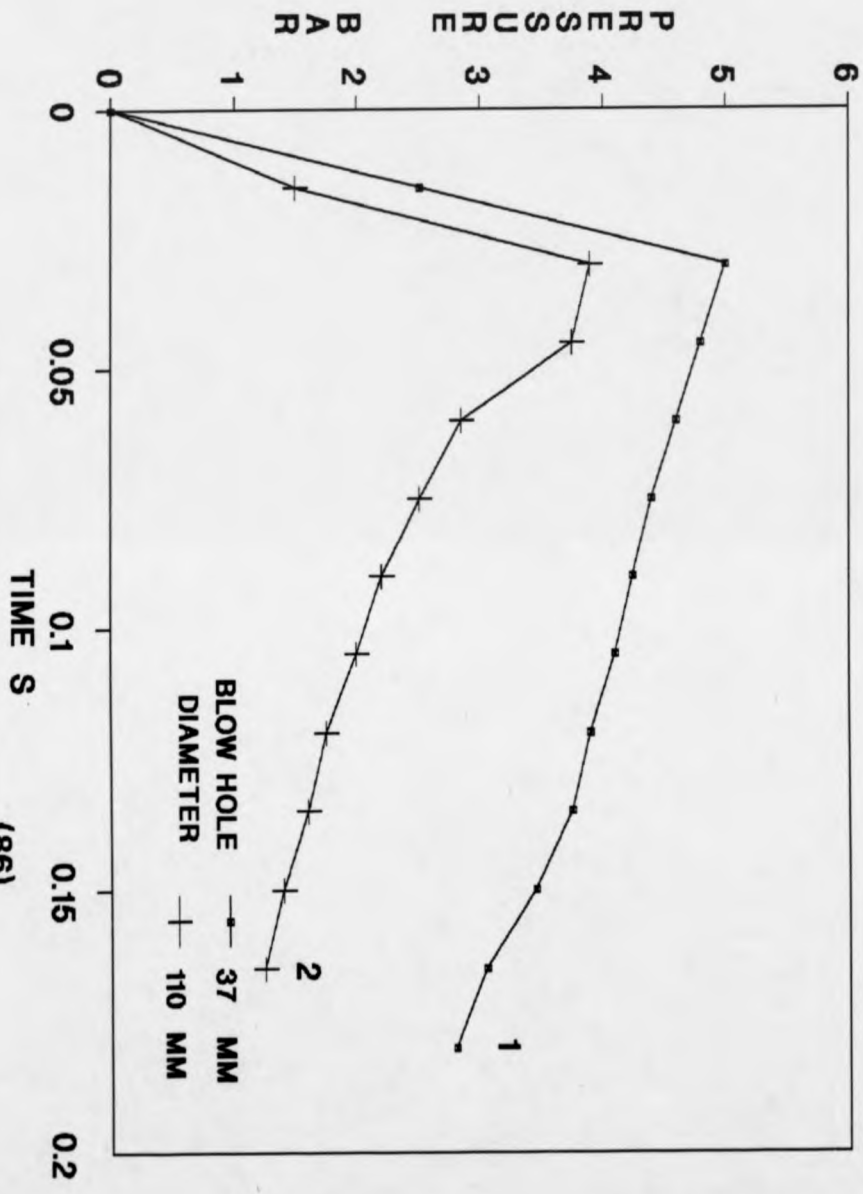


FIG 201. AFTER LESNICHENKO

(86)



Fig 202. Film removal of film build-up
by sand/air jet opposite blow hole



Fig 203. Sand sticking opposite blow hole

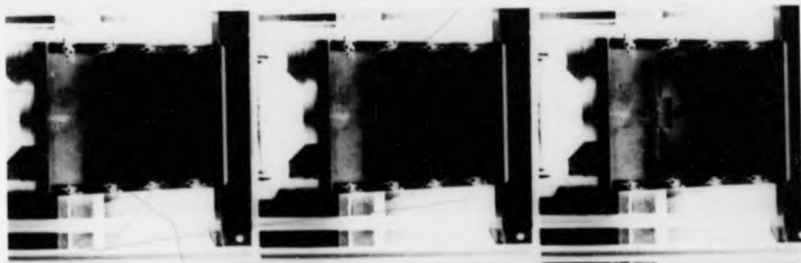


Fig 204. Core-box number 3, $\Phi 10$ mm blow hole, all vents open

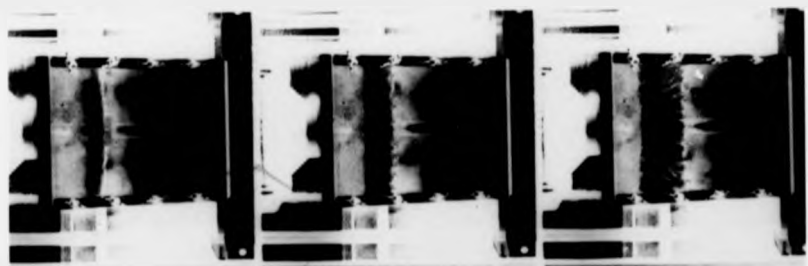


Fig 205. Core-box number 3, $\Phi 10$ mm blow hole, all vents open

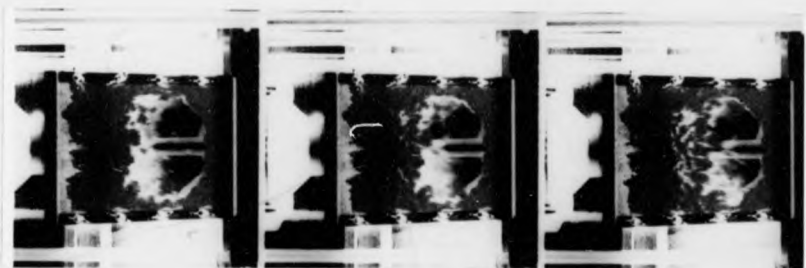


Fig 206. Core-box number 3, ϕ 10 mm blow hole, all vents open

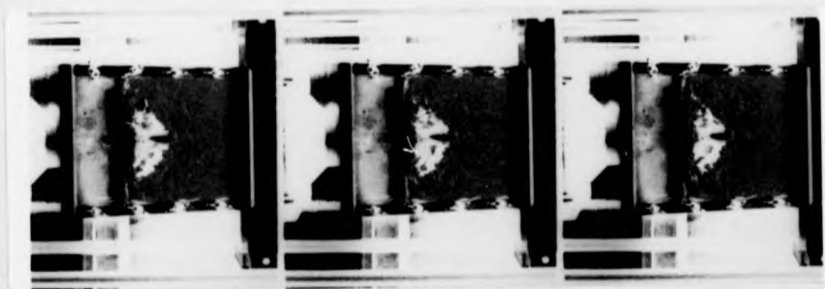


Fig 207. Core-box number 3, ϕ 10 mm blow hole, all vents open

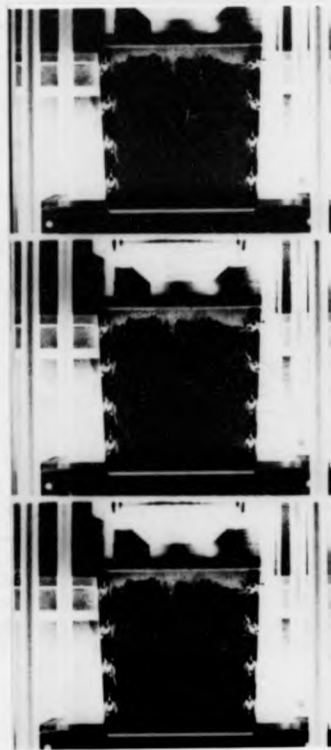


Fig 208. Core-box number 3, Φ 10 mm blow hole, all vents open

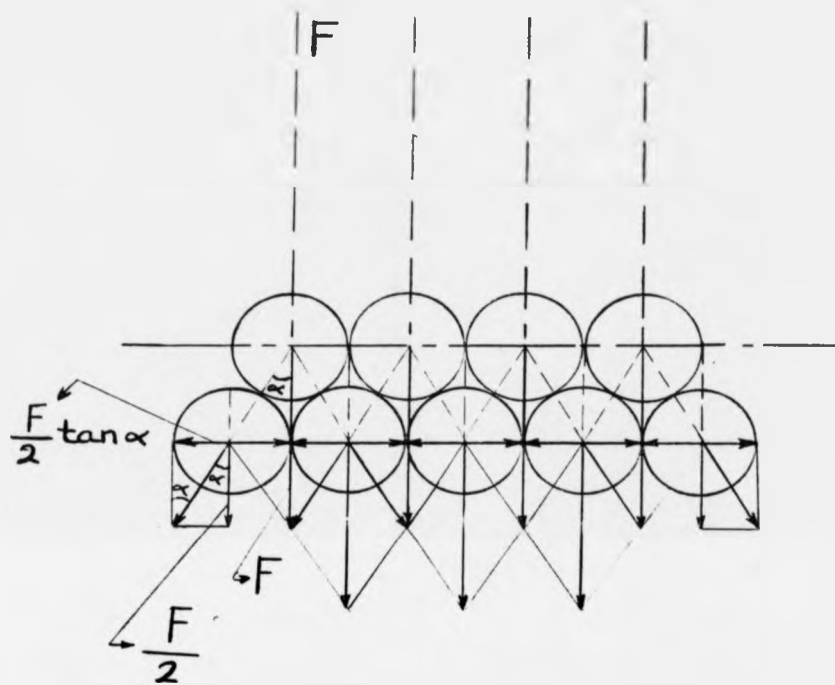


Fig 209. Distribution of forces during collision of the sand particles, after Danko (81)

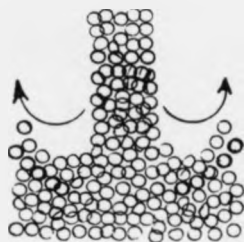
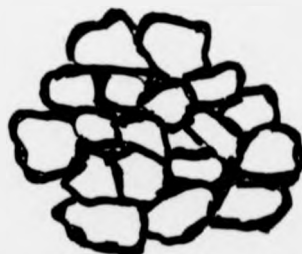


Fig 210. Movement of sand particles
on surface of sand layer in core-box



(a)



(b)

Fig 211. Partially and fully resin coated sand particles

CORE-BOX 1
 SILICA SAND
 ALL VENTS OPEN
 PRESSURE = 80 (5.52) PSI (BARS)

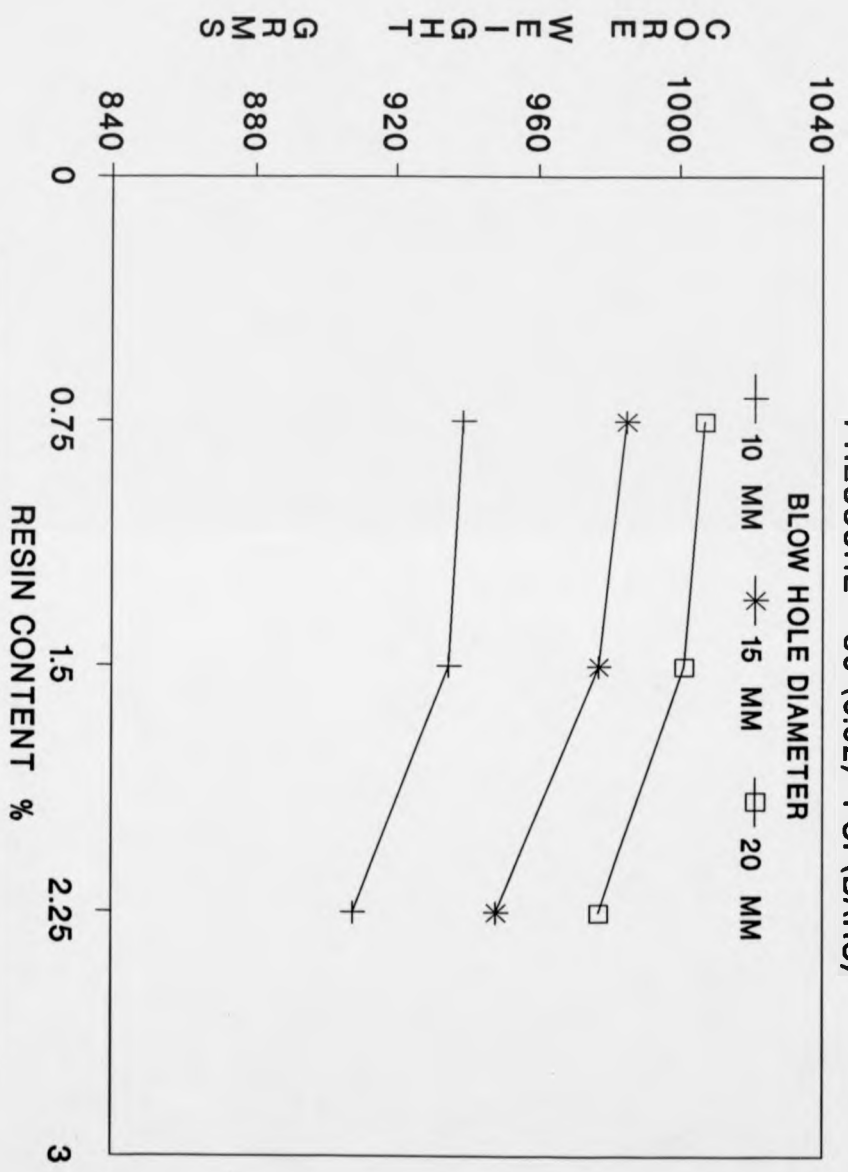


FIG 212a. CORE-WEIGHT vs RESIN CONTENT

CORE-BOX 1
 SILICA SAND
 ALL VENTS OPEN
 PRESSURE = 60 (4.14) PSI (BARS)

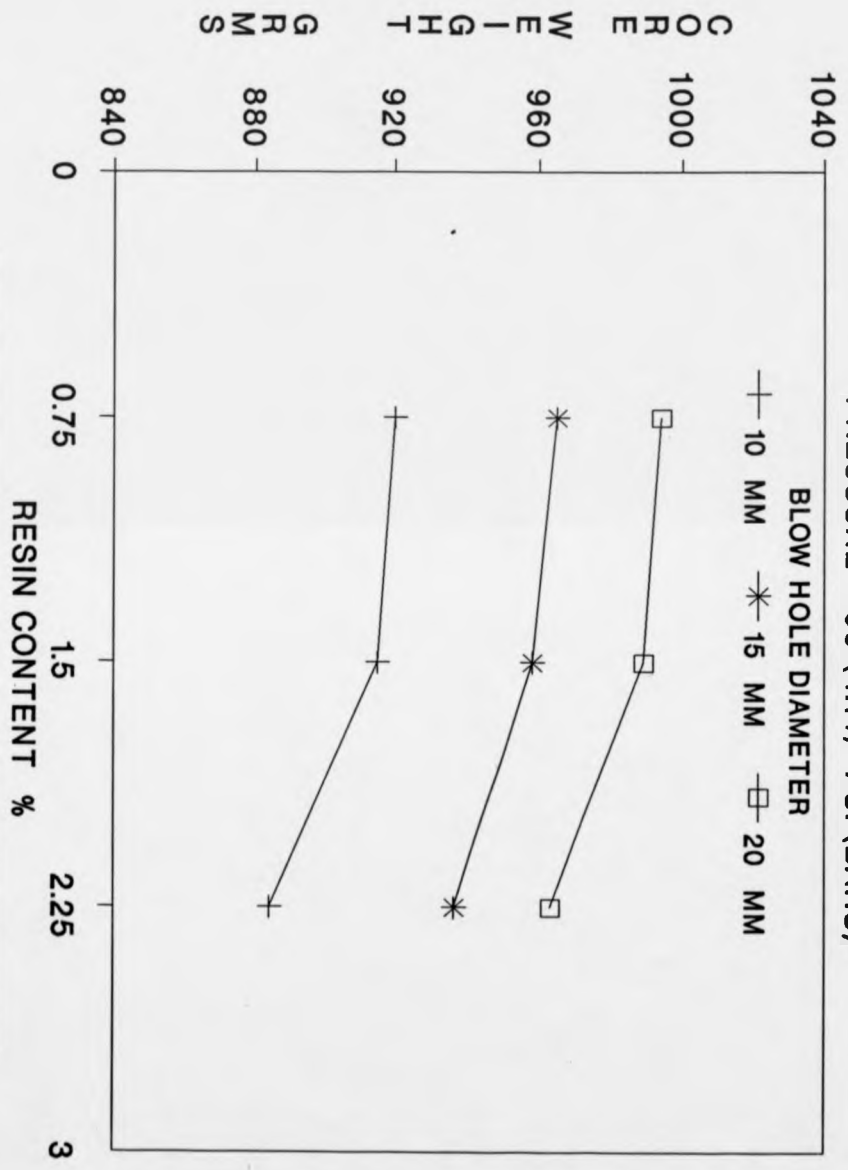


FIG 212b. CORE-WEIGHT vs RESIN CONTENT

CORE-BOX 1
 SILICA SAND
 ALL VENTS OPEN
 PRESSURE = 40 (2.76) PSI (BARS)

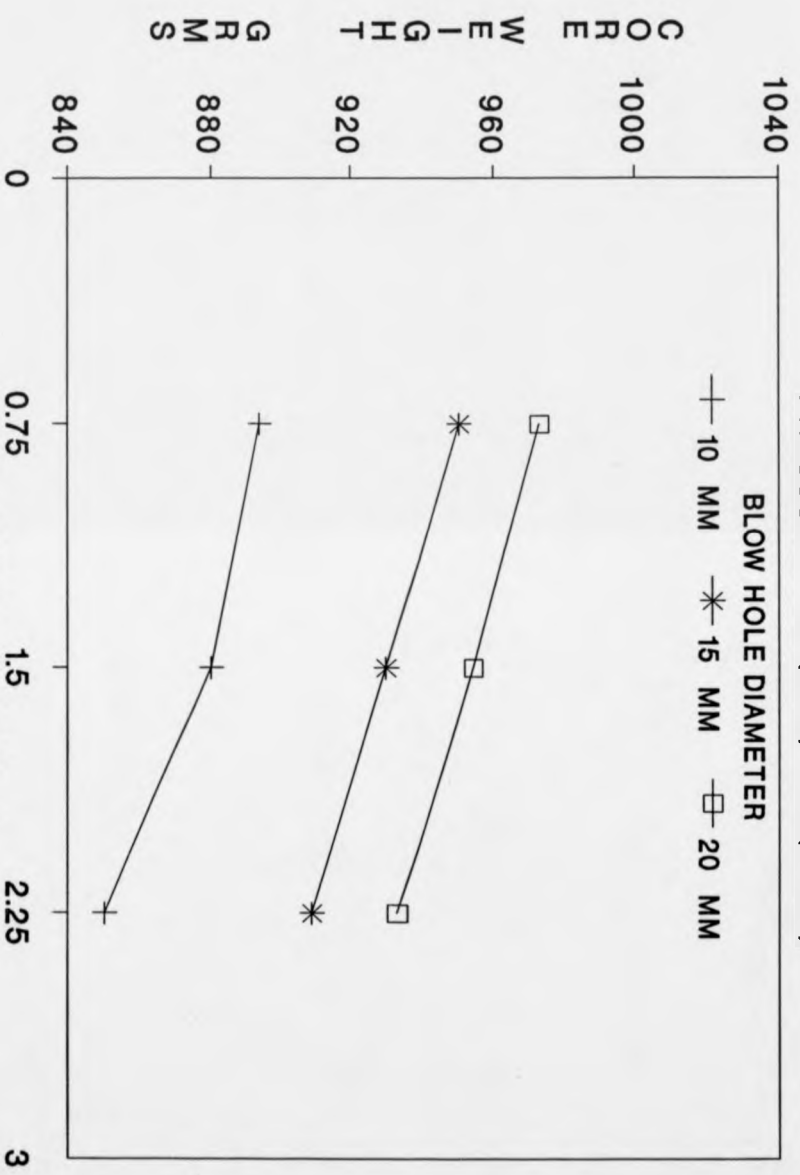


FIG 212c. CORE-WEIGHT vs RESIN CONTENT

CORE-BOX 2
 SILICA SAND
 ALL VENTS OPEN
 PRESSURE = 85 (5.86) PSI (BARS)

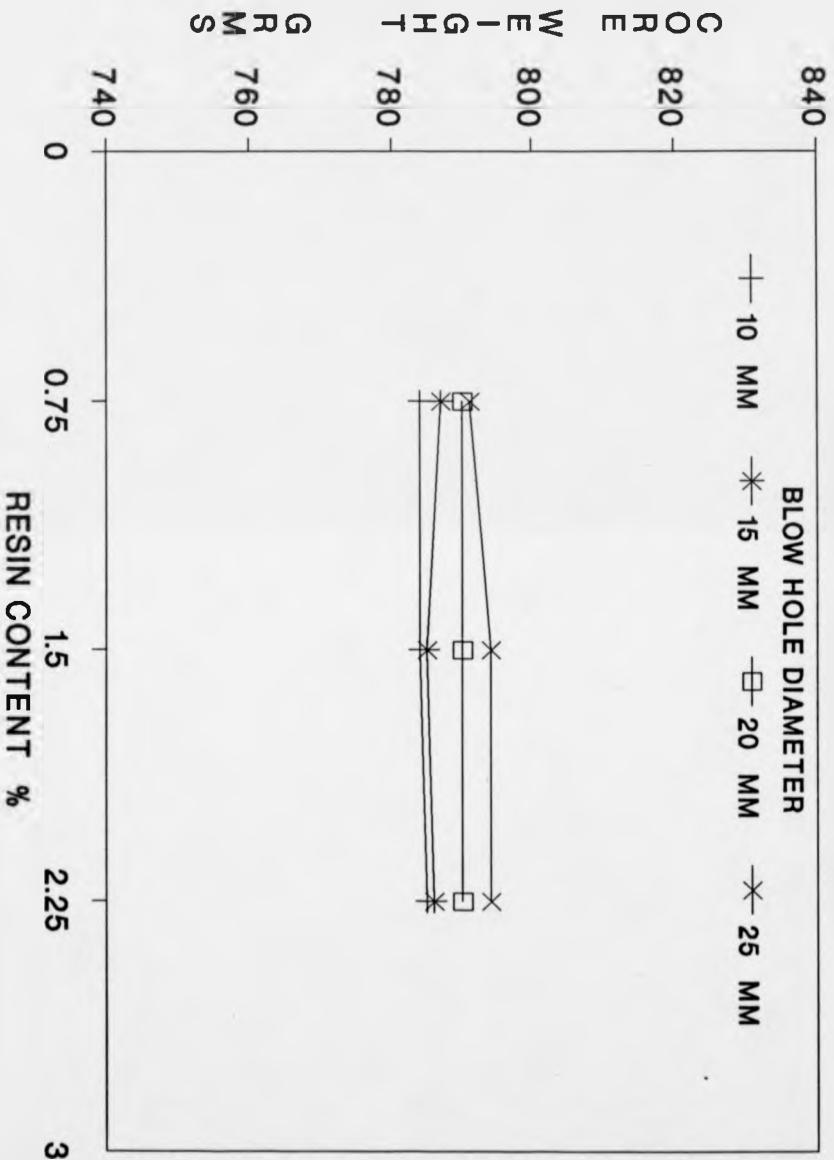


FIG 212d. CORE-WEIGHT vs RESIN CONTENT

CORE-BOX 2
 SILICA SAND
 ALL VENTS OPEN
 PRESSURE = 65 (4.48) PSI (BARS)

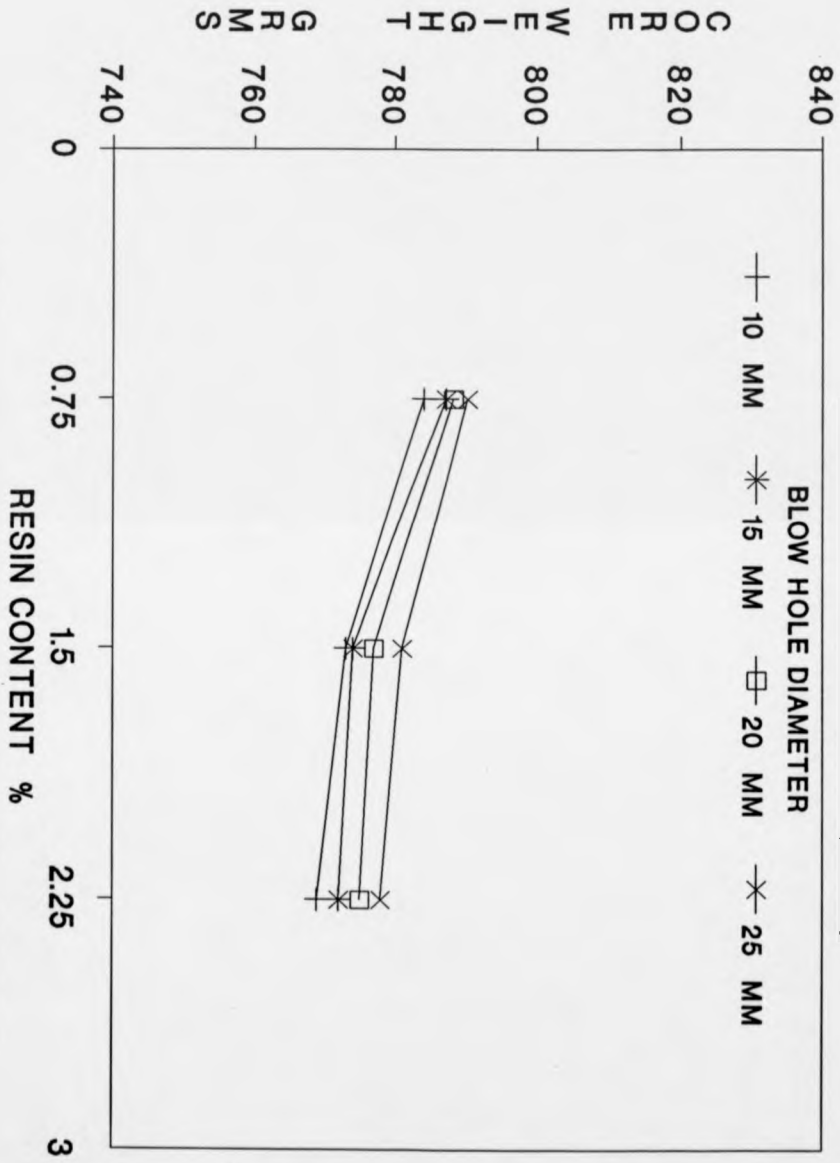


FIG 212e. CORE-WEIGHT vs RESIN CONTENT

CORE-BOX 2
 SILICA SAND
 ALL VENTS OPEN
 PRESSURE = 45 (3.10) PSI (BARS)

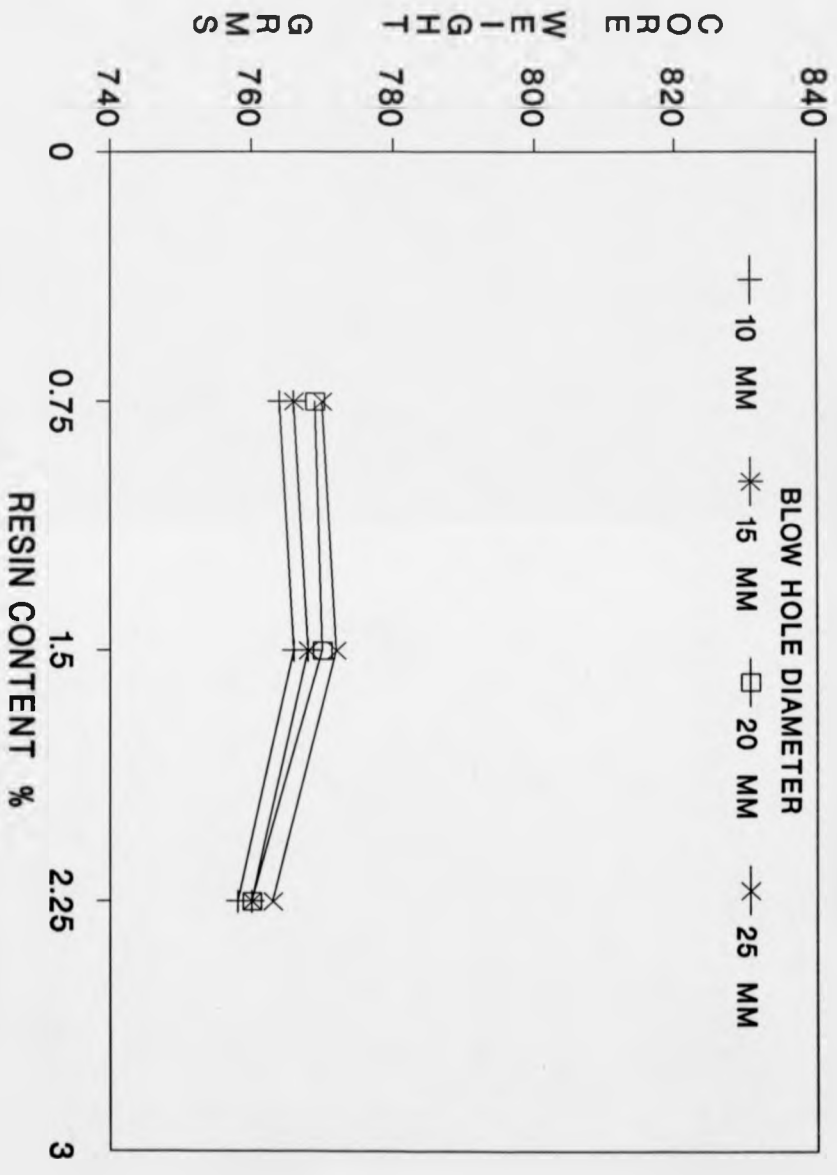


FIG 212f. CORE-WEIGHT vs RESIN CONTENT

7. CONCLUSIONS

7. CONCLUSIONS

The following conclusions are drawn from the present experimental results and the preceding discussions:

1. The filling pattern within a core-box can be controlled by the blowing conditions, such as the blowing air pressure, the blow hole area and shape, and the area and position of the core-box vents.
2. Different filling patterns give rise to different degrees of compaction of the sand in the core-box.
3. The filling time of a core-box with sufficient venting is related to the area of the blow hole and the blowing air pressure. Insufficient venting of a core-box can give rise to prolonged filling times.
4. For a given blowing condition increasing the blowing air pressure to an optimum value, gives rise to increasing the overall compaction of the core and its weight. The rate of increase of the core-weight decreases as the optimum blowing air pressure is approached.
5. For a given blowing condition, increasing the blow hole area to an optimum value, gives rise to increasing the overall compaction of the core and its weight. The rate of increase of the core-weight decreases as the optimum blow hole area is approached.
6. Insufficient venting or over venting of a core-box leads to decreasing the core-weight.
7. Within a symmetrical core-box, one sided venting gives rise to faster filling and better compaction in that side.

8. Compaction of the sand in the core-box is achieved under two different mechanisms; primary and secondary compaction.
9. Primary compaction takes place under the influence of the kinetic energy of the sand/air jet entering the core-box.
10. Secondary compaction takes place under the influence of air blowing through the mass of sand in the core-box.
11. Silica sand showed better flowability and compactability than zircon sand.
12. Increasing the binder level in the mix led to the production of stronger cores. However, it also led to core defects in the form of voids in areas where compaction is largely achieved as a result of the secondary mechanism.

REFERENCES

REFERENCES

1. Dietert, H.W., Foundry Core Practice, Amer. Foundrymen's Soc., 1966.
2. Engineering Industry Training Board (EITB) publications, Core Making, 1985.
3. American Foundrymen's Society, Mould and Core Test Handbook, 1978.
4. Garnar, T.E., Minerology of Foundry Sands and its Effects on Performance and Properties, AFS, vol. 85, 1977.
5. Webster, P.D., Fundamentals of Foundry Technology, Portcullis Press Limited, 1980.
6. Davies, W., Foundry Sand Control, Sheffield, United Steel Companies, 1950.
7. Beeley, P.R., Foundry Technology, Butterworth Scientific, 1982.
8. Hoffman, F., Trans. Am. Foundrymen's Soc., vol. 67, p.125, 1959.
9. Koglin, E.F., The Evolution of a Modern Sand Binder Modern Castings, vol. 49, p.126, June 1966.
10. Campbell, K., Core Making, FWP Journal, February 1984.
11. Marek, C.T. and Wimet, R.J., Trans. Am. Foundrymen's Soc., vol. 61, p.279, 1953.
12. Middleton, J.M. and Bownes, F.F., Br. Foundrymen's Soc. vol. 56, p.473, 1963.
13. Zrimsek, A.H. et. al., Trans. Am. Foundrymen's Soc., vol. 71, p.36, 1963.
14. Bushnell, R.S. et. al., Br. Foundrymen's Soc., vol. 55, p.325, 1965.

15. Fennell, A.G. et. al., Cold Setting Core Metals, British Foundrymen's Soc., July 1978.
16. Parkes, E. et al., British Foundrymen's Soc., vol. 57, p.235, 1944.
17. Mikelonis, P.J., Foundry Technology Source Book, American Foundrymen's Soc., Des plaines, Illinois 60016.
18. Middleton, J.M., Foundry Trade J., vol. 115, p.43, 1966.
19. Kotzin, E.L., 75 Years of Progress in Core Making, Mod. Cast. June 1971.
20. Giolitto, F., Cement-Sand Cores and Moulds, Metal Progress, vol. 25, No.1, p.44, 1934.
21. Davison, S. et. al., Proc. Inst. British Foundrymen's Soc., vol. 46, p.79, 1953.
22. Davison, F. and White, J., Foundry Trade J., vol. 95, p.165, 1953.
23. Sarkar, A.D., Foundry Core and Mould by the CO₂ Process, Progress Press, Oxford, 1964.
24. Schoen, J.R. et. al., Cold-box System Engineering, Trans. American Foundrymen's Soc., vol. 85, p.545, 1977.
25. Slack, B.D., Matching Your Mixer with Your Chemically Bonded Sand System, Mod. Cast., November 1984.
26. Hufton, J.A. and Cowlam, K.W., Developments in the Use of Cold Core Making Processes. Foundrymen Trade J., February 1976.
27. Roper, F.D., Cores and Core Making. Jarrold and Sons Limited, 1957.

28. George, R.D. et al., Advances in the Silicate-CO₂ Process, Foseco Int. Limited, 1986.
29. Atterton, D.W., Proc. Inst. British Foundrymen, vol. 48, 1955.
30. Haley, G.D. et. al., Trans. American Foundrymen's Soc., vol.69, p.189, 1961.
31. Thompson, R.N. and Hugill, R.W., Foundry Trade J., vol. 119, p.529, 1965.
32. Taylor, D.A. Trans American Foundrymen's Soc., vol. 69, p.272, 1961.
33. Lang, E.A. et. al., Trans. American Foundrymen's Soc., vol. 66, 1958.
34. Nishiyama, T., Mod. Cast., vol. 45, Part 3, p.42, 1964.
35. Patterson, L.R. et. al., Mod. Cast., vol. 47, p.94, 1965.
36. Warren, D., IBF Journal, p.449, 1971.
37. George, R.D. et. al., Innovation with CO₂ and Air Curing Systems, BCIRA Int. Conf., 1986.
38. Lepianka, P.D., Epoxy-SO₂ - A New Generation in Coldbox, BCIRA. Int. Conf., 1986.
39. Garbe, G., Wanpaca Foundry's Success with Furan and Epoxy-SO₂ Coldbox, BCIRA, Int. Conf. 1986.
40. Wallbank, J., A Solution to the SO₂ Build up, Foundry Trade Journal, February 1988.
41. Gardzilla, A. et. al., SO₂ Process - Basic Problems, Ways and Progress to their Solution, BCIRA Int. Conference, 1986.
42. Garbe, G. et. al., Progress and Development with SO₂ Coldbox Systems, BCIRA, Int. Conf., 1986.

43. Tordoff, W.L., Advances on Core Making and Casting Technology, 52nd, Int. Foundry Congress, Australia, October 1985.
44. Tordoff, W.L. et al., The Ferrous Applications of the FRC Coldbox Process, BCIRA. Int. Conf., March 1986.
45. Ashland Publications, Training Programme for the Ashland Coldbox Process, 1982.
46. Heckers, H., Practical Experience with the Coldbox Process for Core Making, Foundry Trade J., May 1982.
47. Belcher, M.W. et. al., The Amine-isocure Process - A Success of the 1980s, BCIRA Int. Conf., March 1986.
48. Kunsch, R. and Conderc, P., Recycling Amines for the Coldbox Process, BCIRA Int. Conf., March 1986.
49. Shephard, K.C., The Betaset Process, Theory and Experience in a Modern Grey-Iron Foundry, BCIRA, Int. Conf., 1986.
50. Leomon, P.H.B. and Shephard, K.C., The Betaset Process for the Rapid Production of Moulds and Cores, Steel Castings Research and Trade Association, 29th Annual Conf., June 1984.
51. Shephard, K.C. et. al. The Betaset Process, Theory and Experience in a Modern Grey-Iron Foundry, BCIRA, Int. Conf., 1986.
52. Lemon, P.H.R.B. and Terron, C.A., A New Core and Mould Making Process, Inst. British Foundrymen's Annual Conf., July 1984.
53. Blackburn, C.S., Operating Experiences of a Modern Repetitive Grey Iron Foundry in Changing from Amine-

- Polyurethane to Betaset Coldbox, BCIRA, Int. Conf., March 1986.
54. Broome, A.J., Mould and Core Coatings and their Applications, British Foundrymen, April 1980.
 55. Ashby, G., Applications of Coatings to Mould and Cores, Br. Foundrymen, March 1983.
 56. Vingas, G.J., What to Look For and How to Apply Mould and Core Coatings, BCIRA, Int. Conf. 1988.
 57. American Foundrymen's Society, Mould and Core Coatings Manual, Des Plaines, 1982.
 58. Peterson, E.F., Building and Adapting Core-boxes for Use in Modern Core-blowing Equipment, Mod. Cast., September 1968.
 59. Richards, M., Core-box Rigging for the Coldbox Process, Mod. Cast., vol. 73, No.9, p.34, September 1983.
 60. Cutter, R.T. et. al., Core Blowing and Core Shooting Techniaues, British Foundrymen 74, p.271, 1981.
 61. Baily, R., Pattern Making Today, Mod. Cast., December 1982.
 62. Francis, J.W., Practical Pattern Making Techniques for the Foundry Industry, Br. Foundrymen, September 1980.
 63. Firgard, R.F., Conversion of Core-boxes, AFS, Transactions, vol. 91, p.275, 1983.
 64. Clark, A.M., Core-blowing, Mod. Cast. vol.30, p.30, 1956.
 65. Lincoln, R.F., The Arrangements of Cores, Blow Holes, and Vents for Blowing Purposes, AFS, Trans., vol. 50, p.1134, 1942.

66. Lincoln, R.F., Fundamentals of Core-blowing, Foundry, vol. 68, p.23, 1940.
67. Degley, M.F., Blowing Cores on a Mass Production Basis, Foundry, vol. 75, p.72, 247, 1947.
68. Lesnichenko, V.L., Modern Ideas on the Core-blower and Core-shooter Process, Russ. Cast. Prod., vol. 8, p.351, 1961.
69. Geller, R.L. and Poplavskii, V.I., Selection of Optimum Design Factors for the Working Reservoirs of Core Shooters, Russ, Cast. Prod., vol.10, p.435, 1965.
70. Khurtov, L.A. et. al., Factors in the Core Blowing and Core Shooting Processes, Russ. Cast. Prod., Vol.5, p.232, 1970.
71. Gardner, G.H.D., British Foundrymen, vol. 56, p.145, 1963.
72. Pridmore, L.D., Core Blowing Practice, Foundry, vol. 74, p.94, 1946.
73. Lincoln, R.F., Constructing Boxes for Blowing Cores. Foundry, vol. 71, p.106, 1943.
74. Dwyer, P., Blows Moulding Sand into Cores, Foundry, vol. 70, p.262, 1942.
75. Gade, H.M., Core Blowing, Foundry, vol. 78, p.82, 1950.
76. Notkin, E.M. et. al., Liteinoe Proizvodstvo, vol. 2, p.1, 1958.
77. Lesnichenko, V.L., Investigation and Development of the Technique for the Core Blower Production of Thin-walled Moulds, Thesis, 1957.

66. Lincoln, R.F., Fundamentals of Core-blowing, Foundry, vol. 68, p.23, 1940.
67. Degley, M.F., Blowing Cores on a Mass Production Basis, Foundry, vol. 75, p.72, 247, 1947.
68. Lesnichenko, V.L., Modern Ideas on the Core-blower and Core-shooter Process, Russ. Cast. Prod., vol. 8, p.351, 1961.
69. Geller, R.L. and Poplavskii, V.I., Selection of Optimum Design Factors for the Working Reservoirs of Core Shooters, Russ, Cast. Prod., vol.10, p.435, 1965.
70. Khurtov, L.A. et. al., Factors in the Core Blowing and Core Shooting Processes, Russ. Cast. Prod., Vol.5, p.232, 1970.
71. Gardner, G.H.D., British Foundrymen, vol. 56, p.145, 1963.
72. Pridmore, L.D., Core Blowing Practice, Foundry, vol. 74, p.94, 1946.
73. Lincoln, R.F., Constructing Boxes for Blowing Cores. Foundry, vol. 71, p.106, 1943.
74. Dwyer, P., Blows Moulding Sand into Cores, Foundry, vol. 70, p.262, 1942.
75. Gade, H.M., Core Blowing, Foundry, vol. 78, p.82, 1950.
76. Notkin, E.M. et. al., Liteinoe Proizvodstvo, vol. 2, p.1, 1958.
77. Lesnichenko, V.L., Investigation and Development of the Technique for the Core Blower Production of Thin-walled Moulds, Thesis, 1957.

78. Evseev, A.S. et. al., Core Blower Process of Mould and Core Making, INTI Academy of Sciences, Gostekhnik, 1956.
79. Rakogon, V.G., Investigation of Compaction of Core-sand by the Core Blower Process, Thesis, 1956.
80. Geller, R.L. and Poplavskii, V.I., The Working Process in Core-shooters, Russ. Cast. Prod. PT9, p.393, 1965.
81. Pelczarski, S.M. and Danko, J.S., Phenomena Occurring During the Filling of the Core-box on Core Blowers and Shooters, British Foundrymen, vol. 64, p.1, p.2, 1971.
82. Danko, J. and Pelczarski, S., The Dynamic Action of Sand Air Jets on Layers of Moulding Sand in a Core-box During Production of Cores Using Core-shooters, Metalurgia, vol. 23, P.147, 1975.
83. Danko, J., An Analysis of the Unconventional Methods of Shooting the Sand Mixture into a Mould or Core-box, Metallurgia, vol. 30, p.93, 1983.
84. Aksjenov, P.N., Wybrane Zagadnienia Z Teorii Maszyn Oldewicznych, Wydawnictwo Slask, Katowice, 1965.
85. Rakogon, W.G., Teorija i Praktika Izgotovlenija Sterzuej Peskoduvum Sposobom, Masgiz, Moskva, 1962.
86. Lesnichenko, V.L., Some Aspects of Sand Blower Theory, Liteinoe Proizvodstvo, (11), pp.24-27, 1975.

APPENDIX

Sieve number	Sieve size mm	Weight on sieve gms	% Retained on sieve	Product	
22	0.710	-	-	-	
30	0.500	0.2	0.2	4.4	
44	0.355	1.6	1.6	48	
60	0.250	7.3	7.3	321.2	
72	0.212	5	5	300	
85	0.180	9.9	9.9	712.8	
100	0.150	18	18	1530	
122	0.125	16.1	16.1	1610	
169	0.090	27.2	27.2	3318.4	
237	0.063	1.7	1.7	402.9	
		100	100	10444.7	Total

$$\text{A.F.S. Number} = \frac{10444.7}{100} = \underline{\underline{104.45}}$$

Sieve analysis of silica sand grade 110

Sieve number	Sieve size mm	Weight on sieve gms	% Retained on sieve	Product	
44	0.355	-	-	-	
60	0.250	-	-	-	
72	0.212	0.2	0.2	12.0	
85	0.180	2.1	2.1	151.2	
100	0.150	11.1	11.1	943.5	
122	0.125	19.3	19.3	1930	
169	0.090	52.7	52.7	6429.4	
237	0.063	14.4	14.4	2433.6	
PAN		0.2	0.2	47.4	
		100	100	11947.1	Total

$$\text{A.F.S. Number} = \frac{11947.1}{100} = \underline{\underline{119.47}}$$

Sieve analysis of zircon sand grade 110